ERASMUS MUNDUS MSC PROGRAMME

COASTAL AND MARINE ENGINEERING AND MANAGEMENT
COMEM

MODELING THE EVOLUTION OF THE WAX LAKE DELTA IN ATCHAFALAYA BAY, LOUISIANA

Delft University of Technology
June 2011

Kevin Hanegan
4055284

The Erasmus Mundus MSc Coastal and Marine Engineering and Management
is an integrated programme organized by five European partner institutions,
coordinated by Delft University of Technology (TU Delft).
The joint study programme of 120 ECTS credits (two years full-time) has been
obtained at three of the five CoMEM partner institutions:

- Norges Teknisk- Naturvitenskapelige Universitet (NTNU) Trondheim, Norway
- Technische Universiteit (TU) Delft, The Netherlands
- City University London, Great Britain
- Universitat Politècnica de Catalunya (UPC), Barcelona, Spain
- University of Southampton, Southampton, Great Britain

The first year consists of the first and second semesters of 30 ECTS each, spent at
NTNU, Trondheim and Delft University of Technology respectively.
The second year allows for specialization in three subjects and during the third semester courses are taken with a focus on advanced topics in the selected area of specialization:

- Engineering
- Management
- Environment

In the fourth and final semester an MSc project and thesis have to be completed.
The two year CoMEM programme leads to three officially recognized MSc diploma certificates. These will be issued by the three universities which have been attended by the student. The transcripts issued with the MSc Diploma Certificate of each university include grades/marks for each subject. A complete overview of subjects and ECTS credits is included in the Diploma Supplement, as received from the CoMEM coordinating university, Delft University of Technology (TU Delft).

Information regarding the CoMEM programme can be obtained from the programme coordinator and director

Prof. Dr. Ir. Marcel J.F. Stive
Delft University of Technology
Faculty of Civil Engineering and geosciences
P.O. Box 5048
2600 GA Delft
The Netherlands

Modeling the Evolution of the Wax Lake Delta in Atchafalaya Bay, Louisiana

Kevin C. Hanegan

A thesis presented in partial fulfillment of the requirements for the degree of Master of Science in Civil Engineering within the Coastal and Marine Engineering and Management (CoMEM) program

Delft University of Technology

Delft, the Netherlands

Submitted for approval on

June 27, 2011

Graduation Committee:

Prof.dr.ir. M.J.F. Stive	Delft University of Technology (Chairman)
Ir. A.P. Luijendijk	Delft University of Technology/Deltares
Dr. J.E.A. Storms	Delft University of Technology
Drs. N. Geleynse	Delft University of Technology
Dr.ir. M. van Ledden	Royal Haskoning
Ir. T. M. Kluyver	Royal Haskoning
Ir. M. M. Hillen	Royal Haskoning

TU Delft Delft University of Technology

ROYAL HASKONING

Preface

This thesis represents the conclusion of my MSc work in the Coastal and Marine Engineering and Management program where I studied at the Norwegian University of Science and Technology, the Universitat Politecnica de Catalunya, and Delft University of Technology. I'd like to thank the organizing universities, professors, and CoMEM board for giving us all such a great opportunity to learn coastal engineering in the varying cultures and contexts within Europe, as well as the other CoMEM students who have helped to make it such a great experience.

The majority of this research was carried out with Haskoning, Inc. in New Orleans, Louisiana. I really appreciated the opportunity to live and work in such an interesting place and the great support that I received from everyone there, and thank Professor Stive, Mathijs van Ledden, Maarten Kluyver, and everyone else at Haskoning who made the research possible. It was a pleasure to work with my Dutch colleagues Maarten, Reis, and Martje and fellow students Matthijs and Alissa in New Orleans.

Special thanks to my advisors who offered wonderful guidance despite my being so far away. Nathanael Geleynse and Marten Hillen were especially helpful with particular modeling questions, and in New Orleans, Maarten Kluyver helped to keep the work on track with frequent discussions and review despite his busy schedule.

I want to thank Ioannis Giorgiou of the University of New Orleans, who provided both computer resources and substantial guidance on model development. His expertise on Louisiana coastal processes was very valuable, and the work could not have been completed without his help. Also, I'd like to thank Steve Ayers and others at the USACE New Orleans District who helped with tracking down bathymetry data sets. I'd like to acknowledge the help of my former professor Dr. Clint Willson and colleagues at LSU in developing the initial study idea, and the substantial work by Harry Roberts and others at the Coastal Studies Institute from which any study of the Louisiana Coast and deltaic processes proceeds.

Lastly, I'd like to thank my family for their continued support and for all the opportunities I have had because of their hard work, and especially Hannah for all her support, patience, help, and understanding during the research and throughout my MSc program.

Kevin Hanegan

Delft 2011

Abstract

In this study, a process-based, depth-averaged Delft3D hydrodynamic and morphologic model of the Wax Lake Delta in Atchafalaya Bay, Louisiana was developed to simulate a five year period of delta development from the beginning of 1998 to the end of 2002. The purpose of this modeling effort was to test the ability of process-based modeling tools to successfully simulate typical delta-building processes and the resulting morphologic and stratigraphic characteristics of the delta. Recent developments in conceptual modeling of mouth bar formation and full delta development have confirmed the capability of process-based models to simulate the processes necessary for delta growth and the resulting long-term, geologic scale morphologic and stratigraphic features. In this attempt to model the actual development of a prototype delta using similar techniques to those employed in the conceptual delta models, the applicability of physics-based modeling to delta evolution simulation will be further validated.

Initial model bathymetry was obtained from the grid of a USACE hydrodynamic model of the study area based on 1998 hydrographic surveys augmented with LIDAR survey data for overbank areas. The Wax Lake Delta morphology has been primarily shaped by river mouth processes, where mouth bar formation induces channel bifurcation and further basinward progradation. Because of the Wax Lake Delta river-dominance, marine processes including wave action, tidal oscillation, and wind induced water level changes and currents were neglected in the model. Variation of grain sizes in the bed composition and suspended sediment load was represented by a fine-sand non-cohesive fraction and a cohesive mud fraction. To represent the strong seasonal variation in discharge and sediment transport through the Wax Lake Outlet, the upstream boundary discharge regime was schematized into four periods of constant discharge representative of low flows, the annual flood, the 2-year flood, and the 5-year flood magnitude, with proportion of occurrence during each morphological year assigned based on a sediment transport-scaled frequency-duration curve. Corresponding inflow concentrations for the two sediment fractions were calculated from functional relationships to discharge derived from long-term concurrent measurements at the model upstream boundary. Hydrodynamics and transport were calibrated using measurements of velocity and sediment concentration across multiple transects of delta distributary channels taken during a single flood-condition event. The calibrated model was then used along with the schematized boundary conditions to simulate a five year period of long-term morphological development.

Morphology qualitatively reproduced typical river-dominant delta growth through the establishment of new depositional lobes while maintaining approximate radial symmetry. More specific stratigraphic features were also reproduced. The successive stacking of coarsening upwards sequences observed in Wax Lake Delta mouth bar deposits was evident in the stratigraphy of modeled incipient jet deposits, a result of the varying discharge regime. Though incipient jet deposits developed in the model at the distal ends of distributary channels, the prograding bars did not aggrade sufficiently to induce flow bifurcation and the development of a mature mouth bar depositional lobe. The lack of full mouth bar development could be a consequence of altered jet structure with the extreme channel incision and narrowing, a reduced sediment supply as the full 10 m thick bed is eroded upstream, and a non-representative initial bathymetry that does not capture the already-developing mouth bar deposit. The overall coarsening-upwards, though sand dominant stratigraphic sequence of typical friction-dominant river mouth deposits is reproduced. Significant mud-dominant prodelta deposition is observed basinward of the original delta front location. In the

prototype Wax Lake Delta, deposition of fine sediments in this area is hindered by waves and wind-induced transport, so the modeled mud depositional bodies do not reflect prototype development. Distributary channels are significantly incised and narrowed over the course of the simulation. The narrowing proceeds from significant sand-dominant subaqueous levee deposition on the channel banks. Though distributary channels in the real Wax Lake Delta do frequently incise through the full deltaic sedimentary sequence with channel extension, the modeled incision is persistent throughout the simulation. Upstream accretion of established delta lobes through sand-deposition, similar to the observed primary process of subaerial development in the neighboring Atchafalaya Delta, was also present in the modeled development.

The Wax Lake Delta is clearly river-dominant according to traditional classification schemes; however, the deposition of fine sediments is influenced by basin processes that resuspend and export significant quantities from Atchafalaya Bay. The processes contributing to the coarse sediment depositional features that dominate the Wax Lake Delta are qualitatively simulated under purely riverine forcings, but the fine sediment dynamics cannot be accurately simulated in the present, process-limited model. Recommendations for improving morphological simulation include model redevelopment with an alternative, total load transport formulation and the inclusion of limited marine forcings that inhibit fine-sediment deposition.

Table of Contents

1. Introduction

1.1 Background

1.1.1 The Mississippi River Delta

The Mississippi River delta, which forms a large portion of Southeast Louisiana, began to take shape over 7000 years ago when global sea levels stabilized in the beginning of the Holocene epoch (Blum and Roberts 2009). The complex system of wetlands, lakes, bays, barrier islands, and bayous that make up the Southeast Louisiana coast were formed by sediment accumulated from the Mississippi River's shifting delta lobes. The Holocene delta plain was gradually filled in with sediments as the river shifted to form new shelf-phase delta complexes every 1000 to 1500 years (Penland, Boyd et al. 1988; Blum and Roberts 2009). This concept of Mississippi Delta building through depositional channel switching has been explored extensively since the 1940s, with periodic updates to the chronology and age of each sub-delta complex. Figure 1-1 below gives the current extent of the Holocene delta plain and the locations, maximum extents, and age in thousands of years before present for each sub-delta.

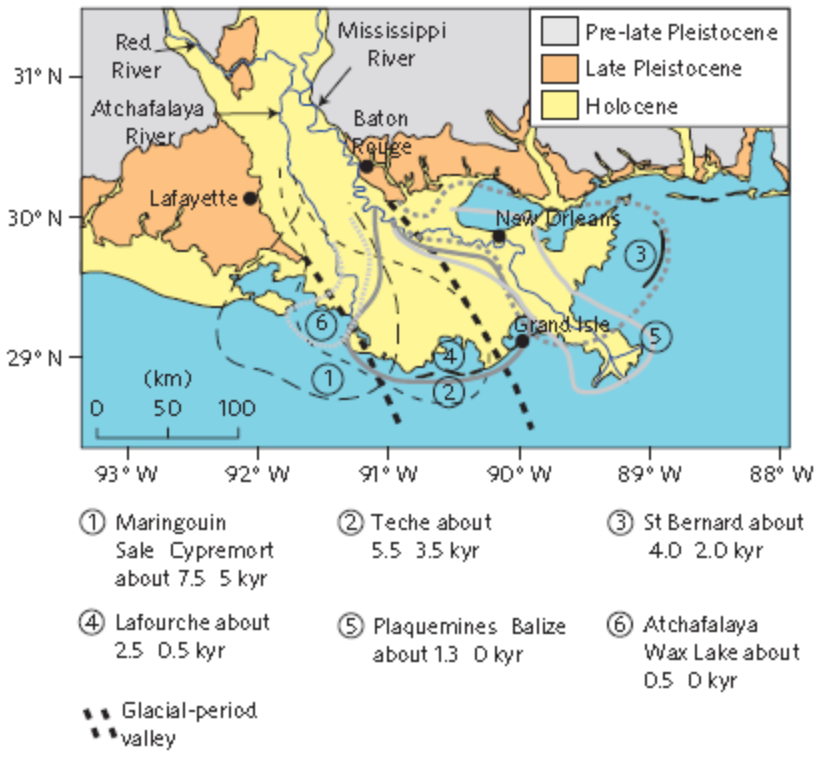

Figure 1-1: Geologic map of the Mississippi River delta plain (Blum and Roberts 2009)

The process of lobe switching and resultant land building was very cyclical, with the accretion following a general pattern for each subsequent sub-delta. As the majority of river flow and sediment began to discharge down a former distributary, the greatly increased sediment load from channel scour began to fill in the interdistributary basins with swamp deposits, eventually being by-passed to the coast to begin forming bayhead deltas. Continued deposition then established prodelta platforms on the continental shelf, the final phase of delta development. Flow bifurcation

would occur upstream of the river mouth, leading to eventual channel switching and abandonment as the original course became hydraulically inefficient with increased distributary progradation. The abandoned sub-delta begins the transgressive phase of the delta cycle, where the seaward boundary of the sediment deposition is reworked into a barrier shoreline as the entire complex subsides (Penland, Boyd et al. 1988; Roberts 1998) . Over the course of the past century, the portion of the Mississippi river flow being discharged through the Atchafalaya River distributary has gradual increased, indicating an in-progress sub-delta switching event. To prevent the eventual shifting of the majority of flow to the Atchafalaya, the Old River control structure, constructed in 1963, limits the flow being discharged through the Atchafalaya to 30% of the combined Mississippi and Red River inflow (Roberts 1998).

1.1.2 Drowning of the Mississippi Delta

Over the course of the last century, anthropogenic influence on the Mississippi River Delta has interrupted the progradation/transgression deltaic cycle. As a result of this intervention in the cycle, as well as natural processes such as subsidence, aerial land in the delta has been lost at a rate of 44 km^2/year over the last several decades (Kim, Mohrig et al. 2008). The transgression of abandoned sub-deltas occurs naturally as the deposited fine sediments consolidate, but the resulting subsidence is typically compensated by new sediment deposition from river overbank flooding and redistribution of discharged sediment by coastal processes. Additionally, the new distributary channel continues to prograde, building land as a new sub-delta. The land area in the entire deltaic plain is naturally maintained as a dynamic equilibrium between subsidence and deposition.

The dramatic decrease in land accretion to balance subsidence can be mostly attributed to the isolation of the current lower river channel from the surrounding deltaic plain (Day, Boesch et al. 2007). After the great flood of 1927, some pre-existing levees were upgraded and integrated into a comprehensive flood protection system that impounded the lower Mississippi River for most of its length, preventing any channel migration or overbank deposition. The sediment load is confined to the canalized channel and delivered to the edge of the continental shelf, isolated from the current Plaquemines-Belize sub-delta and the up and down-drift coasts of the deltaic plain (Kim, Mohrig et al. 2008). Additionally, withdrawal of hydrocarbons and groundwater in the delta plain has been correlated to increased rates of subsidence in the region (Day, Boesch et al. 2007). The mechanisms of subsidence and the degree to which they contribute to the high subsidence rates in Southeastern Louisiana are complex, but the result is extremely high rates of relative sea level rise that contribute to widespread land loss (Yuill, Lavoie et al. 2009). Land loss occurs on the seaward edges of wetlands due to wave erosion and in interior areas due to submergence by relative sea level rise. As more interior marshes are converted to open water through subsidence, wave erosion is having a greater impact on loss rates. Some loss is also attributed to the huge network of canals, dredged for navigation and oil and gas exploitation, that further alter the natural hydrology, allow increased saltwater intrusion, and increase the length of coastline exposed to erosion processes (Day, Boesch et al. 2007). Figure 1-2 below shows the dramatic decrease in land area over the entire Louisiana coast for the past 50 years and the projected continued land loss for the next 50 years, with most of the loss occurring in the Mississippi River delta region (Barras, Beville et al. 2004). The gravity of the situation is emphasized in the map also presented as figure 1-3, where the historical and projected land loss with no further remedial action taken is dramatically displayed in red (USGS 2005).

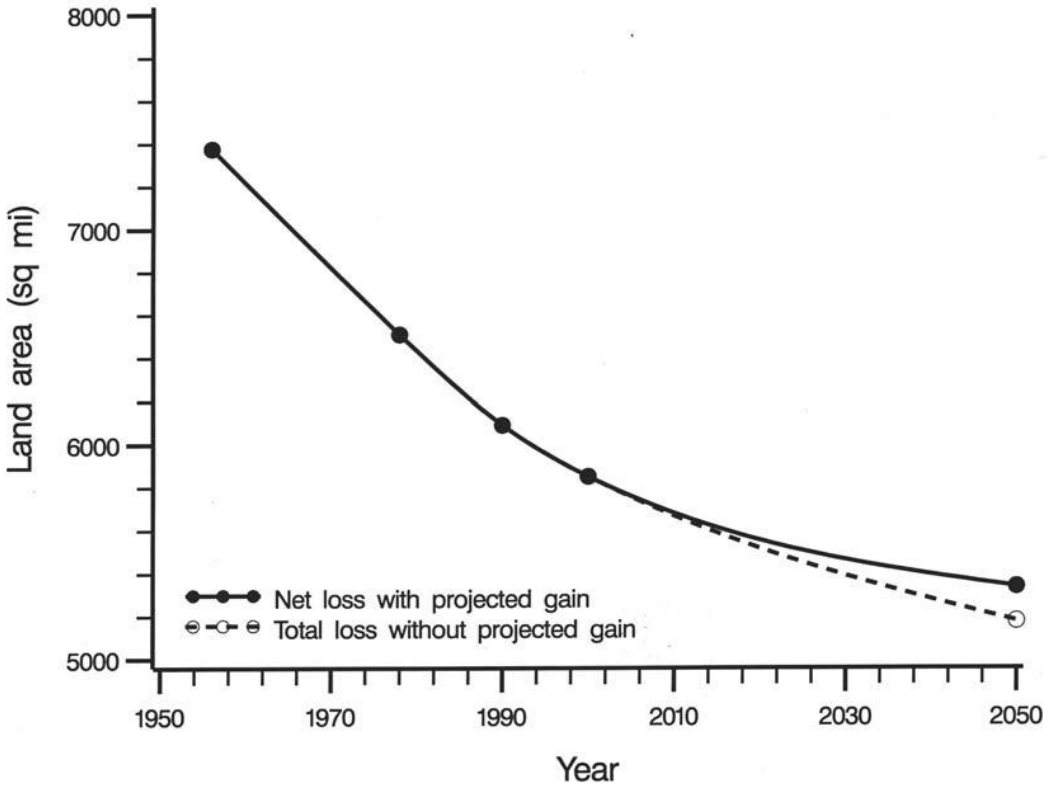

Figure 1-2: Projected Coastal Louisiana Land Loss from 1956 to 2050 (Barras, Beville et al. 2004)

Even if the delta can be re-engineered so that the river's sediment load can be deposited on the surrounding subsiding wetlands, some land loss is inevitable due to the reduced sediment load and projected sea level rise (Blum and Roberts 2009). Upriver damming of tributaries in the Mississippi River watershed has decreased the sediment load in the river by an estimated 50%, leaving a load much less than the time-averaged rates of storage that were necessary to construct the delta during the Holocene. Conservative estimates of the subsidence rate in the delta combined with an accelerating sea level rise rate based on the IPCC predictions dictate that the creation of accommodation space (land loss) greatly exceeds expected deposition based on projected sediment loads and historical trapping efficiencies. It is estimated that over 10,000 km^2 of additional land loss will occur in the Mississippi delta by 2100 if there is no additional sediment input (Blum and Roberts 2009).

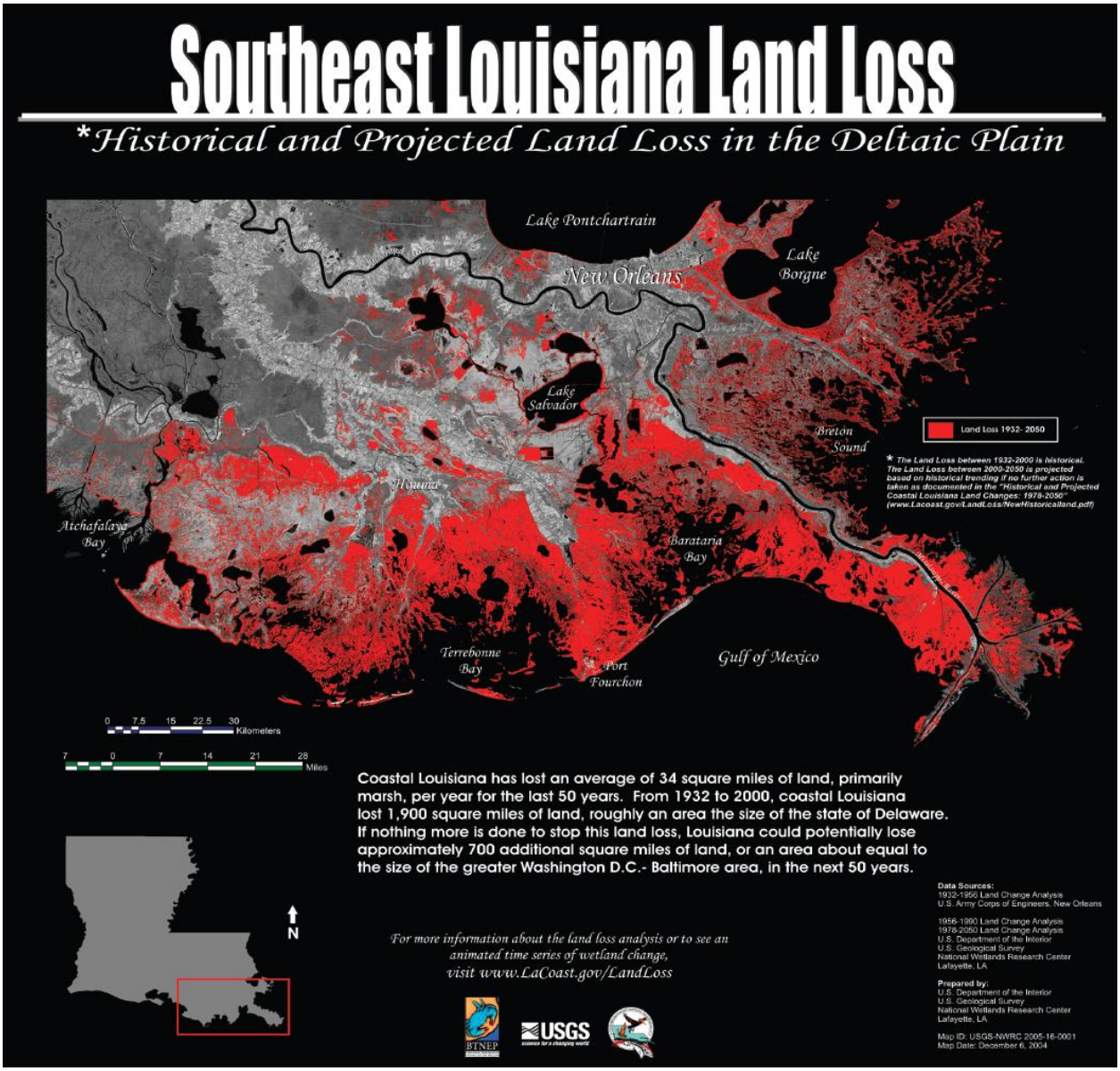

Figure 1-3: Projected Southeast Louisiana Land Loss (USGS 2005).

1.1.3 Diverting Sediment into the Transgressive Delta

The devastation resulting from the hurricanes of the 2005 season reinforced the vulnerability of coastal Louisiana. Hurricane Katrina, due to its very large size and low pressures, caused unprecedented storm surge levels in the Southeast Louisiana-Mississippi Gulf Coast region, leading to catastrophic flooding aided by natural topography and critical engineering failures. Over 1800 people were killed, and nearly 100 km^2 of wetlands in the delta were converted to open water during the single storm event (Day, Boesch et al. 2007; USACE 2009) . Though the magnitudes and mechanisms remain poorly understood, the typical coastal features of the delta region such as wetlands and barrier islands help to attenuate surge height and wave energy, and the erosion and submergence of these features increases the vulnerability of New Orleans and other population centers to disasters like Katrina (Day, Boesch et al. 2007). In response to the recent hurricane disasters, the United States Army Corps of Engineers, the responsible organization for planning, design, and implementation of flood control projects in the U.S., has sought to fully integrate flood

protection and coastal restoration measures into comprehensive risk reduction strategies. In this capacity, the effect of eroded coastal features on storm surge, wave heights, and potential inundation has been evaluated, and coastal landscape restoration is explicitly included in the hurricane risk reduction alternatives (Wamsley, Vann Stutts et al. 2008; USACE 2009).

Though many strategies exist for restoring features of the Mississippi delta coastal landscape, the most promising for large scale impact and self-sustaining wetland creation is the reconnection of the river to the surrounding transgressive deltaic plain (Day, Boesch et al. 2007). This would be implemented through freshwater and sediment diversions in the lower Mississippi and the Atchafalaya distributary that would act as engineered avulsions, diverting significant portions of the water and sediment load of the river into the surrounding delta to recreate the delta building process (Kim, Mohrig et al. 2008; USACE 2009; Allison and Meselhe 2010) . Other proposals even advocate the diversion of the majority of sediment load through the Atchafalaya distributary, leaving only enough discharge through the Plaquemines-Belize Mississippi sub-delta to maintain navigability (Winer 2007). Thus far, only one diversion in the delta has been constructed specifically to divert sediment for land building. The West Bay diversion, constructed in 2003, is an uncontrolled, dredged channel through the West bank levee 7.6 km above Head of Passes. Thus far, the project has not been successful in inducing significant accretion in the adjacent West Bay, mostly due to the large erosion in the area due to Hurricane Katrina and the small discharge of the diversion. This area of the river, located downstream of several large navigational passes, has a reduced sediment transport capacity, and sand transport through the diversion is less than the expected transport for potential upstream diversion locations (Allison and Meselhe 2010). An additional complication for this project is the apparently induced shoaling upstream of the diversion at the Pilottown Anchorage area that requires periodic maintenance dredging to maintain navigability (Allison and Meselhe 2010). Additionally, two small diversions have been constructed at Caernarvon and Davis Pond for freshwater input to control salinity in the surrounding wetlands. Alterations in the basin-side channel and a pulsed management scheme for the Caernarvon diversion encourage significant sediment input to the Breton Sound estuary during high flow events; however, the amount of deposited sediment is insufficient to balance relative sea level rise (Snedden, Cable et al. 2007).

1.1.4 The Wax Lake Diversion

As mentioned earlier, a delta switching event from the Plaquemine-Belize sub-delta to the Atchafalaya distributary has been gradually occurring over the past century but was interrupted through anthropogenic intervention that regulates the division of flow through the two channels. To deal with flooding arising from the gradually increasing flow, the Wax Lake diversion was constructed in 1941 as a more efficient outlet from the Atchafalaya River to the Gulf of Mexico (DuMars 2002). The figure below shows the layout and location of the Wax Lake Outlet in the Lower Atchafalaya Basin.

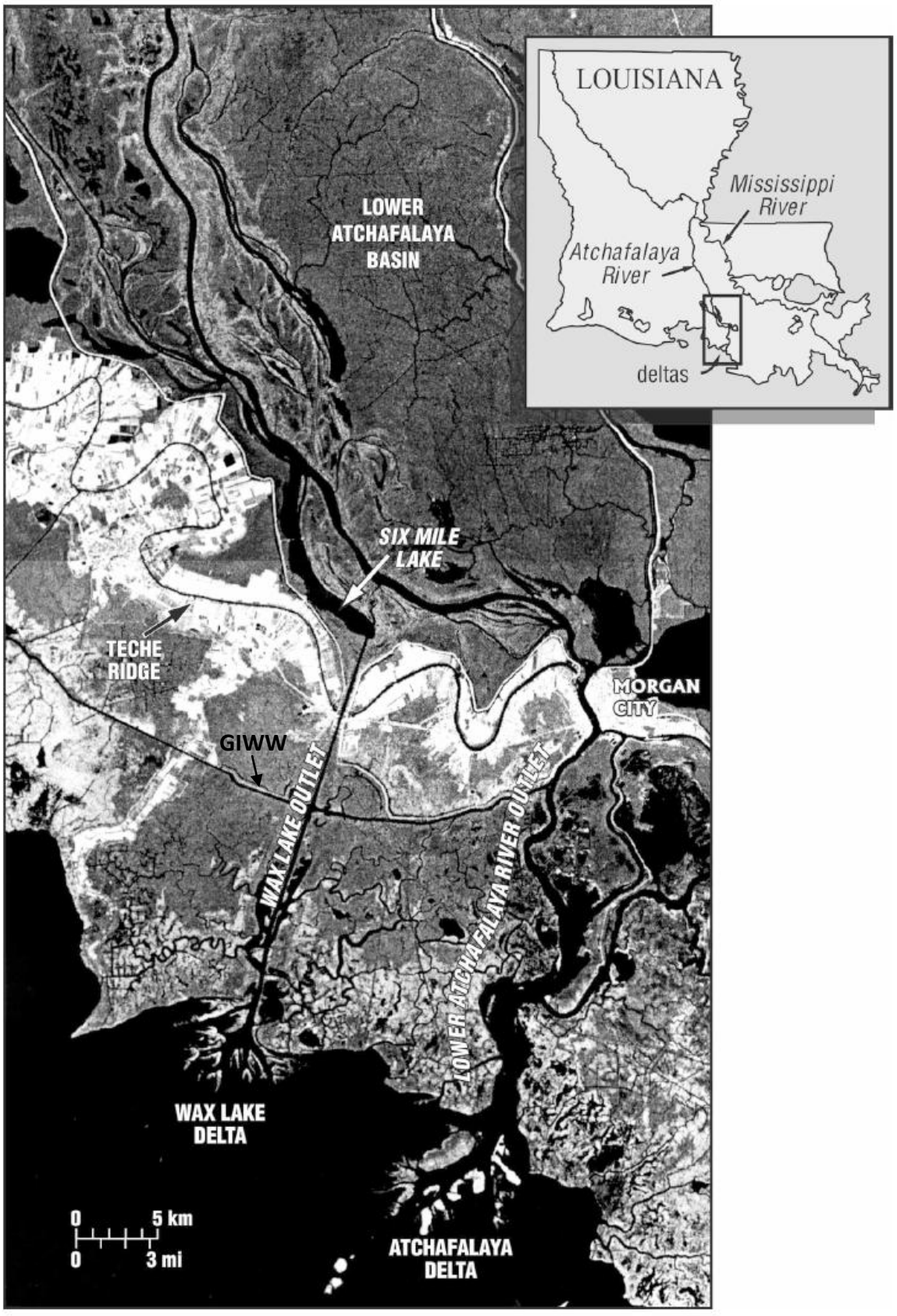

Figure 1-4: Locations of Wax Lake Outlet, Lower Atchafalaya River, and Developing Deltas in Atchafalaya Bay (modified from Roberts, Coleman et al. 2003)

In the mid-20th century, the lakes in the Lower Atchafalaya area were being filled with sand-rich deposits, a process representative of the filling of interdistributary basins that occurs as a stage in delta switching. Between the 1950s and 1970s, deposition had occurred to such a degree in inner-basin features that substantial sand was bypassed into the Atchafalaya Bay, forming subaqueous delta deposits. During a huge flood in 1973 and subsequent high discharge years, coarse sand in the Lower Atchafalaya River was mobilized and transported into both the Wax Lake Outlet and Atchfalaya developing deltas (Roberts 1998). Both are presently continuing to develop as subaerial bayhead deltas, offsetting to a small degree the continuing land loss to the east. While the Wax Lake delta has developed naturally into the Atchafalaya Bay, a maintained navigation channel through the Atchafalaya delta has aided sediment bypass and restricted delta growth (DuMars 2002). The Wax Lake delta has evolved through seaward channel extension, subaqueous mid-channel bar formation, and channel bifurcation. Simultaneously, sand-rich lobes merged and upstream shallow channels accreted (Roberts 1998). The delta building process for the Wax Lake delta has been extensively studied and documented, and as such offers a natural example of how land building could occur for a future large scale sediment diversion in the Mississippi River (Kim, Mohrig et al. 2008). The figure below shows a satellite photo of the fan-shaped delta in 2006 (Parker and Sequeiros 2006).

Figure 1-5: Satellite Image of Wax Lake Delta in 2006 (Parker and Sequeiros 2006)

1.2 Motivation and Research Goal

1.2.1 Problem Statement

The use of large scale sediment diversions to build and sustain wetlands in the Mississippi delta has been discussed extensively, yet none of the recent planning initiatives at the state and federal level contain specific recommendations for their use or location (Allison and Meselhe 2010). Increasing

understanding of the expected land-building magnitudes and morphological configurations resulting from large sediment diversions, as well as the effects on the hydrodynamics and morphology of the main river channel, is essential for moving forward. Admittedly, the main obstacles to implementation are the possible detriments to river navigation by channel siltation and fisheries impacts from large freshwater introduction; however, the knowledge of the expected land building is still important for maximizing project benefits and is interesting for scientific investigations of delta formation and processes. Recent developments in one-dimensional deltaic sedimentation modeling that assumes continued radial symmetry offer a robust tool to predict the expected time-dependent surface area and deltaic front location of a fan-shaped delta, but there is still a need to expand modeling capabilities to be able to predict the evolution of the diversion delta's channel structure (Kim, Mohrig et al. 2008). The conceptual delta-building models developed in the process-based modeling program Delft3D have simulated characteristic delta channel structures, emergent land patterns, and stratigraphy (see section 2.3). The continued development of these modeling capabilities could offer more comprehensive and accurate descriptions of the expected delta morphology arising from large-scale river diversions than is currently available. A numerical model cannot be reliably used as a predictive tool until it has been verified through hindcasting. The goal of this research is to investigate the morphological development of the Wax Lake delta using the process-based model Delft3D. In addition to offering insight on the general processes of delta development, this research will also test the ability of process-based modeling to accurately simulate the real Wax Lake delta evolution.

1.2.2 Objective

The objective of this thesis is to successfully simulate the long-term morphological development of the Wax Lake Delta. In investigating this topic, the following main research question will be answered:

- Can the delta-building processes and the resulting morphologic and stratigraphic characteristics of the Wax Lake Delta be successfully simulated using a physics-based, though process-limited long term morphologic model?

1.2.3 Research Approach

A model of the Wax Lake Outlet, Wax Lake Delta, and a portion of the Atchafalaya Bay receiving basin will be developed. Available velocity and sediment concentration measurements in the delta distributary channels will be used to calibrate the model for hydrodynamics and sediment transport. Schematized flow and transport boundary conditions will be calculated from long term measurement data and implemented with morphologic acceleration techniques so that long time scales can be simulated with reasonable run times. The model will then be used to simulate five years of morphological development from the beginning of the year 1998 to the end of 2002. Though a full bathymetric survey of the Wax Lake Delta at the end of the simulation period does not exist, information from studies of the subaerial development during these years and stratigraphy of new depositional features will be used to assess the validity of the results. The discussion will focus on delta building processes, morphology, and stratigraphic patterns reproduced in the model simulation and how well these results match those observed in the prototype Wax Lake Delta.

1.2.4 Report Structure

In this introductory chapter, background information and research objectives were discussed. Chapter 2 of the report reviews previous work on delta formation, modeling of conceptual delta development, and the specific formation sequence and processes for the Atchafalaya and Wax Lake Deltas. Chapter 3 describes the set-up of a process-based morphologic model for the Wax Lake Delta, and chapter 4 details the calibration process for hydrodynamics and sediment transport in the model. In chapter 5, the actual implementation of the model for the simulation of five years of morphological development is described, and a brief overview of model results is presented. Chapter 6 includes a more in-depth discussion of model results, with a focus on particular delta building processes and the degree to which simulation results reflect the prototype development. Conclusions of the study and recommendations for more successful simulation and future work are given in the final chapter 7.

2. Literature Review

2.1 Delta Classification, Processes, and Characteristics

Deltas have been defined as depositional features that protrude from shorelines where a fluvial sediment source interacts with the redistributing forcings of the receiving marine basin (Orton and Reading 1993). The relative strength of the fluvial or marine forcings has been the traditional basis for examining the various observed delta configurations (Wright and Coleman 1973). The processes occurring at a river mouth influence the nature in which the decelerating effluent's sediment load is deposited which in turn determines the resulting delta's morphology and stratigraphy (Wright 1977). Delta classification schemes have been developed as frameworks in which to discuss the observed variation in modern delta descriptions and as tools to aid in the interpretation of ancient deltaic deposition in the stratigraphic record (Galloway 1975; Nemec 2009). The latter motivation has resulted in some preference for classification based on those properties that are easily observed in sedimentological studies, namely dominant grain size and facies surface gradients. These properties have the additional advantage of being intrinsic to the nature of the depositional body, so classification in this framework does not require difficult-to-verify inferences on the nature of the ancient feeder system and basinal processes (Nemec 2009). In a comprehensive review of classification schemes, Nemec concludes that the use of a particular scheme should be dependent on the characteristics and information on which the particular analysis or comparison is based (Nemec 2009). For the purposes of this current study, classification schemes that focus on the delta-front regime as well as feeder/basin characteristics are preferred because of the insight they can give on delta formation processes which must be understood for analysis of the current delta morphology and the interpretation of predictive modeling results.

The well-known classification system of Galloway (1975) is based on the insight that although many processes affect the deposition and reworking of a delta, only the fluvial flow, wave energy flux, and tidal currents are capable of transporting amounts of sediment in the large quantities necessary to significantly influence the delta morphology and stratigraphy (Galloway 1975). The interaction and relative strengths of fluvial and marine processes are capable of producing a variety of characteristic morphologies and accompanying stratigraphies. The classification scheme characterizes deltas based on three end member types, fluvial-dominated, wave-dominated, and tide-dominated, that exemplify the effects of each process when it is the most important for a deltaic system. A range of intermediate systems exists between the three end-member types that mix delta front process-response characteristics to varying degrees. Figure 2-1 below gives the graphical representation of Galloway's ternary scheme with modern delta representations of each end-member type. The classification of other real deltas can be obtained by a semi-quantitative judgment of the degree of dominance of reworking processes that approximately locates the delta's position on the triangular diagram (Galloway 1975). A weakness of the scheme is its fully genetic nature that relies on judgments and inferences of fluvial and marine forcings that are not always obvious, especially for ancient deltas in the stratigraphic record. Additionally, the classification depends on the degree of reworking value whose method of quantification is not clearly defined (Nemec 2009).

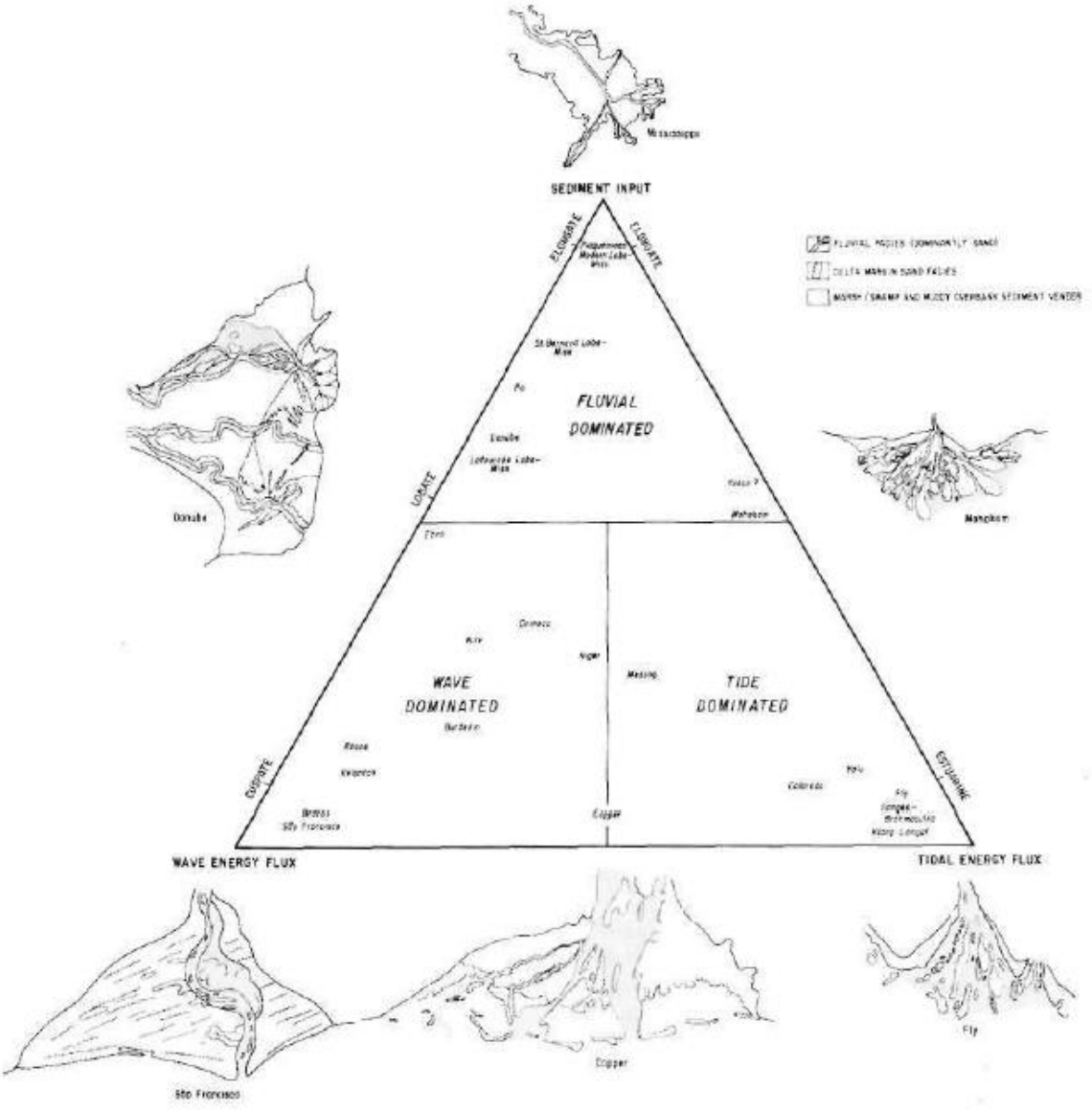

Figure 2-1: Triangular Classification of Deltaic Depositional Systems according to (Galloway 1975)

The importance of sediment supply in the fluvial input of a delta was mentioned by Galloway, 1975, but was explicitly included in the classification scheme of Orton and Reading, 1993. The authors determine that the physical processes and resulting morphology of a delta are significantly influenced by the amount, nature, and grain size of the sediment load of the fluvial input. The dominant grain size in a delta is generally indicative of the other sediment load characteristics, so the range of feeder system characteristics observed in natural deltas is incorporated into Galloway's end-member diagram as a grain size axis (figure 2-2) (Orton and Reading 1993). The scheme still relies on the degree of delta front reworking for primary classification, but the study expands the analysis with a discussion of the influence of sediment input on the channel structure of the deltaic plain, river mouth processes, shoreline response to basin energy, and resedimentation on the seaward delta slope.

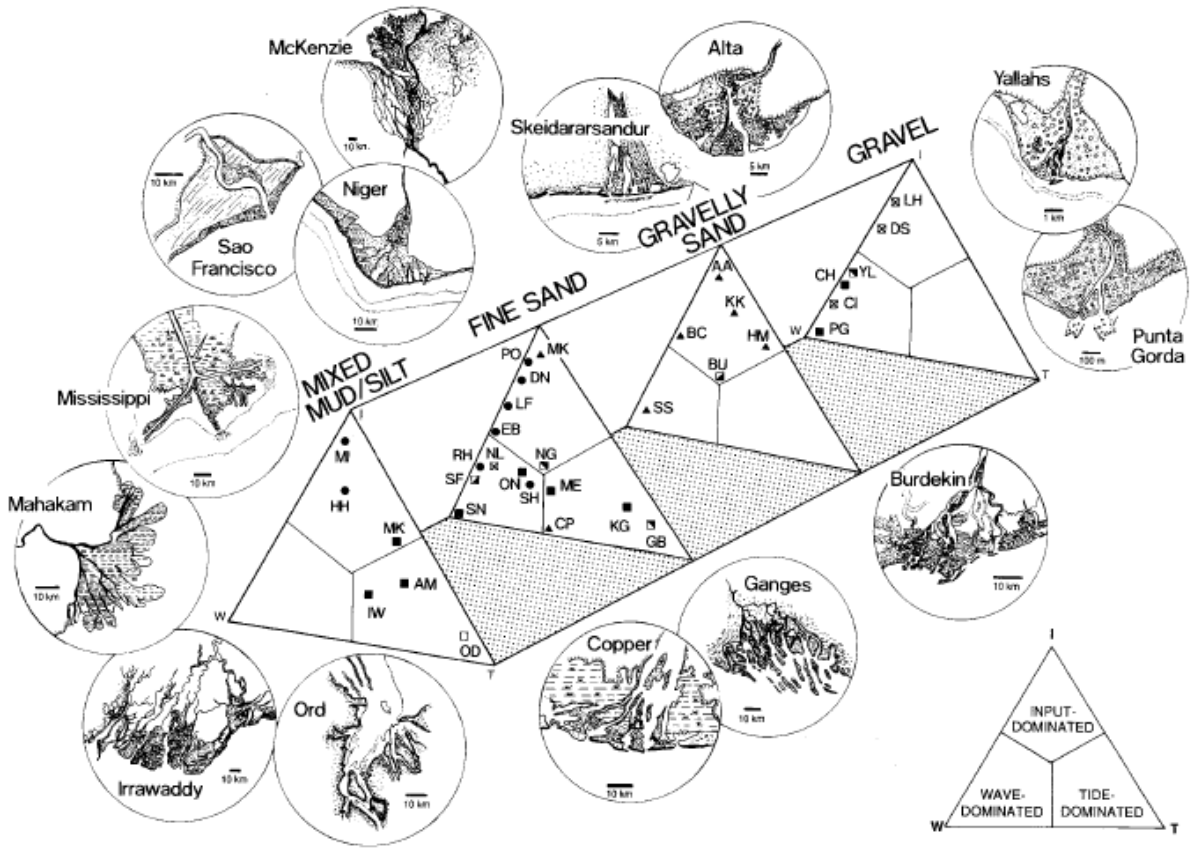

Figure 2-2: Orton and Reading delta classification scheme based on the Galloway, 1975 diagram with consideration of prevailing grain size (Orton and Reading 1993)

For situations in which the riverine forcings are dominant to such a degree that reworking of sediment by tides and waves is negligible, the effluent and associated depositional patterns will be indicative of a further classification of dominant forcing. The spreading and deceleration of the effluent at a river mouth will be dominated by inertia and turbulent diffusion, turbulent bed friction, or buoyancy (Wright 1977). For non-stratified, homopycnal river mouth conditions, inertial forces dominate so that the flow is fully turbulent and spreading, diffusing, and deceleration proceed according to turbulent jet theory. If the receiving basin is shallow, the pronounced bed shear stress induces greater deceleration and alters the jet pattern. If sufficient temperature or salinity gradients exist between the effluent and receiving basin, the resulting density stratification and buoyant forces inhibit turbulent mixing and isolate the outflow boundary layer from the bed (Wright 1977). The work by Wright synthesizes the research on these three effluent forces and presents idealized flow patterns and associated depositional features for each.

River effluents that are fully controlled by the inertia of the outflow resemble the idealized case of a fully-turbulent jet that discharges into a deep receiving basin. The basin must be sufficiently deep so that the expanding jet is not affected by bottom friction and turbulent diffusion dominates. As the discharge exits the river mouth and is no longer laterally or vertically confined, momentum is exchanged from the fully-turbulent jet to the ambient water through eddies generated at the boundaries of the outflow. This transfer of momentum out of the jet (turbulent diffusion) causes flow expansion and deceleration with a constant spreading angle that was found to be approximately 12.5° from the jet centerline. With the exception of a cone-shaped zone of laterally

and vertically constant velocity that decelerates from the mouth seaward, the full width of the jet is composed of turbulent eddies that induce a Gaussian velocity distribution. The maximum non-fluctuating velocity occurs at the jet centerline and progressively slows as the effluent moves seaward and spreads. The two flow regions and associated transverse velocity distribution are shown in plan and longitudinal cross section view in figure 2-3 below (Wright 1977). The depositional pattern associated with an inertia-dominated effluent is also known as a Gilbert-type profile after the first researcher to examine deltaic sedimentation in the context of turbulent jet diffusion. The dominant feature of this type of depositional environment is the lunate bar, where sedimentation in a narrow zone (roughly corresponding to the spreading jet boundaries) builds up a subtle back-bar slope with a steeper, seaward bar front. Because the turbulent diffusion greatly reduces the transport capacity of the effluent, most of the coarse material carried by the flow is deposited at the boundary between the initial cone-shaped zone of constant velocity and the fully-turbulent, diffusion dominated jet zone (Wright 1977). The idealized sedimentation pattern is shown in figure 2-4, where characteristic sediment sorting and the prograding delta-front sequence are given. This effluent type and associated deposition is rarely observed in nature because bed-friction is in most cases non-negligible. Though the necessary conditions often occur when steep rivers discharge into deep, freshwater lakes or when newly formed river mouths discharge into the sea, the deposition occurring seaward of the mouth eventually reduces the water depth so that bed friction begins to affect the flow (Wright 1977).

Many natural river outlets discharge into basins that are of equal or shallower depth than that of the outlet, where velocities near the bed produce high shear stresses and friction that dominate the flow structure. The vertical expansion of the jet is restricted so the vertical velocity distribution is controlled by bed friction rather than turbulent diffusion. Laterally, the effluent spreads and decelerates due to plane jet diffusion, though at much higher rates than in the fully turbulent jet case. Laboratory experiments have shown that these rates are inversely dependent on basin depth seaward of the outlet and that the transverse velocity distribution in the plane jet is Gaussian as well (Wright 1977). The idealized spreading pattern and vertical velocity distribution for friction-dominated effluent is given below in figure 2-5. The rapid spreading and deceleration of the plane turbulent jet induces shoaling seaward of the mouth, forming a positive-feedback loop in which the shallower depth increases deceleration and the deposition rate. Subaqueous levees form at the outward boundaries of the effluent, and once the middle ground shoal reaches a critical height, the effluent bifurcates around the shoal to form two channels of concentrated flow.

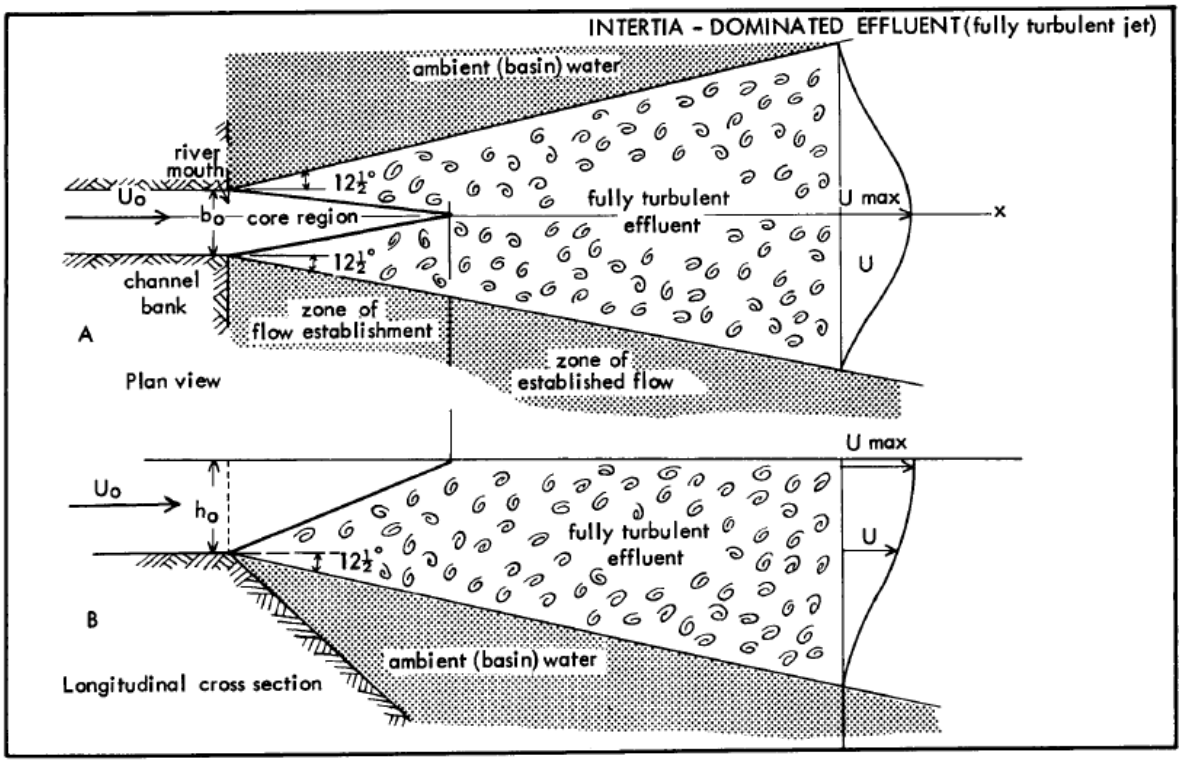

Figure 2-3: Idealized Inertia-Dominated Effluent Flow Pattern (Wright 1977)

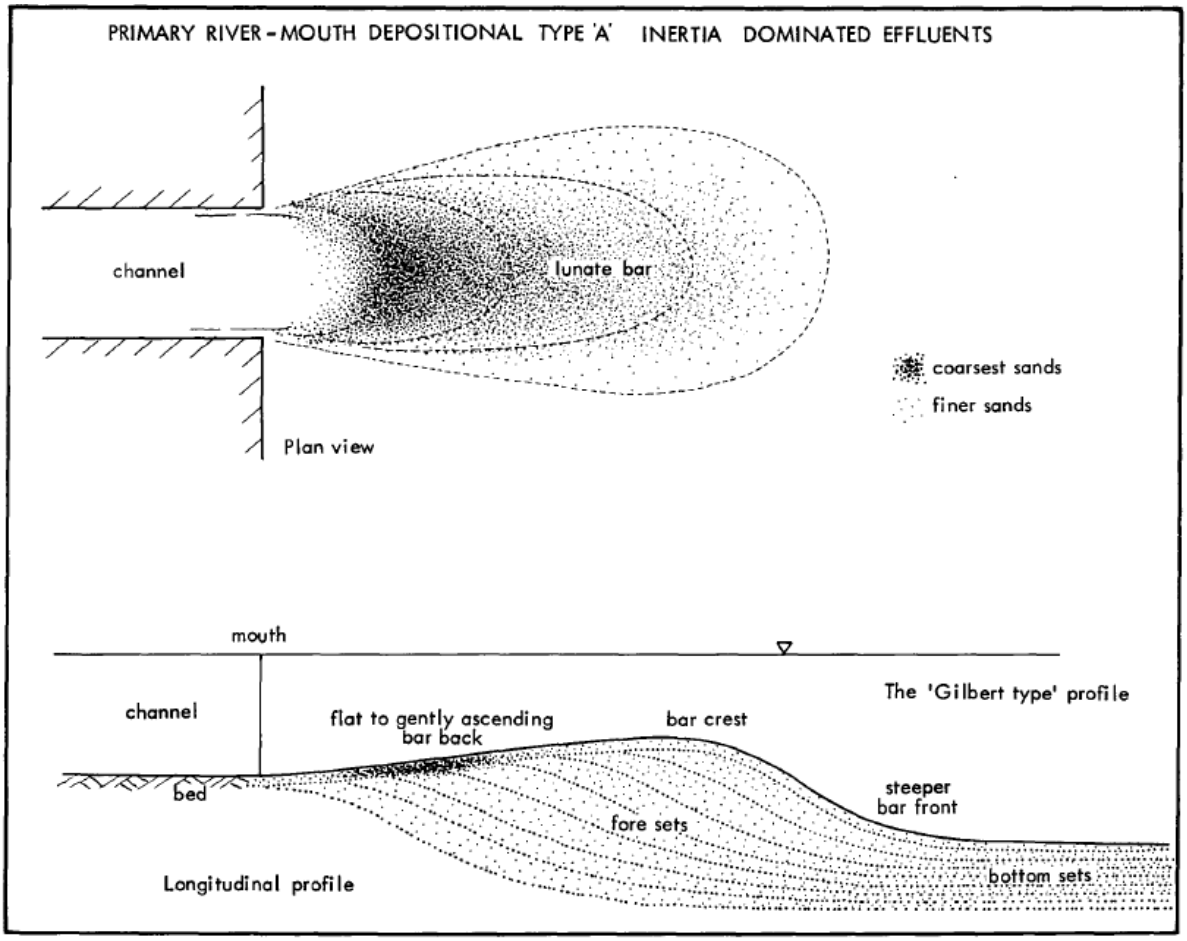

Figure 2-4: Idealized Depositional Pattern for Inertia-Dominated Effluents (Wright 1977)

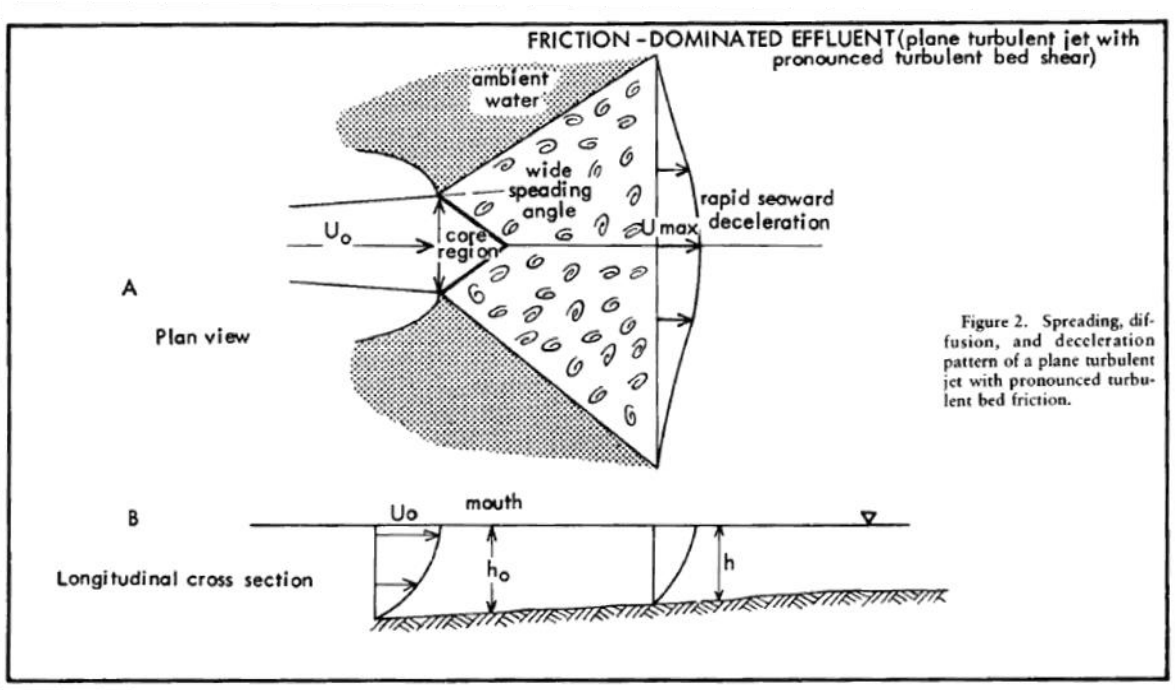

Figure 2-5: Idealized Friction-Dominated Effluent Flow Pattern (Wright 1977)

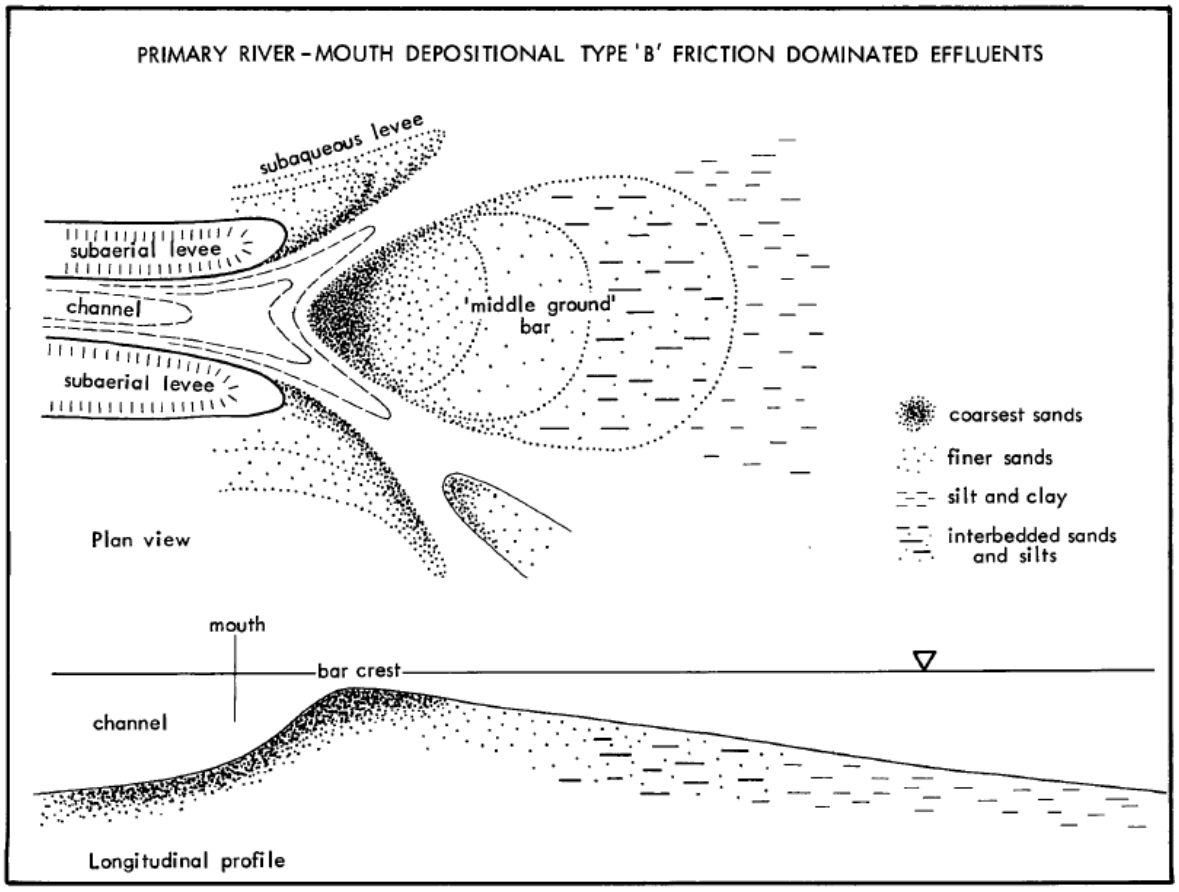

Figure 2-6: Idealized Depositional Pattern for Friction-Dominated Effluents (Wright 1977)

The triangular shoal separating the channels has a relatively high-angle foreslope where the coarsest sediments have been deposited at initial jet expansion. After bifurcation, shear stresses on the middle-ground bar are sufficiently low to allow the accumulation of silts and clays on the seaward, mildly-sloped portions of the bar. The characteristic depositional patterns and features associated with frictionally-dominant effluent are given in figure 2-6. Deltas that prograde onto flat, shallow receiving basin platforms and transport sufficient sediment form through the process of successive middle-ground bar formation, subaqueous levee extension, and channel bifurcation (Wright 1977).

When effluents issue from channels that have high depth to discharge rates into relatively deep receiving basins where tidal-induce mixing is low, high vertical density gradients and flow stratification can occur. The less dense fresh water effluent remains in the upper water column, spreading over the more dense salt water as a buoyant plume. The high depth-discharge ratio stipulation allows a dense salt wedge to propagate into the river mouth, causing buoyancy dominance in the zone of primary spreading and deposition. In other cases, however, discharge is great enough to force the pycnocline beyond the depositional zone so that other forcings dominate (Wright 1977). The most accurate descriptions of the stratified effluent flow structure rely on higher order buoyant jet theory; however, field observations suggest that turbulent diffusion is in most cases negligible, so flow patters can be adequately described from buoyancy alone. From the river mouth to a distance of 4 to 6 channel lengths away, superelevation of the freshwater plume induces lateral pressure gradients which drive flow expansion with relatively homogenous lateral and vertical velocity distributions. As the plume expands, the thickness decreases while velocities remain approximately constant so that flow becomes supercritical in the upper layer. The increased shear between the fresh plume and ambient salt water drives internal wave development that induces mixing and rapid flow deceleration. Coarse sediment deposition drives the development of a distinct bar crest around 4 to 6 channel widths away from the mouth. Seaward of this form, continued deceleration returns the flow to subcritical and deposits fine silt and clay on the bar front slope (distal bar) and prodelta. Secondary flow patterns arising from the effluent superelevation drives flow divergence at the surface and convergence at the layer interface. The convergence aids in the development of subaqueous levees as the channel progrades and keeps the deposition of the coarsest sediment confined to laterally narrow bar structures (Wright 1977). Characteristic flow patterns and depositional features for buoyancy-dominated effluents are given in the figures below.

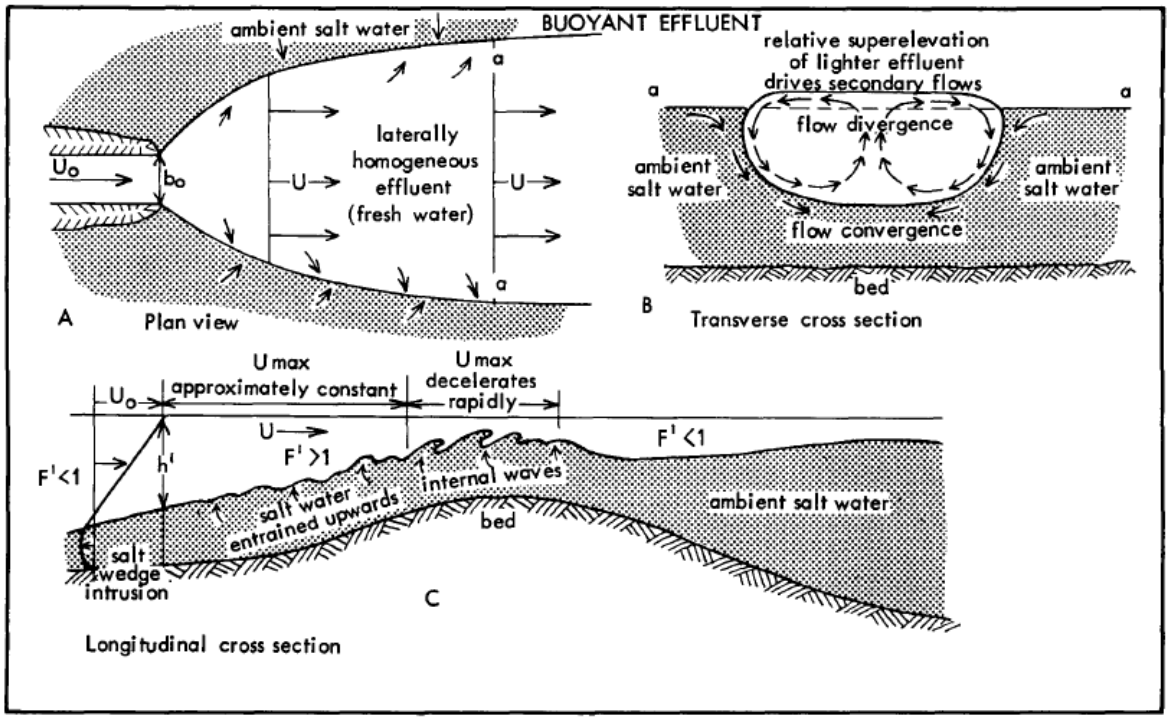

Figure 2-7: Idealized Buoyancy-Dominated Effluent Flow Pattern (Wright 1977)

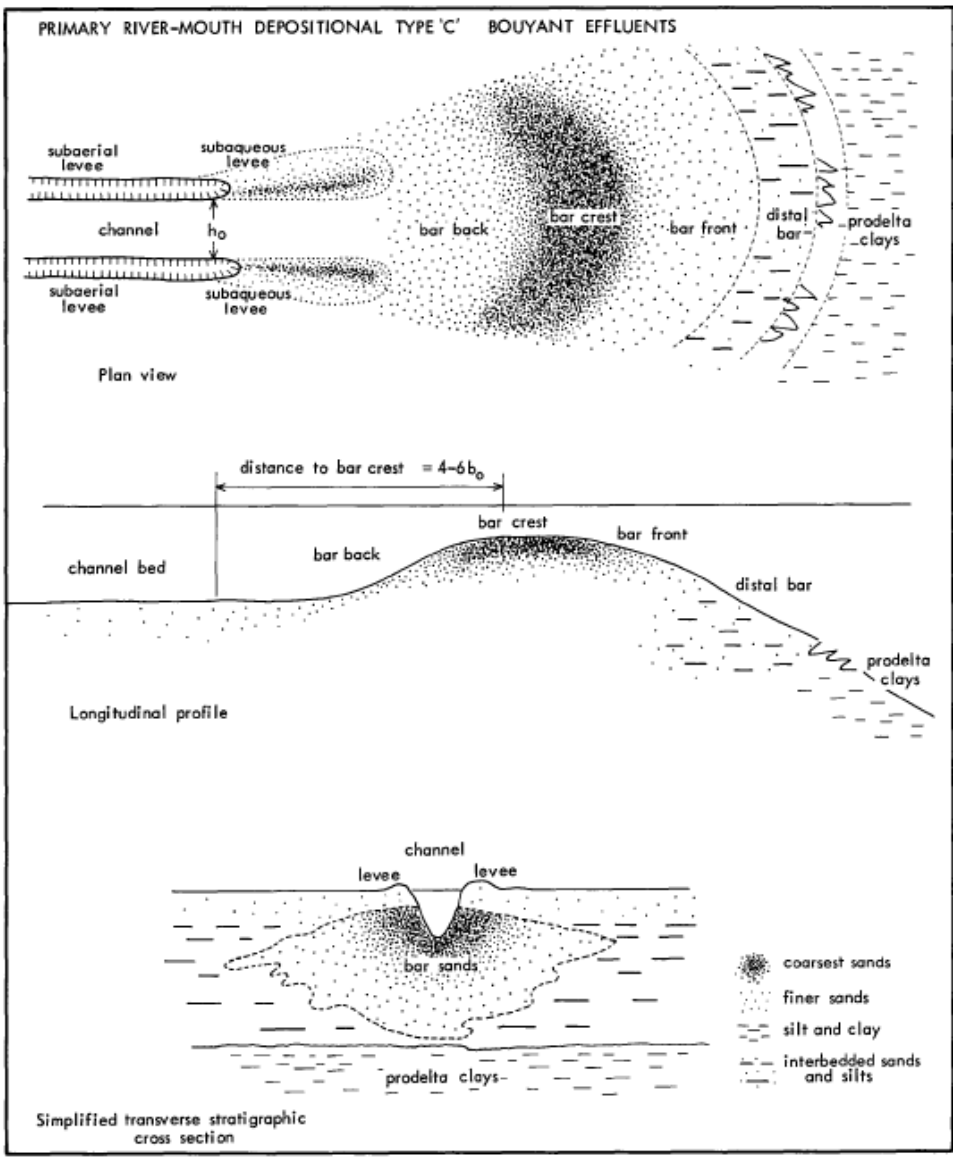

Figure 2-8: Idealized Depositional Pattern for Buoyancy-Dominated Effluents (Wright 1977)

2.2 River Mouth Bar Formation

Observations of modern, river-dominant delta distributary networks suggest that the process of channel bifurcation around river mouth bars is primarily responsible for the development of network structure (the planview orientation of delta distributary channels). In a topological survey of eleven such deltas, Edmunds and Slingerland conclude that decreases in a bifurcating channel's width and depth can be predicted as a function of the decreasing discharge through successive bifurcations. An observed systematic decrease in channel length (defined as the distance between successive bifurcation points) towards the distal ends of distributary networks cannot be explained through hydraulic geometry relations; however, because each bifurcation is initiated by bar formation at the location of a former distributary mouth, the mechanics of mouth bar formation can contribute to understanding of the decreasing length trend and overall organization of delta distributary networks (Edmonds and Slingerland 2007). The decreasing channel length away from the initial channel mouth can be observed in the bifurcation-dominant Mossy delta in fig 2-9 below. Though the work presented in Wright, 1977 conceptually relates mouth bar formation to the characteristic

hydrodynamic and depositional patterns observed in turbulent plane jets, the conceptual model fails to quantify formation processes and does not fully describe the dynamic nature of mouth bars (Edmonds and Slingerland 2007). Field observations indicate that mouth bars can prograde basinward great distances before sufficient aggradation forces channel bifurcations that establish upstream channel length and that, in certain situations, evolution continues after bifurcation through upstream accretion (Edmonds and Slingerland 2007).

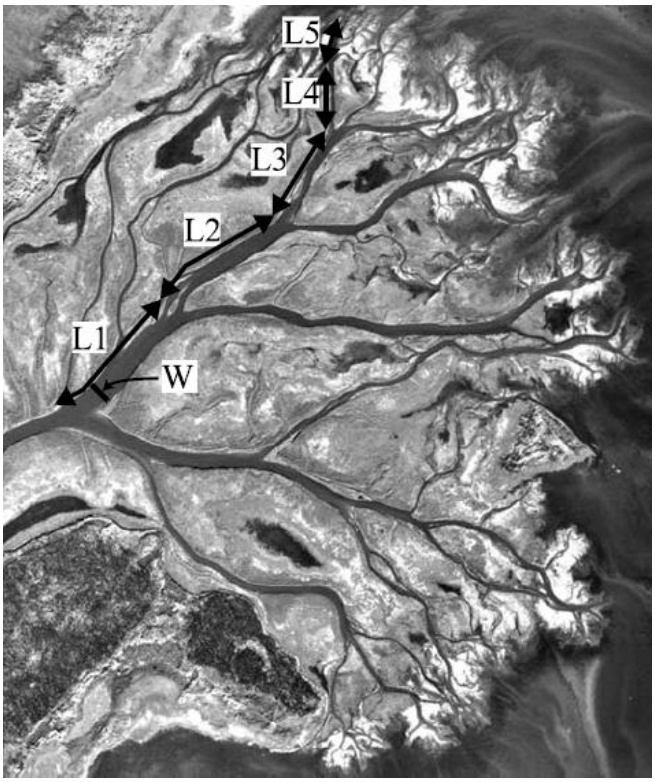

Figure 2-9: The Mossy Delta in Saskatchewan, Canada. Development of the distributary network structure is primarily through channel bifurcation around former river mouth bars. (Edmonds and Slingerland 2007)

In order to quantitatively characterize the formation of river mouth bars including dependency on relevant hydraulic and sedimentologic variables, a Delft3D numerical model of river mouth bar evolution was developed by Edmonds and Slingerland (2007). The model consists of a trapezoidal channel with constant flow and sediment concentrations discharging into a sloping-bed basin with a constant water level at the boundaries, discretized in three-dimensions with seven vertical flow layers to adequately simulate secondary flow circulation associated with mouth bars. The functional relationship of deposition patterns on channel width, channel depth, initial channel velocity, and grain size was determined by conducting 55 model runs where the channel aspect ratio, channel Froude number, and grain Froude number were systematically varied. First, the accuracy of the model's simulation of expanding plane turbulent jet hydrodynamics was established by comparison of jet centerline velocity decay with the theoretical function and was found to reproduce theoretical values with 95% confidence (Edmonds and Slingerland 2007). The multiple simulations allowed the authors to characterize the formation of mouth bars as follows: a small bar initially forms basinward of the discharging channel, progrades some distance basinward away from its initial point of formation, then ceases to prograde as it widens and aggrades (see fig 2-10 below)(Edmonds and Slingerland 2007).

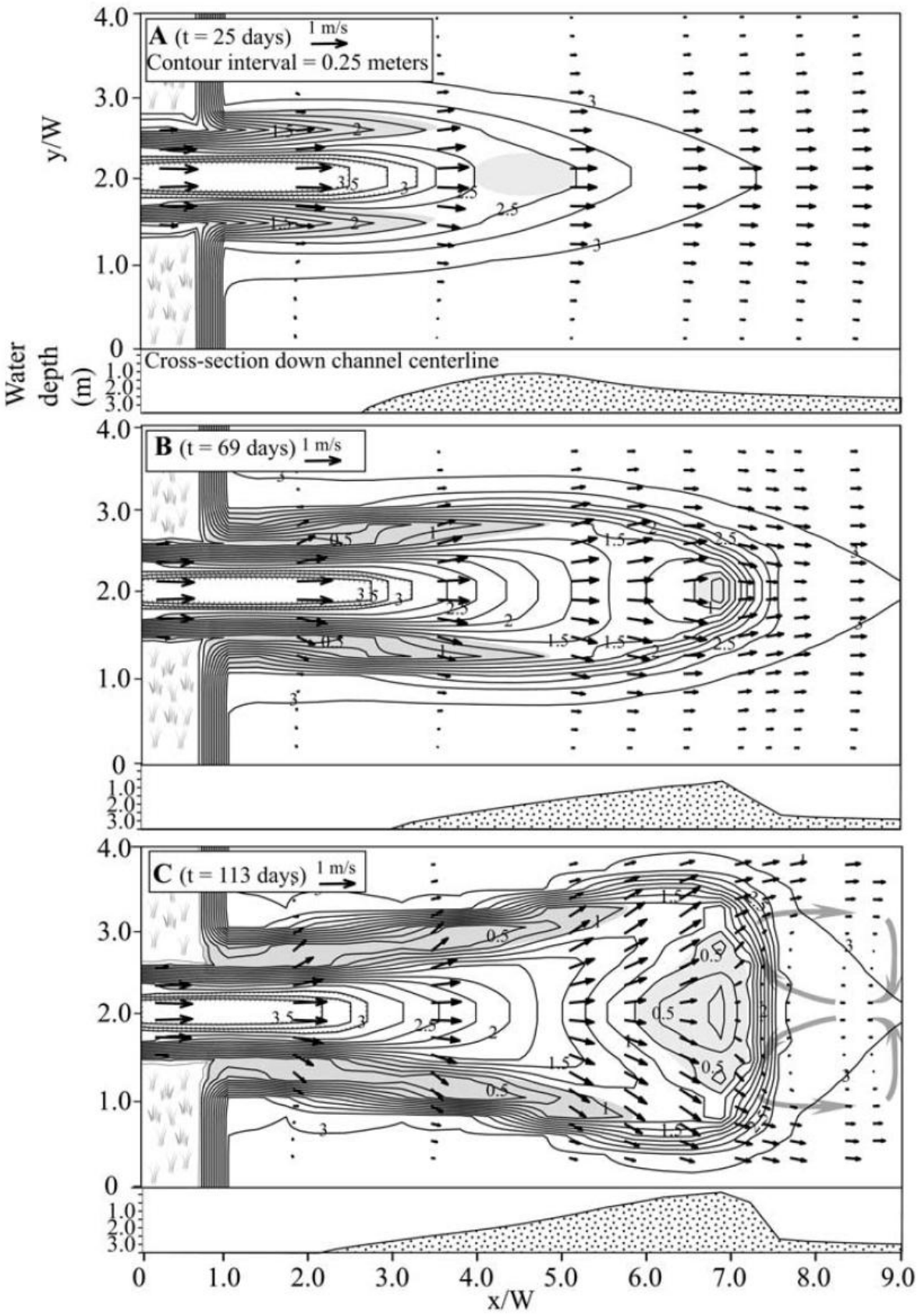

Figure 2-10: Modeled bathymetric and velocity field evolution during river mouth bar formation (Edmonds and Slingerland 2007)

The process begins with simultaneous extension of subaqueous levees from the initial shoreline to a distance of three times the initial channel width and a narrowing and scouring of the channel to the levee ends. Levees extend out from the channel walls and are built primarily from bedload, the individual grains of which are less likely to laterally spread due to less intense near-bed turbulent eddy advection. The small mouth bar initially forms at a distance of 4.5 channel widths from the mouth with a very gentle fore- and back-slope (see the channel centerline cross-section in figure 2-10A). As time progresses, the bar progrades to a distance of 7 times the channel width from the mouth and the levees extend to the initial location of the bar. The fore-slope of the bar is still very gentle with the initial scour hole failing to migrate with levee extension, though the basinward slope is now much steeper (see figure 2-10B). The bar has stopped prograding but has aggraded to such a degree as to cause flow spreading that increases the distance between the continually extending levee tips. The high pressure in front of the aggrading bar induces foreslope deposition and the upstream accretion that is commonly observed in the field. The now stationary bar continues to develop and gradually channelizes the two diverging flows (Edmonds and Slingerland 2007).

Examination of the sediment transport rate along the jet centerline indicates that maximum deposition (and the initial location of the mouth bar) occurs where the negative slope of the sediment flux curve is highest. This minimum in divergence of the sediment transport curve occurs at the point where the turbulent jet momentum flux begins to decrease, a distance that varied between 0 and 2 channel widths from the initial mouth in all the numerical experiments. Figure 2-11 shows the divergence in the transport curve and deposition along the centerline of the jet as functions of distance from the initial mouth (Edmonds and Slingerland 2007). When the mouth bar initially develops, the flow accelerates in the shallower depths over the foreslope and bar crest and decelerates in the deeper water over the basinward slope. This increases the sediment flux up to the bar crest which gradually erodes the fore slope and deposits sediment on the basinward side of the crest as sediment flux decreases, resulting in a basinward progradation of the mouth bar. The bar stops prograding when depth above the bar crest becomes low enough to force flow around the bar which in turn decelerates flow above the crest, inducing significant aggradation that soon fully establishes the flow bifurcation. Numerical tests indicate that most river mouth bars stagnate when the depth above the bar crest is less than 40% of the initial depth (Edmonds and Slingerland 2007). The distance to the point where the bar ceases to prograde is a function of turbulent jet momentum and sediment grain size, with initial channel depth having the greatest influence on the eventual basinward location of the river mouth bar. The number of simulations conducted in the Edmonds and Slingerland (2007) study facilitated conclusions on the sensitivity of numerical modeling of mouth bar formation to various parameters and modeling techniques. The authors found that simulation of mouth bar development is not sensitive to changes in the turbulence closure scheme, changes in the degree of effluent buoyancy, and changes in the Delft3D morphological acceleration factor up to values of 200 (Edmonds and Slingerland 2007).

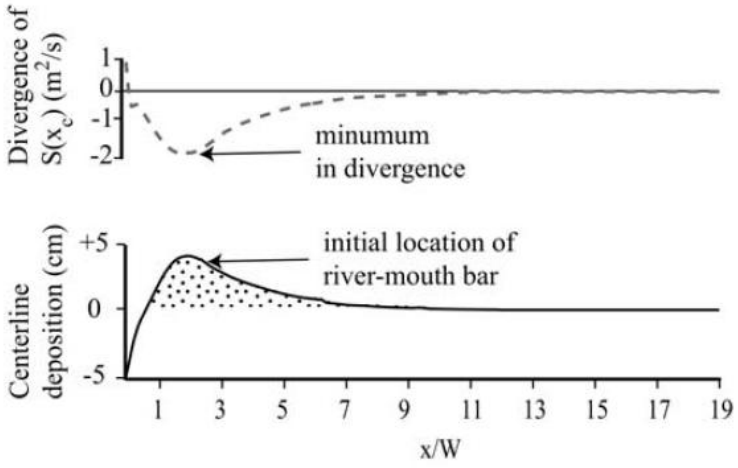

Figure 2-11: Plot of slope of sediment transport curve S(x) and deposition along centerline of jet against distance from initial channel mouth (Edmonds and Slingerland 2007).

2.3 Conceptual Delta Formation Models

Until recently, the study of deltas through development of classification systems and conceptual models of formation processes has relied on field observations of modern deltas and sedimentological investigations of stratigraphically-preserved ancient deltas, from which detailed process data, including time series of forcings and morphologic/stratigraphic response, has been scarce. The difficulty of obtaining time series measurements on the order of the typical time scales of delta formation dictates that any conclusions on genetic processes will require significant inferences, and the preserved sedimentary record in deltas which reflects sufficient time is not always complete as not all deposited sediments are preserved. Numerical models, provided they are accurate for the scales and processes of interest, can offer a means to examine the relationship between delta processes and the resulting morphology/stratigraphy, especially prevailing theories on dominant forcings and distributary channel network formation (Storms, Stive et al. 2007). Continued developments in process-based hydrodynamic and sediment transport modeling, especially progress in morphological upscaling methods, have expanded the applicability of these models to the larger spatial and temporal scales relevant to sedimentary geology, including simulation of delta development (Storms, Stive et al. 2007).

Work by Storms, et al. 2007 uses Delft3D to model the initial delta formation from a river dominant effluent discharging constant flow and sediment loads into shallow and deep receiving basins under homopycnal conditions. Both simulations used a flow of 1000 m^3/s discharging through an intentionally undersized channel with a 5 m erodible bed composed of 50% volume fraction fine sand and 50% cohesive clay (Storms, Stive et al. 2007). Figure 2-12 below gives the morphological development of each delta in a shallow basin (SIM A) and a deep basin (SIM B). In the shallow basin case, a sandy lunate bar quickly forms in front of the effluent mouth and grows basinward as the initial point of deposition develops into a mouth bar. Bifurcation occurs around the mouth bar, and subsequent mouth bar formation and bifurcation develop a system of channels divided by shoals that accrete both upstream and basinward. As discharge per channel is reduced with each bifurcation, the corresponding reduction in channel cross-sectional area leads to an adverse bottom

gradient as the channels moves basinward (Storms, Stive et al. 2007). Though a mouth bar induced bifurcation initially occurs in the deep receiving basin case, the largely unstable bifurcations lead to channel abandonment and delta growth through main channel basinward progradation and levee breaches (Storms, Stive et al. 2007). In simulation A, the initially prograding sandy lunate bar builds out over the clay prodelta deposits, forming a sharp but non-erosive contact between the two sediment fractions. As the delta continues to form, channel and shoal formation increases stratigraphic complexity, and initial deposits are reworked near the dominant channels. The constant discharge throughout the simulations implies that variable floods are not needed for delta development, though increases in water level with delta expansion were sufficient for sub-aerial development. Though the model was not meant to simulate any real location, the authors mention that the simulation A results resemble the morphology and stratigraphy of the Wax Lake Delta. More importantly, the results suggest that process-based hydrodynamic and transport models are capable of simulating important delta formation processes (Storms, Stive et al. 2007).

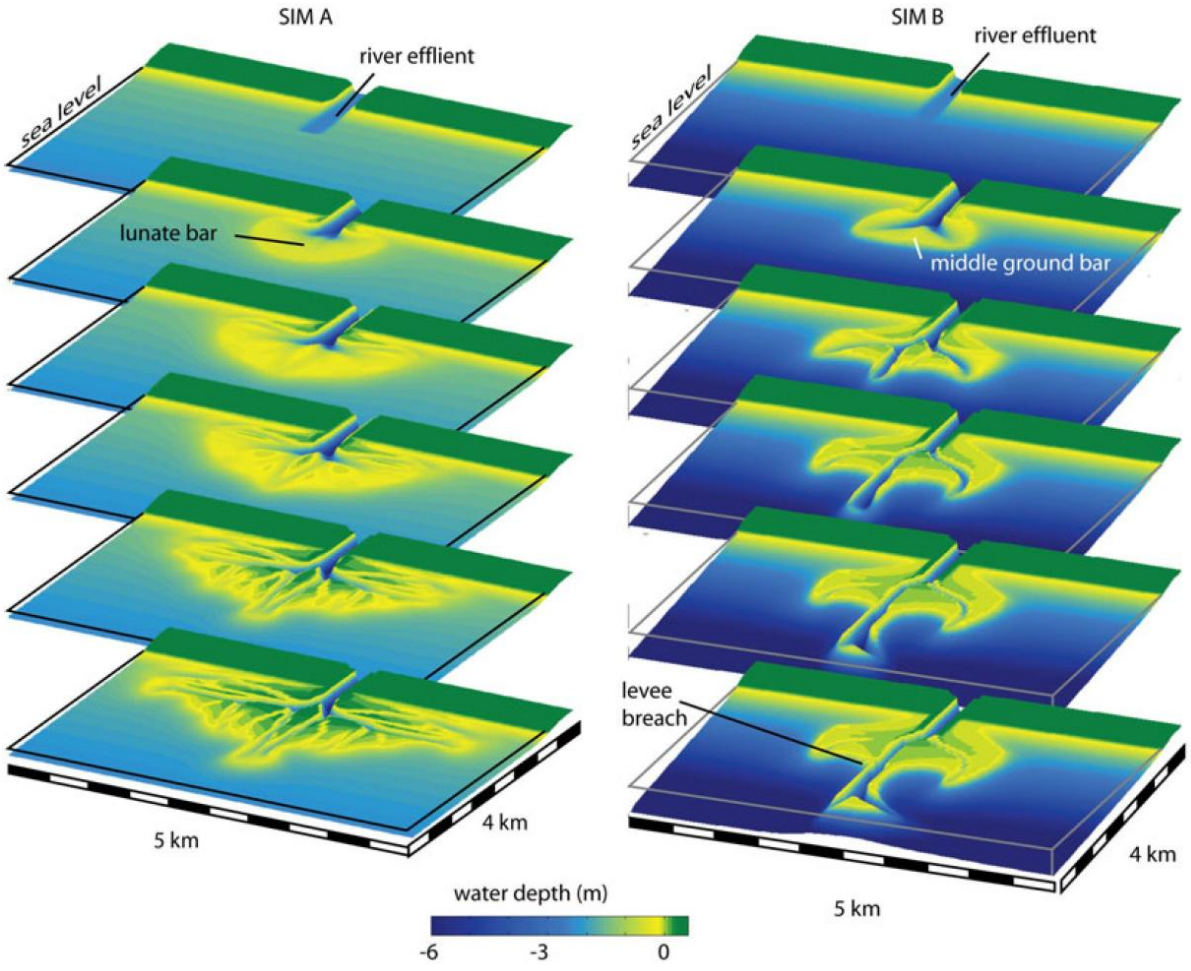

Figure 2-12: Simulated delta evolution for effluent discharging into shallow (SIM A) and deep (SIM B) receiving basins (Storms, Stive et al. 2007).

Further work by Geleynse, et al., 2010 applies Delft3D process-based modeling to simulate conceptual delta formation but locates the boundary much further upstream so that the dynamics of the feeder channel and it's interactions with downstream depositional processes can be explored

(Geleynse, Storms et al. 2010). The model begins with a straight, non-sloping channel that discharges a constant flow carrying sand and silt into a sloping-bed basin. Initial bed stratigraphy for the full domain consists of a 5 m thick, fully-mixed sand/silt layer. As the simulation progresses, the lower river channel planform is altered through the formation of bars and meanders that are influenced by the downstream delta depositional patterns initiated by mouth bar formation. As the delta progrades from the point of initial bifurcation, upstream accretion of the mouth bar into the lower river channel forms distinct feeder channels. Continued bifurcations form a recognizable delta network composed of passive floodplains separated by active channels that prograde basinward in such a way as to maintain an approximate delta radial symmetry (Geleynse, Storms et al. 2010). The importance of morphodynamic feedback resulting from downstream deposition has been established; however, Geleynse, 2010 finds that upstream river channel bar migration affects the feeder channel flow distribution to such a degree as to nearly isolate the northern delta lobe, indicating possible upstream controls on avulsion (Geleynse, Storms et al. 2010).

Since the ability of process-based models to simulate delta-development processes and the resulting morphology/stratigraphy has been established (Edmonds and Slingerland 2007; Storms, Stive et al. 2007), the most recent research in modeling conceptual delta evolution has focused on testing the influence of various sediment properties and forcings on the morphological development. Though the influence of sediment characteristics has been acknowledged in delta classification schemes (Orton and Reading 1993), the effect of sediment load and type on delta morphology has been considered less important, and the role of cohesion in particular is not well established (Edmonds and Slingerland 2010). Research by Edmonds and Slingerland, 2010 uses depth-averaged Delft3D process-based modeling of conceptual delta development to establish sediment bulk cohesion's control on overall distributary network and floodplain structure, shoreline smoothness, and bifurcation angle. Initial model geometry includes a linearly sloping basin of 1 to 3.5 m depths, similar to Atchafalaya Bay bathymetry, and a 250 m wide by 2.5 m deep rectangular channel that extends basinward from a subaerial shoreline for 1000 m (Edmonds and Slingerland 2010). The bed consists of a uniform 5 m thick layer of evenly mixed non-cohesive and cohesive sediment. Each simulation approximates river-dominant mouth processes by discharging a constant flow of 1000 m^3/s with equilibrium non-cohesive and cohesive sediment concentrations into a basin with constant offshore boundary water levels, no waves, and no salinity-induced density gradients. The bulk cohesion of the sediment is varied by systematically altering the critical shear stress for erosion of the cohesive sediment or the proportion of cohesive to non-cohesive sediment load (Edmonds and Slingerland 2010).

Findings confirm the processes of delta formation observed in field and model studies; the delta distributary network is generated by the growth of subaqueous levees and mouth bars, mouth bar stagnation and channel bifurcation, breaching of mouth bars and subaqueous levees to form multiple bifurcations, and channel avulsion. Overall, the results indicate that deltas formed from more cohesive sediment tend to be elongate with long channels, complex floodplains, and rough shorelines; whereas, deltas formed with less sediment cohesion tend to be fan-shaped with approximate radial symmetry and smooth shorelines (Edmonds and Slingerland 2010). Cohesion increases the shear stress needed to re-erode deposited sediments, so the depositional structures involved in channel bifurcation are more stable. Subaqueous levees, resistant to erosion due to high cohesion, concentrate the flow into a narrow channel that easily progrades basinward. When a mouth bar is able to form, it generally forms stable bifurcations and is not easily breached by new

channels. Similarly, avulsion frequency is low due to the difficulty in breaching high-cohesion levees. Low cohesion forms fewer bifurcations because mouth bars are continually re-eroded and deposited basinward so the stagnation that is required for bifurcation occurs less frequently. Levees are more easily eroded, allowing numerous breaches that distribute flow to the full delta and promote radially-uniform progradation (Edmonds and Slingerland 2010). Deltas with intermediate cohesion form the most bifurcation-dominant network structures because the balance of mouth bar stability and subaqueous levee breaching forms the most stable bifurcation angles. Figure 2-13 below presents the shorelines of a portion of the deltas simulated in the study.

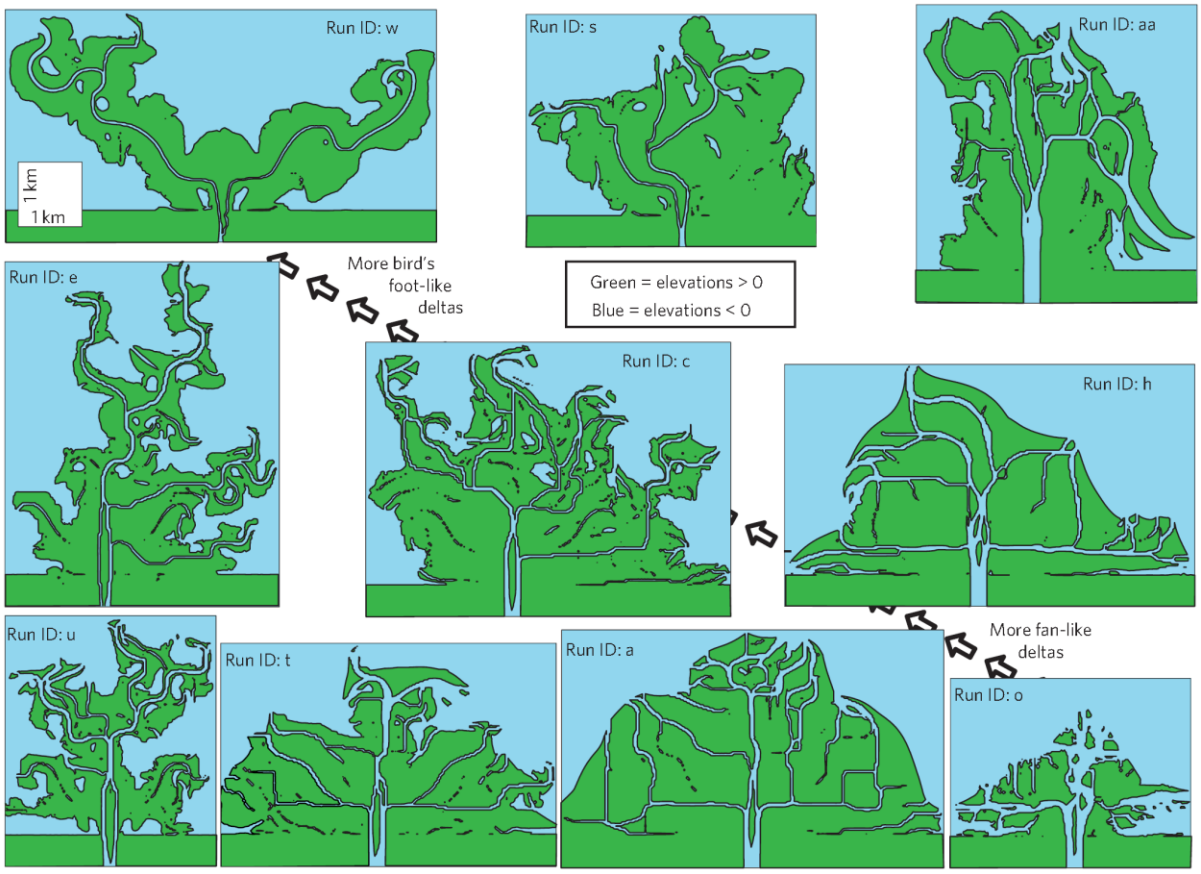

Figure 2-13: Simulated delta shorelines in the study of Edmonds and Slingerland, 2010. The horizontal axis represents decreasing critical erosion shear stress from left to right and the vertical axis represents increasing proportion of cohesive sediment load. Bulk sediment cohesion in the deltas increases from the lower right corner to the upper left corner (Edmonds and Slingerland 2010).

Continued work by Geleynse et al. 2011 has used process-based modeling of conceptual delta development to explore the hydraulic and sedimentary controls on river delta formation that have previously been postulated from observations of modern deltas (i.e. in the classification schemes of Galloway, 1975 and Orton and Reading, 1993). The Delft3D model investigations are based on depth-averaged hydrodynamic calculations coupled to bed level updating with stratigraphy bookkeeping. Initial model geometry consists of a wide, rectangular river channel discharging a constant 2000 m^3/s into a linearly sloping basin. For simulations where wave forcings are present, a low-energy wave climate with a significant wave height of 1.0 m and a peak period of 5.0 s is imposed at the basinward offshore boundary. For simulations where tidal forcings are present, a semi-diurnal tide of 1.5 m amplitude is imposed at the basinward offshore boundary with varying water level gradients imposed at the lateral boundaries (Neumann boundary conditions) (Geleynse,

Storms et al. 2011). The incoming sediment load is discretized using a non-cohesive sand and a cohesive fine fraction (silt). Though the upstream boundary cohesive fraction concentration is kept at a constant .04 kg/m^3, the incoming sand concentration is calculated so that the time derivative of the sand flux across the boundary section is zero. For each simulation, the initial bed is composed of 20 m of erodible sediment with a vertically and horizontally uniform sand-silt volume ratio. The influence of different initial bed sediment configurations was assessed using three cases with varying volume fractions: sand-dominant with 100% sand and 0% silt, mixed with 50% sand and 50% silt, and silt-dominant with 25% sand and 75% silt. Figure 2-14 below gives the simulated delta morphologies for the three initial bed configurations under only riverine forcing, under river and tidal forcings, and under river and short wave forcings (Geleynse, Storms et al. 2011). Several trends in bulk morphology parameters were identified and are noted in the figure; the symbols noting the lower-left to upper-right trend include (α) mean distributary depth, (β) sinuosity, (γ) shoreline roughness, (δ) subaerial delta volume, (ε) river valley width, and (ζ) longitudinal slope.

Examination of the deltas under combined riverine and wind-wave forcings indicates that smoother, radially symmetric delta fronts develop. Subaerial progadation rates are reduced as wind waves hinder the deposition of fines as a prodelta and at the developing delta front. The normally incident wave field deflects the sediment load at the distal ends of distributaries, resulting in enhanced shore-parallel channel orientation (Geleynse, Storms et al. 2011). For both the river-dominant and wave-dominant simulations, results indicate that distributaries are more incisive as the volumetric fraction of silt increases. In addition to the increase in mean distributary depth, the sinuosity and delta front roughness increase with increased silt fraction; subaerial delta volume and cross-delta water level gradients decrease (Geleynse, Storms et al. 2011). Tidal forcings were found to form the roughest shorelines and longest channels. Though initial mouth-bar deposits occurred at the distal ends of distributaries, the increased jet velocities during ebb flow continued the channel incision and subaqueous levee extension. Results from all simulations indicate that the initial bed configuration can have large effects on the resultant delta morphology, and that even relatively low-energy basin conditions can substantially transform delta morphologies, rendering an assumption of river-dominance with negligible tidal and wind-wave effects suspect for situations where basin energy is still present (Geleynse, Storms et al. 2011).

The effect of waves on depositional patterns can be clearly seen in figure 2-15 below. In the case of riverine forcing only (the leftmost delta stratigraphic sections), significant prodelta deposits that are fully composed of the fine sediment fraction (dark blue coloring indicates 0% sand fraction) develop at the basinward and flanking delta fronts. The thickness of these silt deposits are significant, and are nearly subaerial even without significant sand delivery. Alternatively, the rightmost delta stratigraphic sections represent delta development under combined riverine and wave forcings. Fine sediment prodelta deposits are completely absent, resulting in a more-steeply sloped delta front where sand-rich deposits prograde over the mixed fraction basement. In a more detailed modeling study of wave reworking of deltas, Hillen (2009) found that even for already formed conceptual deltas with well-developed silty delta fronts, a low-energy wave climate removes significant volumes of silt from the deltaic environment (Hillen 2009). Fine sediment deltaic deposits are eroded by waves and transported by wave-induced and fluvial currents large distances both laterally and offshore from the delta and are ultimately deposited in thin sheets on the deep, offshore basin slope or transported out of the model domain (Hillen 2009).

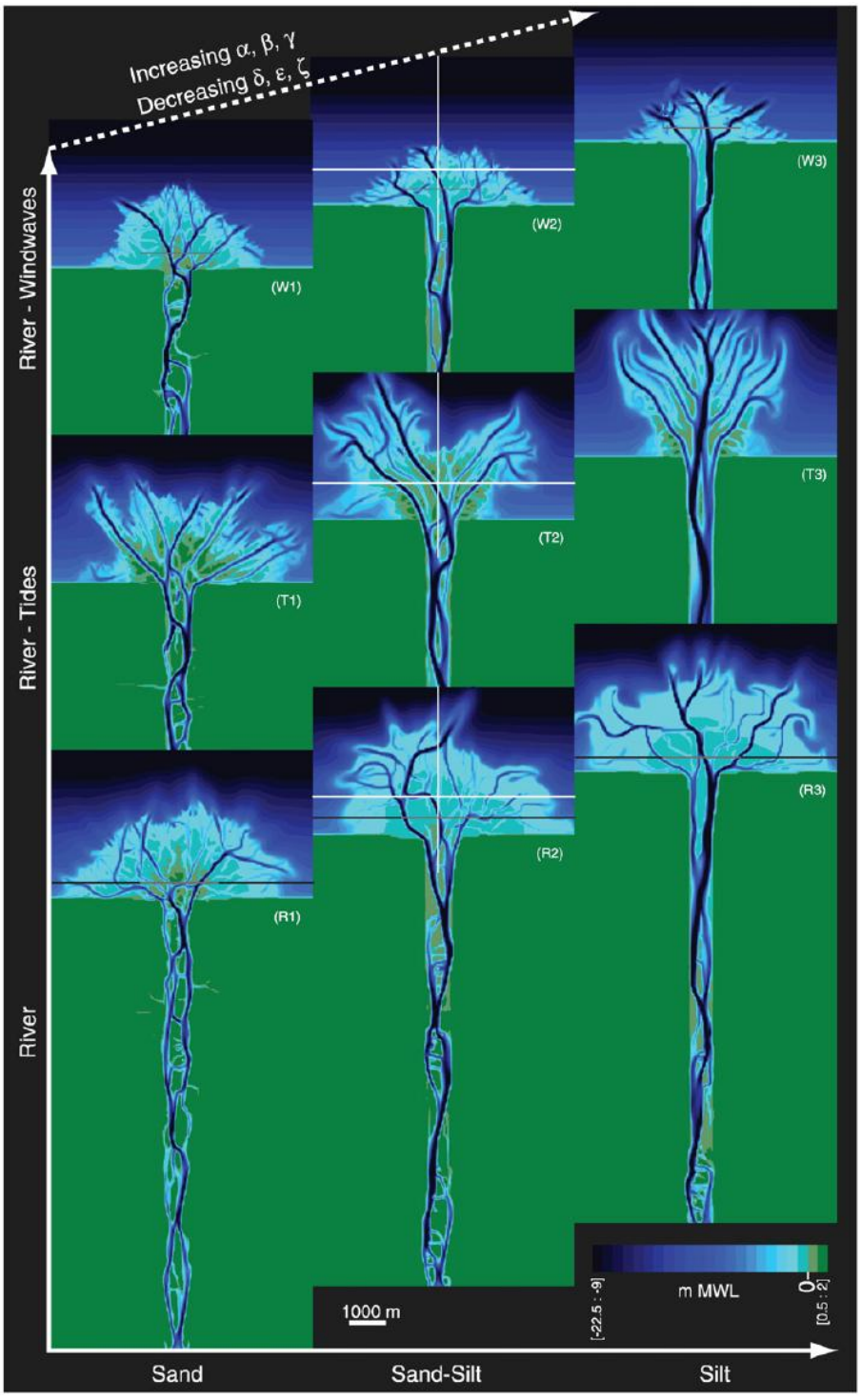

Figure 2-14: Simulated delta morphologies under riverine, river and tidal, and river and wave forcings for different initial bed sand-silt volume fractions. Sand-dominant corresponds to 100% sand and 0% silt, mixed sand-silt corresponds to 50% sand and 50% silt, and silt dominant corresponds to 25% sand and 75% silt. (Geleynse, Storms et al. 2011)

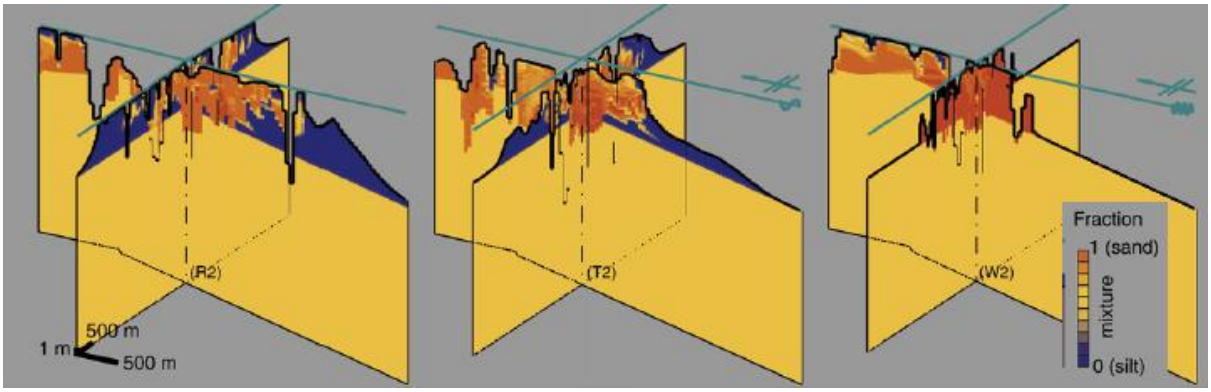

Figure 2-15: Simulated stratigraphy in strike and dip directions for mixed sand-silt initial bed condition simulations. Cross-sections marked R2 correspond to the river only simulation, T2 to riverine and tidal forcings, and W2 to riverine and wave forcings. Locations of cross-sections are indicated by the solid white lines overlaying the corresponding simulated delta planview morphology in figure 2-14 above (modified from Geleynse, Storms et al. 2011).

2.4 Atchafalaya and Wax Lake Deltas

The in-progress diversion of Mississippi River flow to the Atchafalaya river distributary, the latest in a series of delta switching events that successively built the Holocene Mississippi River deltaic plain, has created a new locus of deltaic deposition in Atchafalaya Bay, Louisiana (Roberts 1998). The Atchafalaya River basin, characterized by extensive swamps, wetlands, and lakes, has formed in the low-lying area between the higher natural levees of two former Mississippi delta systems (Roberts, Adams et al. 1980). If left unregulated, the gradient advantage created by the Atchafalaya's shorter path to the gulf (307 km shorter than the modern Mississippi path through the Plaquemines-Balize delta lobe) promotes the eventual abandonment of the modern Mississippi delta in favor of the Atchafalaya (Roberts, Adams et al. 1980). Despite the continued restriction of Atchafalaya River flow by the Old River Control Structure to 30% of the combined Mississippi/Red River inflows, sediment has been delivered to the bay in sufficient volumes to encourage the rapid development of two bay-head deltas. The abnormally high Mississippi River flows of the early 1970's initiated subaerial land-building in the Atchafalaya and Wax Lake Deltas which has continued to build a combined 153 km^2 of new land above the -0.6 m level (Roberts, Walker et al. 1997; Roberts 1998). The growth of subaerial land in each delta from the 1970's onward is given below in figure 2-16. The depositional environment of the microtidal (approximately .3 m tidal range) (DuMars 2002) Atchafalaya Bay consists of a semi-protected, shallow, and mildly-sloping basin that receives low-wave energy and experiences weak littoral drift; thus, the developing Wax Lake and Atchafalaya deltas can be classified as fluvially-dominant according to the system of Galloway (1975) discussed previously (van Heerden and Roberts 1988).

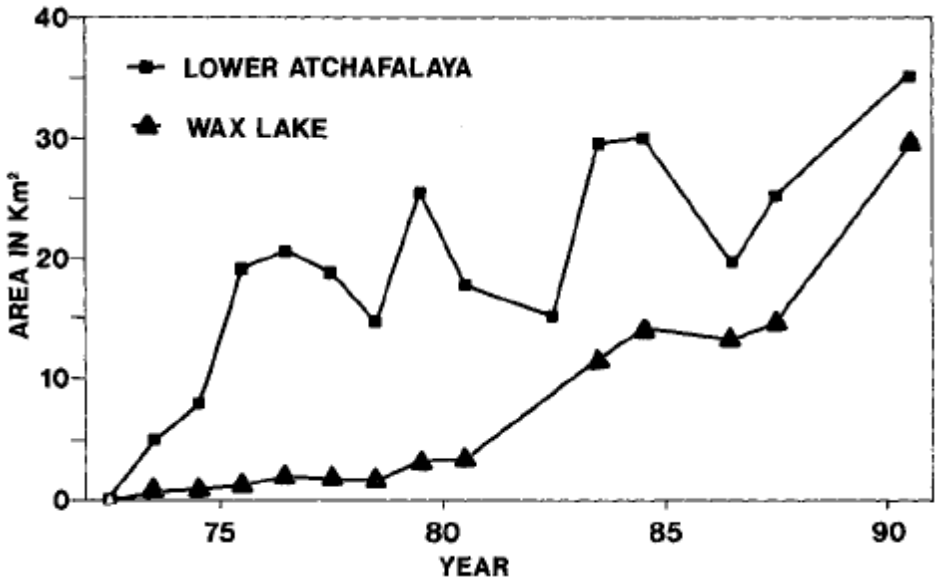

Figure 2-16: Area in km^2 of subaerial land in the Atchafalaya and Wax Lake deltas through time (Roberts, Walker et al. 1997)

2.4.1 Atchafalaya Delta

Though significant sediment from Mississippi inflow and channel scour due to gradually increasing flow has continually been transported through the Atchafalaya River distributary, the infilling of the basin through lacustrine deposition has prevented significant sediment delivery to the Atchafalaya bay until the mid-20th century. At this point, the shallow lakes and swamps of the basin had been filled to such a degree that sediment could finally be bypassed to the bay (Roberts, Adams et al. 1980; Roberts 1998). The substantial suspended load of the Atchafalaya is composed primarily of fine silt and clay-sized particles (DuMars 2002); beginning in the early 1950's, subaqueous delta growth began as these fine sediments were deposited in broad, seaward-thinning sheets (prodelta deposits) extending into Atchafalaya Bay from the river mouth (van Heerden and Roberts 1988). As the upstream portions of the Lower Atchafalaya River became increasingly efficient at transporting sediments through to the mouth, silt and fine sand began to be deposited as a distal bar, a depositional feature that forms a continuous, coarsening-upwards platform onto which the delta can prograde (Roberts, Adams et al. 1980). Mouth bar deposits of increasingly coarser material instigated the formation of subaqueous distributary channels that concentrated flow. The distributary mouth bar deposits are characterized by an overall coarsening-upwards trend; however, cyclic depositional patterns result in stacked sequences consisting of fine sand overlain with clayey layers. The major flood of 1973 induced substantial scour in the lower reaches of the Atchafalaya River, contributing to the uncommonly-large coarse sediment load reaching the developing delta. Coarse depositional lobes began to emerge at distributary mouth bar locations as subaerial and subaqueous levee deposits continued the seaward extension of distributary channels. Continued large flood flows through 1975 expanded subaerial delta lobes through levee deposits and extended the distributary network with further mouth bar formation and channel bifurcation (van Heerden and Roberts 1988).

After the high flow years accompanied with rapid subaerial expansion in the early 70's, the delta distributary network extension ceased, marking a change in dominant depositional processes. Growth of subaerial land area continued, however, through the processes of lobe fusion and upstream accretion. Small, secondary and tertiary channels formed during the high flow years began to narrow and were eventually closed off with major channel levee deposits. Additionally, coarse sediment, no longer transported to the delta front, was deposited at the upstream ends of delta lobes. Established depositional bodies thus continued to accrete and fuse with others as minor channels were abandoned, ultimately concentrating flow into a smaller number of more prominent channels (van Heerden and Roberts 1988). The two dominant delta growth phase processes and the resulting sedimentary facies are demonstrated conceptually in figure 2-17 below. The continued dredging of the main Atchafalaya Delta distributary channel for navigation has resulted in an artificially-elongated delta shape that bypasses sediment into the bay, decreasing the potential delta growth. Dredged sediment disposal in the Western half of the delta has resulted in artificial aggradation, though the Eastern half of the delta has developed naturally (DuMars 2002).

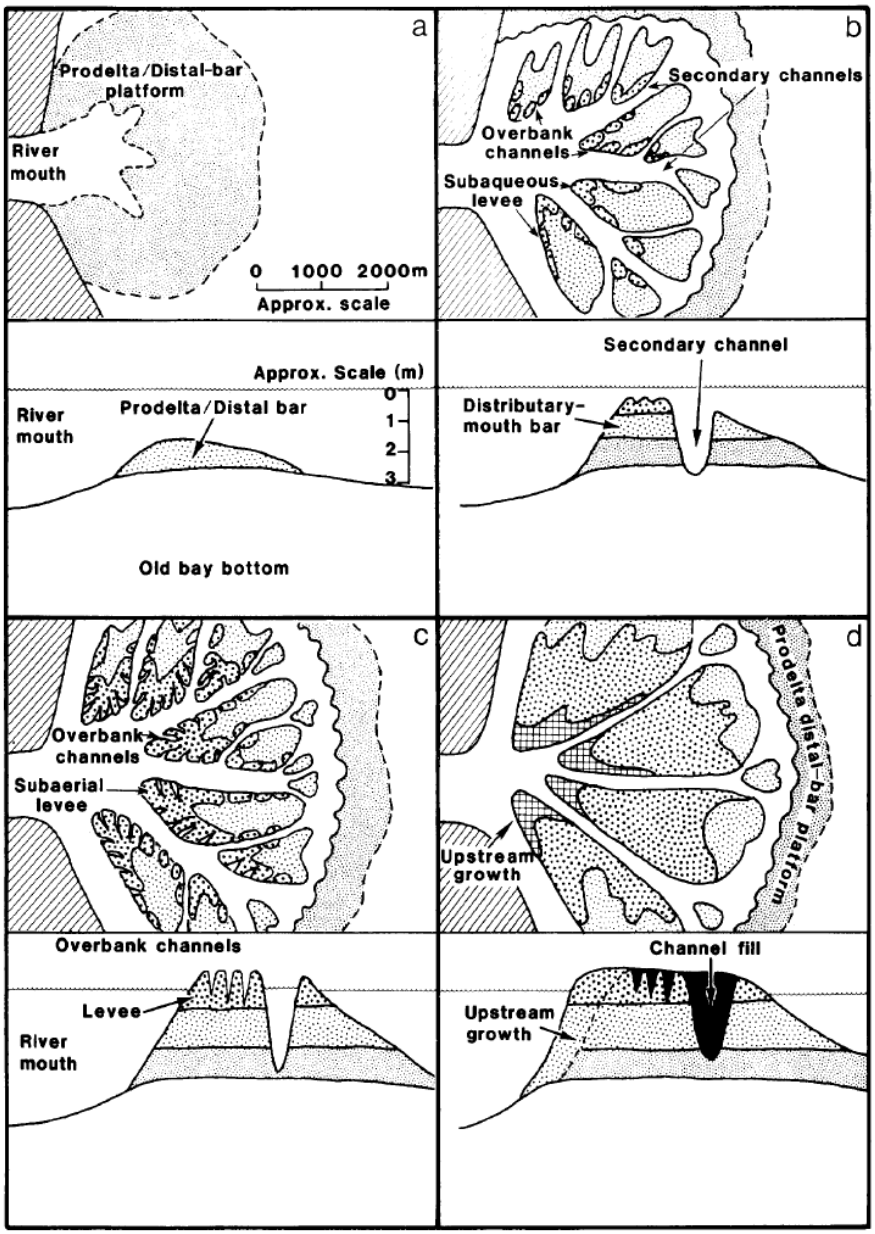

Figure 2-17: Conceptual description of delta growth processes and sedimentary facies development in the Atchafalaya Delta (van Heerden and Roberts 1988)

2.4.2 Wax Lake Delta

After the 1941 construction of the Wax Lake Outlet as a more efficient flow outlet from the Atchafalaya Basin, subaqueous deltaic deposition at the outlet mouth proceeded in a similar manner to that of the adjacent Atchafalaya Delta (Roberts, Walker et al. 1997; DuMars 2002). Subaerial land development in the Wax Lake Delta also commenced during the extremely high flows of 1973, when approximately 31% of the of the substantial suspended sediment load reaching the Atchafalaya Bay was discharged through the Wax Lake Outlet channel (Roberts, Coleman et al. 2003). During the later part of the decade, however, subaerial growth of the Wax Lake Delta was overshadowed by substantially higher growth rates in the Atchafalaya Delta. At this point, the Lower Atchafalaya had become more efficient at delivering the coarse sediments necessary for delta growth to the river mouth, while basins upstream and along the Wax Lake Outlet (Six-Mile Lake and Wax Lake,

respectively) were still trapping large amounts of course sediment delivered to the diversion. By 1980, interior basin infill had progressed to such a degree that subaerial land growth rates increased to similar values observed in the early formation of the Atchafalaya Delta, initiating a prolonged period of rapid subaerial development (Roberts, Walker et al. 1997). In a similar situation to the much-larger scale progressive flow capture occurring upstream at the Atchafalaya distributary diffluence, the gradient-advantaged Wax Lake Outlet began to widen and discharge much more than the design value of 20% of the upstream Atchafalaya discharge. To prevent eventual flow capture, a rock weir was constructed across the upstream channel inlet in Six Mile Lake in 1988 that substantially inhibited sand transport through the outlet; however, weir-induced elevated flood stages near Morgan City, LA resulted in its eventual removal in 1994 (DuMars 2002). The subaerial development in the Atchafalaya Delta was separated into the earlier period of mouth-bar deposition and channel extension dominance and the later period characterized by upstream accretion and lobe fusion; though these processes have also been observed in the Wax Lake Delta, all have continued to occur concurrently with no periods associated with the dominance of a particular process (Roberts 1998).

Wax Lake Delta sedimentary facies mimic those documented in the development of the Atchafalaya Delta, described in the previous section. Though sedimentary investigations of the Wax Lake Delta do not specifically correlate observed facies to the depositional features presented in figure 2-17 above, the overall coarsening-upward sequence reflects depositional order as the Lower Atchafalaya System became increasingly efficient at transporting coarser sediment to the Wax Lake Outlet mouth (Roberts, Walker et al. 1997). Very thin, clay-rich prodelta facies underlie most of the delta. These prodelta deposits transition upwards into a much thicker layer of interlaminated fine sands, silts, and clays, representative of the distal bar deposits that underlie the sand dominant features responsible for subaerial expression. The uppermost sand-rich facies, deposited as distributary mouth bars, subaqueous levees, and upstream depositional lobe expansions, dominate the deltaic sequence, occupying an average of 67% of the depositional facies (Roberts, Walker et al. 1997). In the stratigraphic section given below in figure 2-18, it can be seen that the proximal portions of delta distributary channels incise through the full stratigraphic sequence into the pre-delta, bay bottom sediments. Though distal sections of distributary channels generally do not incise through the full deltaic sequence, channel beds still scour into previously-deposited stratigraphic sequences with basinward extension (DuMars 2002).

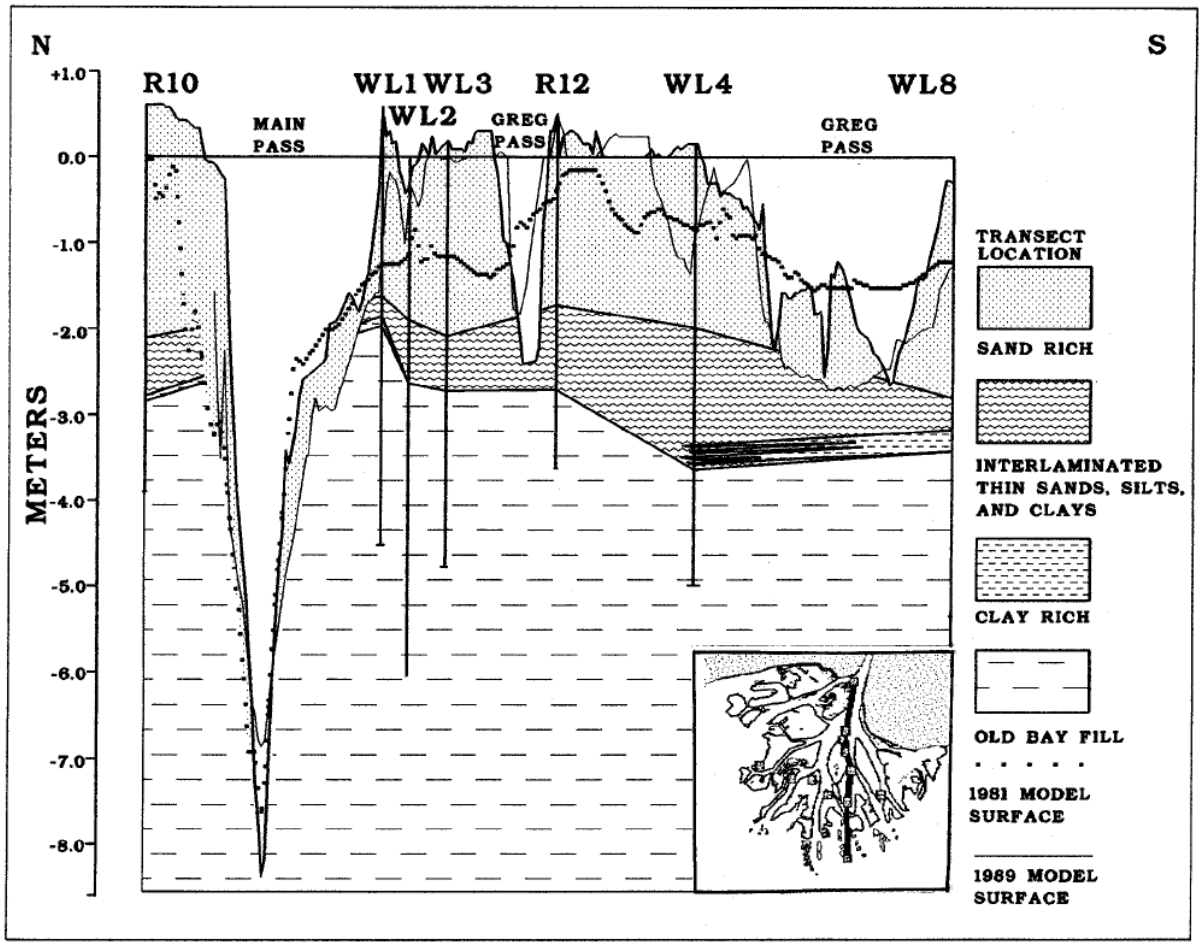

Figure 2-18: Dip-oriented stratigraphic section of the Wax Lake Delta from 1994 with interpreted dominant sedimentary facies and previous bed levels to demonstrate morphological development (Roberts, Walker et al. 1997).

Recent research on the Wax Lake Delta proposes a new conceptual formation model that better reflects the more complex stratigraphic sequences evident in higher resolution sampling, challenging the prevailing theory correlating sedimentary facies with delta development as demonstrated conceptually in figure 2-17 above. Instead of stratigraphic sequences that reflect the gradual coarsening of the sediment load delivered to the river mouth, the model of Wellner, et al. 2005, proposes a morphology and resulting stratigraphy that arise from the stacking and lateral merging of individual turbulent jet deposits (Wellner, Beaubouef et al. 2005). Each individual jet deposit consists of a region of erosion at the current jet mouth location followed by an aggrading bar whose sedimentary structure from the proximal to distal ends represents the gradual transition from deposition of bedload to deposition of suspended load. The central portion of the upstream tip of the deposit is composed of the coarsest sediment, with grain sizes gradually fining both towards the distal end and away from the flow-oriented central axis (Wellner, Beaubouef et al. 2005). In the Wax Lake Delta, partial or complete jet deposit sequences are stacked and merged to form a jet deposit complex. This larger body still has predictable coarsening upwards and distal-fining grain size trends, though the stratigraphy is somewhat cyclical and much more complex than in the single jet deposit. Once the jet deposit complex sufficiently accretes to induce flow stagnation at the proximal end, flow splits around the bar head and forms new channels in the lower areas along the flanks of the deposit, initiating the formation of new deposition complexes that expand the delta basinward (Wellner, Beaubouef et al. 2005). Figure 2-19 below demonstrates conceptually the structure of a

single jet deposit, the stacking of jet deposits to form a complex, and how a succession of complexes can form the Wax Lake Delta.

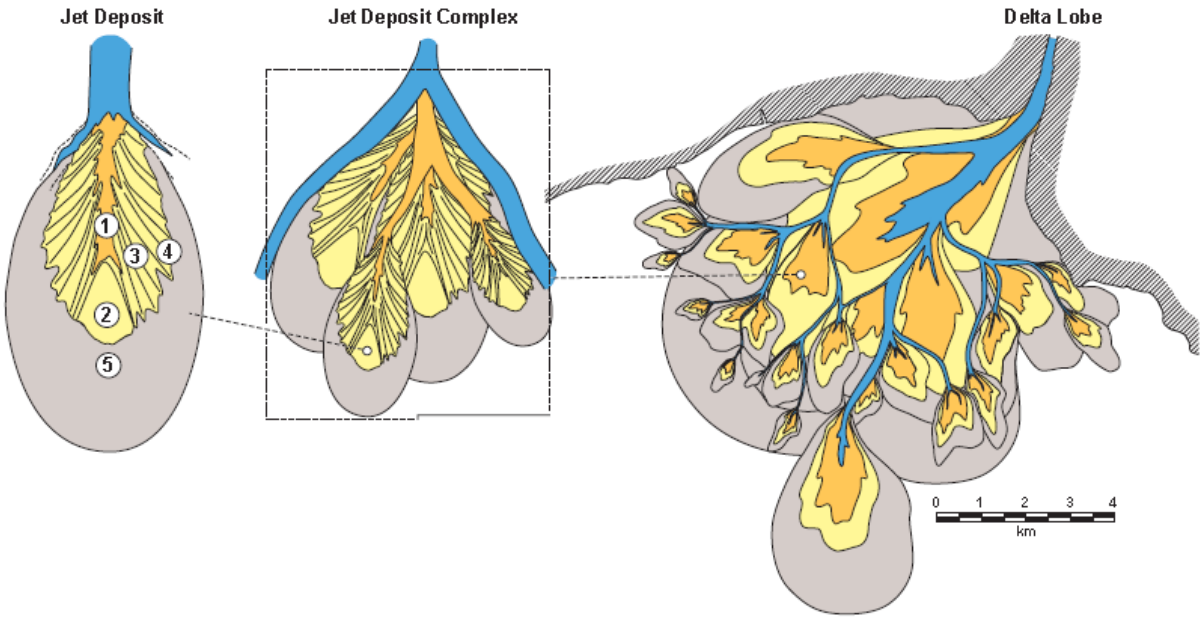

Figure 2-19: Schematic of individual deposits and jet deposit complexes in the conceptual delta formation model presented in Wellner, 2005. In the jet deposit, the orange color represents the central portion of coarse sediment bedload deposition, the lighter tan color represents the transition from coarse sediment bedload to suspended load deposition, and the gray area represents the deposition of fine sediment from suspension. (modified from Wellner, Beaubouef et al. 2005)

In an analysis of successive aerial photographs throughout the course of delta formation, Wellner, 2005 was able to identify the progression of jet deposit complex development in the Wax Lake Delta through time (Wellner, Beaubouef et al. 2005). Figures 2-20 and 2-21 below show the subaerial extend of the delta in 2000 and 2002, respectively, highlighting the different jet deposit complexes and changes in subaerial land area between photograph periods. Actual dates for the first two aerial photograph were not given, so it was assumed that a five year period is represented from the beginning of 1998 to the December, 2002 photo. Between 1998 and 2000, subaerial growth occurs through the basinward expansion of already established deposit complexes and the establishment of new jet deposit locations after mouth bar formation at distal ends of major distributary channels. The most active deposition occurred at the new jet deposit complexes at the mouths of Gladwell and Greg Pass, with minor growth accompanying the establishment of a mouth bar at Main Pass. The lobe-fusion process observed in the Atchafalaya Delta (van Heerden and Roberts 1988) occurs with the infill of minor channels, further expanding established delta lobe subaerial land . The period from 2000 to 2002 is characterized by limited subaerial land area expansion. The mature depositional bodies generally do not expand; however, there is some basinward growth of the incipient jet deposits formed between 1998 and 2000. The mouth bar at the distal end of Main Pass develops into a deposit complex, representing the most active deposition during this period. Overall, the period between the aerial photograph dates is characterized by the establishment and expansion of new jet deposit complexes and large increases in subaerial exposure through aggradation of established depositional bodies.

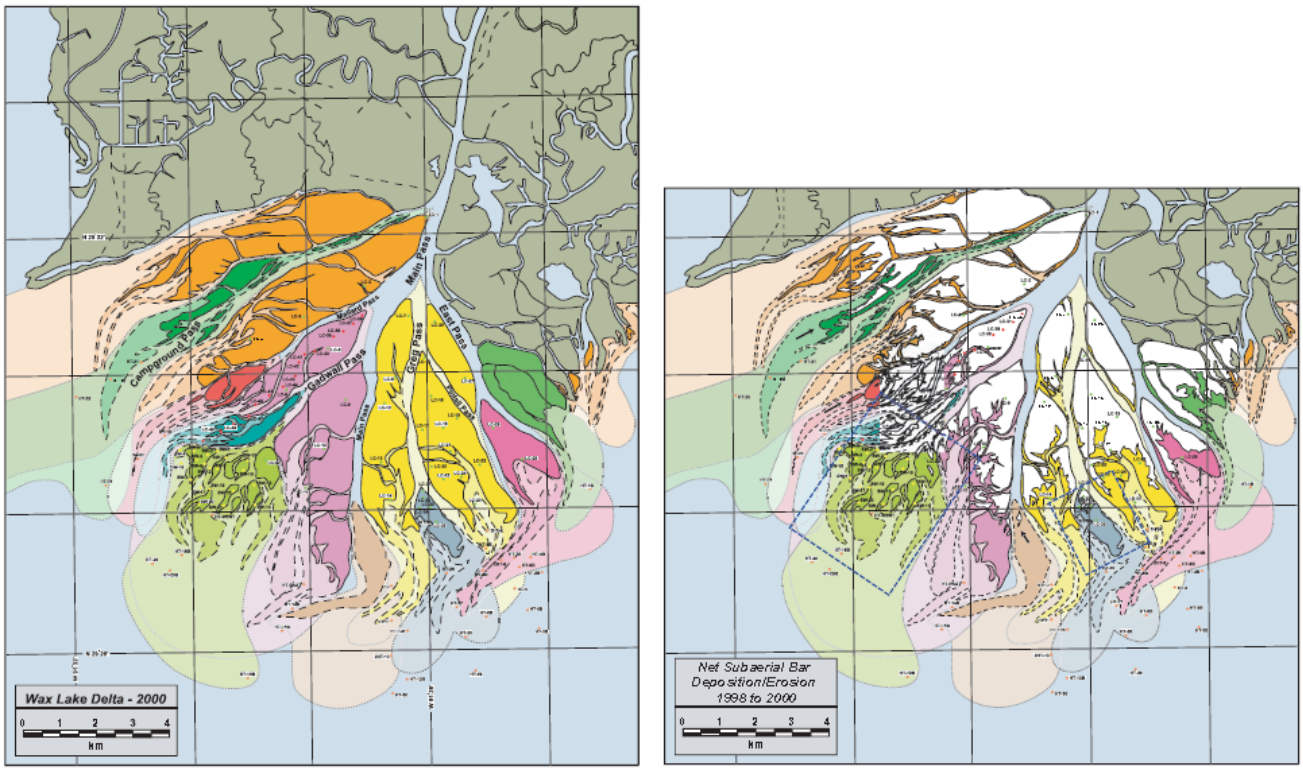

Figure 2-20: Subaerial portions of the Wax Lake Delta in 2000. The different colors in the left figure indicate different jet deposit complexes. The colored areas in the right figure represent the change in subaerial exposure from the white areas representing the 1998 subaerial extents. Dashed boxes indicate the most active areas of deposition (Wellner, Beaubouef et al. 2005).

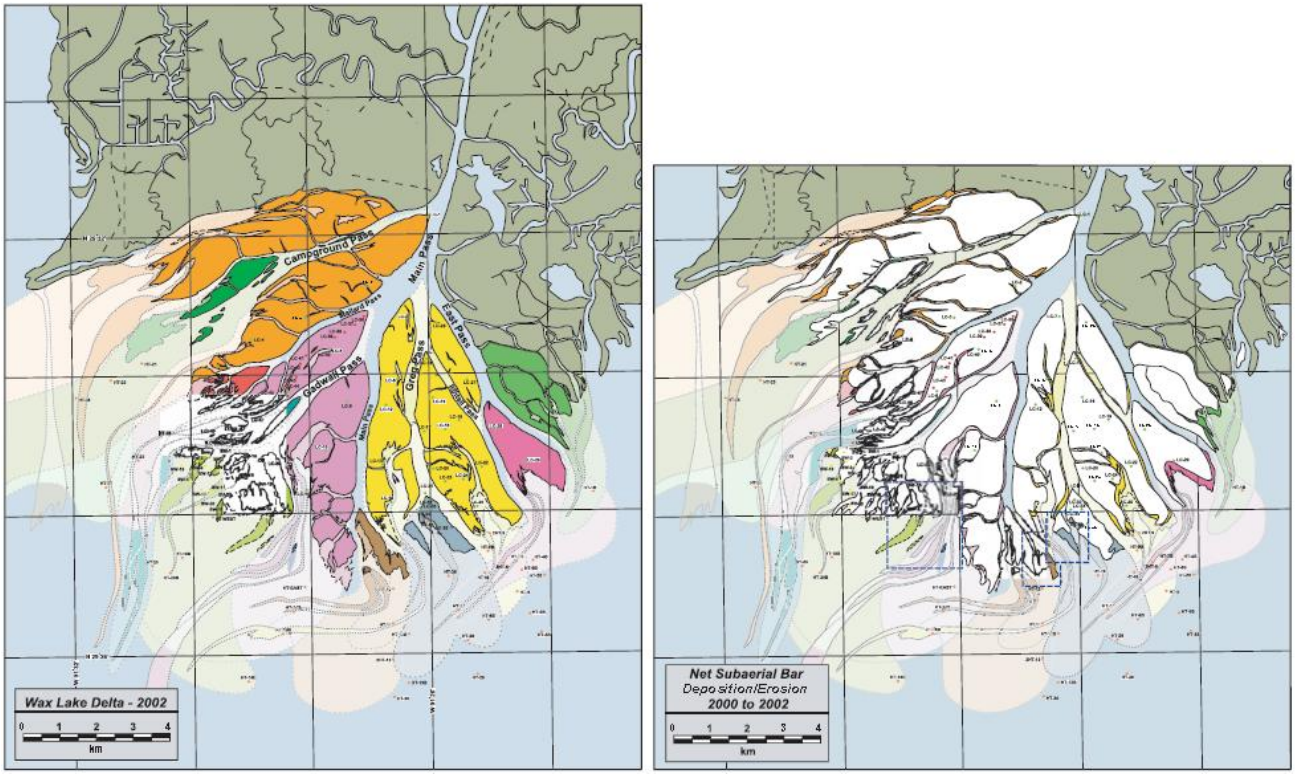

Figure 2-21: Subaerial portions of the Wax Lake Delta in 2002 (left figure), along with changes in subaerial exposure between 2000 and 2002(right figure) (Wellner, Beaubouef et al. 2005).

2.4.3 Effect of Cold Fronts on Delta Development

Remote sensing of suspended sediment concentrations in Atchafalaya Bay as well as observed shoreline changes on the downdrift Southwestern Louisiana coast indicate that significant fine suspended sediment is transported beyond the confines of the Atchafalaya and Wax Lake Delta receiving basin (Roberts, Walker et al. 1997). Historically, extensive oyster reefs at the Atchafalaya Bay-gulf boundary limited saltwater intrusion into the bay, inhibiting the flocculation of the extensive cohesive sediment load beginning to bypass the river mouth. Though some fine sediment was certainly deposited in the bay as Atchafalaya and Wax Lake Delta prodelta facies, bypassed suspended sediment was sufficient to induce accretion of the previously erosive downdrift shoreline through nearshore fluid mud deposition (Roberts 1998). Despite the typically low-energy wave climate, wind waves are at times capable of resuspending basinward fine sediment prodelta deposits, increasing the extents and concentration of the suspended sediment plume (Roberts, Walker et al. 1997).

The prevailing current along the Louisiana coast west of the Mississippi Delta advects the fine sediment plume bypassing the bay westward to be deposited as accreting mudflats. The more significant cause for the export of fine sediment from Atchafalaya Bay, however, is the passage of winter cold fronts over the Gulf coast (Roberts, Walker et al. 2005). Cold fronts are the boundary zones between cold, dry air moving southward over the continental U.S. and warm, moist air moving landward from the Gulf of Mexico. Though producing much milder storm conditions than the tropical systems that can affect the area during the late summer and early fall, cold fronts have a much more significant impact on sediment dynamics along the coast because of their frequency. During the winter months, cold fronts typically approach the coast from the northwest every four to seven days, resulting in twenty to thirty cold front passages per year (Roberts 1998; Roberts, Walker et al. 2005). During the prefrontal period when a cold front is approaching the coast front the north, strong winds typical blow landward from the south or southeast, elevating water levels at the coast with up to 0.6 m of wind-induced set-up. The enhanced wind wave action resuspends fine sediments deposited on the bay floor. As the cold front passes over the coast, the wind direction abruptly shifts to the north, causing rapid water level reductions at the coast and flushing the high-concentration suspended sediment plumes seaward (Roberts 1998). Figure 2-22 below shows the seaward flux of sea surface suspended sediment from Atchafalaya Bay directly after the passage of a cold front. The yearly transport of fine sediments from Atchafalaya Bay due to the passage of cold fronts is estimated to be as large as 15% of the total amount of sediment transported to Atchafalaya Bay through the Lower Atchafalaya River and Wax Lake Outlet (Roberts, Walker et al. 1997). This frequent and extensive bypass of fine sediment from the Atchafalaya Bay has effectively removed prodelta mud deposition from its typical location at the delta front, resulting in primarily coarse-grained deltas that preserve only a small fraction of the large fine-dominant suspended load reaching the deltas (Roberts, Walker et al. 2005)

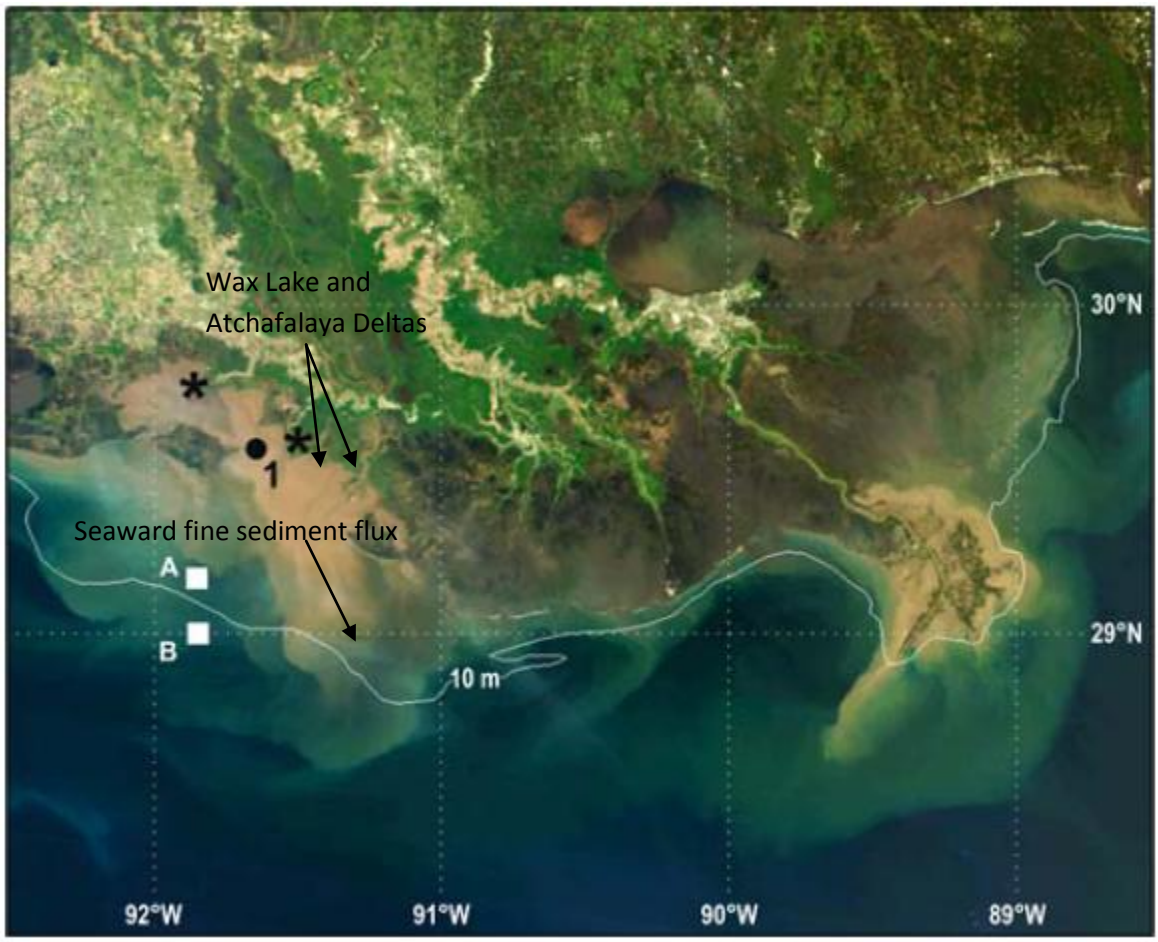

Figure 2-22: Satellite image of the Louisiana coast and surface suspended sediments after cold front passage (modified from Roberts, Walker et al. 2005)

3. Model Set-Up

The following chapter details the construction of the long-term morphological model of the Wax Lake Delta. First, important aspects of the Delft3D modeling suite most relevant to the current study are discussed. The necessary assumptions required in model development, especially the assumptions involved in limiting simulated processes, are presented. The development of various model aspects is detailed, including the computational grid, boundaries sections, initial domain bathymetry, and representative sediment fractions. Finally, the boundary condition schematization from available prototype measurements for the long-term simulation is described.

3.1 Delft3D

In accordance with the research objective to simulate the morphological development of the Wax Lake Delta for a five year period, the coupled hydrodynamic and morphologic modeling software Delft3D was used to construct a model of the study area. Delft3D is a modeling suite developed by Deltares that has the capability to simulate hydrodynamics, sediment transport, and resulting changes to bed levels and bed sediment composition. The Delft3D-FLOW module integrates the computation of hydrodynamics, sediment transport, and morphology in a simultaneous, "online" approach where changes to bathymetry in one time step are immediately available to calculate hydrodynamics in the next time step (Lesser, Roelvink et al. 2004). The online approach is essential for the simulation of delta development, where the complex interactions between a growing mouth bar and the evolving delta distributary channel mouth flow pattern are important (Edmonds and Slingerland 2007). A schematic of this modeling approach is given below in figure 3-1.

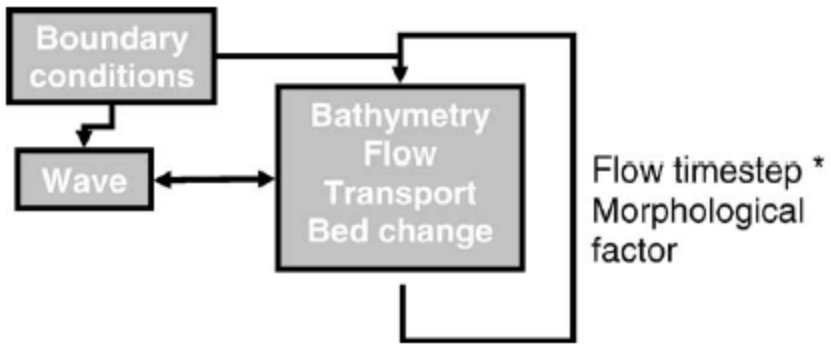

Figure 3-1: Schematic of "online" modeling approach for flow, sediment transport, and morphology used in Delft3D. The WAVE module available in Delft3D and shown in the figure was not used in this research (Roelvink 2006)

Hydrodynamics in Delft3D are simulated by solving the unsteady shallow water equations on a finite-difference rectilinear, curvilinear, or spherical grid (Lesser, Roelvink et al. 2004). Though the program is capable of simulating flows in three dimensions, the depth-averaged mode is implemented for the current study, an assumption justified by the success of conceptual delta development models using depth-averaged flow conditions (see section 2.3). The sediment transport portion of the FLOW module can compute both bed load and suspended load transport for non-cohesive sediment fractions and suspended load transport for cohesive sediment fractions. Suspended transport for both sediment types follows from the advection-diffusion equation. The erosion and deposition from suspension of cohesive sediment is calculated according to the Partheniades-Krone formulations that determine flux to and from the bed based on ratios of bed shear stress to user-defined critical

shear stress values for erosion and deposition. Transport of non-cohesive sediment is calculated using the formulations of Van Rijn, 1993, the default sediment transport formula in Delft3D (Deltares 2009).

The Van Rijn formulation for non-cohesive sediment transport was chosen because of its inclusion of both transport modes, bed load and suspended (van Rijn 1984, Part I; van Rijn 1984, Part II). The use of this formula allowed for calculation of depth-averaged sand concentration at particular model locations for comparison to prototype measured values. The detailed formulation is dependent on many physical parameters; however, high sensitivity to several parameters with high uncertainty could result in inaccuracies (Camenen and Larroudé 2003).

The capability of computing transport for multiple sediment fractions requires a system for keeping track of bed sediment fraction composition changes from preferential deposition or erosion of particular fractions. Delft3D gives the option of implementing one of two bed composition models. The first assumes that the bed is composed of a single layer of uniformly mixed sediments where the proportion of each fraction present at each computational point can change based on fluxes of each fraction to our away from the bed. The second model implements multiple sediment layers so that the order in which certain fractions are deposited or eroded will be preserved as stratigraphy. A user-defined number of composition bookkeeping underlayers each of the same user-defined thickness underlie a transport layer at the bed surface from which sediment can be eroded or deposited. A base layer is also present under the bookkeeping layers to merge properties of sediment layers that do not fit within the depth extent of the bookkeeping layer system (Deltares 2009). The stratigraphy model available for use in Delft3D is conceptually demonstrated in figure 3-2 below.

For more detailed information on the theoretical background, numerical implementation, and practical use of Delft3D, please refer to the program user manuals and Lesser, et al., 2004 (Lesser, Roelvink et al. 2004; Deltares 2009).

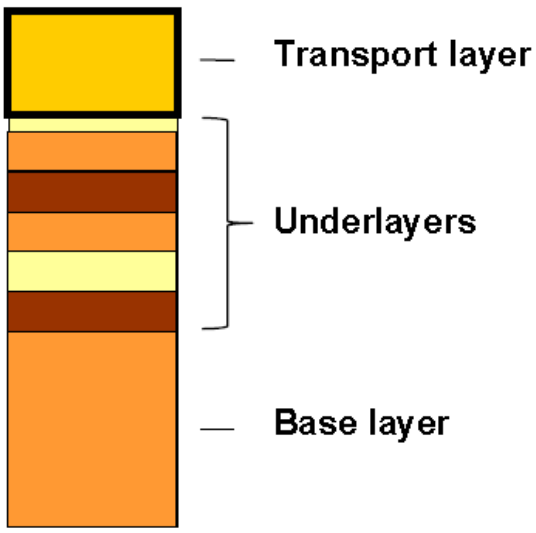

Figure 3-2: Stratigraphy bed composition model in Delft3D, utilizing bookkeeping underlayers, a transport layer, and a base layer. The varying colors represent different sediment fraction compositions (Hillen 2009).

3.2 Assumptions and Limitations

3.2.1 Full River Dominance

The advancing capability to simulate morphological developments on longer time scales and larger spatial scales with acceptable resolution still requires substantial computational power. If certain processes are found to be negligible for the long term model results, substantial gains in simulation efficiency can be obtained when these processes are excluded from the computations. For this simulation in particular, the delta development is assumed to be fully river dominant, so tidal oscillations, wave action, and wind-driven currents and water level fluctuations are not included. The Atchafalaya Bay is a microtidal environment with an average tidal range of only 30 cm. Though this range is sufficient to induce oscillations in velocities through the delta distributary channels during periods of low flow, the oscillatory velocity component becomes negligible during the higher flows that have the greater influence on delta morphology (DuMars 2002). The wave climate in Atchafalaya Bay is typically very mild, with significant wave heights rarely exceeding 0.5 m. Figure 3-3 below gives the average cumulative frequency distribution of significant wave heights measured within Atchafalaya Bay for the period from November 1981 through December 1982. Wave and tidal forcings are both clearly diminutive relative to the significant river discharge through the delta, creating a river dominant deltaic environment (Wright 1977). Field measurements of velocity, suspended sediment concentration, salinity, and water temperature in Wax Lake Delta distributary channels during non-flood and flood conditions in 2000 and 2001, respectively indicate that the system is well-mixed. The lack of density gradients or any other complex vertical flow patterns justifies the use of a 2-D, depth-averaged modeling framework that does not include the effects of varying salinity.

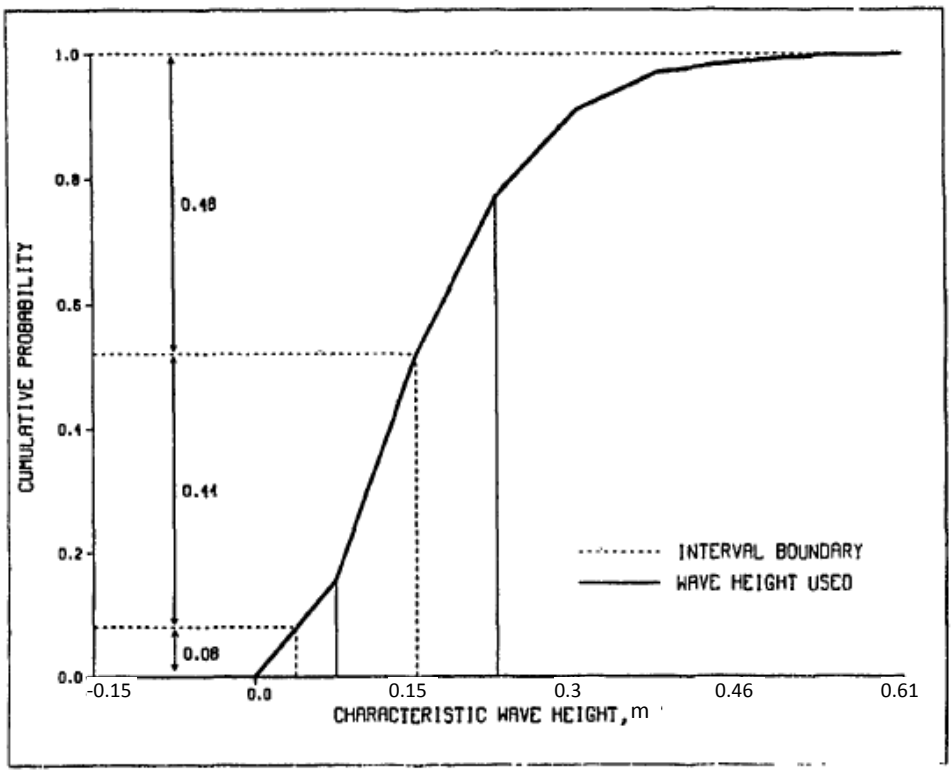

Figure 3-3: Average cumulative frequency distribution of significant wave heights in Atchafalaya Bay from November, 1981 through February, 1982 (modified from Donnell, Letter et al. 1991).

3.2.2 Negligible Influence of GIWW

The Gulf Intracoastal Waterway (GIWW) shipping canal is an extremely important waterborne commerce route that traverses the Louisiana Gulf Coast roughly along the boundary between low-lying coastal wetlands and higher elevation uplands parallel to the Gulf coast (Swarzenski, United States. Army. Corps of Engineers. New. Orleans District et al. 2003). Maintained with a minimum width of 61 m and depth of 6 m, the GIWW intersects both the Wax Lake Outlet and the Lower Atchafalaya River in the study area (see figure 1-4 in section 1.1) and comprises a portion of the upstream model domain (see figure 3-4 in section 3.3 below). In general, the GIWW acts as an additional flow and sediment conduit from the Atchafalaya Basin to the Gulf of Mexico. Though discharge through the GIWW is highly variable and depends on stage levels in the Gulf, Lower Atchafalaya River, and Wax Lake Outlet as well as local precipitation and runoff, flow during floods is generally directed from East to West, capturing small amounts of discharge and sediment from the Lower Atchafalaya and Wax Lake Outlet (Swarzenski, United States. Army. Corps of Engineers. New. Orleans District et al. 2003).

During a three year measurement campaign from 1996 through 1999, a period that includes the significant flood of 1997, average discharges through the GIWW on each side of its intersection with the Wax Lake Outlet were both equal to 268 m^3/s towards the West, indicating that on average no flow exchange occurred between the Wax Lake Outlet and GIWW. The maximum discharge recorded during this period in the GIWW west of the Wax Lake Outlet was still only 568 m^3/s (Swarzenski, United States. Army. Corps of Engineers. New. Orleans District et al. 2003). Based on the relatively small discharges in the GIWW compared to typical Wax Lake Outlet outflows and the lack of a non-zero average flow exchange between the two channels, this study assumes that flow and sediment passing through the GIWW and into or out of the Wax Lake Outlet is insignificant to the delta morphological development. Thus, no boundary conditions are defined where the GIWW intersects the model domain boundaries to simplify the required data collection and boundary condition schematizations. As there will be no flow through the GIWW perpendicular to the Wax Lake Outlet, siltation of the normally-maintained navigation channel is expected but is assumed to have minimal impact on flow and sediment transport to the delta.

3.3 Grid and Boundaries

With the study focus on Wax Lake Delta development, a curvilinear grid that encompasses the direct upstream Wax Lake Outlet channel, the delta distributary channels and depositional formations, a portion of the receiving basin, and upstream low-lying areas flanking the main channel was generated. The main depositional features of the Wax Lake Delta form an approximately radially symmetrical geometry on the order of 10 km wide. The grid boundaries were oriented to include between 5 and 10 km of accommodation space basinward of the delta. Because upstream channel development was of less interest in the current study, the upstream boundary of the grid was located approximately 20 km from the delta apex at the closest available long-term gauging station on the Wax Lake Outlet. Though a defined distributary channel network structure had already developed in the prototype Wax Lake Delta at the start of the simulation period, no effort was made to follow the orientation of delta bathymetry and distributary channels during grid development. This approach was justified based on the success of previous conceptual modeling efforts with producing representative meandering and fan-shaped delta distributary networks despite use of

purely rectilinear grids (see section 2.3). Grid resolution ranges from over 100 m in the most offshore portions of the receiving basin to as little as 25 m in the distal portion of the delta, with most grid cell sizes being on the order of 50 m. This resolution allowed for accurate representation of delta distributary channels captured in the bathymetry with a minimum of approximately 5 grid cells representing a channel cross-section. Overall, the model domain comprises an area of approximately 35 by 20 kilometers, represented by 185339 grid cells. With the assumption of full river dominance and corresponding assumption of negligible basinal energy, only an upstream flow and an offshore water level boundary were needed. The model grid along with the locations of the two boundaries is given below in figure 3-4.

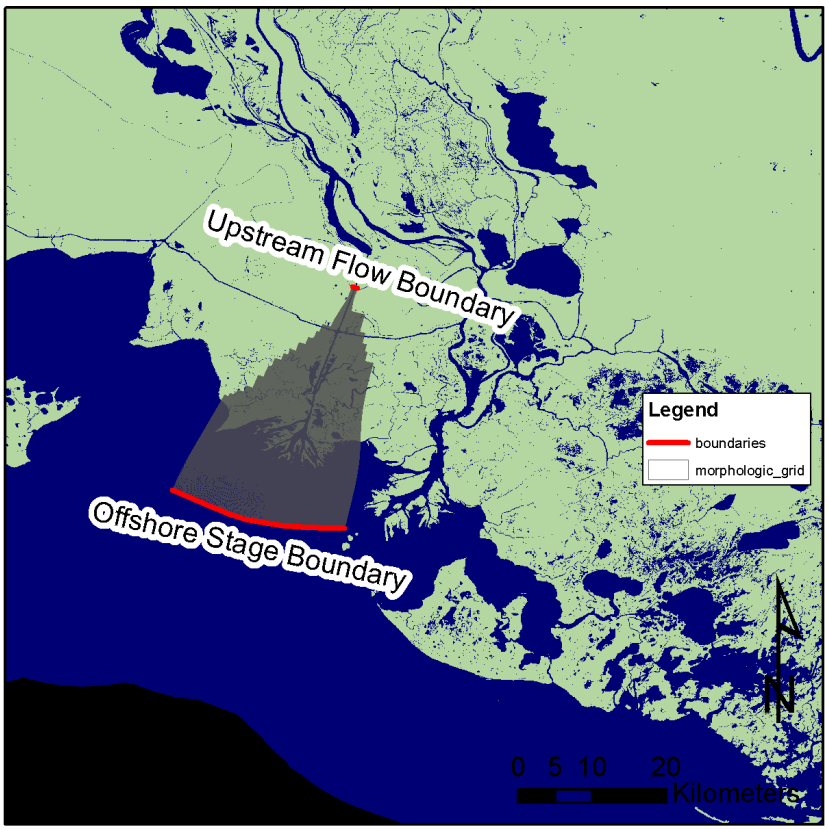

Figure 3-4: Model computational grid and upstream and offshore boundary locations

3.4 Bathymetry

Though the U.S. Army Corps of Engineers has conducted hydrographic surveys of the Lower Atchafalaya River including the Wax Lake Outlet approximately every decade beginning in 1967, the surveys generally do not cover the Wax Lake delta and portions of the Atchafalaya Bay of most interest for the current study. The survey of 1998 was the most complete, providing transects through the delta distributary channels and over depositional lobes. A finite-element hydrodynamic model of the Lower Atchafalaya system including Atchafalaya Bay and portions of the Gulf of Mexico has been developed by the USACE with bathymetry primarily derived from the 1998 hydrographic survey. The bathymetric data set for this model was augmented with Light Detection and Ranging (LIDAR) survey data for overbank areas not covered in the hydrographic survey (USACE 2010, Appendix A). The bed level at each node in the finite-element mesh was available as an xyz point file, so was used to establish the bed level at each grid point for the present simulation. The locations of

each node at which the bed level is defined in the study area are given below in figure 3-5. Depths at each model grid point were assigned by triangular interpolation from the USACE model bathymetry sample points. Figure 3-6 gives an overview of the initial bathymetry in the model domain, along with a three-dimensional visualization following in figure 3-7.

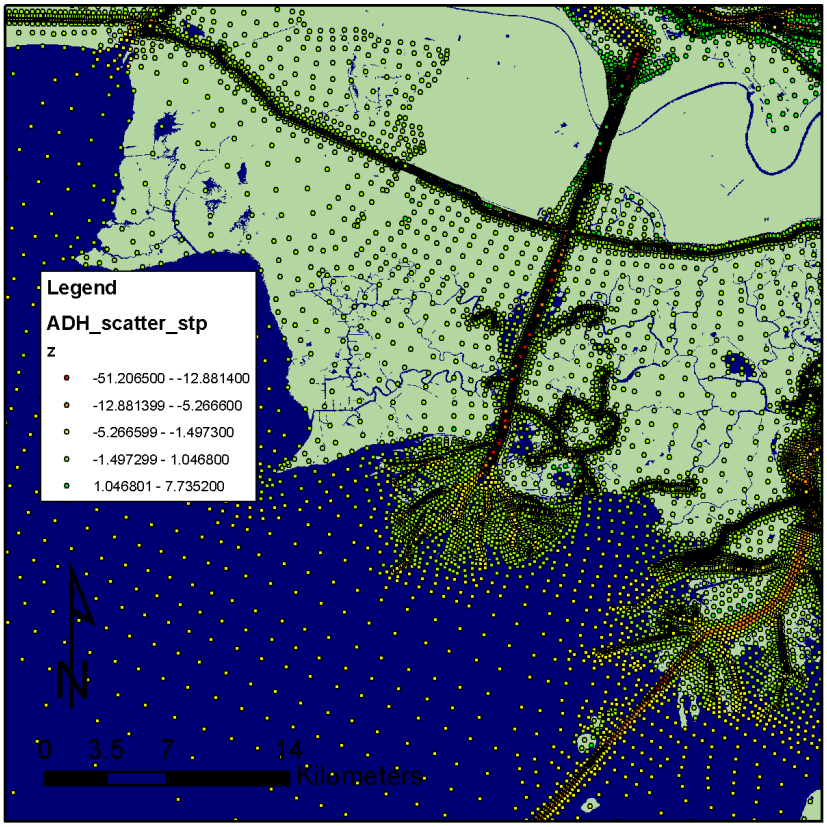

Figure 3-5: Locations of the model nodes used in the USACE finite-element hydrodynamic model of the Lower Atchafalaya River system (USACE 2010). Bed levels were assigned from the 1998 USACE Lower Atchafalaya hydrographic survey combined with LIDAR survey data for overbank areas.

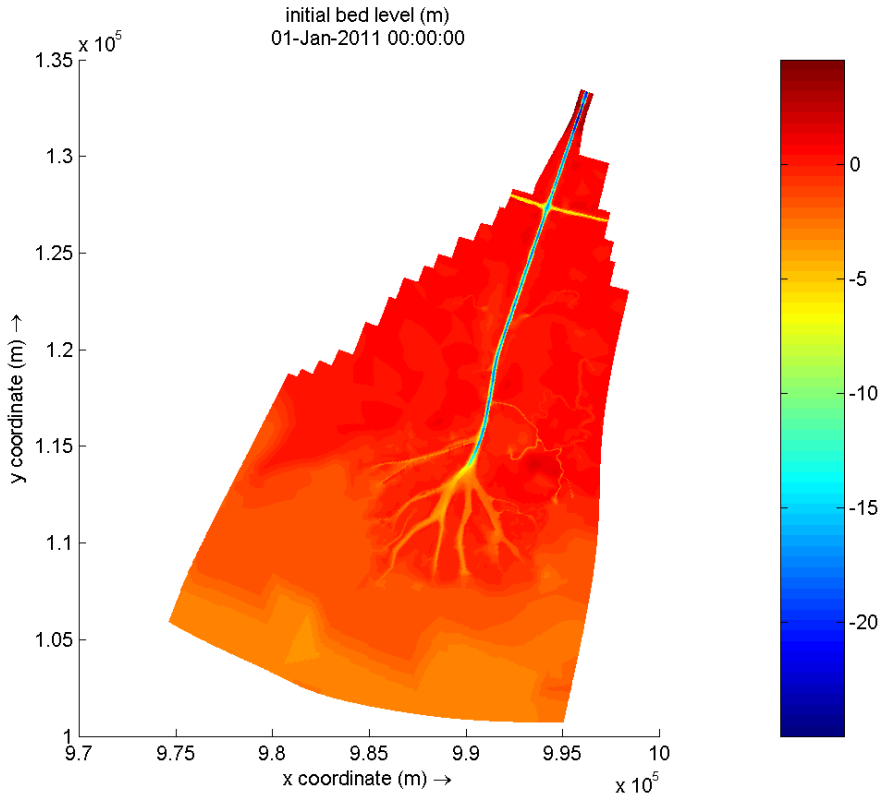

Figure 3-6: Initial Model Bathymetry

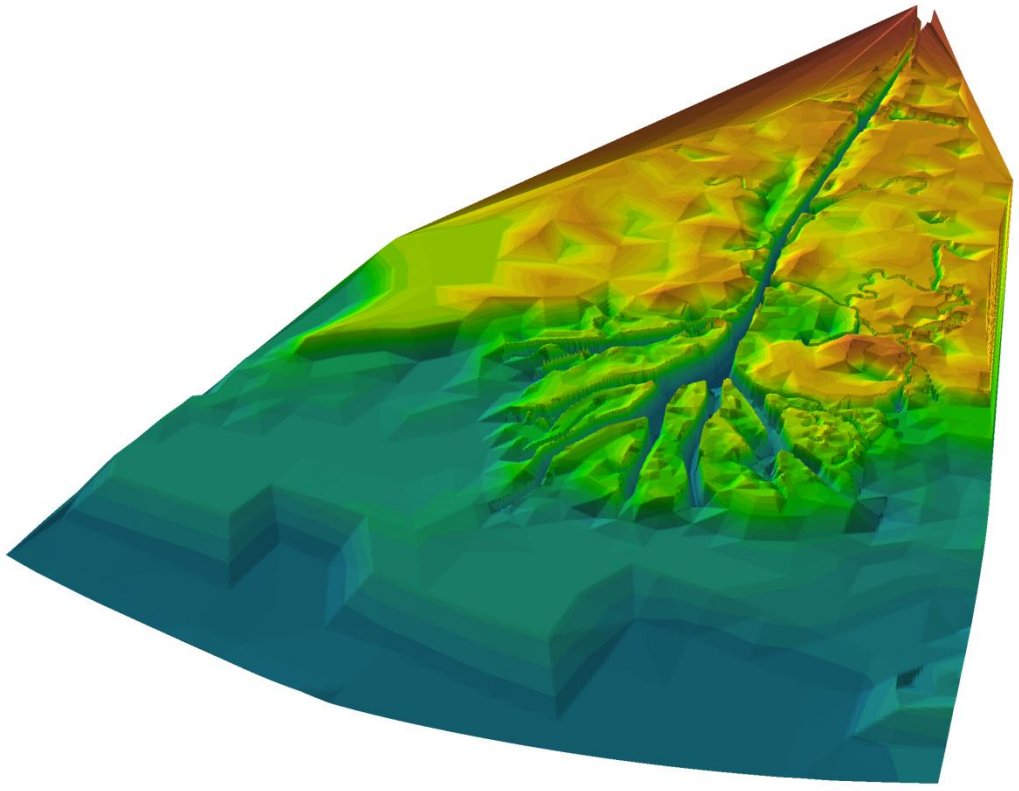

Figure 3-7: 3-D representation of the initial morphology of the model domain used in the simulation with 250x vertical exaggeration. Note that the higher elevations to the East and West of the Wax Lake Outlet that lie outside the modeled area are unrealistic, a result of visualization surface creation through triangulation.

3.5 Sediment Schematization

The Wax Lake Delta is primarily composed of coarse sediment depositional features despite a large, fine-sediment dominant suspended load (Roberts, Walker et al. 1997). Still, sedimentary facies underlying subaerial delta features can be characterized by coarse or fine sediment dominance, and depositional bodies initiated by mouth bar formation and channel bifurcation exhibit characteristic sediment sorting patterns reflected in surface sediment distributions and stratigraphy (DuMars 2002; Wellner, Beaubouef et al. 2005). In order to schematically reproduce the stratigraphic patterns created with delta growth, the model uses two sediment fractions, each representing a range of coarse and fine sediment portions of the inflowing sediment load and preserved depositional sequences. Analysis of suspended sediment load and bedload samples taken during the low flow and flood condition field campaigns of DuMars, 2002, indicate that grain sizes range from very fine sand to coarse silt with a small clay fraction (DuMars 2002). Analysis of many bed sediment vibra-cores throughout the delta indicate a similar bed material grain size distribution (Wellner, Beaubouef et al. 2005). Figure 3-8 gives a plot of the grain size distribution as a linear function of delta deposit thickness, indicating the range of grain sizes present in the Wax Lake Delta. Based on this field information, the sand sediment fractions were approximated by a single, very fine sand fraction with a d_{50} of 100 µm, a specific density of 2650 kg/m^3, and a dry bed density of 1600 kg/m^3. Though the fine sediment fractions would surely be better represented with a non-cohesive fine silt fraction and a cohesive clay fraction, a single cohesive fine sediment fraction was used to approximate all fine sediment. This mud fraction was assigned a density of 2650 kg/m^3, a dry bed density of 500 kg/m^3, and a fall velocity of .00025 m/s. The fall velocity was calculated using the Van Rijn formulation and an assumed d_{50} of 15 µm corresponding to a fine silt classification (van Rijn 1984). The properties of the two sediment fractions used in the model are summarized below in table 3-1.

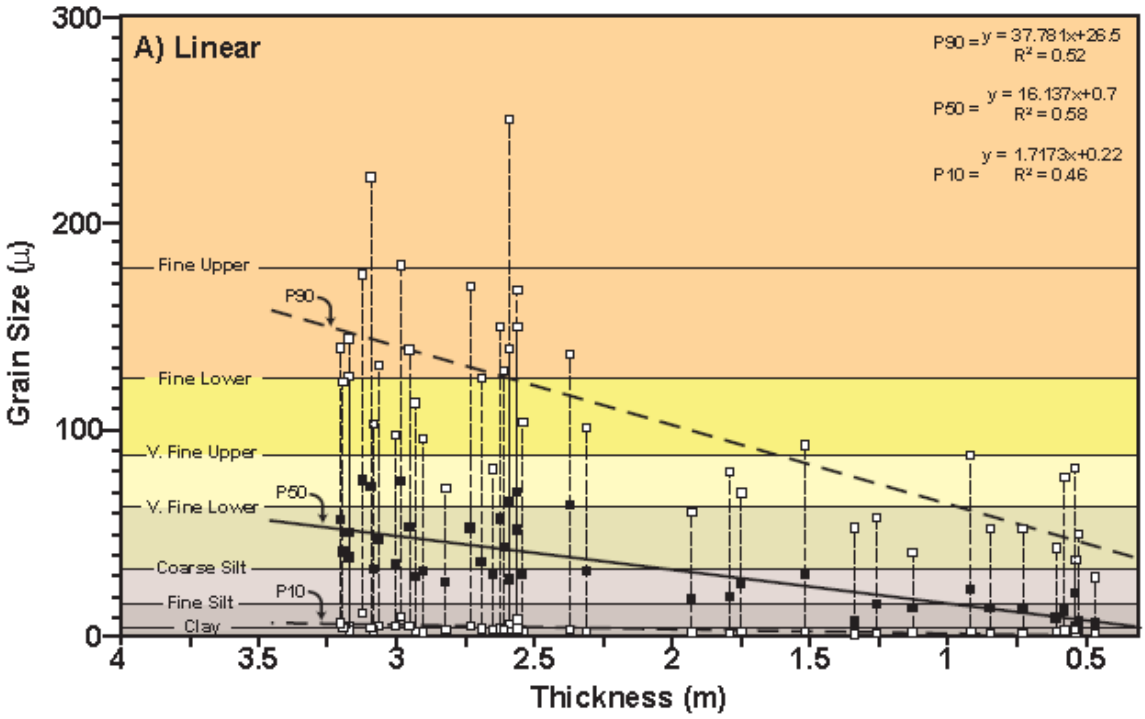

Figure 3-8: Plot of grain size distribution from many vibracores taken throughout the Wax Lake Delta as a linear function of delta depositional facies thickness (Wellner, Beaubouef et al. 2005)

Table 3-1: Properties of sand and mud sediment fraction used in model

fraction name	type by size	size (μm)	specific density (kg/m^3)	dry bed density (kg/m^3)	fall velocity (m/s)
sand	fine sand	100	2650	1600	--
mud	fine silt	15	2650	500	0.00025

3.6 Boundary Conditions

The following section recounts the process undertaken to determine hydrodynamic and sediment transport boundary conditions for both the upstream and offshore model boundaries. In order to conduct a successful long-term morphological simulation, the applied boundary conditions should reflect the actual prototype conditions to the greatest degree possible; however, computational limitations that come with high-resolution process-based modeling require a reduction in boundary condition input from the ideal measured time series. The available prototype hydrodynamic and sediment transport measurements were thus used to develop a representative average morphological year composed of four periods of constant flow. To more accurately represent the sediment delivered to the delta, the number of days per morphologic year that each flow occurs was scaled to reflect the greater proportion of sediment transported during higher flows. Corresponding sand and mud input boundary sediment concentrations were assigned for each flow condition based on functional relationships to discharge calculated from concurrent, long-term measurements.

3.6.1 Available Data

Two measurement gages in the study area were used to assign boundary conditions to the upstream inflow boundary and downstream outflow boundary. The upstream model boundary was located at the U.S. Geological Survey-operated Wax Lake Outlet at Calumet, LA gage, and the model offshore boundary was located very near the U.S. Army Corps of Engineers-operated Atchafalaya Bay near Eugene Island gage. The locations of the two gages along with the model area bathymetry are shown below in figure 3-9. Nearly continuous daily mean discharge data is available at the Calumet, LA gage in the period from June 1, 1986 to March 22, 2011 (USGS 2011). Data on the suspended load at the same location is available from April 20, 1973 to December 7, 2010, though at a sampling frequency of approximately once per month with slight increases in frequency during significant floods (USGS 2011). For each Calumet, LA gage sediment sampling event, instantaneous values of suspended sediment discharge in tons/day, suspended sediment concentration in mg/l, and the percent of the suspended sediment load that has a grain size finer than .0625 mm are available. The Atchafalaya Bay near Eugene Island gage records consist of instantaneous stage (NGVD datum) recorded daily at 8:00 a.m. from February 25, 1976 to April 9, 2006 (USACE 2006). A timeline giving the periods of record at each gage in relation to the calibration event and simulation period is given in figure 3-14.

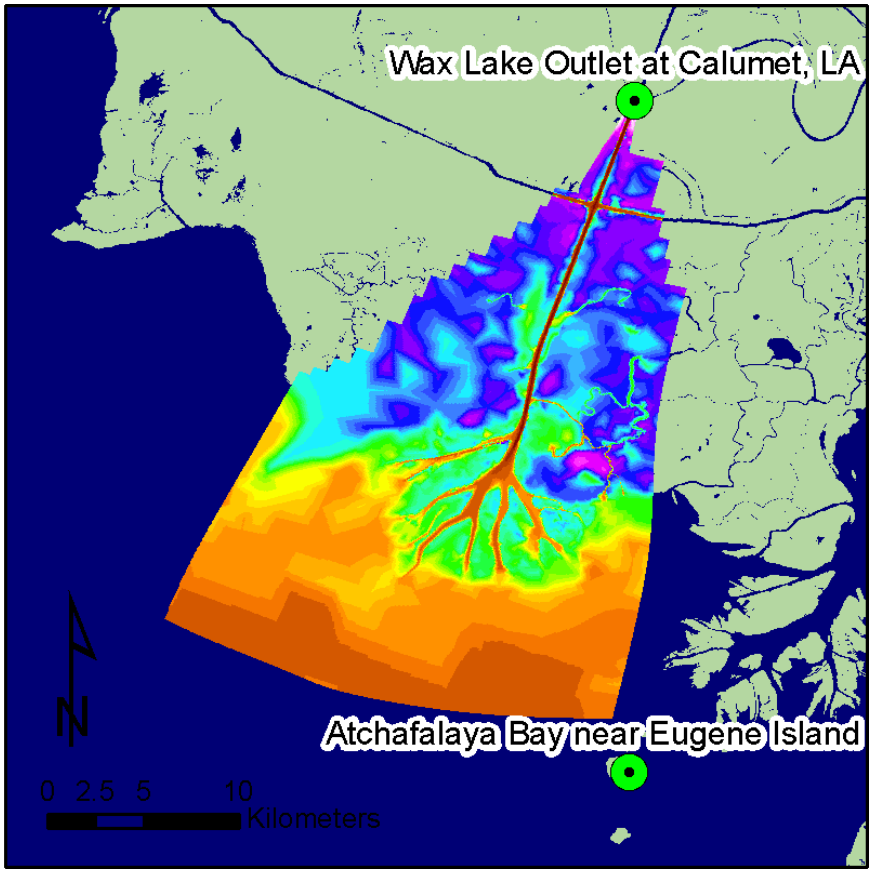

Figure 3-9: Locations of the Wax Lake Outlet at Calumet, LA and Atchafalaya Bay near Eugene Island gages used in determining model boundary conditions. The multi-colored overlay represents the modeled area and corresponding bathymetry.

3.6.2 Hydrodynamic

In accordance with the assumed negligible influence of tides and waves on long term morphology, the offshore boundary was assigned a constant water level equal to the average water level recorded in the approximately thirty year record of the Atchafalaya Bay near Eugene Island gage. The mean offshore water level was calculated as .32 m above NGVD. The use of a constant water level offshore boundary for models of the area is not unprecedented; a one-dimensional USACE hydrodynamic model of the Lower Atchafalaya River system used a nearly identical value of .30 m for offshore stage boundaries (USACE 2010, Appendix D).

Because of the complexity and computational expense of the process-based Delft3D model, the number of simulated boundary conditions must be reduced from the continually-varying time series of inputs that occurs in the prototype during the simulation period to obtain suitable run times. Though measured time series of hydrodynamic and sediment transport boundary conditions exist for the simulated period of the beginning of the year 1998 to the end of the year 2002, the model input boundary conditions were reduced to a few instances of constant values whose repetition would approximate the simulated period discharge and sediment load regime. Each year was approximated with four levels of constant discharge, applied for varying time periods based on the flows' probability of occurrence in the full prototype flow record and scaled based on contributions to sediment load, which were then repeated five times for the five year simulation.

First, an annual flood frequency analysis was performed to determine the discharge levels corresponding to various return periods (probability of exceedance). The U.S. Geological Survey program PeakFQ fits the annual maximum discharges from the Calumet gage's 24 year period of measurement to the log-Pearson type III frequency distribution to obtain the annual probability of exceedance as a function of discharge (Flynn, Kirby et al. 2006). The PeakFQ annual exceedance probability output for the 5 year, 2 year, and approximately annual flood are given below in table 3-2.

Table 3-2: Annual Flood Frequency Analysis Results using PeakFQ

annual exceedance probability	return period (yr)	Q (m^3/s)
0.995	≈1	2961.94
0.5	2	5077.21
0.2	5	5977.69

The entire flow record was then used to construct a flow-duration curve that gives the cumulative frequency of occurrence of the observed flow values. The flow-duration curve communicates the proportion of time that a certain discharge value occurred during the measurement period. The flow-duration curve for the Wax Lake Outlet at Calumet, LA gage is given in the upper subplot of figure 3-11 along with the 5 year, 2 year, and annual flood flows plotted at their corresponding locations on the curve. To account for the non-flood conditions encountered in the discharge regime, a representative low flow of 1149.7 m^3/s was also used to complete the discharge schematization. Each of the four schematized discharge values was treated as the median of a group of discharges for which the constant value occurring for a set proportion of time would approximate the occurrence of the full group of discharges. Probability of occurrences which also equal the proportion of time that the specified discharge level will occur were calculated based on the proportional area under the flow duration curve for each schematized discharge level's corresponding discharge range. The probabilities were found to equal .1582, .7232, .0799 and .0387 for the low flow, annual flood, 2 year flood, and 5 year flood, respectively.

Because the sediment concentrations and resulting sediment flux in the Lower Atchafalaya system have a non-linear relationship to discharge, much greater volumes of sediment are delivered to the Wax Lake Delta during the highest flows (Roberts, Walker et al. 1997), so an effort was made to scale the proportional time of occurrence to reflect the increased morphologic influence of the higher flows. A power relationship was established between discharge and sediment transport based on concurrent discharge/transport measurements at the Calumet, LA gage location taken on an approximately-monthly basis for the 37 year period of record (see figure 3-10 below for plot of data, regression, and goodness of fit information). This functional relationship ($Qs=6.194*Q^{.4659}$) was used to construct a sediment transport-duration curve with the transport value at each cumulative frequency calculated from the discharge value at the same frequency. The proportional areas under the curve were recalculated and found to be .1243, .7365, .0923, and .0469 for the low flow, annual flood, 2 year flood, and 5 year flood, respectively. The scaling to sediment transport has predictably given less emphasis to the low flow and more emphasis to the higher flood flows. The transport-duration curve, proportional areas, and probability of occurrence for the four schematized discharge levels are presented in the lower subplot in figure 3-11. Translating the probability of occurrence

into the actual flow durations for a representative year yields a 1149.7 m^3/s discharge for 45 days, a 2961.9 m^3/s discharge for 269 days, a 5077.2 m^3/s discharge for 34 days, and a 5977.7 m^3/s discharge for 17 days. The proportioning of flow durations for each of the four discharge conditions is summarized in table 3-3.

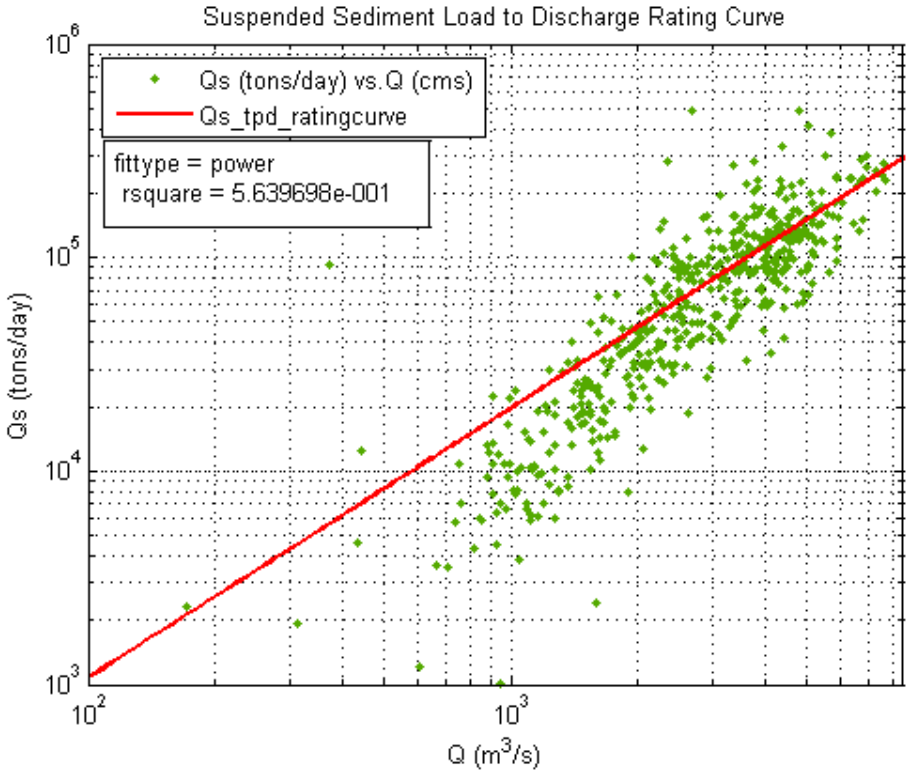

Figure 3-10: Relation between discharge and sediment transport at the Wax Lake Outlet at Calumet, LA gage

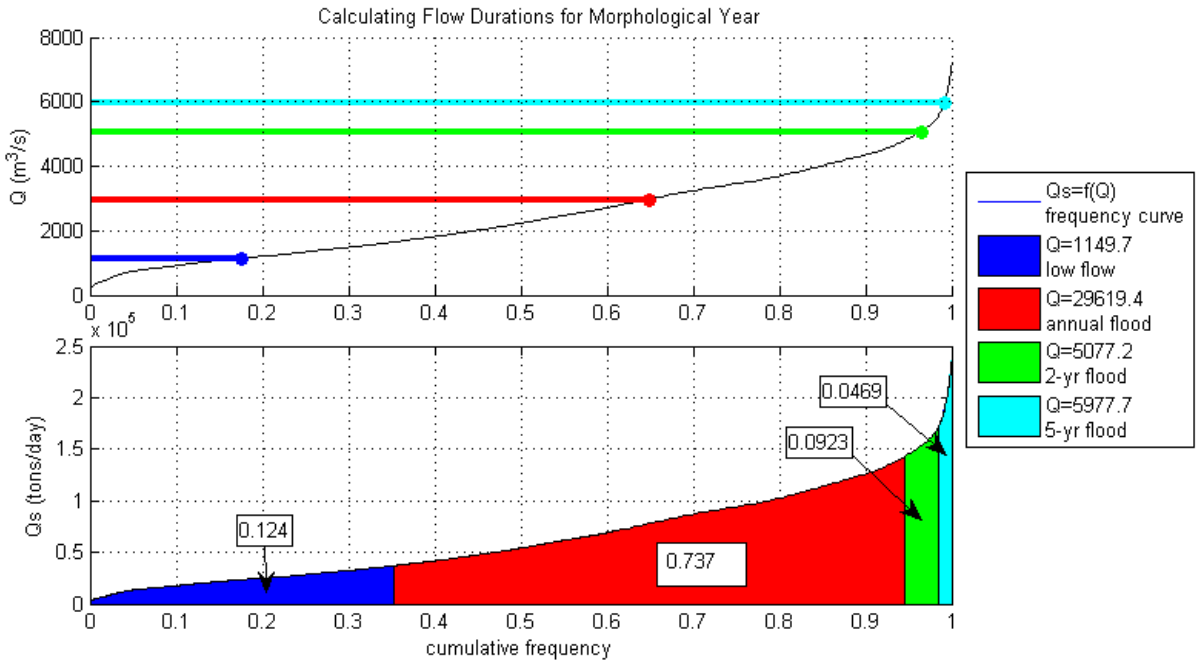

Figure 3-11: Flow duration curve and transport duration curve used in the calculation of flow durations for the long-term morphology simulation. The colored circles in the upper plot represent the four discharge levels that will schematize the full flow regime. The colored areas in the lower plot represent the portion of the flow regime that corresponds to each discharge level. Each discharge level's area as a proportion of the total curve integral was used to calculate the probability of occurrence displayed in text in the lower plot.

Table 3-3: Summary of flow condition proportioning for each morphologic year

Flow condition	Discharge (m^3/s)	scaled probability of occurrence	days per morphologic year (days)
low flow	1149.7	0.124	45
annual flood	2961.94	0.737	269
2-yr flood	5077.21	0.0923	34
5-yr flood	5977.69	0.0469	17

3.6.3 Sediment Transport

The development of a functional relationship between discharge and sediment transport was detailed in the above section (see figure 3-10). Similarly, a second-order polynomial fit was used to establish the relationship of the percent of suspended sediment finer than .0625 mm measurement to discharge at the Wax Lake Outlet at Calumet, LA gage. The data set, polynomial regression (percent finer= -6.88e-007*Q^2-0.000614*Q+100.6), and the r^2 value of the fit are presented below in figure 3-12.

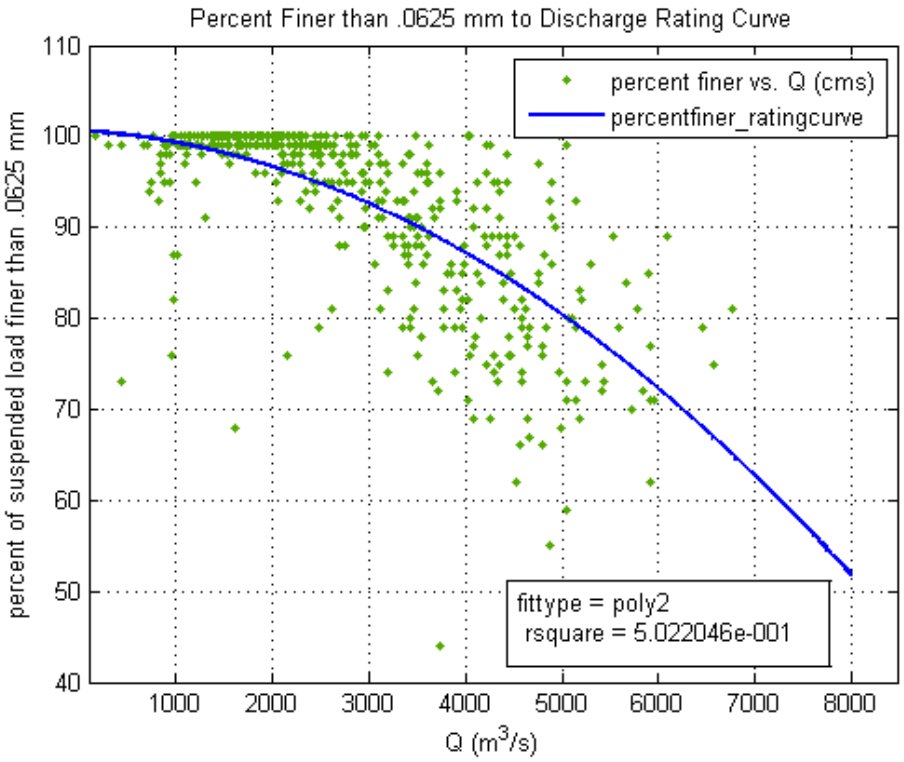

Figure 3-12: Relation between discharge and percent of suspended sediment finer than .0625 mm at the Wax Lake Outlet at Calumet, LA gage

Once the four discharge levels and the number of days that each occurs in the morphological year were determined, the functional relationships for sediment transport parameters were used to assign corresponding inflow boundary sediment transport concentrations for the two grain size fractions used in the model. The sediment transport value obtained from the transport-discharge relationship was used to calculate a total inflow sediment concentration. The percent finer than .0625 mm value corresponding to each discharge was then used to distribute the total inflow concentration between the fine sand and mud fractions. A summary of the four discharge levels and corresponding suspended sediment concentrations used at the upstream boundary is given below in table 3-4.

Table 3-4: Upstream boundary conditions - four constant discharge levels and corresponding sand and mud suspended sediment concentrations

Discharge level	Discharge (m^3/s)	Sediment Transport (tons/day)	Total suspended sediment concentration (mg/l)	Percent finer than .0625 mm (%)	Sand suspended sediment concentration (mg/l)	Mud suspended sediment concentration (mg/l)
1	1149.70	23447.63	165.16	99.03	1.60	163.56
2	2961.94	77524.36	256.68	92.79	18.50	238.18
3	5077.21	153175.08	329.94	79.79	66.67	263.27
4	5977.69	188273.65	356.01	72.39	98.29	257.72

3.6.4 Comparison to Prototype Conditions

A key assumption in the process of schematizing the discharge regime is that the flow-duration curve developed from 24 years of daily discharge data is applicable to the development of a typical annual discharge regime. It is assumed that the average year that is repeated for the long term simulation will have cumulative frequencies for discharges that are identical to those calculated from the much longer data set. The discharge regime in any given year for the prototype, as well as the actual modeled five year time period, will likely differ substantially from the representative year used in the schematization; however, the need for reduction in the number of modeled discharge scenarios necessitates this approximation. Still, it is useful to compare the simulated discharge regime with what actually occurred in the prototype during the model period.

Figure 3-13 below presents the observed discharge and suspended sediment transport at the Wax Lake Outlet at Calumet, LA gage during the model period of simulation, January 1, 1998 to December 31, 2002. The four constant discharge and transport levels used in the model boundary condition schematization are also given in each plot for comparison. It can be seen that the prototype discharge does not exceed the highest discharge level used in the model during the simulation period; however, the total suspended sediment transport significantly exceeds the highest modeled value at various points in the simulation period. Additionally, the total volume of water and mass of sediment discharged through the upstream boundary during the full simulation period was calculated for the prototype and model discharge and transport regimes for comparison. The modeled volume of water (5.6137e+006 m^3) significantly exceeded the measured prototype water volume (4.5835e+006 m^3), though this is expected due to the scaling of flow duration to favor the higher flows that are responsible for much higher values of sediment transport. The total mass of sediment discharged during the modeled simulation period is much closer to the prototype measured value, though the modeled value of 151.59 megatons still exceeds the prototype measured value of 132.22 megatons.

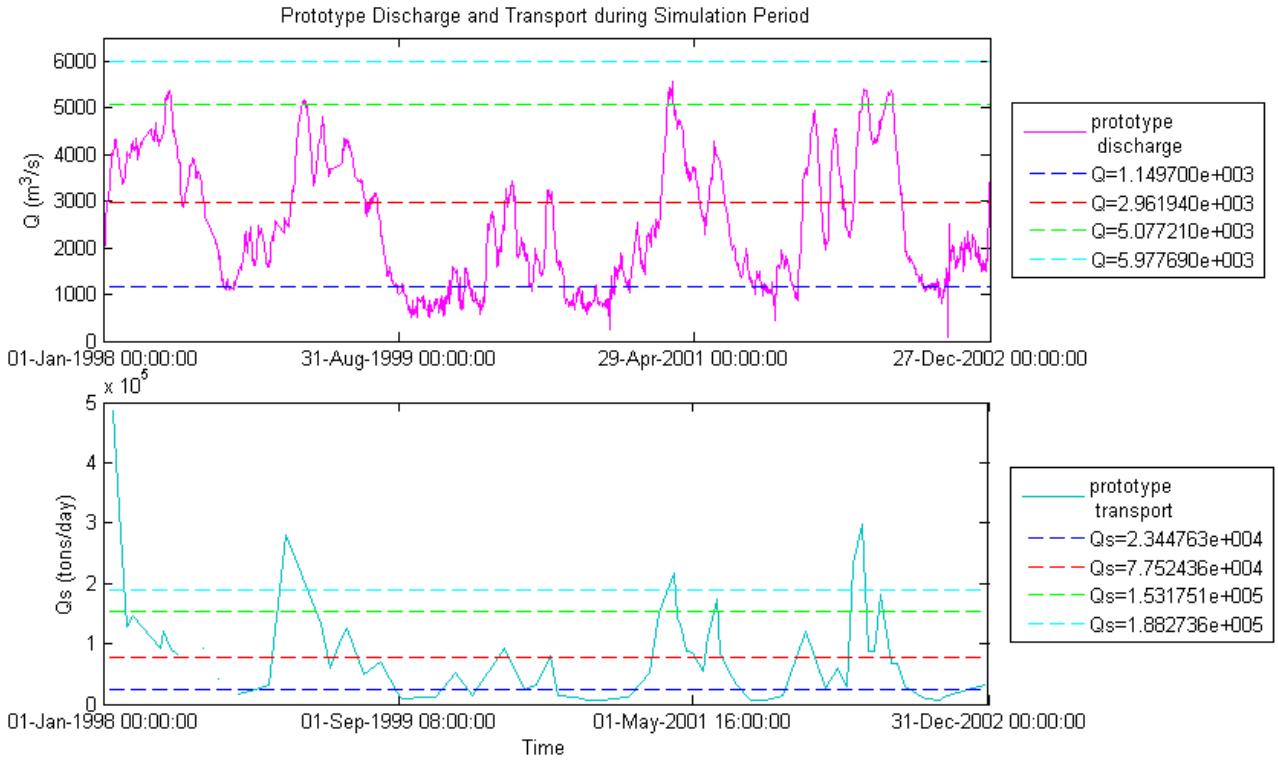

Figure 3-13: Prototype discharge (upper subplot) and suspended sediment transport (lower subplot) during simulation period. The four constant discharge and transport levels used in the model boundary condition schematization are also shown for comparison.

3.7 Conclusion

The initial set up of the long-term morphological model of the Wax Lake Delta in the process-based modeling program Delft3D has been described. The computational grid extents were located to include portions of the Wax Lake Outlet feeder channel and the Atchafalaya Bay receiving basin surrounding the fan-shaped delta. Bathymetry from a 1998 hydrographic survey augmented with LIDAR data for overbank areas was interpolated to the computation grid. The range of sediment sizes in the suspended load and bed is represented by a fine sand non-cohesive fraction and a fine-silt sized cohesive mud fraction. An upstream flow boundary was located at the site of the long term flow and sediment measurement station at Calumet, LA; the basinward water level boundary was located near the long term Eugene Island gage. Measurements from these two gages were used to calculate suitable schematized boundary conditions to best represent the actual prototype flow regime. An average morphological year is represented by four periods of constant flow whose duration was determined from a flow-frequency curve scaled according to the sediment transport typical of each flow. Upstream suspended sediment concentrations for each of the two sediment fractions were determined from rating curves derived from long-term concurrent flow-sediment transport measurements. The validity of the boundary condition schematization was explored through comparison of total volumes of flow and suspended sediment passing through the upstream boundary during the simulation period in both the prototype Wax Lake Delta and the model. Figure 3-14 below summarizes the measurement periods from which boundary condition data were derived, the dates of bathymetry and sediment grain size data used in the model, the dates of the

calibration event, and the long-term morphologic simulation period. Information on the model calibration follows in chapter 4.

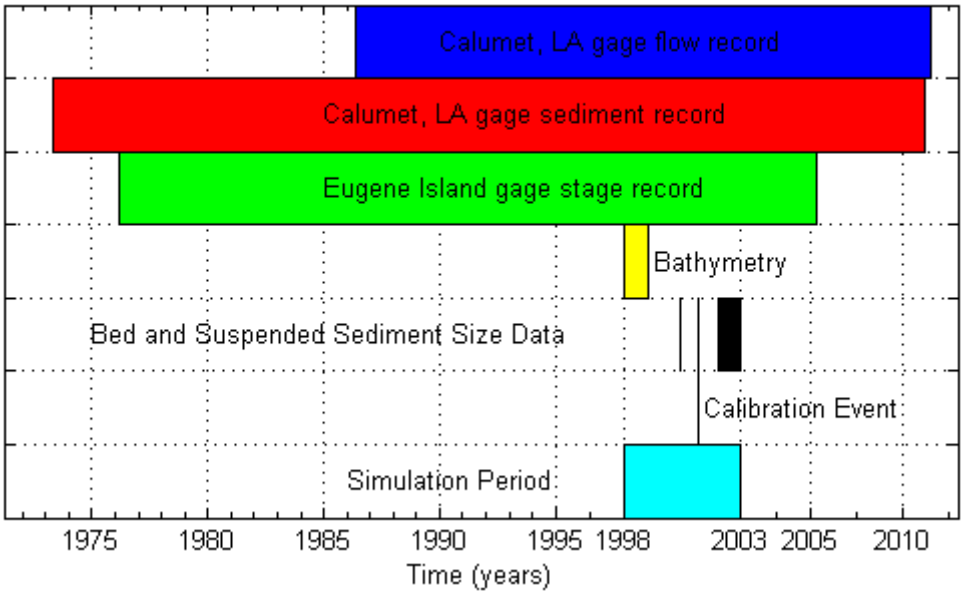

Figure 3-14: Timeline for model set-up and simulation

4. Model Calibration

4.1 General

To successfully simulate the morphodynamic development of the Wax Lake Delta, both the hydrodynamics and sediment transport in the model domain during high flows must be calibrated so that the modeled depositional patterns at the delta front approximate the real Wax Lake Delta (prototype) behavior to the greatest extent possible. Though a typical model calibration will include simulation of time varying boundary conditions with comparison of modeled results to observed values at some interior measurement point, the lack of a long term measurement station in the Wax Lake Delta forces a reliance on field measurements recorded during discreet events. The velocity and suspended sediment measurements made in the channels of the Wax Lake Delta for the Dumars, 2002 study form the basis for both the hydrodynamic and sediment transport calibration effort. In Atchafalaya Bay, a mixed-diurnal tidal cycle with a 30 cm average range strongly affects flow velocities in the delta during low-flow conditions; however, this influence is significantly diminished during annual flood periods (DuMars 2002). The effect of tidal fluctuations and winter storm-induced water level gradient changes (both neglected forcings in this model) on measured velocities during low flow would be impossible to accurately simulate given the assumptions and simplifications made during model development. Though measurements were made during flood and non-flood conditions, only the measurements made on February 25-27, 2001 under flood conditions were used for calibration. Velocities observed during this period were so high as to render tidal and wind influences negligible and correspond to the more-morphologically active flood discharges which will be the focus of this model.

During the flood condition field campaign of DuMars, 2002, measurements were taken at various sample points along eight channel transects of the Wax Lake Delta distributaries. Measurements were made at transects 8, 15, 17, 18, 19, 24, and 25 during flood conditions, and their locations are given below in figure 4-1. Initial transect bathymetry profiles were used to locate sample points at inferred high and low energy locations. At each point, velocity and suspended sediment concentrations were taken at .05, .5, and .95 of the total sample site depth (DuMars 2002). Figure 4-2 below gives a schematic of the sampling scheme for a typical transect, where measurements are taken at the indicated depths for each measurement point along the transect. The model hydrodynamics were calibrated first by running a steady-state hydrodynamic simulation with a fixed bed and no sediment input or transport considered. The spatially varying manning's roughness values were adjusted to minimize the percent error between simulated and observed transect-averaged, depth-averaged velocity. An aggregate velocity parameter was used to assess model deviation from prototype instead of comparison at specific sample points. The inevitable deviations between the real and model bathymetries due to survey resolution and depth interpolation mean that accurate simulation of specific velocity vectors is very difficult.

Once velocity differences were reduced to within acceptable limits, a sediment transport simulation was performed with constant boundary discharge and sediment inflow concentrations. Once the specific sediment schematization, bed schematization, initial bed composition, and sediment transport formulation were determined and implemented, various sediment transport calibration parameters for both fractions were altered to minimize the percent error between simulated and observed transect-averaged, depth-averaged sediment concentration without regard to the

distribution of the measured suspended sediment between the two modeled grain-size fractions. The sections below discuss specific aspects of the calibration simulations and present the calibrated parameter results.

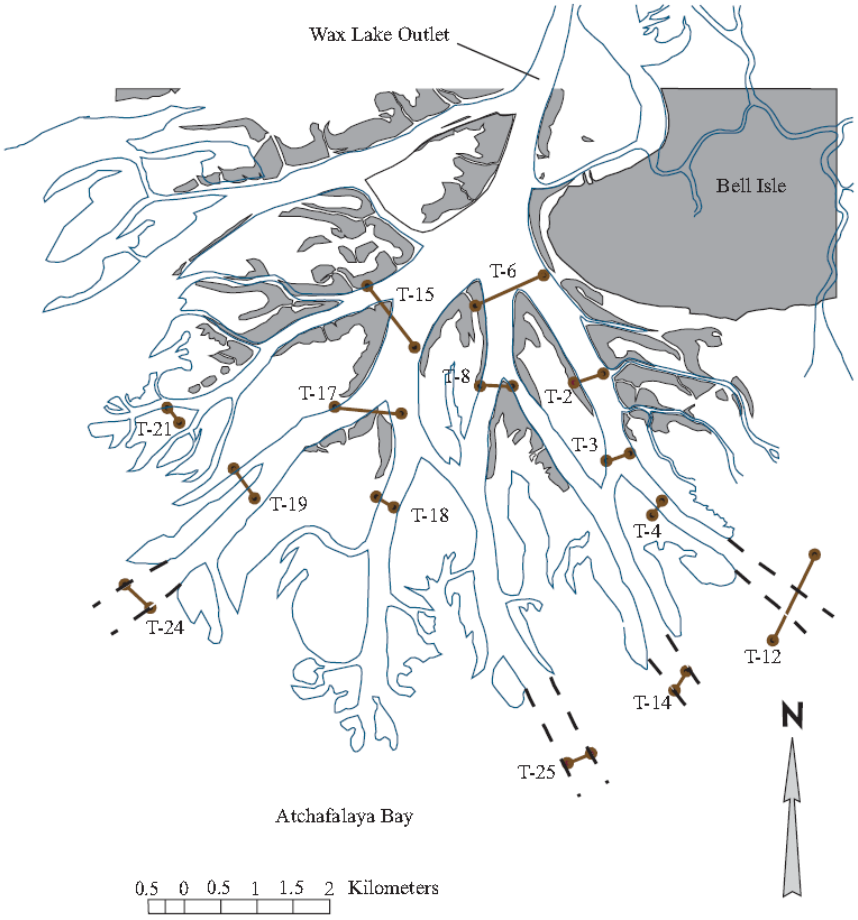

Figure 4-1: Transect locations for field measurements used in calibration. T-8, T-15, T-17, T-18, T-19, T-21, T-24, and T-25 correspond to measurements made during flood conditions on February 25-27, 2001. (DuMars 2002)

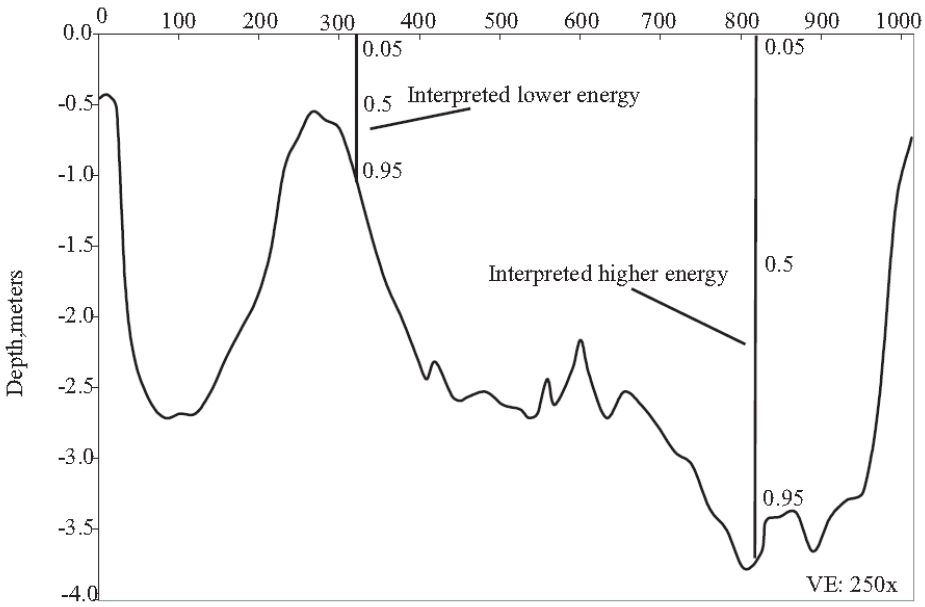

Figure 4-2: Velocity and suspended sediment sampling scheme demonstrated for typical transect (DuMars 2002)

4.2 Hydrodynamic Calibration

4.2.1 Hydrodynamic Calibration Run Description

The simulation run for hydrodynamic calibration used a constant upstream boundary discharge to try to simulate observed velocities in the delta distributary channels. For each calibration run, the upstream boundary discharge was set to 4012 m^3/s, the mean discharge measured at the Calumet, LA gage for the period of field measurement. The open boundary was given a constant stage boundary condition of .32 m, the average water level measured at the Eugene Island gage for the entire period of record. To obtain the channel-averaged velocity from the field measurements, the three velocities at .05, .5, and .95 of the depth at each sample location were fit to a logarithmic velocity profile, and a depth-averaged value was calculated. It was assumed that the velocity measurement device would align with the primary direction of flow, so measurements were treated as magnitudes. The channel-averaged value was then calculated by multiplying the depth-averaged velocity at each sample point by the incremental flow area then dividing by the total area according to the standard procedure for computing discharge from velocity measurements (Chow, Maidment et al. 1988). Because at most 5 samples were taken along each cross-section, a substantial amount of flow near the banks was unaccounted for in the averaging procedure. Thus, a 10 cm/s depth-averaged velocity was assumed to occur at the start and end point of each cross-section transect so that the incremental discharge occurring outside the measurement points would still be included.

4.2.2 Exclusion of Non-representative Cross-sections

Once the model was sufficiently stabilized, depth-averaged velocity magnitudes at each intersecting grid velocity point within the cross-section transect were extracted from the model results. These values were similarly channel-averaged, though no assumed velocities were used as the grid resolution was sufficient to fully represent the flow through the transect. Additionally, the modeled

depth-averaged velocity values were averaged in the direct vicinity of each sample point for a direct comparison with observed values. Initial model runs indicated that substantial discrepancies existed between the measured and modeled velocity magnitudes at several of the cross-sections located at the distal ends of distributary channels. Examination of the velocity measurements implied developing channel structures at these transects that were not present in the model bathymetry. Because the measurements are from approximately three years after the model bathymetry surveys were conducted, it is expected that the morphologic change at the mouths of distributary channels in the intervening years would be significant. Figure 4-3 below gives the modeled and observed depth-averaged velocity magnitudes at transect 24, and is representative of the discrepancies at transects 19 and 25 as well. Also given is a plot comparing the observed and modeled depth-averaged velocity magnitudes at each sample point. Because of the substantial errors at cross-sections 19, 24, and 25 due to non-representative bathymetry, these transect measurements were excluded from the calibration process.

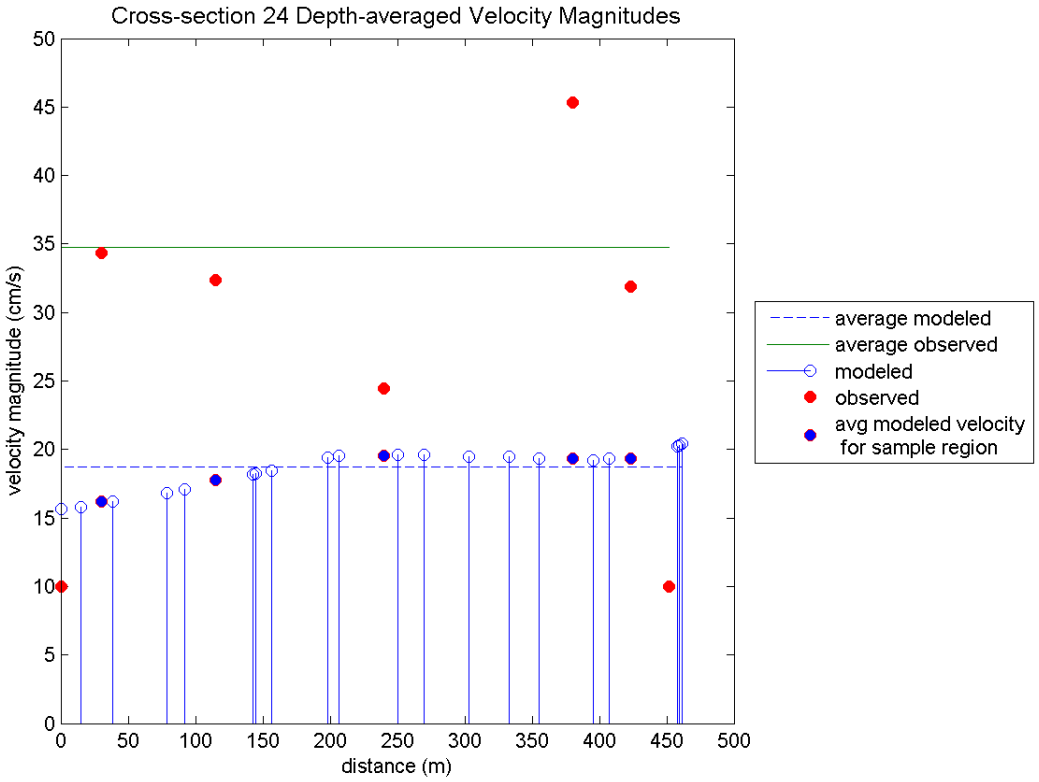

Figure 4-3: Comparison of Modeled and Observed Depth-averaged Velocity Magnitudes at Cross-section 24

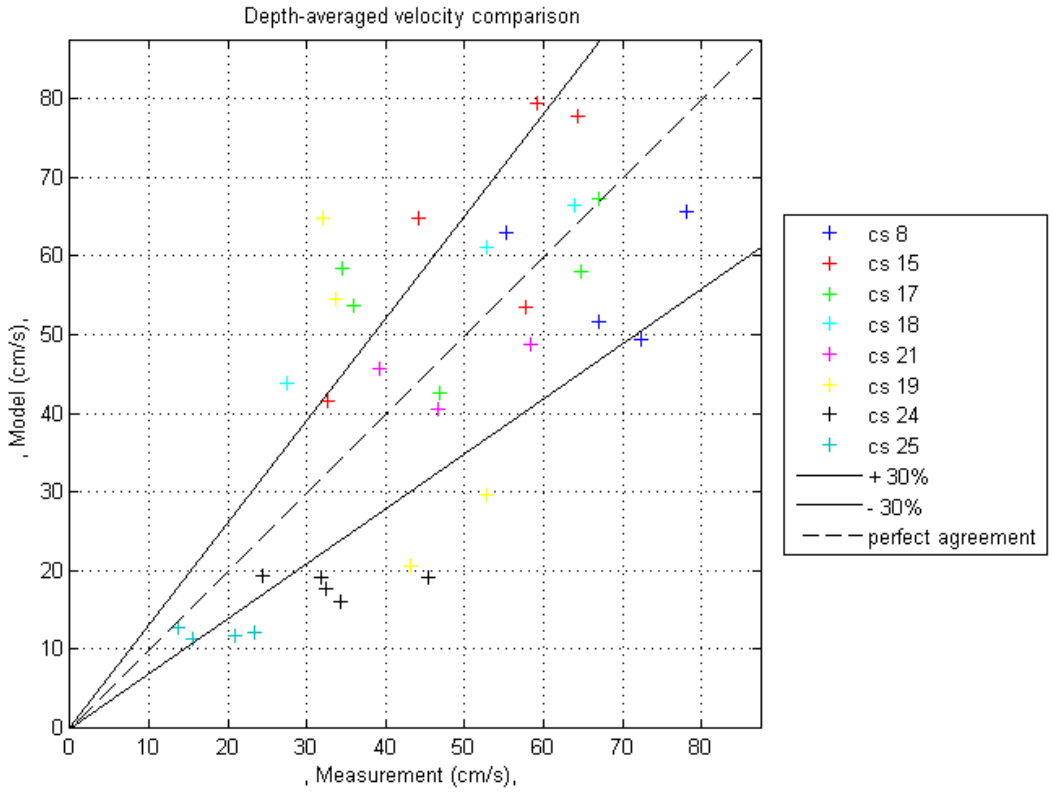

Figure 4-4: Measured vs. modeled depth-averaged velocities at each sample point. Most points for cross-sections 19, 24, and 25 lie outside the 30% error lines.

4.2.3 Hydrodynamic Calibration Results

Alteration of spatial-varying manning's roughness values was used to minimize the mean error between modeled and observed channel-averaged velocity magnitudes for the five remaining cross-sections. Values obtained in calibration of the ADH model of the Lower Atchafalaya River system were used for initial runs (USACE 2010, Appendix A). The ADH model roughness values were initially based on land use and vegetation type in the model domain but were altered to better simulate stages at multiple gage sites for historic floods (USACE 2010, Appendix A). Figure 4-5 gives the spatial-varying manning's roughness value distribution used in the ADH model. These values were then altered over successive runs until errors were minimized. Figure 4-6 gives the final manning's roughness distribution for the calibrated model. The modeled and observed depth-averaged velocity magnitudes and channel-averaging results are presented in Appendix A in for all transects used in the calibration process, and a direct comparison of modeled and observed magnitudes at each measurement point is presented in figure 4-7. Figure 4-8 compares the modeled and observed channel-averaged velocity magnitude for each cross-section. The mean difference between modeled and observed channel-averaged velocity magnitudes is 6.4 cm/s which corresponds to a mean percent error of 10.99%, and most of the errors between modeled at observed values at specific measurement points fall within the $\pm$ 30% lines in the comparison plot. Channel-averaged values all lie within $\pm$ 30% error.

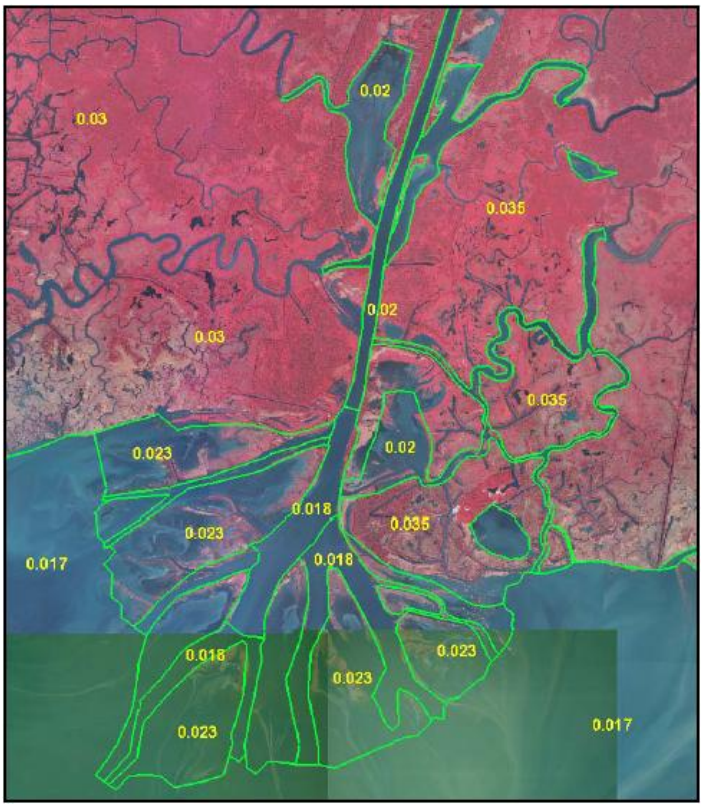

Figure 4-5: Manning's roughness values obtained in ADH model calibration used as initial roughness values (USACE 2010, Appendix A)

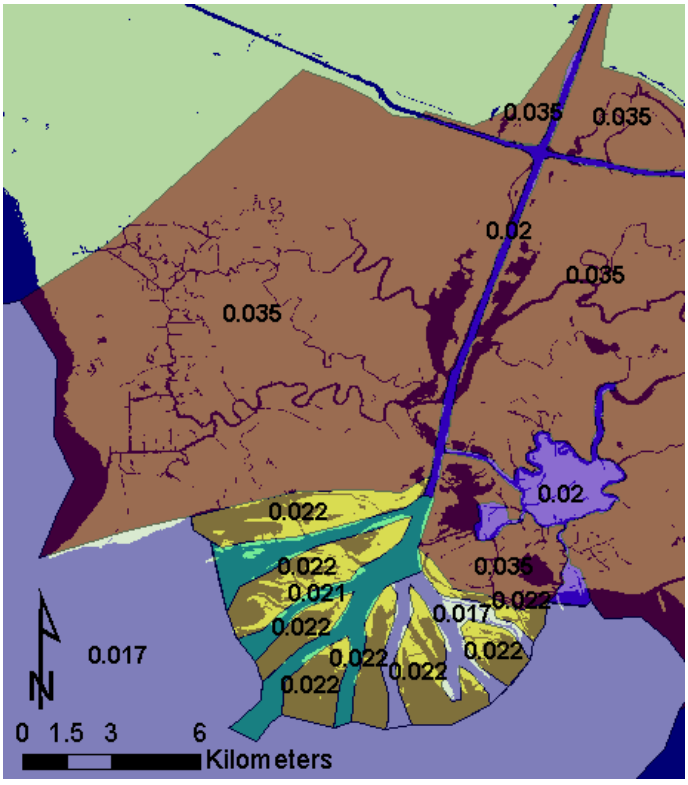

Figure 4-6: Manning's roughness values for calibrated model

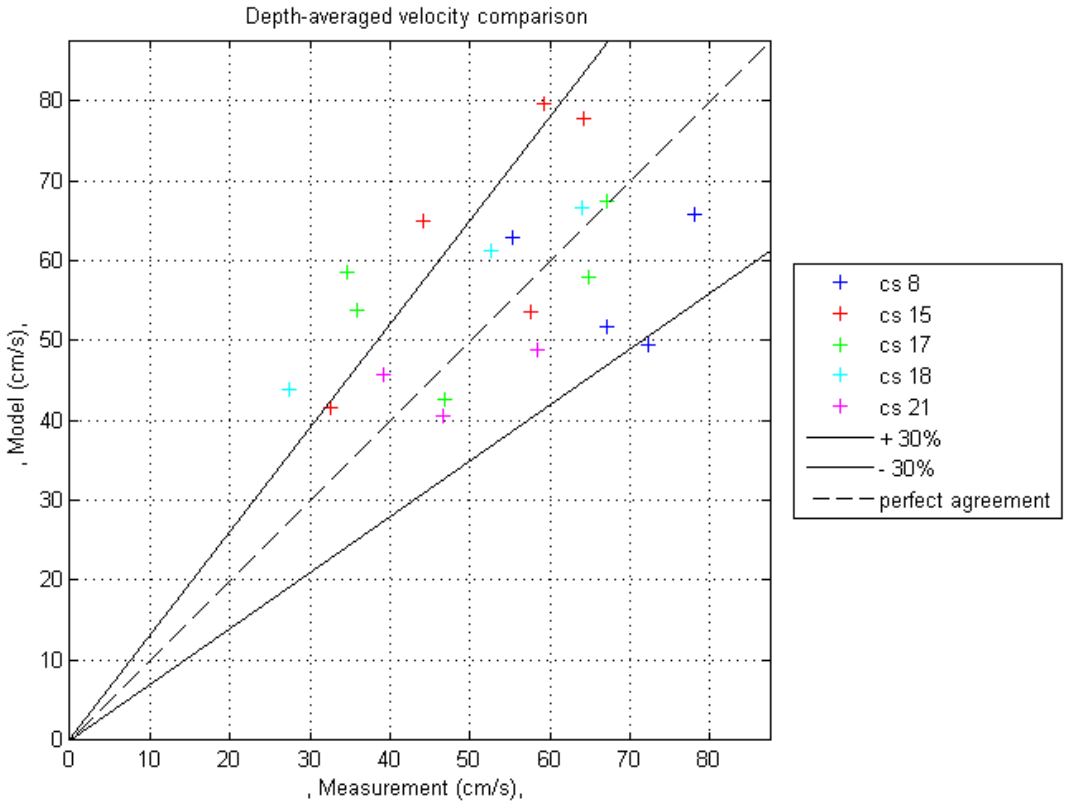

Figure 4-7: Measured vs. modeled depth-averaged velocities at each sample point for cross-sections used in calibration.

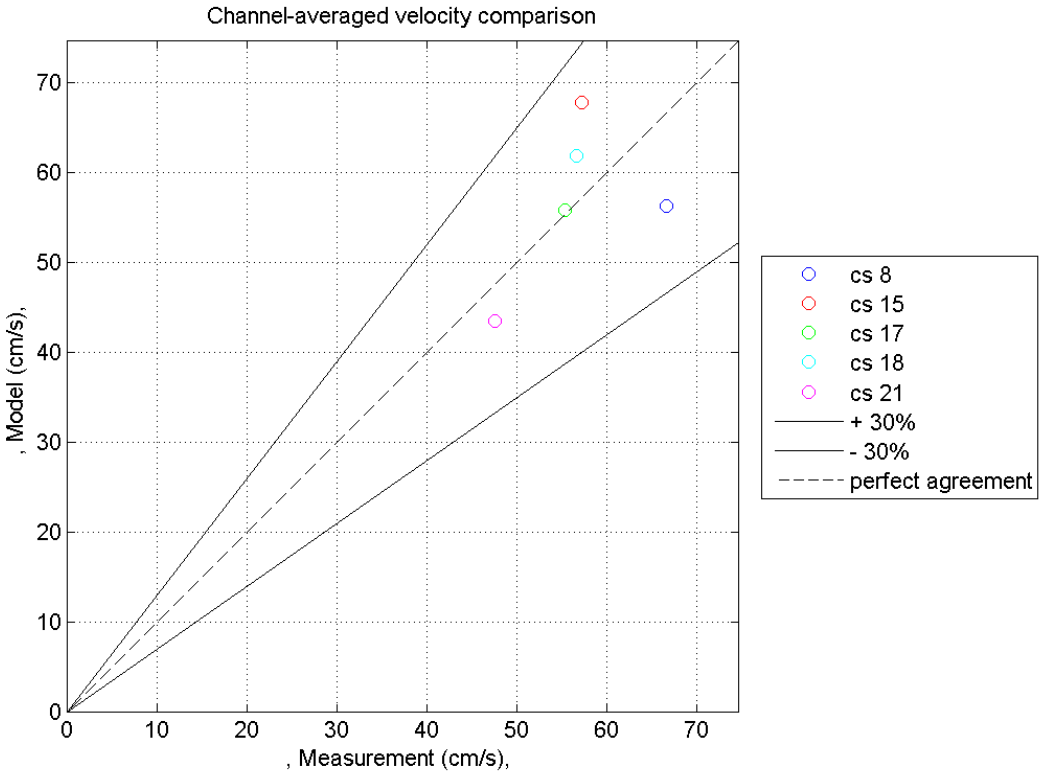

Figure 4-8: Measured vs. modeled channel-averaged velocity magnitudes for cross-sections used in calibration.

4.3 Transport Calibration

4.3.1 Transport Calibration Run Description

The simulation used to calibrate the model sediment transport employed the same hydrodynamic boundary conditions used in the hydrodynamic calibration. The basinward offshore boundary was kept at a constant water level of 0.32 m; the discharge through the upstream boundary was kept at a constant 4012 m^3/s with the addition of a constant inflow sediment concentration. Though the measurement period for the delta channel calibration data was from February 25 – 27, 2001, the closest upstream boundary sediment measurement available at the Calumet gage was from February, 21. The measured suspended sediment concentration at this point it time was 444 mg/l and the percent of the suspended load finer than .0625 mm was 87%; thus, the assigned model inflow concentrations for the calibration period were .333 mg/l mud and .111 mg/l fine sand. The suspended sediment concentration measurements by DuMars, 2002 were obtained according to the procedure outlined in the hydrodynamic calibration section above. Though grain size distributions obtained from each suspended sediment concentration measurement were presented in DuMars, 2002, the measured concentration was treated as the sum of all size fractions and no attempt was made to determine the proportion of each modeled fraction present in the measurements. Examination of the measurements indicated a very well-mixed system with no correlation of suspended sediment concentration to sample location, channel depth, or velocity (DuMars 2002). To calculate the observed transect-averaged suspended sediment concentration value used for comparison to simulated values, the three measurements at varying depths for each sample point were first depth-averaged using a weighted-averaging method based on the proportion of total depth represented by each depth measurement point. The measurements at .95 and .05 of the total depth were both given a weight of .275 and the measurement of at .5 of the total depth was given a weight of .45. Because concentration is not a vector quantity, the channel averaged value was obtained through simple arithmetic averaging. It is expected, however, that the method of averaging would have little impact on the calculated value given the near uniformity in measured and modeled depth-averaged concentration values over each transect. The model output includes depth-averaged concentration values for both grain-size fractions at each grid point, so the values for sand and mud fractions were extracted from the gridded results along each transect used in the calibration process. The two concentration values for each fraction at each output point were then summed to obtain total suspended sediment concentrations which were then averaged across the transect. As in the hydrodynamic calibration data processing, the concentrations were also averaged in the direct vicinity of each measurement point for direct comparison with observed values.

The measured depth-averaged suspended sediment concentrations in the delta distributaries range from approximately 600 to 800 mg/l, values that are much greater than the upstream input concentration. Because of this discrepancy, sediment from erosion of the upstream channel must be an important internal contribution to the sediment concentrations in the delta for this particular flood event. The eroded sediments' contribution to sediment delivery at the delta front during high flows places an increased importance on the initial bed composition. For the transport calibration simulations, the bed was composed of a uniformly-mixed 10 m think layer of .7 volume fraction sand and .3 volume fraction mud based on the findings that the Wax Lake Delta is composed of approximately 70% sand deposits (Roberts, Walker et al. 1997). The real distribution of sediment grain size in the modeled area is obviously more complex, but this was considered an adequate

approximation for calibration purposes. An adequate supply of both sediment fractions was insured by implementing the default bed schematization option; this treats the full bed thickness as a transport layer so that the order in which sediments are deposited or eroded is not preserved and the full sediment volume is available for erosion. Though the spatial distribution of sediment sizes may be altered through the simulation, the composition remains vertically uniform at each output point (Deltares 2009).

4.3.2 Calibrated Transport Parameter Results

Through successive model runs, the simulated suspended sediment concentrations in the delta distributaries were altered through variation of four sediment transport parameters: the Sus and Bed calibration factors in the Van Rijn non-cohesive transport formulation and the critical erosion (TcrEro) and sedimentation (TcrSed) shear stress values for cohesive sediment erosion and deposition. Initially, the non-cohesive transport calibration parameters were left unaltered from the default values of 1; whereas, the cohesive sediment transport critical shear stress values were taken from a calibrated one-dimensional, moveable-bed model of the full Lower Atchafalaya system (USACE 2010, Appendix D). The initial values of .09576 N/m^2 for TcrSed and .114912 N/m^2 for TcrEro were altered over multiple runs to obtain the final values of TcrSed=.07288 N/m^2 and TcrEro=.35 N/m^2. Additionally, the non-cohesive sediment transport calibration parameters Sus and Bed were raised to values of 2.5 and 1.5, respectively, to increase the total amount of sand transport. Because a restart file from a previous, similar run was used to ascribe spatially-varying initial conditions, the water levels, velocities, sediment concentration, and resulting suspended sediment transport reached a steady-state condition very quickly, and suspended sediment values were extracted after 3 days of simulation. Figure 4-9 below gives the depth-averaged total suspended sediment transport at various observation points throughout the model domain as a function of time; the locations of the observation points are given as well in figure 4-10.

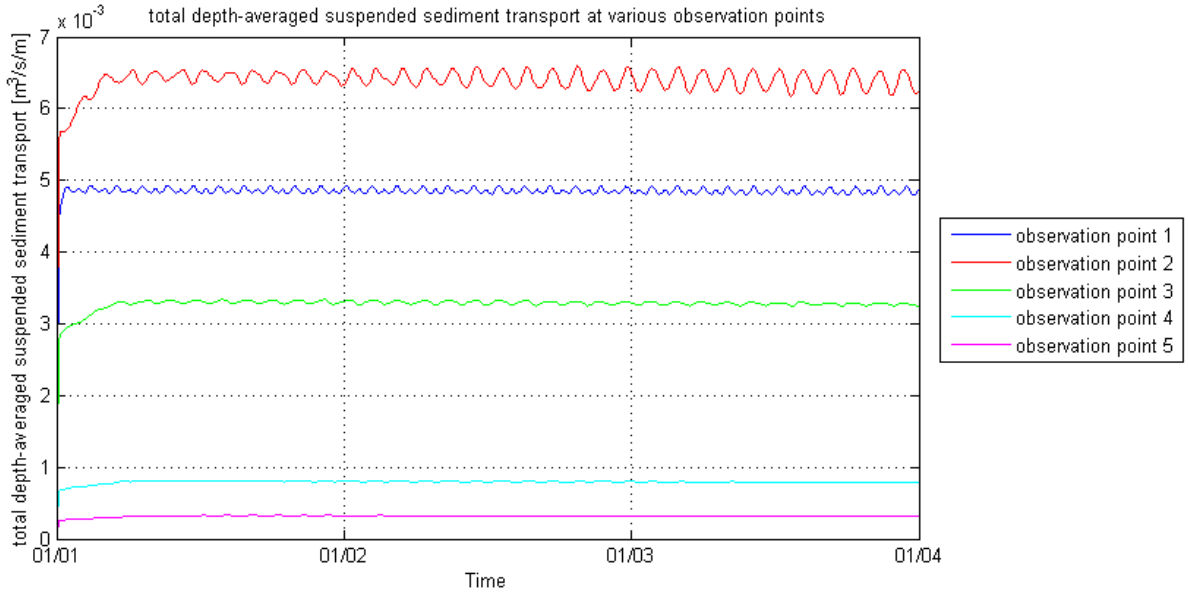

Figure 4-9: Total depth-averaged suspended sediment transport at various observation points within the model domain. Spin-up time to approximately steady-state conditions is very short due to spatially-varying initial conditions.

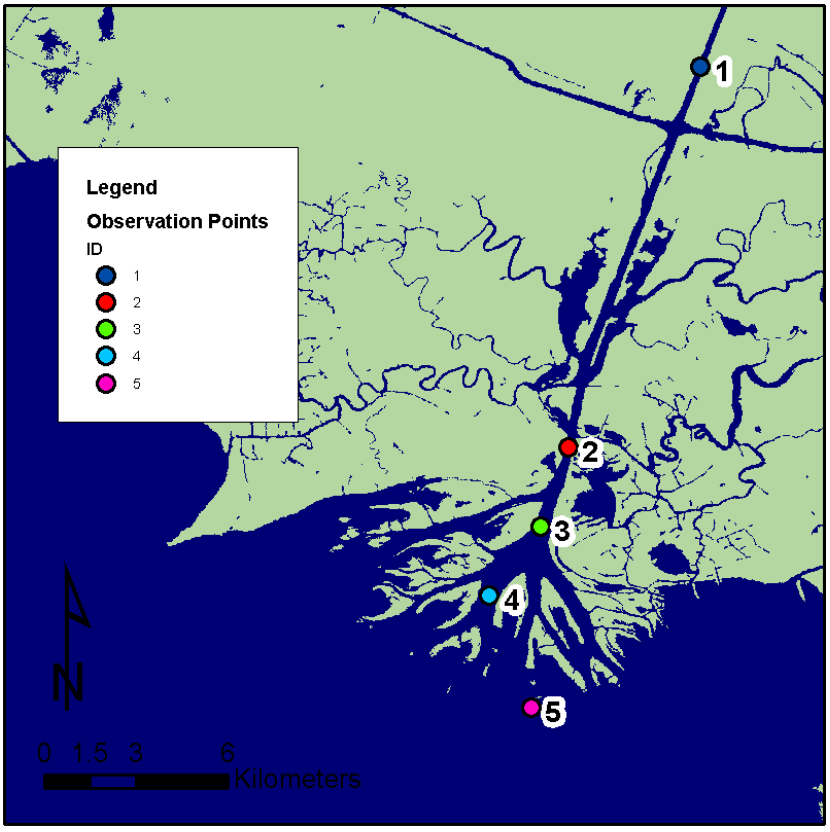

Figure 4-10: Location of observation points where the depth-averaged total suspended sediment transport was measured for figure 4-9

The modeled and observed depth-averaged total suspended sediment concentrations and channel-averaging results are given in Appendix B for all transects used in the calibration process, and a direct comparison of modeled and observed magnitudes at each measurement point is presented in figure 4-11 . Figure 4-12 compares the modeled and observed channel-averaged velocity magnitude for each cross-section. The mean difference between modeled and observed channel-averaged total suspended sediment concentration is 141.68 mg/l which corresponds to a mean percent error of 17.64%. Discrepancies between modeled and measured values are very low, with both channel-averaged values for all transects used in calibration (figure 4-12) and nearly all of the values at specific measurement points (figure 4-11) falling within the $\pm$ 30% error lines in the comparison plots.

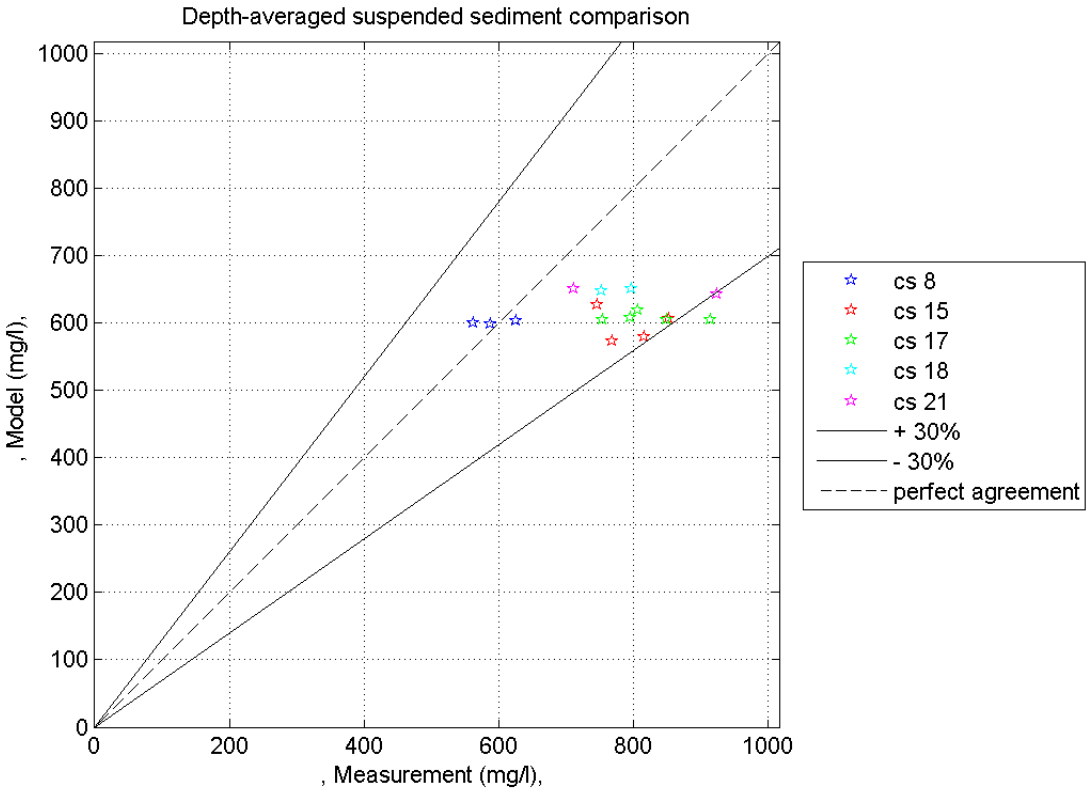

Figure 4-11: Measured vs. modeled depth-averaged total suspended sediment concentration at each sample point for cross-sections used in calibration.

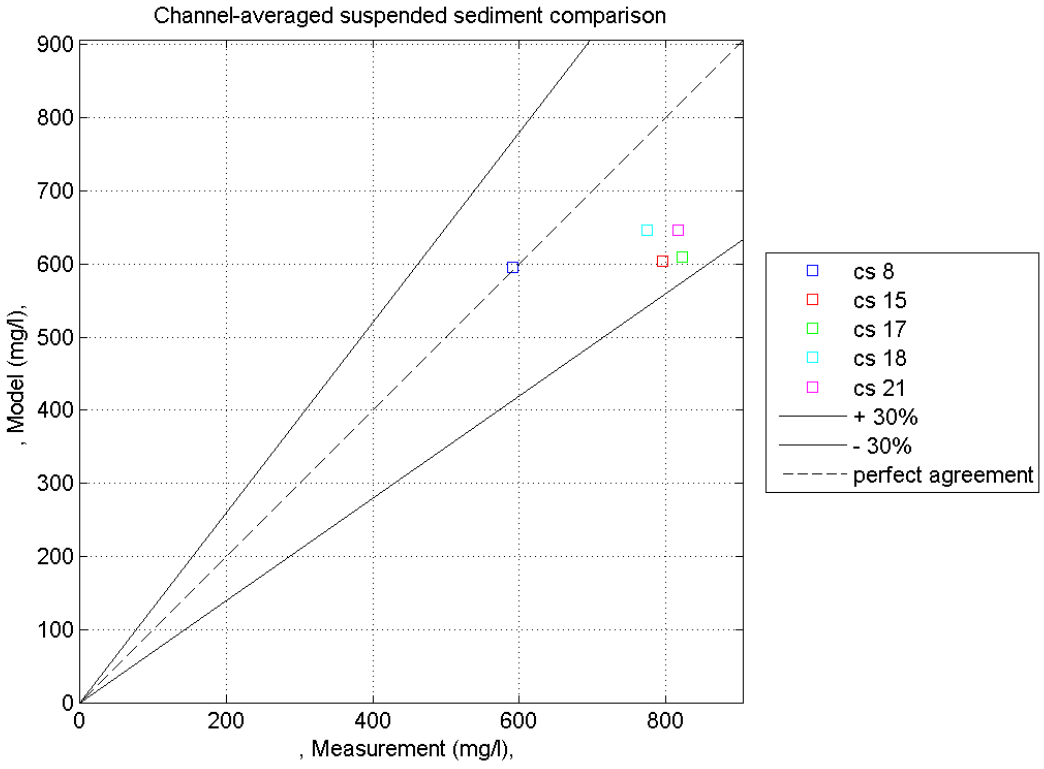

Figure 4-12: Measured vs. modeled channel-averaged total suspended sediment concentration for cross-sections used in calibration.

4.3.3 Critical Shear Stress for Deposition of Fine, Cohesive Sediment

Though a value was set for the TcrSed parameter during the calibration process, the use of a single, flood-condition calibration event does not offer a situation in which this parameter would have an effect on the suspended sediment concentrations in the delta distributary channels. In the Partheniades-Krone cohesive sediment erosion and deposition formulations used in Delft3D, deposition flux is dependent on the ratio of bed shear stress to the critical shear stress parameter, which also defines the maximum bed shear stress at which deposition will occur (Deltares 2009). Consequently, if the bed shear stress remains greater than the defined critical value in a situation where only currents contribute to bed shear stress (no waves or wave-current interactions), deposition of cohesive sediment fractions will not occur, and this parameter will have no effect on sediment concentrations in the flow channels. Field measurements of suspended sediment concentrations only exist along the certain channel transects pictured in figure 4-1, so no detailed field concentration data exists for portions of the model domain where cohesive sediment deposition could occur. Figure 4-13 below gives a plot of the maximum bed shear stress that occurs in the transport calibration simulation. It can be seen that shear stresses do not drop below the value necessary for deposition in any of the distributary channels and over most of the subaerial and subaqueous delta, so the critical shear stress for deposition should not have any effect on the modeled concentrations at the comparison transects. The choice of a TcrSed value is thus somewhat arbitrary, though the calibrated value is very similar to other values used for cohesive sediment in the study area in other modeling studies (USACE 2010, Appendix D).

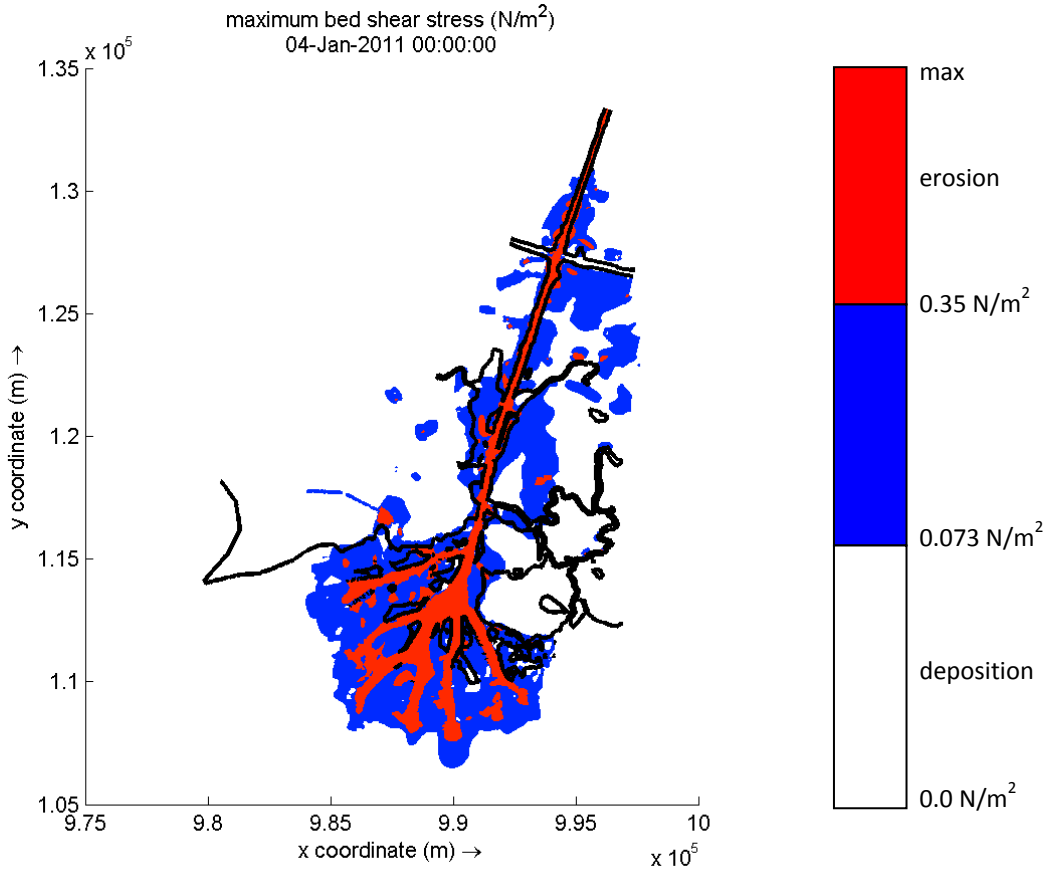

Figure 4-13: Plot of the spatial distribution of maximum bed shear stress that occurred during the transport calibration simulation. The thick black line marks the 0 m contour for the model bathymetry. Red areas indicate that bed shear stress exceeds the critical shear stress for erosion, blue areas indicate that bed shear stress is between the critical shear for erosion and deposition, and white areas indicate that bed shear stress is below the critical shear for deposition.

4.3.4 Contributions of Suspended Sand, Suspended Mud, and Bedload to Total Transport

The parameters controlling the erosion of fine, cohesive sediment are the most relevant to the total suspended sediment concentrations in the distal distributary channels of the fine sediment suspended load dominant Wax Lake Outlet (Roberts, Walker et al. 1997); however, the fine sand typically carried as bedload can be entrained as suspended load in significant quantities during high flows (Roberts, Adams et al. 1980) so non-cohesive transport calibration is important for accurate representation of the suspended sediment load. Transport calibration was performed based on the sum of the two sediment fractions' concentrations, but the accurate proportioning of the load between sand and mud fractions can be verified from the findings of previous studies on the Lower Atchafalaya River system. Long term suspended sediment measurements near the point of diversion from the Mississippi River indicate an average 17% sand contribution to the suspended load with the proportion of sand load increasing with increasing discharge (Allison, Kineke et al. 2000). Figure 4-14 below shows the mean total suspended sediment transport magnitude, mean sand suspended transport magnitude, and mean mud transport magnitude along the main channel centerline from the model upstream boundary to the approximate location of the delta front. Figure 4-15 shows the suspended sand transport and bedload transport magnitudes as a proportion of the total suspended sediment transport. Though the mean proportion of suspended sand transport to the total suspended transport is less than 17%, the location specific transport proportions are closer to this

value in the upstream reach of the channel but drop well below in the delta distributaries where flow velocity rapidly decreases. No information on bedload transport rates in the Wax Lake Outlet and delta is available, so the only means of assessing the validity of the modeled bedload transport is comparison with measurements in other rivers. Nittrouer et al., 2008, computed bedform transport rates in the Lower Mississippi River at four reaches downriver of New Orleans and found that yearly-averaged bedload transport rates are approximately 2.5% of the yearly-averaged total suspended sediment transport (Nittrouer, Allison et al. 2008). The mean bedload transport rate over the channel centerline distance is an order of magnitude less than the 2.5% in the Mississippi; however, this value is an annual average so it is possible that much greater rates would occur in the model with larger floods. Additionally, bedload transport rates as a proportion of the total suspended sediment transport in the Wax Lake Outlet could be fundamentally different from the proportion observed in the Lower Mississippi due to the substantial differences in channel geometry and discharge.

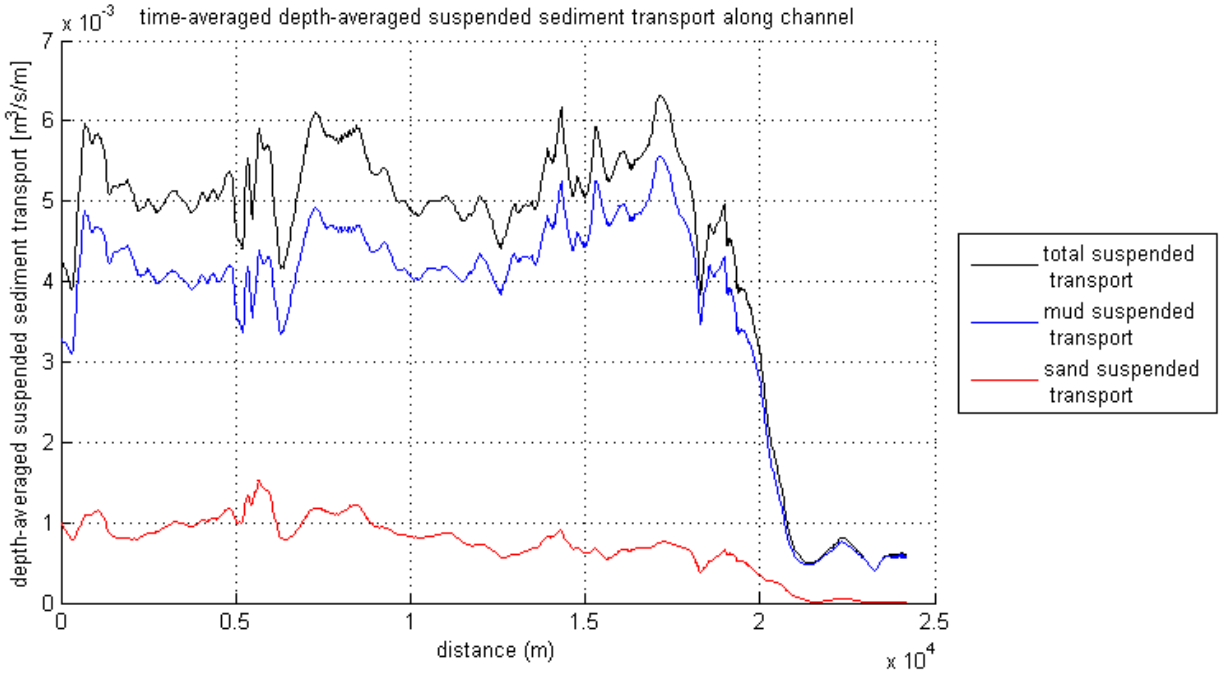

Figure 4-14: Time-averaged depth-averaged suspended sediment transport along the Wax Lake Outlet and Delta main channel centerline

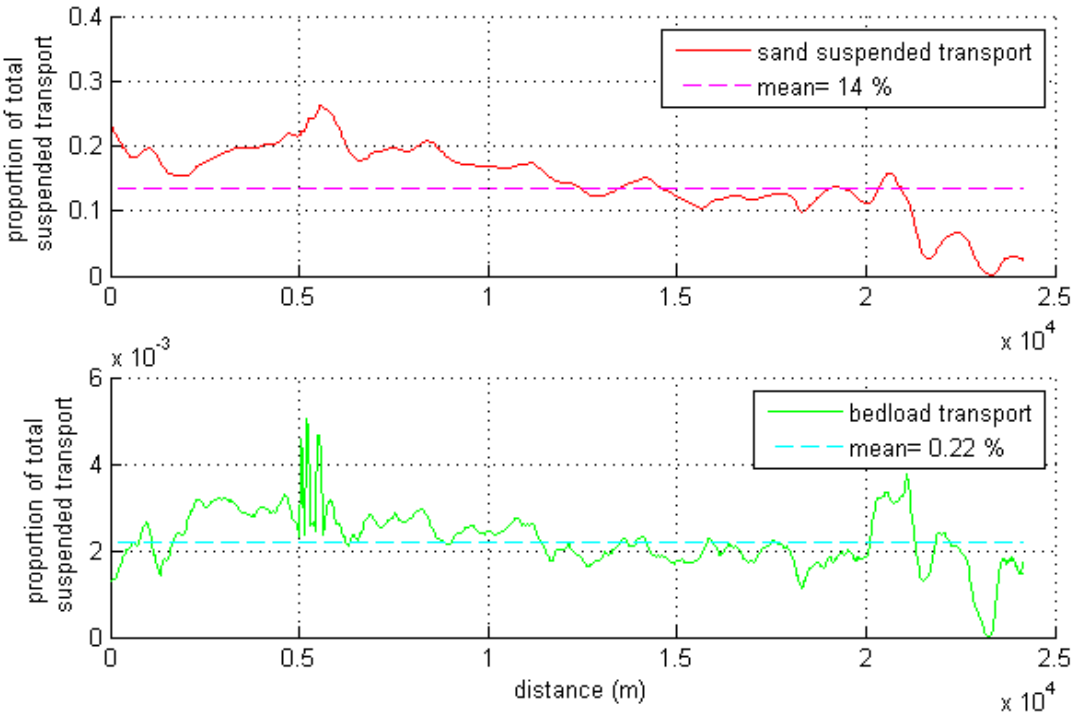

Figure 4-15: Plot of suspended sand transport and bedload transport as a proportion of the total suspended sediment transport along the Wax Lake Outlet and Delta main channel centerline

The calibration process for model sediment transport was based only on combined channel- and depth-averaged suspended sediment concentrations along transects of the delta distributary channels during a discreet period of constant discharge. Though no measurements were available to assess the accurate simulation of transport by sediment fraction or bedload transport, the reasonableness of the model performance in these areas was established through comparisons with each transport mode's contribution to total transport in similar situations.

5. Long-term Morphologic Simulation

The following sections details the actual implementation of the already set-up and calibrated Wax Lake Delta model to attempt to reproduce the observed prototype long-term morphological development for a period of five years beginning in 1998 (see figure 3-14). Specific implementation aspects necessary for the long-term simulation including the sequencing of boundary conditions, morphologic acceleration techniques, and required deviation from calibrated parameter values are discussed. The resulting morphology and stratigraphy at the conclusion of the simulation are briefly presented. A more in depth analysis of the model results is given in chapter 6. This subsequent chapter examines the results in light of the general delta features and forming mechanisms and the specific features and development observed in the Wax Lake and Atchafalaya Deltas. A substantial discussion of the effects of varying upstream boundary conditions is also included.

5.1 Model Description

5.1.1 Morphological Acceleration Factor

In addition to the boundary condition input reduction described in the flow and transport regime schematization, acceleration of the morphodynamic changes can also be used to simulate long term morphologic development with realistic model run times. An inherent difficulty in simulating morphologic change with process-based models (bed level changes are controlled by sediment transport and hydrodynamics without use of any empirical or equilibrium relations) is the difference between morphodynamic and hydraulic timescales (Deltares 2009). Morphodynamic changes occur over years to decades (e.g. the formation of a delta) but are controlled by flows that vary over much shorter timescales (tides or the annual flood cycle). In Delft3D, a morphologic acceleration/upscaling factor (MorFac) is available to resolve the difference in timescales; at each time step, the bed sediment flux is multiplied by a constant factor which effectively increases the simulated morphologic timestep from the hydrodynamic time step to that time step times the MorFac (Lesser, Roelvink et al. 2004). Figure 5-1 conceptually summarizes the use of a MorFac in a typical process-based morphologic model. The MorFac acceleration technique allows for simulation of long morphologic time scales with short time steps, and the coupling of bathymetry and flow changes on the same time step eases the modeling of complex flow-morphology feedback processes (Roelvink 2006).

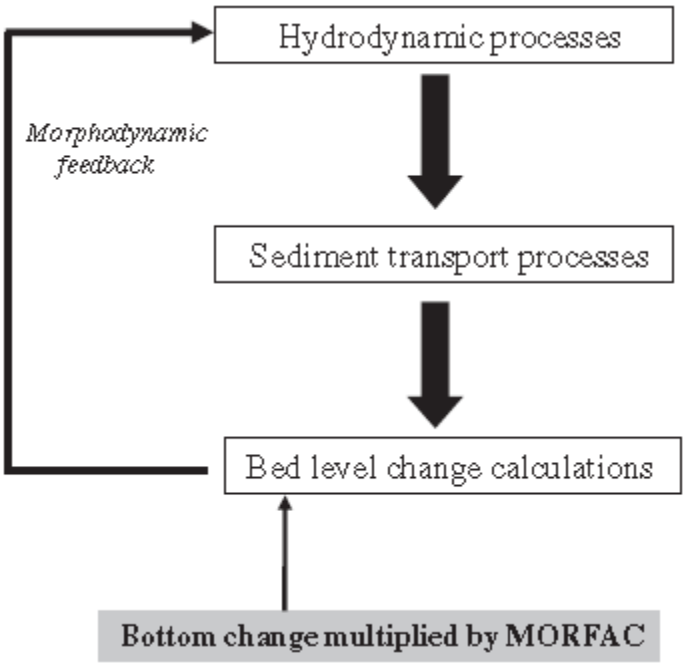

Figure 5-1: Conceptual description of the use of a morphologic acceleration factor (MorFac) in a process-based morphologic model (Ranasinghe, Swinkels et al.)

Despite the clear advantage of using morphologic acceleration techniques for long-term simulations, quantitative guidance for choosing maximum MorFac values (that minimize simulated hydrodynamic time and corresponding model run time) is mostly absent, so the selection of a valid value is reliant on judgment through sensitivity testing and experience (Lesser, Roelvink et al. 2004). Delft3D has been used in several conceptual delta models and studies on delta-forming processes (see sections 2.2 and 2.3), so previous experience can offer some indication of valid upper MorFac limits for simulating delta development. Table 5-1 summarizes the MorFac used for each study. Additionally, sensitivity testing in the model development for Edmonds and Slingerland, 2007 found that the process of mouth bar formation is independent of the morphologic acceleration factor for values below 200, so it is assumed that this is the limiting case for the validity of delta development simulations as mouth bar formation is the primary forming process for river-dominant systems (Edmonds and Slingerland 2007).

Table 5-1: Morphologic acceleration factors (MorFac) used in Delft3D conceptual delta development and delta-forming process models.

Reference	Study Subject	MorFac
Edmonds and Slingerland, 2007	High-resolution, 3-D model of conceptual mouth bar formation	75
Edmonds and Slingerland, 2009	Delta development dependence on cohesion	175
Storms, Stive, et al., 2007	River-dominant conceptual delta development	50
Geleynse, Storms et al. 2010	Conceptual modeling of mixed-load, fluvio-deltaic system	60
Geleynse, Storms et al. 2011	Conceptual delta development with various basin forcings and initial stratigraphy	60

To simulate a year of morphologic change within the simulation period, each constant boundary condition level was applied for a multiple of 24-hours; a varying MorFac was applied to upscale the hydrodynamic simulation time to a full year of morphologic change. MorFac values of 45, 67.3, 34, and 17 were used to upscale the low flow, annual flood, 2-year flood, and 5-year flood discharge levels to their respective average year durations of 45 days, 269 days, 34 days, and 17 days. The discharge levels, corresponding MorFac values, and average morphologic year durations are given in table 5-2.

Table 5-2: Discharge level hydrodynamic and morphologic times of occurrence

Discharge Level	Discharge (m^3/s)	Hydrodynamic days (day)	MorFac	Morphologic days (day)
Low-flow	1149.7	1	45	45
Annual flood	2961.94	4	67.3	269
2-yr flood	5077.21	1	34	34
5-yr flood	5977.69	1	17	17

5.1.2 Flow Sequencing

The discharge regime recorded over 24 years of measurement at the Wax Lake Outlet at Calumet, LA gage has been schematized into four periods of constant discharge that approximate the variation in boundary conditions in a typical year. Durations for each flow have also been determined based on flow frequency of occurrence scaled to reflect sediment transport –discharge functionality. In the interests of simplicity and shorter run times, an idealized hydrograph sequence with low flows increasing to the highest discharge level at mid-year then decreasing again to low flows at the yearend was not used; rather, the four flows occurring each morphological year were applied one after the other, increasing stepwise from the lowest discharge (low flow) to the highest (five year flood) in each year cycle. Additionally, a one hydrodynamic day transition period of linearly increasing flow was including between each period of constant flow to minimize the large oscillations that could occur from abrupt flow changes; the morphological impact of any possible unrealistic oscillations resulting from these transition periods was negated by implementing a MorFac of zero between constant discharge periods. Setting the morphological acceleration factor to zero effectively turns off bed updating so that flows can develop without effect on bathymetry or bed composition. Figure 5-2 below gives the discharge sequence and accompanying morphological acceleration factor for one year of morphologic simulation. This sequence was repeated a total of five times for the full five year simulation.

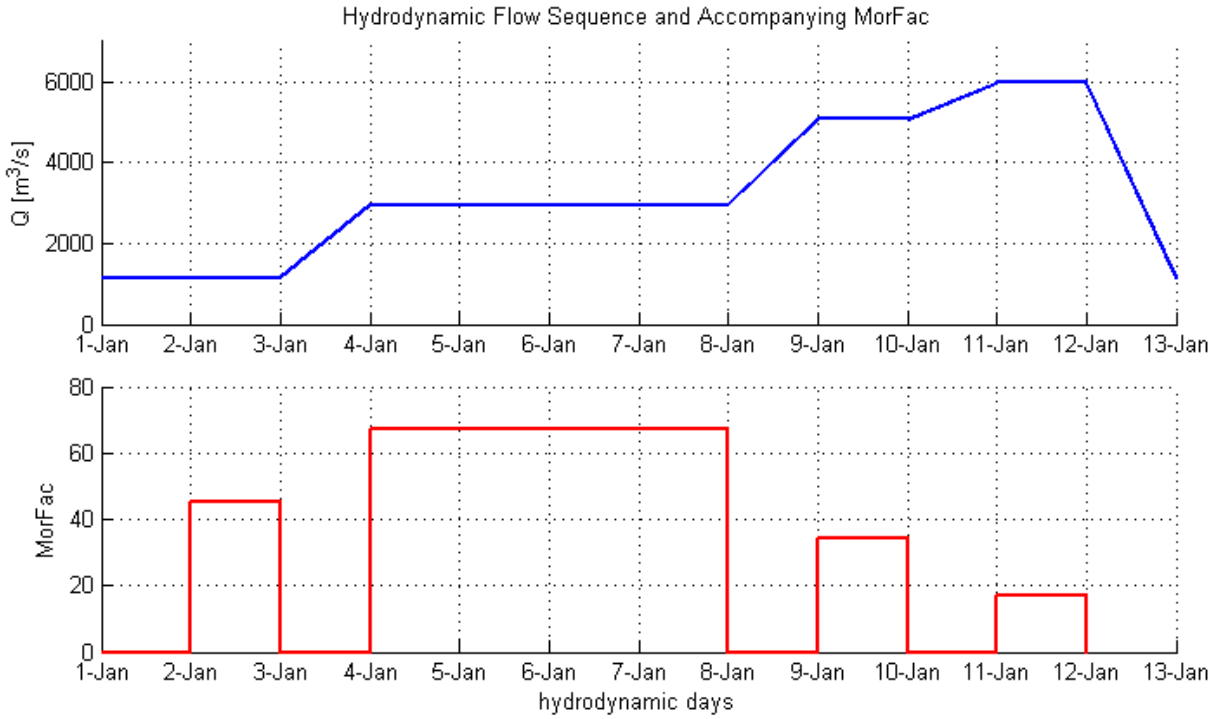

Figure 5-2: Sequence of discharge and accompanying morphological acceleration factor (MorFac) for one hydrodynamic year in simulation period. This sequence was repeated a total of five times for the full 5 year morphologic simulation.

5.1.3 Alteration of Calibration Parameters

In the course of multiple long-term morphology simulation trials, it became evident that some of the parameters whose values were established in the transport calibration phase would need to be altered to produce more realistic morphologic results. Preliminary runs could not complete the full simulation due to excessive deposition in the first grid cells directly downstream from the upstream boundary. Thus, instead of assigning a sand concentration boundary condition dependent on the discharge through a functional relationship derived from historical measurements, a zero-gradient in sand suspended sediment concentration across the boundary is maintained. Inflow suspended sand concentration is set equal to the suspended sand concentration in the first grid cell, so a near-equilibrium concentration enters the model and inhibits excessive bed level change near the boundary (Deltares 2009).

Subsequent runs and the resulting morphology were characterized by excessive channel narrowing and deepening, with incision in the main channel so significant as to fully erode the ten-meter initial sediment layer and reach the inerodible basement. The already substantial suspended sediment load augmented with the eroded channel sediments contributes to unrealistic deposition in the delta and receiving basin. The existing delta lobes experience excessive upstream accretion and subaqueous levee growth that together serve to continually decrease delta distributary channel widths. Though upstream accretion and continued levee development have been identified as important processes in the growth of the more mature Atchafalaya Delta (van Heerden and Roberts 1988), the degree to which this occurred in preliminary runs is obviously unrealistic. Additionally, excessive deposition of suspended cohesive sediments in the area basin-ward of the delta front succeeds in establishing large, subaerial mud depositional lobes. The establishment of new

depositional lobes is a key morphological development in the simulation period; however, these deposits are primarily composed of sand and form at the distal distributary mouths (Wellner, Beaubouef et al. 2005).

In an effort to reduce the unrealistic channel narrowing and mud deposition, the sediment transport parameters obtained in the calibration process were subsequently altered. The volume of cohesive sediment eroded from the upstream channel and the volume deposited basinward of the delta front could both be altered by raising and lowering the critical shear stress for erosion and the critical shear stress for deposition, respectively. For production five-year morphological change simulations, the TcrEro parameter was raised from .35 N/m^2 to .5 N/m^2, and the TcrSed parameter was reduced from .07288 N/m^2 to .05 N/m^2. Because the upstream lobe accretion and levee expansion responsible for excessive channel narrowing is driven by non-cohesive sand deposition, the transport of this sediment fraction was reduced by changing the Sus calibration parameter from 2.5 to .75 and the Bed calibration parameter from 1.5 to 1.

The need to alter calibrated transport parameters for more accurate long term morphological development simulation is especially justified considering the very limited nature of the calibration. The difficulty in calibrating the TcrSed parameter from the limited field measurement data has already been discussed, so the long term simulation and the resulting depositional patterns offer a much more robust means of assessment to find a suitable value. A hysteresis in sediment loading during flood periods has been documented for both the Lower Mississippi and Atchafalaya River near its diversion from the Mississippi (Mossa 1996; Mashriqui 2003). Peak sediment concentrations occur during the rising portion of the flood hydrograph before peak discharges; the time lag between peak concentration and discharge generally decreases with decreasing flood magnitude. It is likely that this phenomenon also occurs in the lowermost portion of the Atchafalaya system at the Wax Lake Outlet and the Atchafalaya River below Morgan City, LA; however, the relatively infrequent concurrent sediment-discharge measurements at gage locations in these reaches have been unable to definitively capture a consistent lag (Mashriqui 2003). Still, the effect may not be as pronounced in the lowermost reaches of large rivers, where resuspension of deposited fine sediments contributes to concurrent sediment and discharge peaks (Mossa 1996). The flood measurement period used for calibration (DuMars 2002) occurs during the rising limb of the flood hydrograph, so sediment concentrations are expected to be greater than for the same discharge occurring on the falling limb. The approximately weeklong gap between the sediment concentration measurements used as an upstream boundary condition and the downstream measurements used for calibration could also be responsible for the calibrated parameters that favor greater erosion in the Wax Lake Outlet channel than what may have actually occurred. Whether or not a hysteresis in sediment concentrations actually exists at the upstream boundary of the model, the sediment dynamics are complex, and any attempt at calibration based on a steady-state case that does not take into account the time relative to sediment-discharge peaks and previous fine-sediment channel deposition is clearly an approximate approach.

5.1.4 Initial Stratigraphy

In an effort to further reduce the unrealistic mud deposition described in the previous section, the initial bed composition was changed from the uniform .7 volume fraction sand and .3 volume fraction mud mixture used in the transport calibration phase. The initial sediment layer prescribed in

the calibration scenarios, in addition to being uniformly mixed in the vertical, was also spatially uniform across the full model domain. In all simulations, this uniform distribution was quickly altered by preferential erosion and deposition of the two modeled sediment fractions. Both the main Wax Lake Outlet channel's and the delta distributary channels' beds become sand dominant, with the fine cohesive mud fraction being preferentially depleted with channel incision. Pro-delta deposition of the primarily mud suspended load increases the mud volume fraction directly basinward of the delta. The initial use of a uniformly-mixed, uniformly distributed bed was driven by the ease of implementation; however, the simulated sediment redistribution as well as the real observed distribution of sediment fractions in the wax lake delta (DuMars 2002; Wellner, Beaubouef et al. 2005) suggest that an initially non-spatially uniform sediment distribution is a much better approximation.

For the long-term morphology simulation, an initial sediment distribution that better reflects the expected redistribution was used to avoid unrealistic erosion and resulting fine sediment loads resulting from beds composed of more fine sediment than in reality. The basis for the new initial bed condition was derived from the results from a previous preliminary run, where bed levels were kept constant but the two sediment fractions' respective volumetric fraction in each grid cell could change to reflect calculated sediment fluxes. Though the redistribution from the initial spatially-uniform configuration was only evident in the first few layers of this multiple bed layer simulation, the initial bed configuration for the long-term simulation assigned the resultant sediment fractions in the top layer to the full sediment thickness, resulting in a vertically-uniform but spatially-varying bed sediment distribution. Figure 5-3 below gives the spatial distribution of the sand volume fraction in the model domain; as only two fractions are used, the remaining volume fraction from what is shown is mud. Figure 5-4 demonstrates the vertically-uniform nature of the initial bed composition and spatially-uniform 10 m thickness with dip (from main channel upstream of distributary bifurcations through delta to basin, roughly parallel to main channel) and strike (across delta, roughly perpendicular to main channel) stratigraphic sections, the locations of which are presented as thick white lines overlaying the spatial distribution of sediment fractions in figure 5-3.

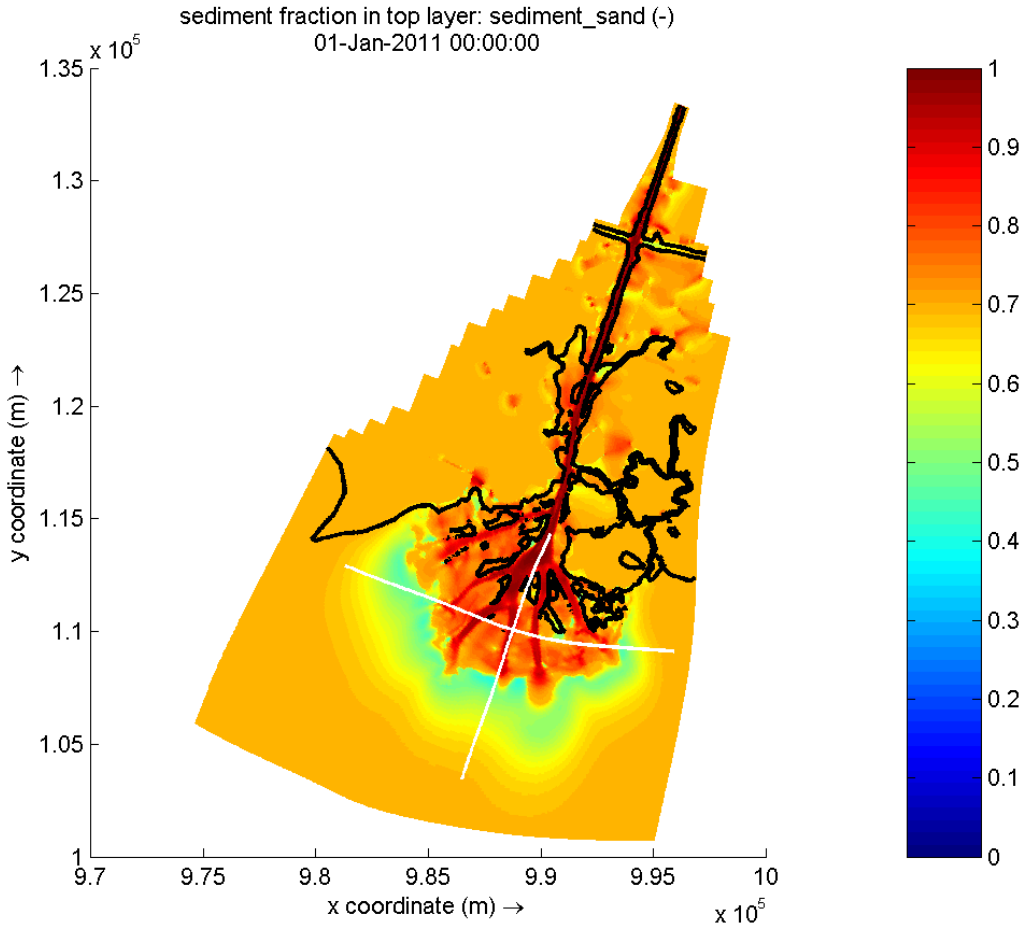

Figure 5-3: Spatial distribution of sand volume fraction for initial bed configuration used in the long-term morphology simulation. As only two sediment fractions are used, the mud volume fraction at each point is equal to one minus the sand fraction. The thick black line represents the 0 m contour line of the model bathymetry. The two white lines mark the locations of the dip and strike stratigraphy sections presented in figure 5-4 below.

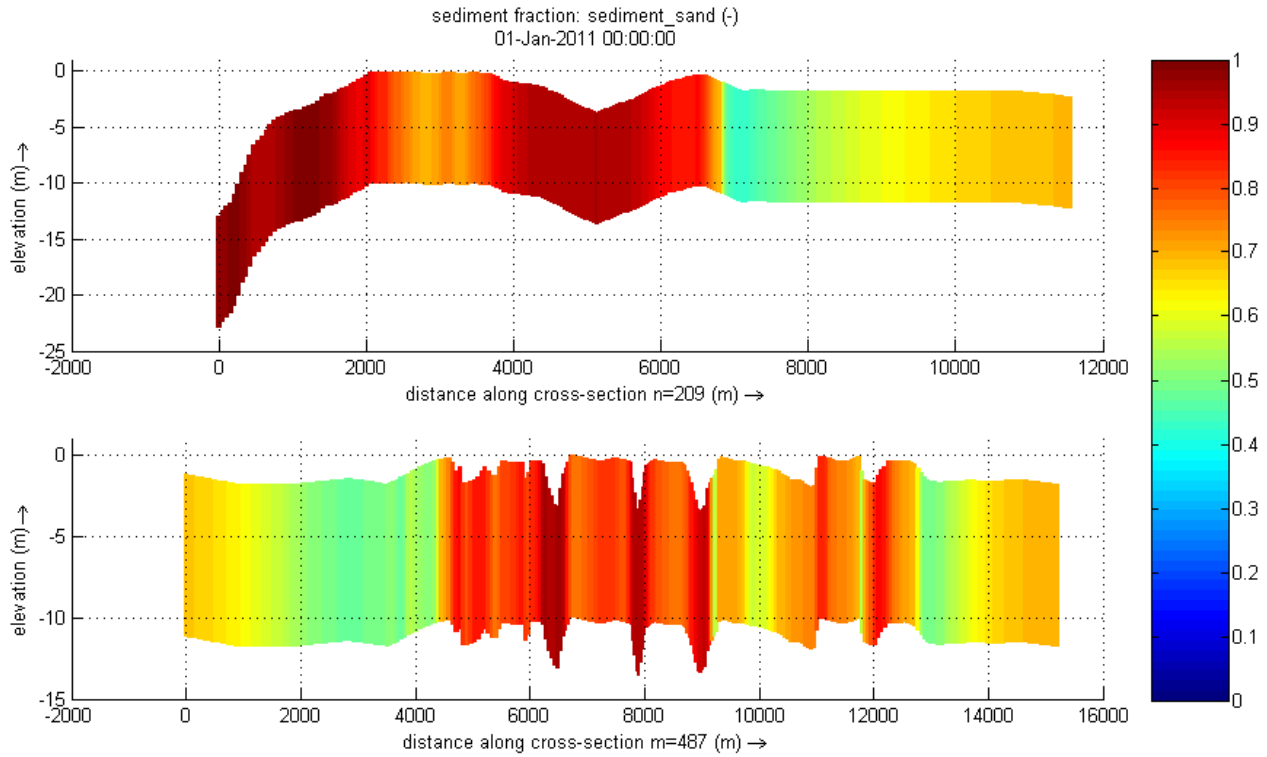

Figure 5-4: Initial delta bed composition by sand volume fraction along dip (upper plot) and strike (lower plot) sections located at the white lines in figure 5-3 above. Note that both the vertical and horizontal scales are different in the two subplots.

The ability to model the stratigraphy of any morphological development with multiple sediment fractions has been an important development, especially for validation of accurate simulation in conceptual delta models. Mouth bar formation and subsequent channel bifurcation is the primary mechanism of delta formation in river-dominant settings, and theoretical stratigraphic sequences for these features have been proposed in literature (Wright 1977) and validated in conceptual delta formation models (Storms, Stive et al. 2007) and field coring of representative deltas (van Heerden and Roberts 1988; Wellner, Beaubouef et al. 2005). To be able to assess the stratigraphy of the resultant depositional bodies in the five year long-term morphology simulation, the second bed schematization method available in Delft3D was utilized (see section 3.1 for a more detailed discussion of bed representation in Delft3D). The schematization represents the bed with fifty .1 m thick bookkeeping underlayers, a well-mixed base layer of variable thickness, and a .2 m thick active transport layer. The high resolution vertical schematization allows for the preservation of detailed information on the depositional history of each sediment fraction in the uppermost five meters of the movable bed. The use of a well-mixed, variable thickness base layer below the upper five meters implies that detail on depositional sequences will be lost as the lowermost bookkeeping layer is incorporated into the base layer; however, this should not be an issue as the Wax Lake Delta progrades into the very shallow Atchafalaya Basin where accommodation space for deposition does not exceed five meters.

5.2 Results

The main purpose of this study is to simulate the morphological development of the Wax Lake Delta over the five year period from January, 1998 to December, 2002. The model whose development,

calibration, and boundary condition formulation is described in previous sections was used for the long-term morphologic simulation. The following sections will give a broad overview of the morphological development after five years of simulation. The main delta features and some observed trends will be presented; specific analysis of the simulation validity, detailed process information, and examination of results in light of specific Wax Lake Delta studies and conceptual delta development will follow in chapter 6.

5.2.1 Overview of Simulated Morphology

The bathymetry of the full model domain after the five year simulation is given below in figure 5-5 followed by a three-dimensional representation. The model is generally successful in producing a typical river-dominant delta morphology that maintains the delta's radial symmetry through basinward formation of elongate depositional lobes. Persistent and massive erosion in the main Wax Lake Outlet channel significantly increases the overall bathymetric gradient in the modeled area, so more refined visualization is necessary to discern the more subtle bathymetric changes and depositional features in the delta and receiving basin.

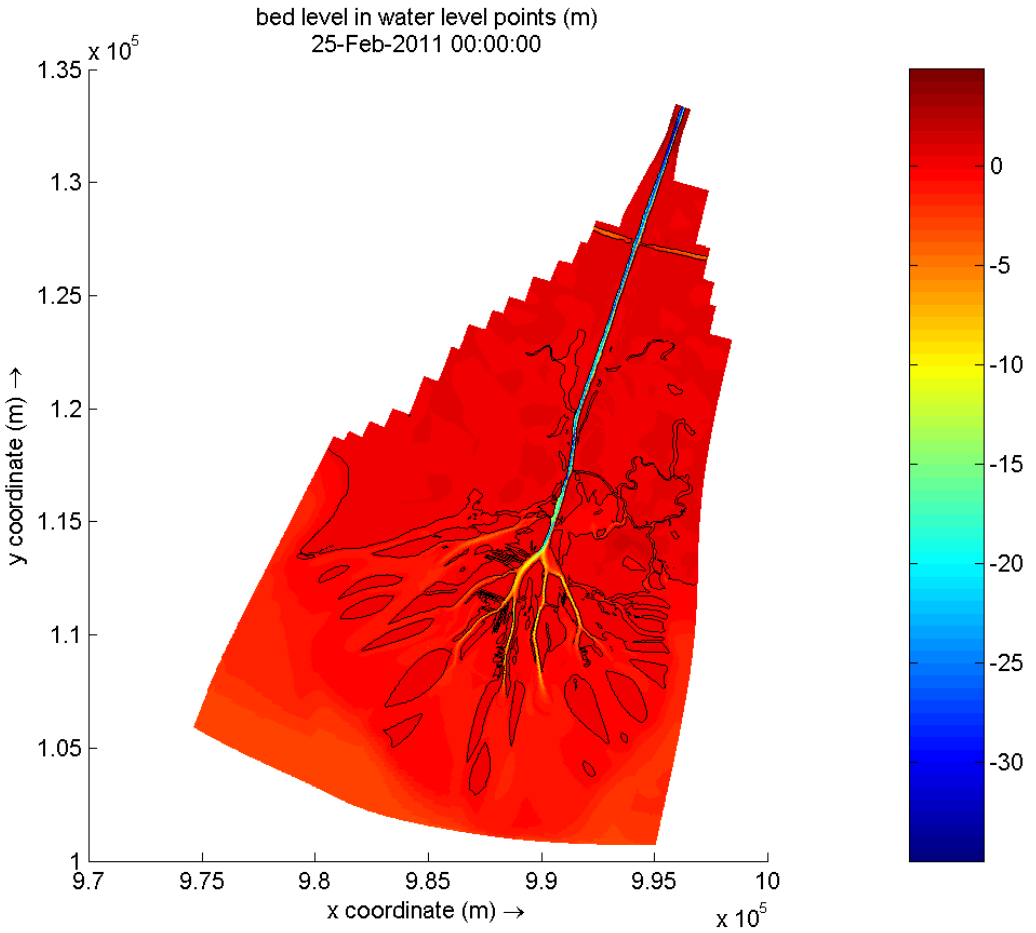

Figure 5-5: Bathymetry of full model domain after five years of morphologic simulation along with 0 m contour line. The date in the title marks the final hydrodynamic simulation time; morphodynamic acceleration techniques allow a nearly two month hydrodynamic simulation to represent five years of morphological development.

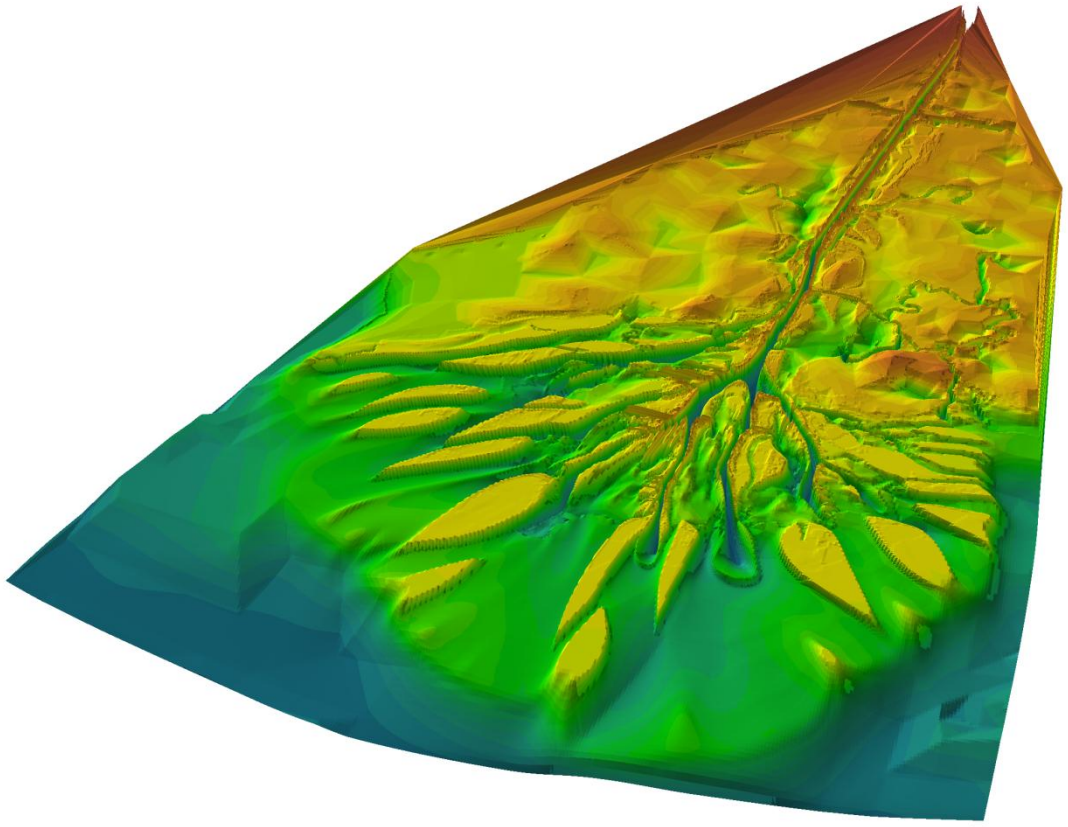

Figure 5-6: 3-D representation of the final morphology after the five year simulation with 250x vertical exaggeration. Note that the higher elevations to the East and West of the Wax Lake Outlet that lie outside the modeled area are unrealistic, a result of surface creation through triangulation.

Figure 5-7 below presents a more focused view of the final bathymetry in the delta and receiving basin. The limits of the color map were intentionally set at 0 m and -10 m so that the elevations between these limits that dominate the delta expansion would be shown with more precision. The white line is the 0 m contour, so any area bounded by the line could have a higher elevation that is not reflected by the color; similarly, areas that are the darkest shade of blue represented in the color map may have depths that exceed what is implied by the color due to the defined lower limit. The most dramatic morphological changes that were modeled in the simulation period include the development of multiple, sub-aerial depositional lobes basinward of the original delta front location, significant distributary channel incision and narrowing, and incipient jet deposit forms at the distal ends of the two major channels that do not evolve into fully-developed mouth bars. Figure 5-8 shows the cumulative erosion and deposition that occurred in the delta area and receiving basin over the course of the five year simulation and identifies representative locations of the main features/morphological developments just described. Again due to the very high magnitudes of erosion and deposition that occur in the main channel with incision and narrowing, less extreme values are shown with less precision; consequently, areas with morphological change of magnitudes less than approximately one meter are still identified in the figure as white areas of zero erosion/deposition.

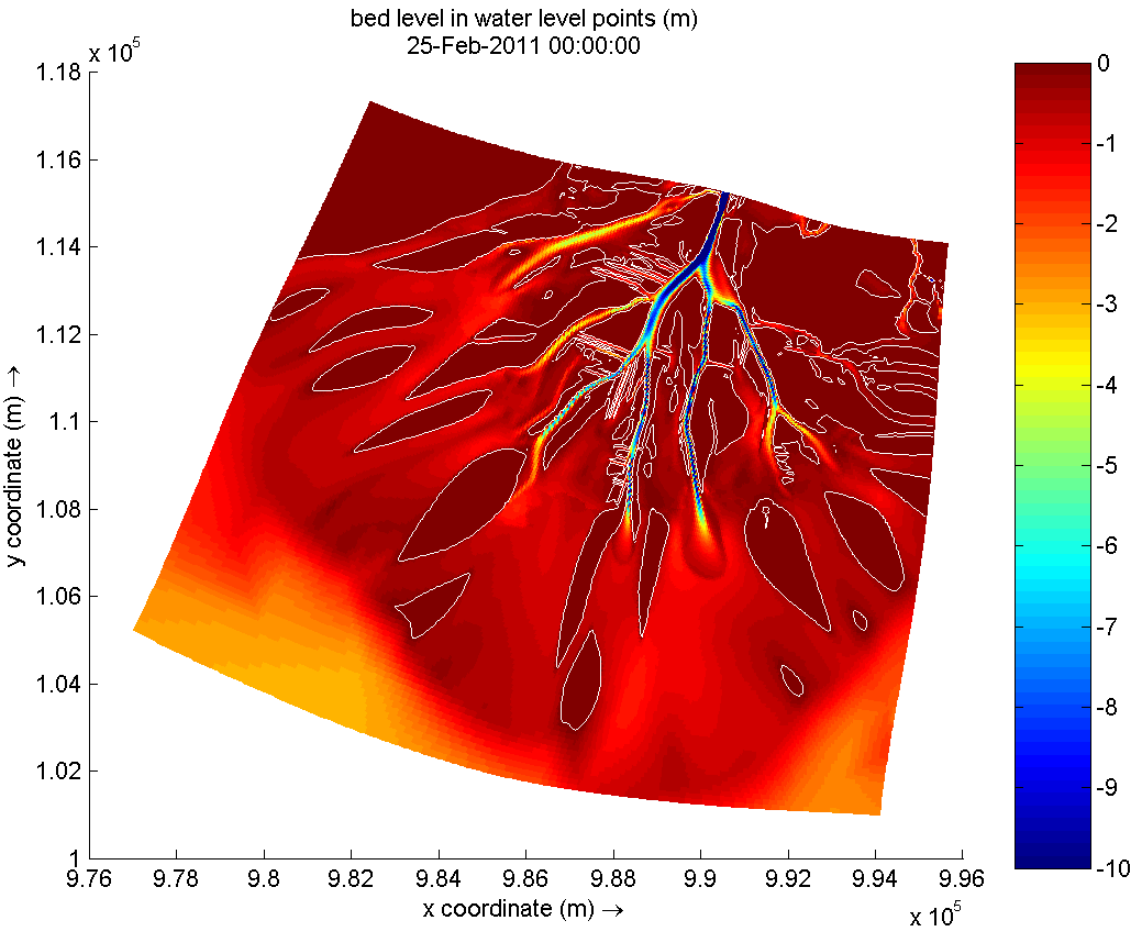

Figure 5-7: Bathymetry of developing Wax Lake Delta and receiving basin after five years of morphologic simulation along with 0 m contour line. Upper and Lower color limits were defined so that elevations between limits could be viewed with more clarity.

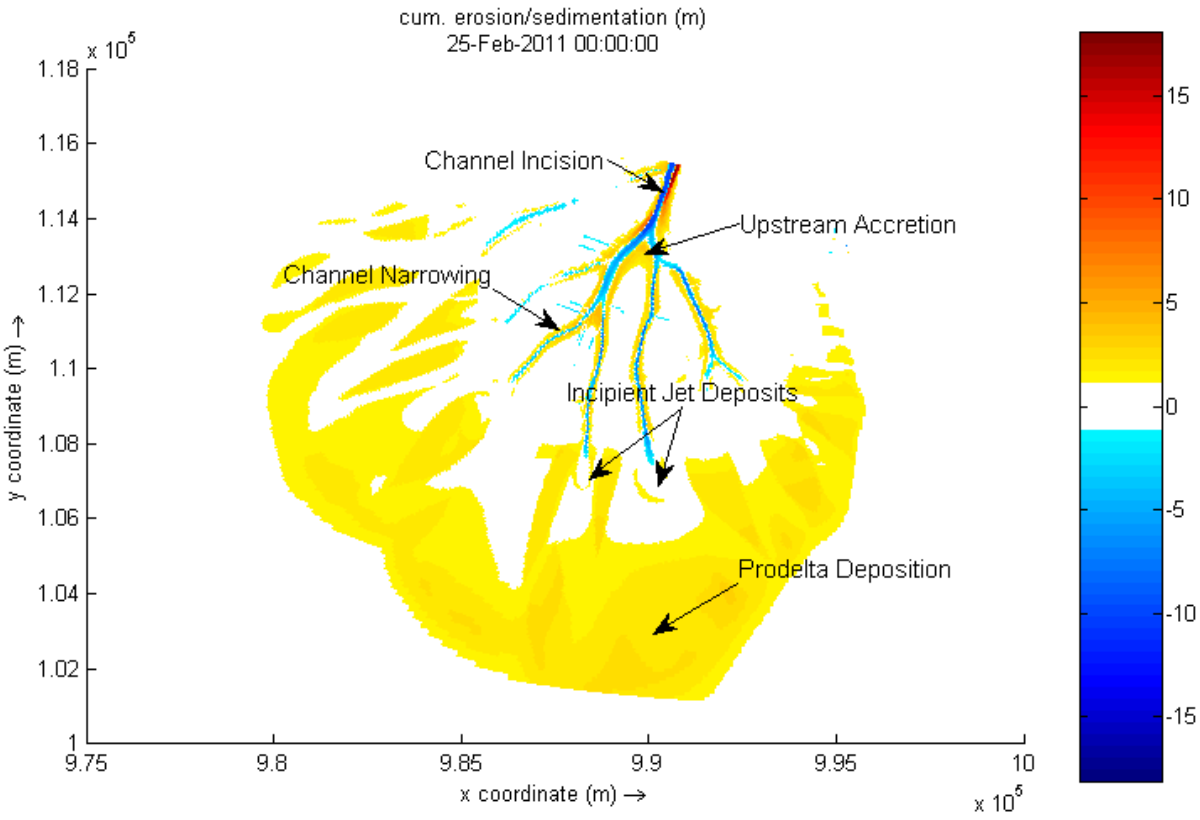

Figure 5-8: Cumulative erosion (cool colors) and deposition (warm colors) in the delta and receiving basin after five years of morphologic simulation. Examples of simulated morphologic features mentioned in the text are noted.

5.2.2 Overview of Simulated Stratigraphy

Figure 5-9 presents the spatial distribution of the sand sediment fraction in the uppermost .2 m layer of the bed (transport layer) in the delta and basin areas. It can be seen from the bed surface composition that with the exception of small areas at the distal ends of the main delta channels, the area basinward of the original delta front lacks any recent sand deposition so is overlain fully by the mud fraction. The bed surfaces in distributary channels become more sand-dominant as the channel erosion that depletes the mud fraction from the bed in the upstream Wax Lake Outlet channel reaches the delta. The incipient jet deposits located at the distal ends of the two major distributaries (see figure 5-8 above for locations) are almost fully composed of the sand fraction. Figure 5-10 gives the dip and strike-oriented stratigraphic sections denoted by the white lines in figure 5-9. The black, dotted line marks the elevation of the initial bed level; in non-erosional areas the bed composition below this line has not been altered by the simulation and only reflects the assigned initial bed condition. The significant mud deposition basinward of the original delta front is even more evident in these sections. The rightmost, basinward portion of the dip section and the right and left portions flanking the central delta in the strike section show mud deposition that fills basin accommodation space above the original bed level, ultimately producing multiple subaerial lobes separated by broad, shallow, non-erosional “channels” where flow energy is still sufficiently low to accommodate the settling of fines. The absence of any inter-laminated sandy layers in the zones of basinward mud deposition indicate that even during the highest flows, velocities are not sufficient to transport suspended sand and bedload beyond the delta front. Upstream accretion of the existing delta

depositional bodies is evident in the dip stratigraphic section as significant deposition above the original bed level beginning at approximately 2000 m from the starting point of the section. The observed channel narrowing, evident in the three main channels near the central portion of the strike section plot, is a consequence of subaqueous levee deposition near the channel banks that is in some cases sufficient for subaerial expression. The stratigraphic section plots demonstrate that the development of both of these morphologic features is driven by exclusively-sand deposition.

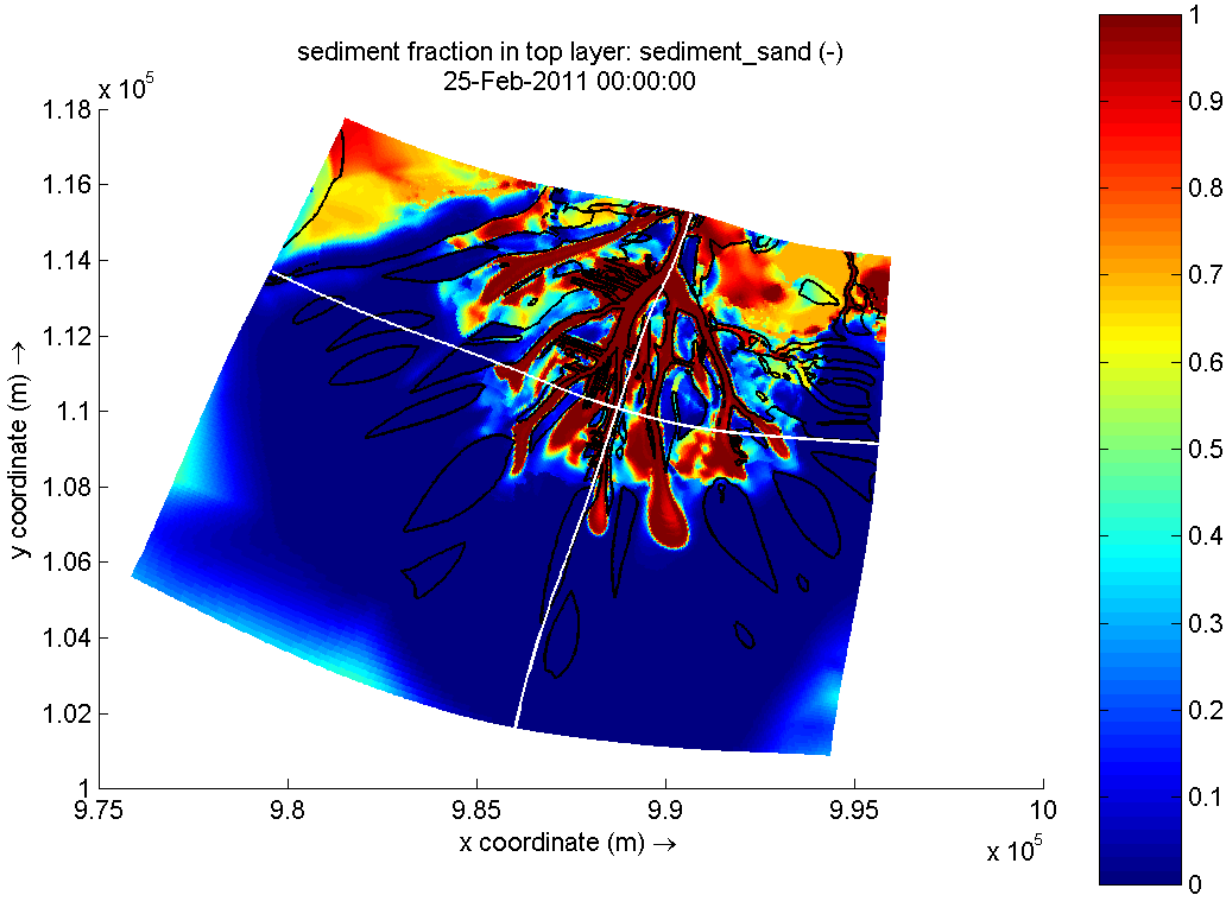

Figure 5-9: Spatial distribution of sand volume fraction in the top bed layer after five year morphologic simulation. As only two sediment fractions are used, the mud volume fraction at each point is equal to one minus the sand fraction. The black line represents the 0 m contour line of the modeled bathymetry. The two white lines mark the locations of the dip and strike stratigraphy sections presented in figure 5-8 below.

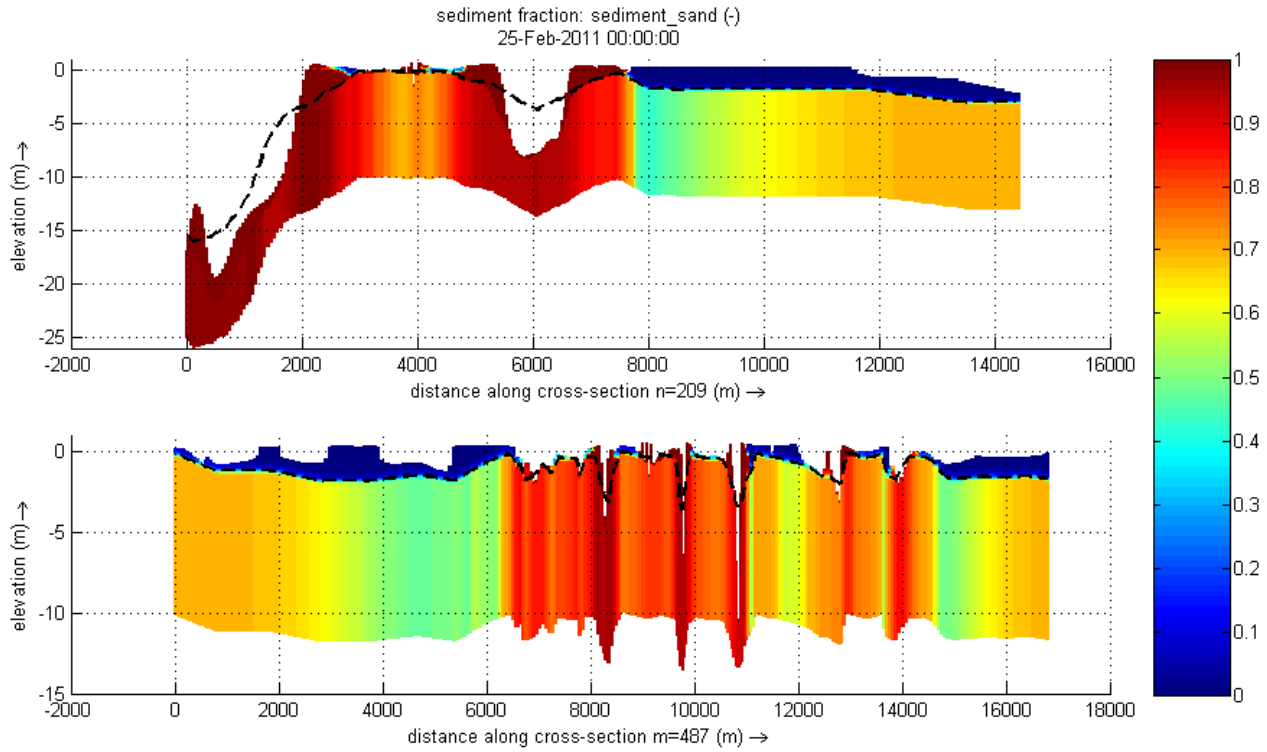

Figure 5-10: Final delta bed composition by sand volume fraction along dip (upper plot) and strike (lower plot) sections located at the white lines in figure 5-9 above. The black dotted line marks the bed level at the beginning of the simulation. Note that both the vertical and horizontal scales are different in the two subplots.

6. Discussion

As previously stated, the following chapter discusses the simulated delta features and forming mechanisms and assesses the degree to which the simulated delta development processes reflect those typically observed in river-dominant deltaic environments, with emphasis on the processes that contributed to the actual development of the Wax Lake Delta during the simulation period. The discussion includes sections on the four predominant morphological developments simulated in the long-term model: channel narrowing and incision, upstream accretion of depositional lobes, excessive prodelta mud deposition, and incipient mouth bar formation through jet deposits. To contrast the results of successful conceptual delta development simulations that implement a constant discharge upstream boundary condition, the specific morphologic and stratigraphic developments that can be attributed to the varying discharge boundary condition schematization method are discussed as well.

6.1 Simulated Delta Features and Forming Mechanisms

6.1.1 Channel Narrowing and Incision

Examination of the cumulative erosion and deposition in figure 5-8 above indicates that the main Wax Lake Outlet and all distributary channels experience significant channel deepening and narrowing through the course of the simulation. Figure 6-2 below shows the bed level in a cross-section across a narrowing, incisive channel as a function of time, with line colors getting progressively darker as time passes. The cross-section location is shown as a thick white line marked as “Channel Narrowing Plot” in figure 6-1. The cross-section evolves from shallow, broad channel to a much deeper, steeply sloped channel accompanied on both sides by significant subaqueous depositional levees that ultimately develop into subaerial features. Though distributary channel narrowing has been observed in field deltas as part of the eventual lobe fusion process (van Heerden and Roberts 1988), this morphological development has not been observed in the prototype Wax Lake Delta during the simulation period. No full bathymetry data set of the Wax Lake Delta exists after the initial condition for comparison, but transects of the distributary channels taken during the field campaign of DuMars, 2002 give an indication of channel bathymetry after approximately half of the simulation time. Channel thalweg elevations do not fall below approximately 3 meters, and maintain width-to-depth ratios of over one hundred (DuMars 2002; Olariu and Bhattacharya 2006). The channel narrowing and incision is clearly an unrealistic representation of what occurred during the simulation period; however, previous work indicates that more moderate incision and levee accretion did occur in the Wax Lake Delta during past periods of development. Figure 6-3 shows a strike-oriented stratigraphic cross-section constructed from data collected in the mid 1990’s. The difference between the section surface and the 1981 bathymetry, represented in the plot by a dotted line, shows the intervening incision of the distributary channels and narrowing through subaerial levee deposition. Channel incision into underlying stratigraphic sequences is typically observed as distributary channels initially form and elongate (Roberts, Walker et al. 1997), but the massive depth increase in the mature delta channels would only be expected in the case of drastic changes to flow regime. The time steps used for the time-dependent bed level plots in figure 6-2 correspond to the initial condition and the end of each period of constant boundary inflow. Though it is clear that greater change occurs during certain periods, it is notable that the narrowing/incising trend is present during the full flow regime, not just during flood flows.

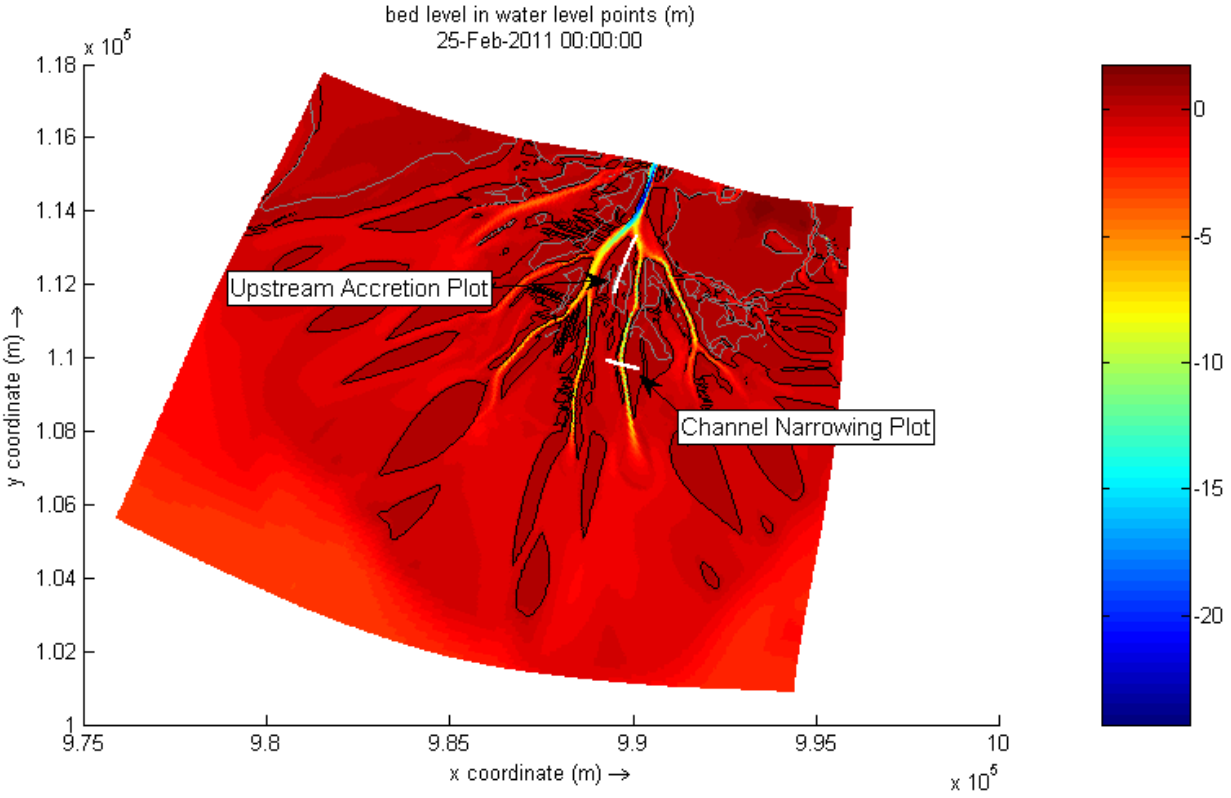

Figure 6-1: Locations of Channel Narrowing Plot (figure 6-2) and Upstream Accretion Plot (figure 6-6) cross-sections. Cross-sections used in the subsequent plot are represented by the thick white lines and labeled. The thin grey line marks the 0 m contour of the initial bathymetry, and the thin black line marks the 0 m contour at the end of the five year simulation.

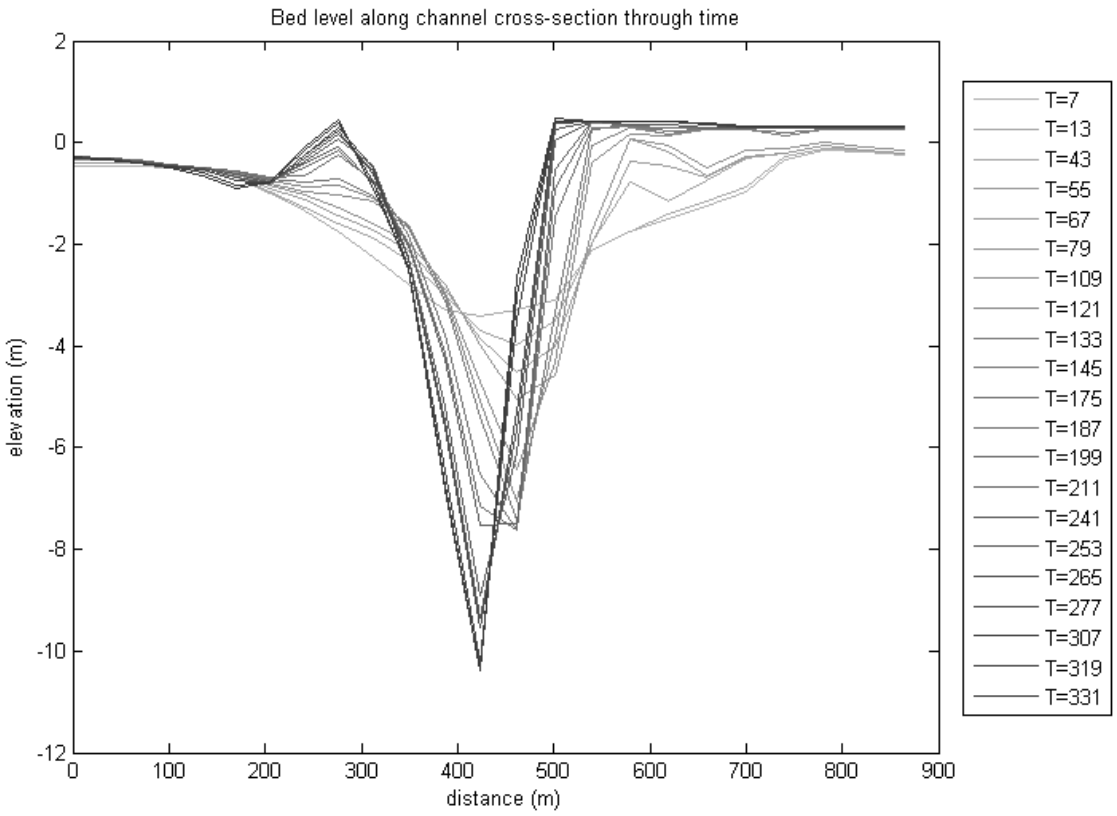

Figure 6-2: Plot of bed level elevations in a channel cross section as a function of time to demonstrate the persistent narrowing and deepening. Line colors represent time, with the lightest line (T=7) representing the initial condition and the darkest line (T=331) representing the bed level at the end of the five year simulation. The location of the cross section is given by the thick white line labeled "Channel Narrowing Plot" in figure 6-1 above.

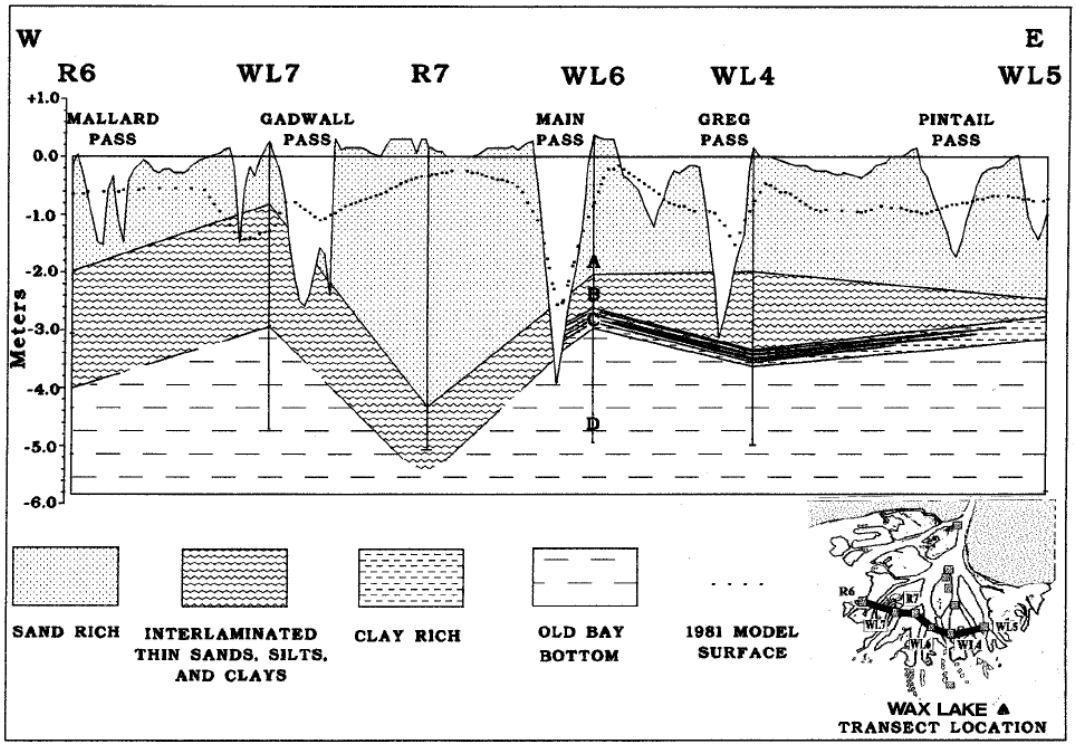

Figure 6-3: Strike-oriented stratigraphic section of Wax Lake Delta from 1994, showing the incision and levee accretion that occurred in the distributary channels since 1981 (Roberts, Walker et al. 1997).

The cause for this misrepresentation of channel development during the simulation period is not immediately clear. The fact that the incision and levee accretion occurs even during low flow periods indicates that a possible invalid discretization of the discharge regime with more intense floods than what actually occurred is probably not responsible. A plot of the depth-averaged velocity distribution across the same cross section at time steps corresponding to the end of each five year flood period of constant discharge is given in figure 6-4. It can be seen that the peak velocity does not change very much with the reduction in width and increase in depth; however, the locations on both sides of the channel where velocities are reduced to near zero levels continually move inward towards the channel center. Because there have been no prototype velocity measurements near channel banks, the representativeness of the distribution across the channel cannot be validated, but it is expected that the very low velocities at the channel banks are responsible for the excessive levee deposition.

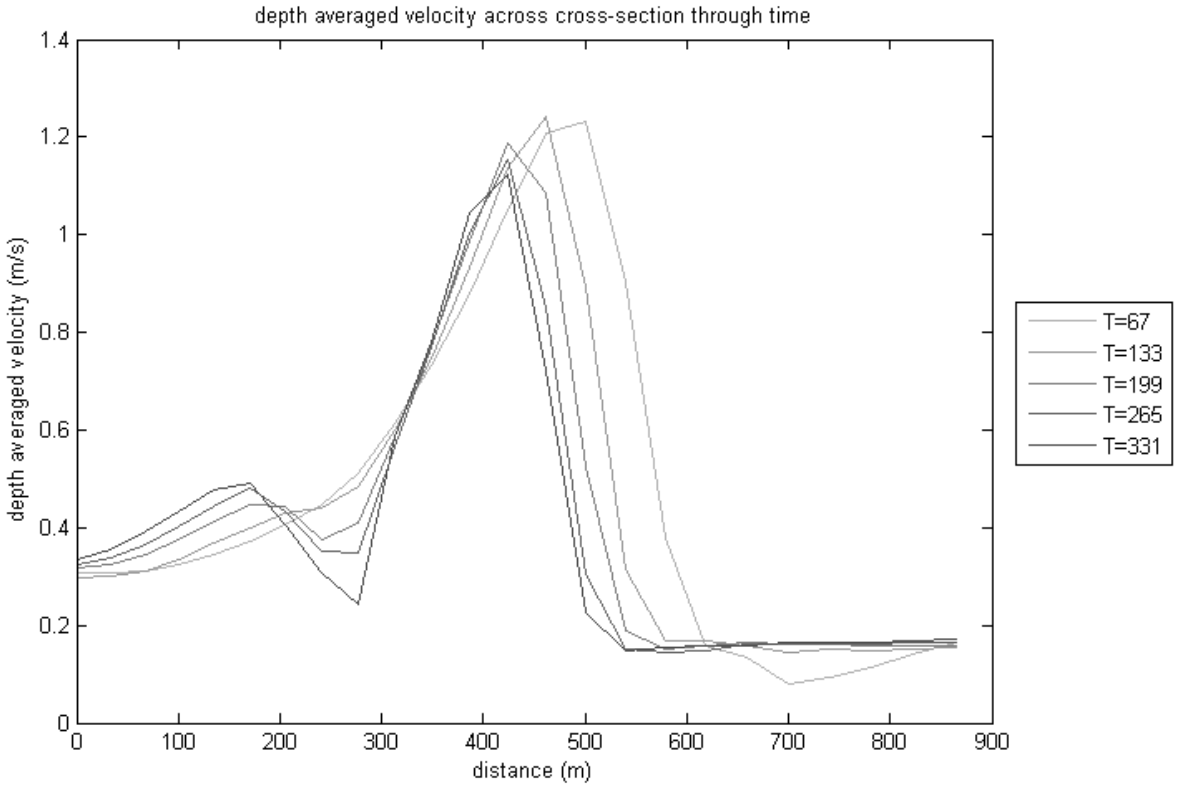

Figure 6-4: Plot of depth averaged velocity magnitude distribution in a channel cross section as a function of time. Line colors represent progression through time with increased darkness. The location of the cross section is given by the thick white line labeled "Channel Narrowing Plot" in figure 6-1 above.

As described in the grid development section, no effort was made to orient the computational grid to the distributary channels or other bathymetric features. This approach was justified based on the success in previous studies of modeling conceptual delta development with rectilinear grids (Storms, Stive et al. 2007; Edmonds and Slingerland 2010; Geleynse, Storms et al. 2011). As the distributary channels narrowed over the course of the simulation, the arbitrary grid orientation resulted in a so-called "zig-zag" channel orientation that represents the limiting case for stability of the time-integration method (Deltares 2009). The small channels that develop towards the end of the simulation and cut through the existing depositional bodies along the grid orientation are most likely a result of instabilities. These grid effects do not become significant until the channels narrow to

widths that are on the order of the grid cell sizes. The "artificial roughness" that is introduced by the grid orientation could also be responsible for the initial deposition on the channel banks that causes the narrowing, which then induces more deposition. Figure 6-5 gives an example initial and final bed level plot along with the hydrodynamic grid to show the described situation.

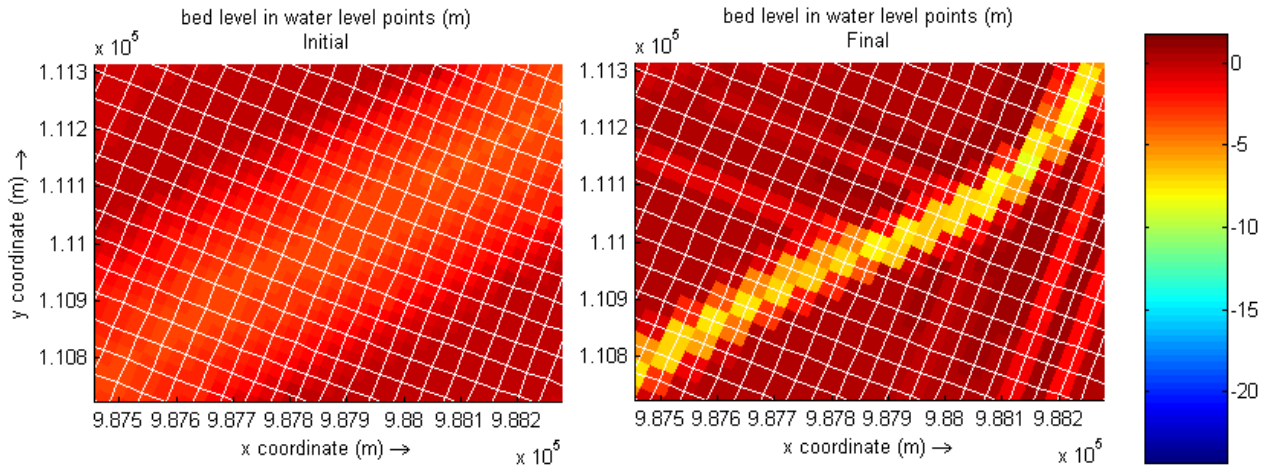

Figure 6-5: Initial and final bed levels along with the hydrodynamic grid. Though initially the grid was sufficiently refined to adequately represent the channel, the persistent narrowing results in the limiting "zig-zag" case shown on the right. The unrealistic, small channels that develop most likely due to limitations in the time-integration scheme are visible in the final condition plot.

Because an already-redistributed sediment bed condition was used to construct the initial bed stratigraphy, the Wax Lake Outlet and delta distributary channels are underlain by an almost-fully sand-dominant layer (see figures 5-3 and 5-4). As the channels begin to incise with moderate flows, preferential entrainment of the more easily eroded mud fraction further increases the sand volume fraction in the upper bed layers. Modeling of conceptual delta development for various initial bed compositions indicates that delta distributary channels are more incisive for initial bed configurations with a greater proportion of fine sediments (Geleynse, Storms et al. 2011), so it is reasonable to conclude that the use of alternative initial bed configurations in the current model that place a greater proportion of fines underlying the channels would result in even greater channel erosion. The continued incision despite increasing sand-dominance of the channel beds could be a result of the very fine sediment used as the coarse fraction (100 µm opposed to the 200 µm sand fraction used in the Geleynse, 2011 model), lessening the distinction between the sand and mud fractions.

6.1.2 Upstream Accretion

Analysis of subaerial features identified in a time series of aerial photographs in Wellner, 2005 indicates that in the simulation period, established depositional bodies continue to develop through downstream accretion and infilling of secondary channels; however, subaerial lobe expansion through upstream accretion does not occur (Wellner, Beaubouef et al. 2005). In the very similar Atchafalaya Delta, subaerial development through time was characterized by the dominance of one of two identified processes: channel bifurcation and elongation, and lobe fusion and upstream accretion. During the later period in which the delta development was observed, no basinward extension or significant channel bifurcation occurred in the Atchafalaya Delta; instead, the increase of subaerial land area came from deposition of coarse sediment on the upstream ends of existing

depositional lobes (van Heerden and Roberts 1988). Though no definitive cause is attributed to the shift in dominant subaerial accretion processes, it is proposed that continued delta network development through bifurcation and channel extension eventually diminishes sediment transport efficiency so that sand fractions are no longer transported to the delta front and, instead, are deposited in the delta plain as upstream accretion (van Heerden and Roberts 1988). If such a mechanism does exist, the Wax Lake Delta has not reached the point where dominant processes shift so continues to expand through mouth bar formation and channel bifurcation (Roberts, Walker et al. 1997).

The model simulations, where upstream accretion of the existing subaerial lobes through sand deposition occurs extensively, are clearly not reflective of prototype reality. Figure 6-6 below demonstrates the modeled upstream accretion through time with plots of the bed level at the upstream end of a subaerial lobe, where time progression is represented by increasingly dark line colors. The channel incision discussed earlier can also be seen upstream of the subaerial lobe in the leftmost portion of the figure. This excessive scouring of the main channel could be a contributing factor to the unrealistic upstream accretion by increasing the sand load through the narrowing distributary channels whose transport efficiency to the delta front is diminished. Though this modeled development was not observed in the prototype during the simulation period, field studies of the very similar but more mature Atchafalaya Delta have demonstrated that it is a valid and expected delta-building process.

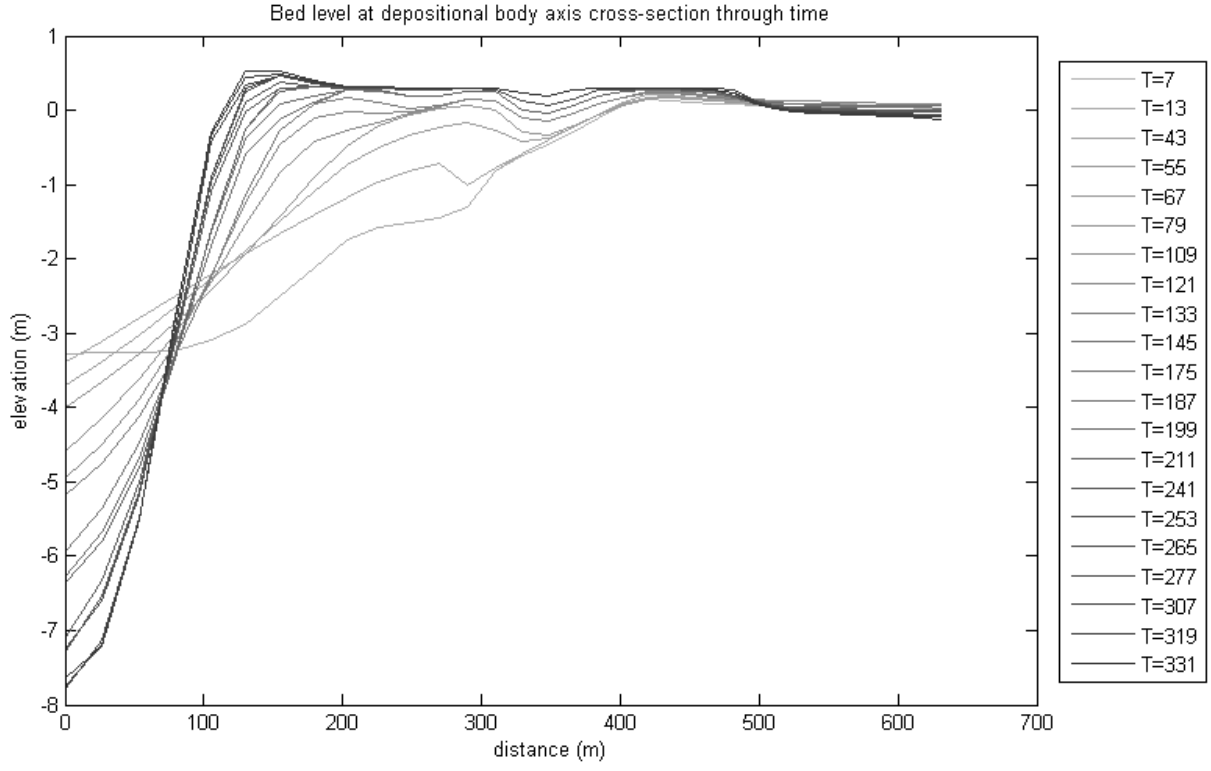

Figure 6-6: Plot of bed level elevations on the upstream end of existing depositional lobe as a function of time to demonstrate the upstream accretion. Line colors represent time, with the lightest line (T=7) representing the initial condition and the darkest line (T=331) representing the bed level at the end of the five year simulation. The location of the cross section is given by the thick white line labeled "Upstream Accretion Plot" in figure 6-1 above.

6.1.3 Prodelta Mud Deposition

Over the course of the five year simulation, the Wax Lake delta progrades into the receiving basin through the development of new subaerial depositional lobes while maintaining its approximate radial symmetry. The subaerial features (see 0 m contour line in figure 5.7) maintain a teardrop shape similar to the shape of previously-established depositional lobes in both the Wax Lake Delta and the Atchafalaya Delta (van Heerden and Roberts 1988; Wellner, Beaubouef et al. 2005) and generally form at the downstream ends of existing lobes between channels or at large distances basinward from distributary channel mouths. The absence of any sand volume fraction in the basinward deposits over the initial bathymetric surface in the dip and strike-oriented stratigraphic cross-sections (see figure 5-10 in section 5.2.2) demonstrates the complete dominance of the mud sediment fraction in the composition of these depositional features.

The initial locations of the most intense mud deposition that eventually develop into subaerial mud deposits are very dependent on the assigned critical erosion and deposition shear stress. Figure 6-7 below plots the maximum bed shear stress in the delta at the end of the first year annual flood period of constant discharge with contour patch limits corresponding to the TcrEro and TcrSed values used in the simulation. The critical shear stress for erosion is exceeded in the red areas, the shear stress falls below the critical shear stress for sedimentation in the white areas, and blue areas represent shear stresses between the two critical values where no erosion or deposition takes place. The contour lines in the figure represent the cumulative deposition at values of 1, .75, and .5 meters. The locations with over 1 m of deposition that eventually develop into subaerial lobes correspond to the first locations where bed shear stress falls below the value necessary for deposition. This determinacy in mud depositional lobe development and clear dependence on the assigned mud critical deposition shear stress parameter is a consequence of the exclusion of prototype processes in assuming river-dominant delta development.

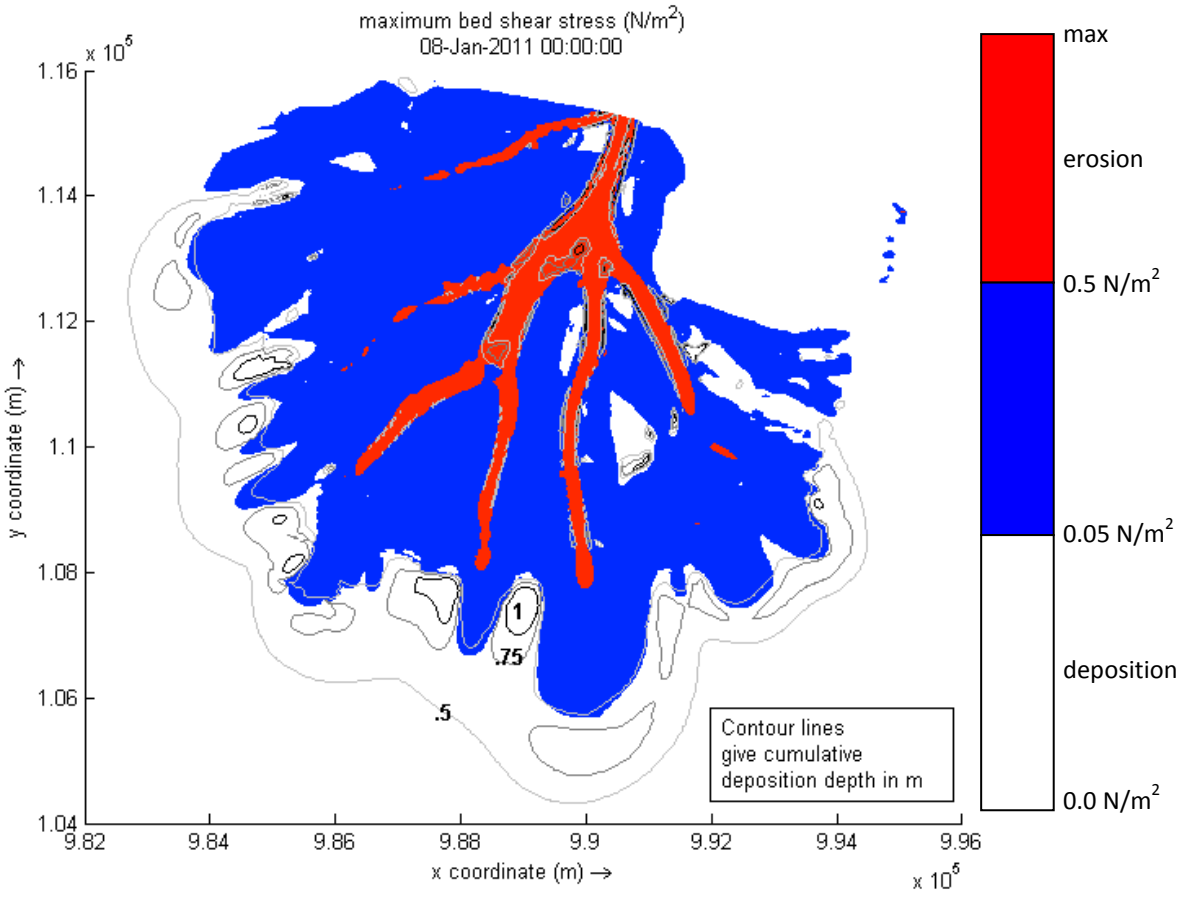

Figure 6-7: Plot of the spatial distribution of maximum bed shear stress that occurred during the first low flow and annual flood periods of constant discharge in the simulation. Red areas indicate that bed shear stress exceeds the critical shear stress for erosion, blue areas indicate that bed shear stress is between the critical shear for erosion and deposition, and white areas indicate that bed shear stress is below the critical shear for deposition. Contour lines mark cumulative deposition at values of 1, .75, and .5 meters.

Though the prototype Wax Lake Delta development during the simulation period is characterized by the formation of new depositional bodies, these arise from mouth bar formation at the distal end of main channels and are initiated through sand fraction deposition (Wellner, Beaubouef et al. 2005). In historic research on the morphology of the Atchafalaya Delta with emphasis on sedimentary facies development, the first subaqueous deposition associated with incipient delta formation consisting of a broad, thin, laterally continuous fine sediment layer is identified as prodelta and distal bar deposits (Roberts, Adams et al. 1980). As coarser sediments began reaching the mouth through suspended load and bed load transport, the developing sand depositional bodies and distributary network structure built upon and, in some cases, incised into the fine sediment prodelta platform. With continued basinward channel lengthening and network expansion, clay rich prodelta and distal bar sediments were deposited as basinward-thinning layers basin surrounding the delta network and depositional body limits (see figure 2-17 in section 2.4.1) (van Heerden and Roberts 1988). The stratigraphy of the Wax Lake Delta also contains a clayey prodelta layer onto which the coarse depositional features prograded; however, the clay-rich prodelta facie is not completely continuous under the emergent delta and is extremely thin (Roberts, Walker et al. 1997). Since only the development of subaerial features was documented for the prototype during the simulation period, information on the exact nature of prodelta mud deposition is not available. Comparison with previously documented depositional patterns in the stratigraphic record do suggest that mud

prodelta deposition basinward of the initial delta front probably occurs, though deposited mud layers would be extremely thin and definitely would not build to the subaerial levels observed in the model results.

Due to the limited basin processes included in the model, the observed transport of fine sediment out of the immediate receiving basin (Roberts, Walker et al. 1997) is not sufficiently modeled. Granted, further calibration of cohesive sediment erosion and sedimentation parameters could decrease the amounts of mud prodelta deposition; however, realistic values for these parameters with only riverine processes modeled are still unlikely to prevent excessive deposition. Conceptual models of delta development under various marine forcings offer insight into possible means for more realistic prodelta simulation. In the presentation of the results of Geleynse, et al. 2011, the ability of modest wave action to prevent prodelta deposition is discussed (see figure 2-15 in section 2.3) . The river dominant simulation results in significant, mud-dominant basinward deposits that are similar to the resultant mud deposits in the present study; the implementation of a constant wave climate in an alternative simulation effectively prevents any offshore mud deposition (Geleynse, Storms et al. 2011). It is expected that exposure of the Wax Lake delta to a very low energy wave climate representative of that in Atchafalaya Bay would modulate the extreme prodelta mud deposition and result in more representative morphologic development.

6.1.4 Mouth Bar Formation

Besides the previously described upstream accretion and subaqueous levee development, the most prominent modeled morphological developments resulting from the deposition of coarse sediment are incipient jet deposits at the distributary mouths of Greg Pass and Main Pass. The locations of these deposits are identified in figure 5-8 in section 5.2.1. Figure 6-8 gives a detailed view of the final bathymetry of the more well-defined jet deposit at the mouth of Greg Pass. At the end of the simulation, a mouth bar has formed and prograded basinward; however, it has not aggraded or developed sufficiently to induce a flow bifurcation and the subsequent formation of a new depositional lobe. Subaqueous levees extend out from the initial mouth location as the bar progrades, though towards the end of simulation the bar and levees continue to develop asymmetrically. The subaerial lobes on each side of the initial jet deposit arise from the unrealistic prodelta mud deposition described in the previous section. It can be seen from the time series of bed levels on a section through the distributary mouth and bar formation (figure 6-9) that after initial formation, the mouth bar progrades basinward with very slight aggradation and some widening as time progresses. The significant scouring at the distributary channel mouth is evident in the leftmost portion of the figure, and the basinward mud prodelta deposition is visible on the far right. Though the very shallow receiving basin clearly indicates a friction-dominant effluent according to Wright, 1977, the bar front and back slopes more resemble the characteristic depositional patterns of inertia-dominant effluents (see figures 2-4 and 2-6) (Wright 1977). A gently sloped bar back face precedes the more-steeply sloped basinward bar front, though encroachment of the extreme channel incision towards the bar front does steepen the front slope. The typical longitudinal profile of deposition at friction-dominant effluents does reflect that of a fully formed middle ground bar, so the difference in simulated bar slopes could reflect more the nascent stage of the formation and not ultimate differences after full development. Results from detailed modeling of mouth bar formation found a gentler bar front slope and steeper basinward slope similar to the

present simulation results (see longitudinal profile of plot B in figure 2-10) (Edmonds and Slingerland 2007).

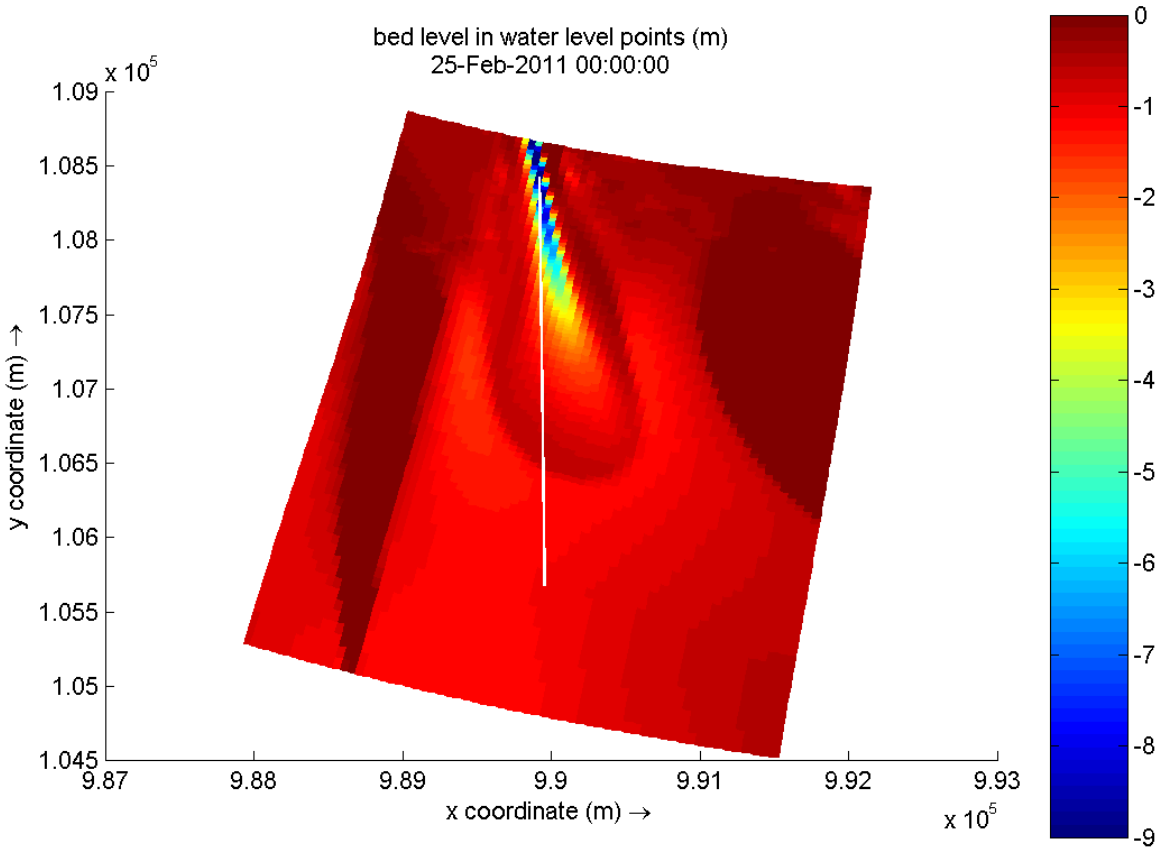

Figure 6-8: Bathymetry of prograding distributary mouth bar at the mouth of Greg Pass at the conclusion of the five year simulation. The white line marks the location of the bed level profiles and stratigraphic section given below in figures 6-9 and 6-10.

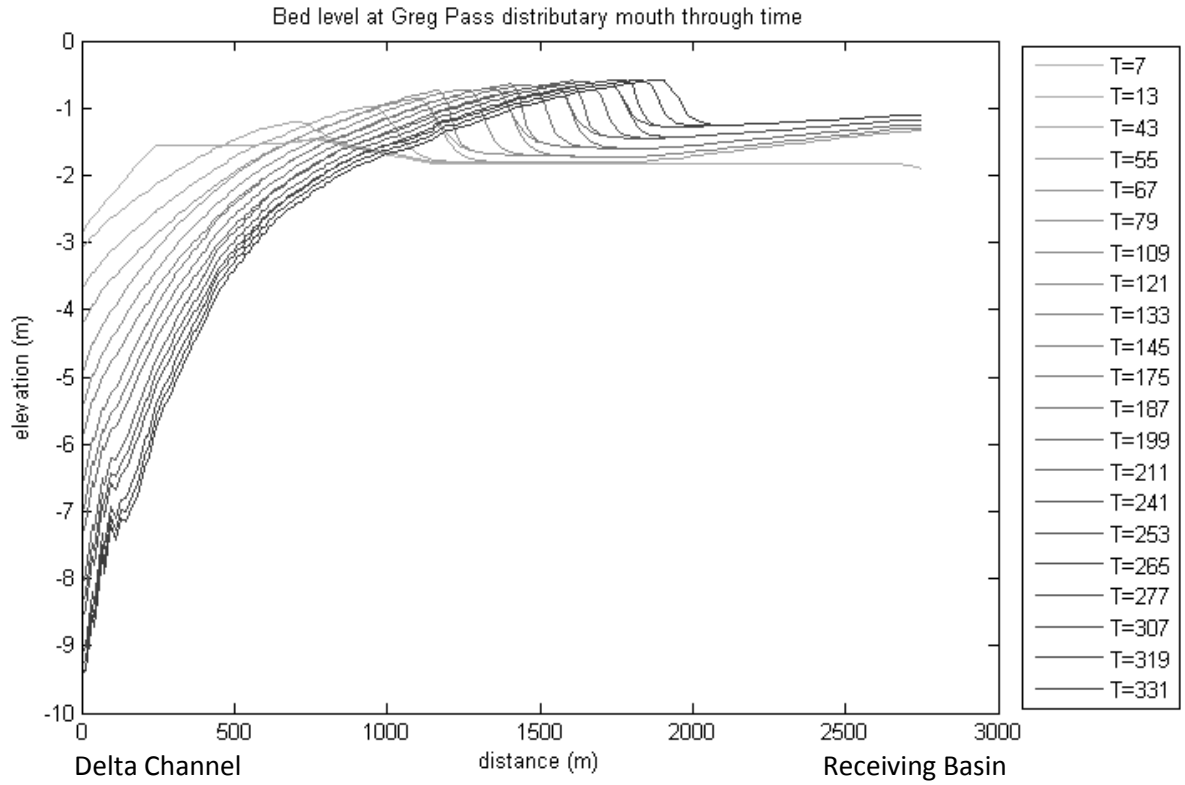

Figure 6-9: Plot of bed level elevation profiles at the mouth of Greg Pass as a function of time. Line colors represent time, with the lightest line (T=7) representing the initial condition and the darkest line (T=331) representing the bed level at the end of the five year simulation. The location of the cross section is given by the white line in figure 6-8 above.

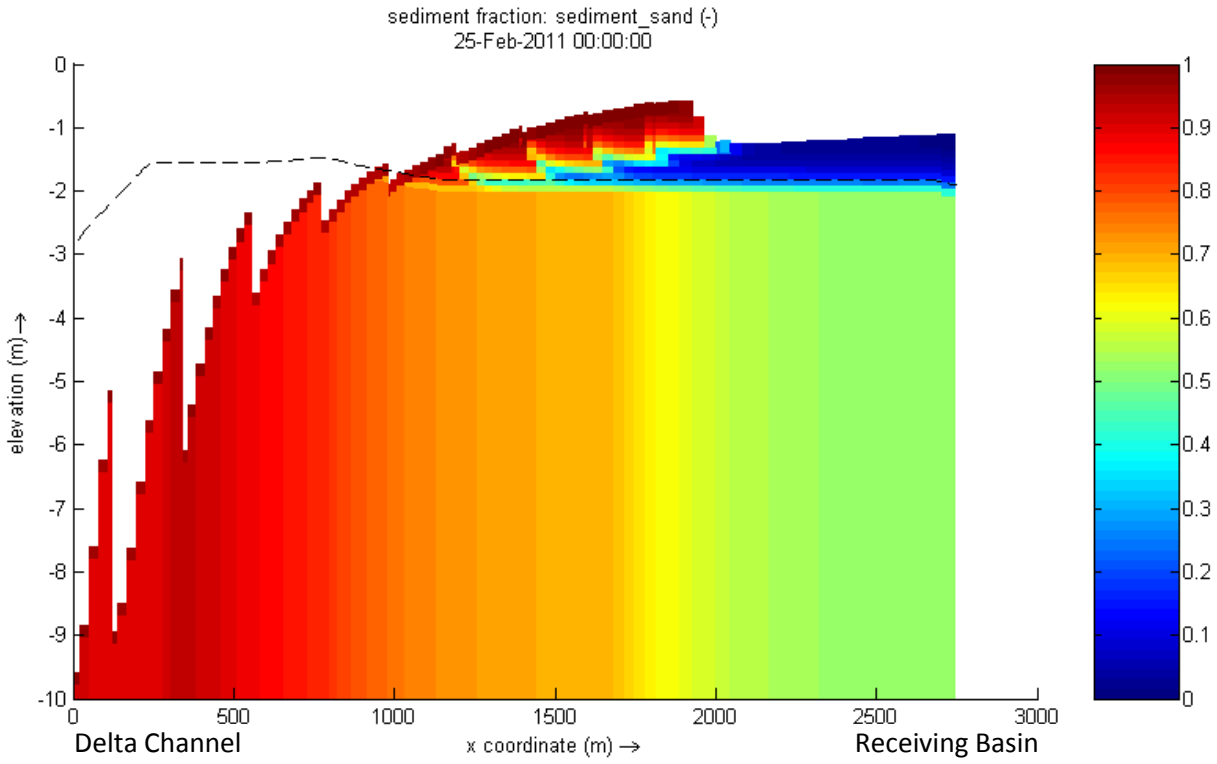

Figure 6-10: Stratigraphic section at the end of the simulation through the incipient jet deposit at the mouth of Greg Pass, the location of which is marked as the white line in figure 6-8 above. The black dotted line represents the initial bed level at the section location.

Figure 6-10 above gives the final stratigraphy at the bed level profile location. Again, the stratigraphy of the non-erosional areas more than a few layers below the initial bed level were not affected in the simulation and only reflect the defined initial bed composition. Though the mouth bar does not fully develop into a subaerial, middle-ground bar and form a new depositional lobe, the stratigraphy of the incipient deposit can still be assessed for validity. The prograding mouth bar is clearly sand dominant and coarsens towards the bed surface. This characteristic stratigraphic sequence was identified as distributary mouth bar facies in the hydrologically and sedimentologically similar Atchafalaya Delta (Roberts, Adams et al. 1980). The bed surface sediment distribution patterns agree well with the typical depositional patterns for friction-dominant effluents (Wright 1977), where the coarsest sediments are deposited on the fore slope and bar crest and finer sediments settle from suspended load basinward of the developing bar.

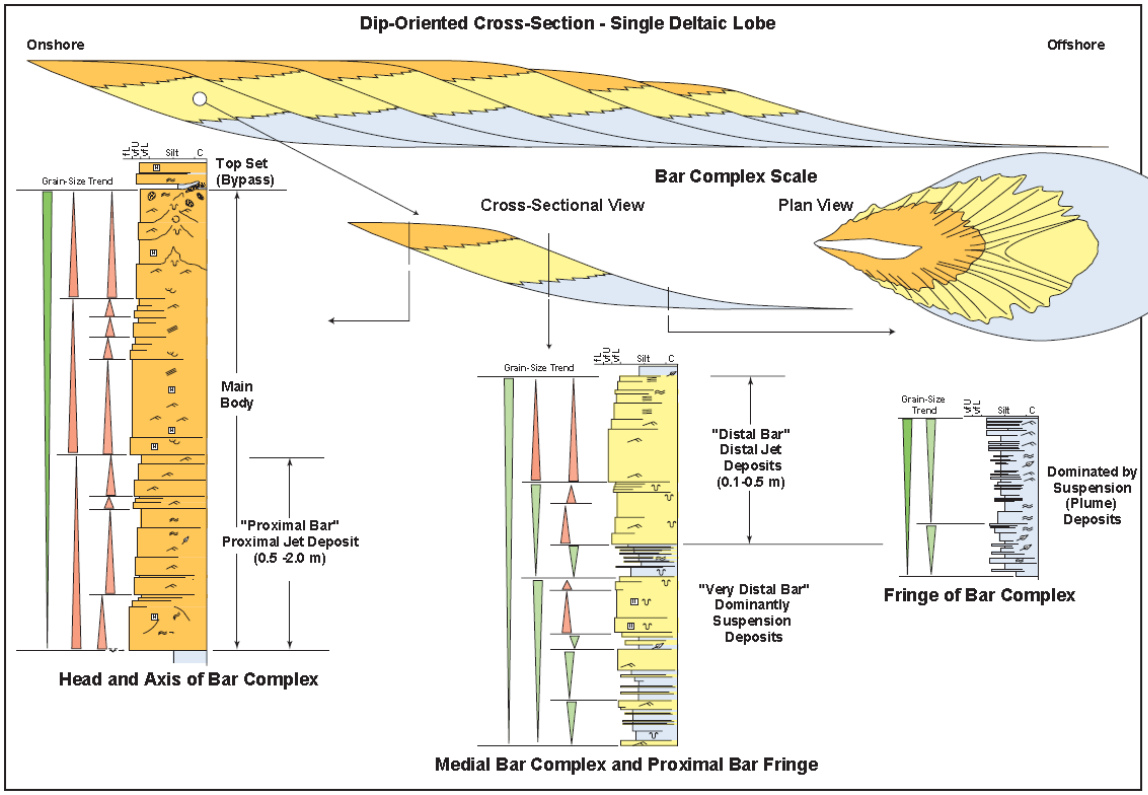

Figure 6-11: Typical grain size trends and stratigraphic bedding structures in Wax Lake Delta Jet Deposit Complexes (Wellner, Beaubouef et al. 2005).

Since the bar does not reach the point were progradation ceases and deposition proceeds basinward from the static crest, comparison to the detailed deltaic lobe stratigraphic sequences in Wellner, 2005 are not as useful. The results, however, do follow the successive stacking of coarsening-upwards sequences observed in the fully-developed jet deposits complexes (see figure 6-11). In a single jet deposit (the part of the figure marked as “Cross-sectional View”), the succession from lower, finer sediments to the uppermost coarse sediments proceeds from the successive deposition of fine suspended sediment, coarse suspended sediment, and bedload as the distributary mouth extends basinward (Wellner, Beaubouef et al. 2005). A clear mechanism for the stacking of these sequences emerges with examination of the simulated final stratigraphy and successive bed level profiles. As the bar progrades, a total of five stacked fining-upwards sequences develop, one for each year of varying boundary conditions. During the long, lower flow periods imposed at the start

of each morphologic year, mud deposition dominates the area basinward of the developing bar. The onset of 2 year and 5 year flood conditions sufficient to mobilize significant amounts of sand as suspended and bedload at the end of each morphological year induces sand deposition and continued mouth bar progradation over the previously deposited mud layer. The most upstream preserved portion of the developing mouth bar lacks the fully-mud layer underlying the successive sequences only because the bar had not yet progressed sufficiently to lower shear stresses for mud deposition directly basinward. The division of the simulation time into multiple periods with varying discharge allows for temporal variations in the dominance of mud or sand deposition in addition to the spatial variation in dominance that would occur with constant boundary conditions. Though a basinward-advancing distributary mouth could create a more complex sequence of jet deposits while still under constant discharge conditions, the sharp transitions between subsequent stacked sequences observed in the Wax Lake Delta would not be adequately reproduced.

As presented in the aerial photograph analysis portion of the Wellner, 2005 study, the morphological development during simulation period from 1998 to 2002 is dominated by the aggradation of new depositional bodies at the mouths of Main and Greg pass. In the prototype delta, mouth bars at these locations induce channel bifurcations, which then promote further development of the mouth bars into middle-ground bars/depositional lobes. Though jet deposits start to develop at the distal distributary mouths in the simulation, they fail to evolve sufficiently to induce channel bifurcation. The unsuccessful simulation of this morphological feature can be attributed to multiple factors. Foremost is the inevitable misrepresentation of prototype bathymetry that is a consequence of limitations in measurement points and interpolation techniques to the computation grid. Observations indicate that the Greg Pass jet deposit began to develop as early as 1990 and reached a point of slight subaerial exposure by 1995 (Wellner, Beaubouef et al. 2005). The first time level profile in figure 6-9 above shows an adverse slope at the mouth rising to a very slightly elevated platform; however, it is clear that the initial model bathymetry does not yet capture the incipient jet deposit, possibly delaying the formation of a fully developed middle-ground bar to beyond the simulation period. The high resolution, focused modeling study on mouth bar formation by Edmonds and Slingerland, 2007 found that although the channel mouth initially narrows and creates a scour hole extending to the subaqueous levee tips, the scour hole remains stationary and no further channel narrowing occurs as the initially formed mouth bar progrades basinward. The mouth bar continues progradation until the depth above the bar crest reduces to less than .4 of the initial mouth depth; runaway aggradation then cements the mouth bar crest position and initiates flow bifurcation (Edmonds and Slingerland 2007). In the present model simulation, the mouth bar progrades in a similar manner to that just described; however, the distributary mouth continues to scour and narrow, altering the flow velocities and the structure of the turbulent jet as the simulation progresses. Still, it appears that the prograding bar is reaching approximately .4 of the initial mouth depth, though the continued channel incision probably exceeds the bounds of applicability for this empirically-determined ratio. Lastly, the sand supply to the distributary mouth during high flows is not constant. Persistent incision in the upstream Wax Lake Outlet channel fully depletes the initial 10 m sediment bed, so erosion sand flux magnitudes are reduced as the channel bed level nears the inerodable basement. This reduction in coarse sediment supply during high flows is demonstrated in figure 6-12 below, which plots the time-dependent depth-averaged suspended sand transport magnitude at a point near the initial diffluence of the main distributary channels (point 3 identified in figure 4-10).

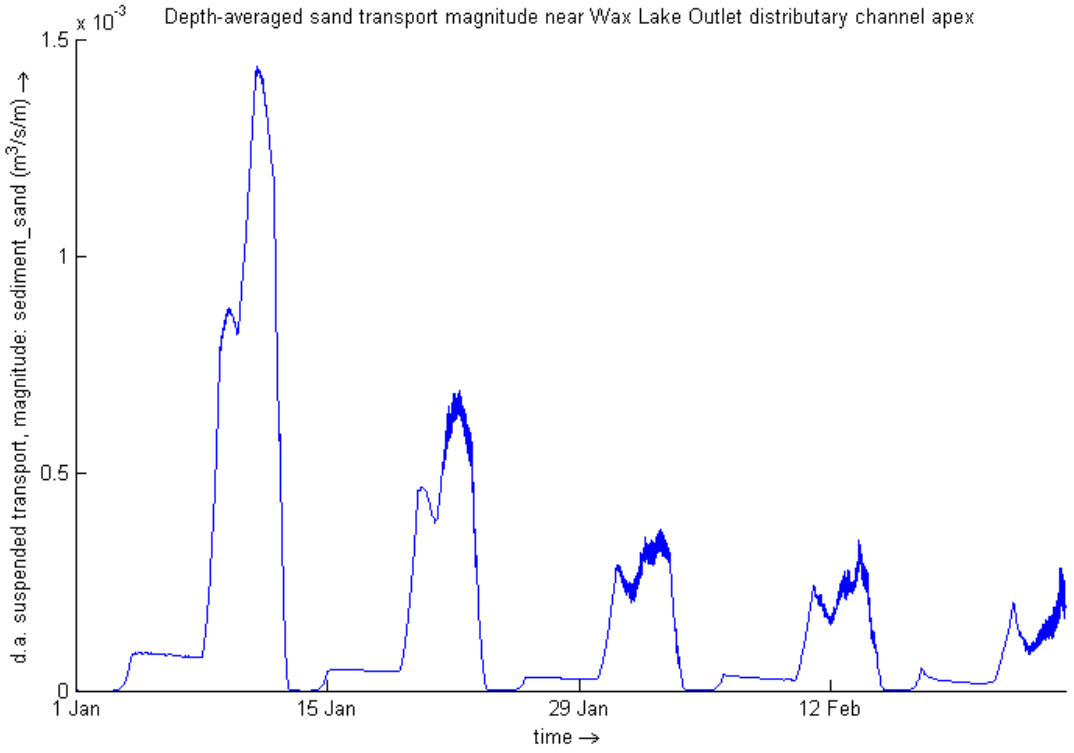

Figure 6-12: Depth-averaged suspended sand transport magnitude at observation point 3 in figure 4-10

The effects of sediment cohesion on delta morphologic development described in Edmonds and Slingerland, 2010, do not seem to be relevant to the current study as the main features of the Wax Lake delta are formed through mostly sand deposition (Roberts, Walker et al. 1997). Though the resulting stratigraphic patterns arising from the conceptual delta modeling with varying sediment cohesiveness are not presented, it is assumed that the modeled dependence of fine sediment deposition only on the critical erosion shear stress, negating the influence of the poorly-defined critical sedimentation shear stress parameter, results in more fine sediment presence in delta depositional features (Edmonds and Slingerland 2010). The modeled Wax Lake Delta development mimics the prototype sand-dominant depositional feature development, discounting the unrealistic formation of subaerial mud depositional bodies already discussed.

6.2 Effect of Varying Boundary Conditions

Thus far, process-based conceptual delta models have been able to successfully reproduce expected delta development despite the use of constant boundary discharge and sediment concentrations. Subaerial expression of both the Wax Lake and Atchafalaya Deltas, however, has been linked to periods of flood discharge sufficient to transport large amounts of suspended coarse sediment to the deltas (Roberts, Walker et al. 1997). The discharges used in the conceptual models are generally sufficient to alter initial feeder channel geometry, thus can be viewed as a series of multiple flood discharges that have been compressed into a continues period of high flow (Geleynse, Storms et al. 2010). Surveys of multiple river-dominant field deltas, including the Wax Lake and Atchafalaya Deltas, suggest that magnitude of seasonal discharge variability still is an important control on mouth bar formation and the dependent delta network structure that follows, in contrast with the

successful constant discharge simulations (Olariu and Bhattacharya 2006). The present simulation, unique not only in its attempted reproduction of the long term development of a real delta through process-based modeling, also imposes time-varying flow and sediment concentration boundary conditions in an approximation of the prototype seasonally-varying discharge regime. The main consequence of this boundary condition schematization is the delineation of the morphological year into periods of prodelta mud deposition dominance and periods of sand deposition dominance. Figure 6-13 below shows the cumulative erosion/deposition that occurred in the delta during the first year of simulation at the end of each of the four periods of constant discharge. The absence of color in the plot representing the cumulative erosion/sedimentation after the low flow period indicates that the discharge is insufficient to significantly erode the upstream channel and entrain the volume of sediment necessary to induce deltaic deposition. Alternatively, the massive prodelta mud deposition discussed earlier occurs most significantly during the annual flood period of constant discharge, where bed shear stress distributions favor erosion of fines from the Wax Lake Outlet and distributary channels and mud sedimentation immediately beyond the bounds of the delta front (see figure 6-7). It can be seen from the upper-right plot that while mud deposition is most dominant during this period, sand deposition as subaqueous levee expansion and depositional lobe upstream accretion still occurs. Flow is insufficient to transport the coarse sediment all the way through the distributary channels to the delta front; instead, it is sequestered within the delta. The discharge schematization process resulted in dominance of the annual flood discharge level in time of occurrence during the morphological year (see section 3.6.2), so this level was applied for the most hydrodynamic days and utilized the largest morphological acceleration factor of the four levels. The two lower plots representing the cumulative erosion/deposition after the 2 year flood and 5 year flood flow periods show the dominance of sand deposition during these periods. While the prodelta mud deposit does extend basinward slightly from its offshore limit after the annual flood, the most prominent developments are the formation of incipient sand jet deposits at the distributary mouths of Main and Greg Passes and the continuation of channel narrowing through levee deposition and upstream accretion, all processes driven by coarse sediment transport. Though the results from only the first year are presented because of their clarity, the delineation of the morphological year into sand and mud deposition dominant periods continues through the full simulation.

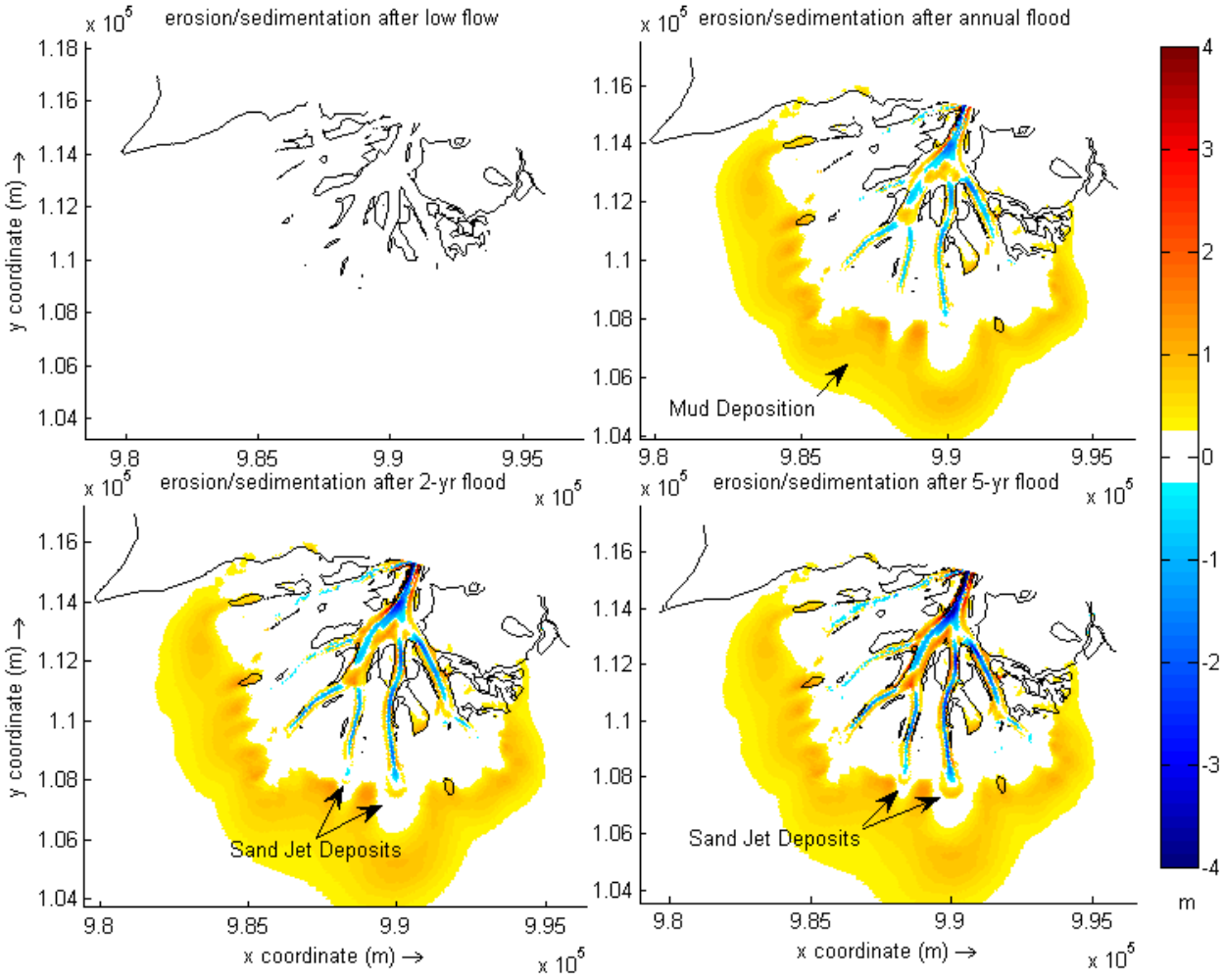

Figure 6-13: Cumulative erosion and deposition during the first year of morphologic simulation, presented at the end of each period of constant discharge. Black lines in each plot represent the 0 m contour line.

The use of a more representative, time-varying discharge regime in this case does not necessarily result in more valid morphologic simulation. The development of sand-dominant depositional lobes through mouth bar formation and channel bifurcation dominates the prototype morphologic development during the simulation period, but the flow conditions that induce the necessary levels of sand transport only occur for a fraction of the simulation time. Instead, the discharge level that induces the most unrealistic basinward prodelta mud deposition is applied for by far the largest proportion of time. Though this distribution of flow proportion of occurrence clearly reflects the prototype reality, the lack of a basin mud sedimentation hindrance or resuspension process (an average wave climate or winter cold front storm conditions) in the model combined with the flow proportioning produces unrealistic prodelta mud deposition that is disproportionally represented in the simulation results.

The consequences of using a time-varying flood discharge regime on the stratigraphy of the incipient mouth bars were discussed in detail in section 6.1.4. The successive stacking of sloped, upward-fining sequences in the incipient mouth bar formation that mimic the cyclic sequences observed in Wax Lake Outlet depositional lobes can be directly attributed to the varying discharge regime. Cyclicity in generally sand-dominant delta plain deposits has been successfully simulated in conceptual delta models, though only with the inclusion of tidal action (Geleynse, Storms et al.

2011). The cyclicity in the prototype Wax Lake Delta depositional lobes, however, is most likely due to seasonal variability in discharge. The modest wave action of Atchafalaya Bay would clearly affect the morphological development of the delta by preventing excessive prodelta mud deposition, but the effect on features arising from sand deposition is much less consequential. Results from conceptual delta modeling support the hypothesis that pronounced wave action inhibits mouth bar formation and the resulting bifurcations that form delta network structure (Geleynse, Storms et al. 2011), so the fact that the Wax Lake Delta's formation has been dominated by mouth bar formation could indicate little wave influence on delta building through sand deposition. The successful simulation of the stratigraphic cyclicity in a setting with only riverine forcings further supports the dependence of this feature on seasonal discharge variations.

7. Conclusions and Recommendations

This research sought to investigate delta development processes through the successful simulation of a long-term period of morphological development in the Wax Lake Delta in Atchafalaya Bay, Louisiana. To accomplish this goal, a hydrodynamic and morphologic model of the study area was developed using the process-based Delft3D modeling program. This final chapter discusses the main conclusions drawn through examination of model results and gives recommendations both for more successful simulation of the Wax Lake Delta development as well as opportunities to advance the understanding of delta development processes through long-term morphological modeling.

7.1 Conclusions

The model was generally successful in simulating the growth typical of river dominant systems. The simulated Wax Lake Delta expanded basinward with the establishment and growth of elongate subaerial depositional bodies while maintaining its approximate radial symmetry. While reproducing the very large scale, qualitative morphodynamic behavior of the prototype delta, more specific stratigraphic features were also reproduced. The successive stacking of coarsening upwards sequences observed in Wax Lake Delta mouth bar deposits was evident in the stratigraphy of modeled incipient jet deposits, a result of the varying discharge regime that represents the strong seasonality in the Wax Lake Outlet discharge regime.

The long-term morphological model results unfortunately did not accurately reproduce the specific prototype Wax Lake Delta morphological development during the five year simulation period. The simulated delta experienced growth in subaerial land exposure to a much greater degree than the prototype, which only experienced modest growth through basinward expansion of established depositional lobes, the continued growth of new jet deposits at main delta distributary mouths into fully-developed mouth bars, and the infill of several very-minor distributary channels. Alternatively, the most dramatic morphological change observed in the simulated delta is the development of extensive, sub-aerial depositional lobes basinward of the existing depositional lobes present in the initial bathymetry. Examination of the resulting stratigraphy indicates that these sub-aerial features are composed exclusively of the mud sediment fraction. Both the main Wax Lake Outlet channel and the delta distributary channels were significantly incised during the simulation, leading to a full depletion of the initially-10 m thick sediment bed layer in the upstream feeder channel over the course of the simulation period. The narrowing proceeds from subaqueous levee deposition near the distributary channel banks and accretion at the upstream ends of established depositional lobes. Incipient jet deposits develop at the mouths of Greg and Main Passes, mimicking the most active depositional sites during the simulation period in the prototype Wax Lake Delta; however, the deposits do not evolve into fully-developed mouth bars that have aggraded sufficiently to induce flow bifurcation.

Though the resulting morphology of the delta did not accurately simulate real delta development, each modeled morphological development is representative of typical river dominant deltaic processes observed in the Wax Lake and hydrologically and sedimentologically similar Atchafalaya Delta. Despite the discrepancies between simulated and observed delta development, this study reinforces the conclusion, established by the conceptual delta development models discussed in

section 2.3, that process-based models of hydrodynamics and resulting morphology are capable of simulating the larger spatial- and time-scale geologic developments involved in delta formation.

The accurate simulation of the actual development of a real delta requires a corresponding accurate representation of dominant processes, model domain bathymetry and sediment composition, and the calibration of hydrodynamics and sediment transport. Though the hydrodynamic calibration process was fairly straightforward, the subsequent need to alter calibrated sediment transport parameters for more accurate long-term simulation highlights the difficulty of transport calibration based on a single, discreet measured event. In this case, the possible storage of fine sediment in the prototype upstream channel during low flows, hysteresis in transport and discharge peaks at the upstream boundary, and the limited model representation of marine processes create significant complications for calibration.

The cause of the channel incision and narrowing is not immediately clear in the model results. Though distributary channels in the real Wax Lake Delta do frequently incise through the full deltaic sedimentary sequence into the old bay bottom with channel extension, the incision simulated in the model is clearly excessive. The incision is persistent throughout the imposed flow cycle of the morphological year, so a misrepresentation of discharge regime with higher flows is likely not the main cause. As distributary channels become increasingly narrow to widths on the order of the grid resolution, the oblique channel orientation to the curvilinear grid begins to induce small, grid-oriented erosive channels. The initial grid orientation without regard to channel network structure could also be a contributing factor to the levee deposition that initiates narrowing. Sensitivity runs utilizing an alternative non-cohesive sediment transport formulation were able to more accurately represent delta development without the excessive channel incision and narrowing occurring in the main simulation.

The modeled upstream accretion of depositional lobes similarly was not observed in the prototype delta; however, it has been a dominant delta-building process in the Atchafalaya Delta. Both the deposits at upstream ends of depositional bodies and along channel banks as subaqueous levees are fully composed of the non-cohesive sediment fraction. The excessive upstream channel erosion could be a cause for this unrealistic representation by increasing the sand load through the narrowing delta channels with reduced transport efficiency to the delta front.

The excessive prodelta mud deposition that leads to the development of unrealistic subaerial features is a consequence of the neglected marine processes as part of the assumed full river dominance. The significant fine sediment resuspension and export from Atchafalaya Bay due to waves and wind-induced transport during the passage of winter cold fronts that occurs in the prototype situation (detailed in section 2.4.3) is not reproduced by the simulation, as no marine processes are imposed in the receiving basin. If the actual receiving basin did not experience marine forcings as in the simulation, substantial mud deposition would be expected from the fine-sediment dominant large suspended load reaching the delta; however, the relatively low-energy marine processes are sufficient to inhibit the accumulation of fine sediment basinward of Wax Lake delta front that develops in the present study.

Though incipient jet deposits developed in the model at the distal ends of distributary channels corresponding to the most active depositional sites in the prototype Wax Lake Delta, the prograding bars did not aggrade to a degree sufficient to induce flow bifurcation and the development of a

mature mouth bar depositional lobe. The lack of full mouth bar development could be a consequence of an altered mouth jet structure with the extreme incision and narrowing, a reduced sediment supply as the full 10 m thick bed is eroded upstream, and a non-representative initial geometry that does not capture the small, though already sub-aerial developing mouth bar. Stratigraphy of the incipient jet deposit evolves as expected, with an overall coarsening-upwards though sand-dominant sequence that conforms to typical stratigraphic patterns arising from friction-dominant river effluents. Additionally, a successive stacking of multiple coarsening upwards sequences corresponding to each morphological year is preserved in the prograding bar stratigraphy. This stacking of sequences was identified in mature Wax Lake Delta mouth bars, and can be attributed to the discharge variability present in the prototype as well as in the schematized varying upstream flow and sediment boundary conditions in the model. The main consequence of using multiple discharges in the discharge regime schematization is the delineation of the morphological year into periods of prodelta mud deposition dominance and periods of sand deposition dominance.

The Wax Lake Delta is clearly a river-dominant delta according to traditional classification schemes as there is no evidence of reworking of the primary delta depositional features by waves or tides. Though the predominantly-sand delta depositional bodies arise from friction-dominant river mouth processes, the deposition of cohesive fractions is much more dependent on the basin processes that inhibit the settling of, resuspend, and export fine sediments from the Atchafalaya Bay. Thus, the processes contributing to coarse sediment depositional features can be at least qualitatively simulated under purely riverine forcing; however, fine sediment dynamics cannot be accurately simulated because the primary processes controlling their deposition in the Wax Lake Delta and Atchafalaya Bay are not included in the present, process-limited model.

7.2 Recommendations

The long-term morphologic model of the Wax Lake Delta developed and implemented in the current study is able to reproduce typical river dominant deltaic processes with varying degrees of success, but many opportunities exist to potentially improve the simulation of the actual morphological development of the real delta during the simulation period. The following expansions to the current modeling study are recommended to achieve more accurate simulation and a corresponding better understand of delta development both in the study area and in general:

- The foremost recommendation is to include the neglected basin processes in the model. This could be achieved with the simple addition of an average wave climate imposed at the offshore model boundary or a more complex boundary condition formulation that includes the effects of wind fields on water levels and fine sediment transport during passing cold fronts.

- A corollary to the above recommendation is the expansion of the model boundaries to include a greater portion of the receiving basin. In the present simulation, delta growth gradually alters bed levels very near to the basinward model boundary. To avoid any complications with imposed boundary conditions, model boundaries should be located a significant distance from the delta so as to be unaffected by any potential delta growth. The effects of any flow from the neighboring Atchafalaya

Delta are disregarded in this model, so any expansion of model domain boundaries would also need to include the Atchafalaya Delta and upstream portions of the Lower Atchafalaya River. The addition of wind and/or wave forcings would especially require model boundary expansion, possibly even to or beyond the bay/gulf boundary, to remove boundary effects from the marine forcings.

- Though tidal currents in the Atchafalaya Bay are not large enough to have a significant effect on delta morphology, the periodic lowering of basin water levels could have a positive impact on the simulation of mouth bar formation as mouth bars were found to stop prograding and aggrade significantly when water levels above the bar were below a certain point. Thus it is recommended to implement a simple mixed-diurnal tide schematization representative of the range experienced in Atchafalaya Bay.

- Though the fine sand sediment fraction included to represent non-cohesive sediment in the suspended load and model domain bed is quite representative of the typically fine sediments of the area, larger sand certainly exists as part of the bed material gradation. Inclusion of another, larger sand fraction could help to reduce the unrealistic channel incision that occurs throughout the simulation period.

- The computational grid could be further refined, especially in the area comprising distributary channel mouths where mouth bar deposition and channel bifurcation is likely to occur. Though conceptual models have successfully simulated mouth bar formation with grid sizes on the order of those used in the models, grid refinement would allow for a more accurate representation of complex flow patterns around developing mouth bars and reduce the observed grid effects as the distributary channels narrow.

- As already discussed, the computational grid was developed without regard to delta distributary channel orientation which may have contributed to excessive channel narrowing with induced, artificial roughness. A better approach for simulating the complex channel networks typical of deltas may be the use of an unstructured, flexible computational grid. This functionality is currently being integrated into the Delft3D modeling program.

- The difficulty of sediment transport calibration, especially fine sediment transport, in the Wax Lake Outlet delta from a single, discreet flow period has been discussed. A more accurate calibration of sediment transport parameters could be achieved if measurements of fine and coarse sediment concentrations in the delta distributary channels were available for a continuous period that ideally would capture both the rising and falling limbs of the annual flood. This more representative calibration period would yield better calibrated parameters that presumably would result in a more accurate simulation of morphology and stratigraphy. Additionally, a more recent full hydrographic survey of the delta channels and depositional lobes would aid in future morphological modeling efforts.

- Sensitivity analysis (see Appendix C) indicates that use of the alternative Engelund-Hansen sediment transport formulation eliminates the unrealistic channel incision and narrowing observed in model results. A redevelopment of the model with this formulation is recommended as a possible means to improve simulation of long-term morphologic development in the Wax Lake Delta.

The results of this study indicate that successful simulation of delta development along the typically low-energy Louisiana coast requires inclusion of marine processes beyond those included in this assumed river-dominant simulation. The inclusion of two sediment fractions, necessary to assess the validity of depositional body stratigraphy, likely results in a less accurate morphologic simulation than if only the coarse sediment fraction was included because of the neglected processes and their effect on fine sediment deposition. Though it was thought that the use of process-based, depth-averaged morphological modeling in Delft3D would offer an ideal method for assessing the expected land building arising from large-scale sediment diversions for land-building in the transgressive Mississippi Delta, the necessary inclusion of multiple marine processes for accurate delta development simulation, especially the difficult to implement wind forcings from periodic cold front passages, makes the use of this modeling technique somewhat inefficient. At the moment, more simplified models that assume delta radial symmetry are more suited for the evaluation of expected diversion land-building for preliminary studies where multiple location alternatives are still in consideration. Detailed process-based modeling, such as that presented in this study, is more suited for much higher level evaluations in the diversion design process that justify the increased effort to adequately represent all processes involved. For situations in which the exact stratigraphy of depositional bodies is of no interest, simulation of the development of the mostly sand-dominant delta features in the Southeast Louisiana Coast may be more efficiently achieved with a single fraction sediment schematization.

8. References

Allison, M. A., G. C. Kineke, et al. (2000). "Development and reworking of a seasonal flood deposit on the inner continental shelf off the Atchafalaya River." Continental Shelf Research 20(16): 2267-2294.

Allison, M. A. and E. A. Meselhe (2010). "The use of large water and sediment diversions in the lower Mississippi River (Louisiana) for coastal restoration." Journal of Hydrology 387(3-4): 346-360.

Barras, J., S. Beville, et al. (2004). Historical and projected coastal Louisiana land changes: 1978-2050: USGS Open File Report 03-334, U.S. Department of the Interior, U.S. Geological Survey: 39.

Blum, M. D. and H. H. Roberts (2009). "Drowning of the Mississippi Delta due to insufficient sediment supply and global sea-level rise." Nature Geosci 2(7): 488-491.

Camenen, B. and P. Larroudé (2003). "Comparison of sediment transport formulae for the coastal environment." Coastal Engineering 48(2): 111-132.

Chow, V. T., D. R. Maidment, et al. (1988). Applied Hydrology. Singapore, McGraw-Hill Book Company.

Day, J. W. J., D. F. Boesch, et al. (2007). "Restoration of the Mississippi Delta: Lessons from Hurricanes Katrina and Rita." Science 315: 1679-1684.

Deltares (2009). Delft3D-FLOW: Simulation of multi-dimensional hydrodynamic flows and transport phenomena, including sediments: User Manual. Delft, the Netherlands, Deltares. Version: 3.14 Revision: 7864: 630.

Donnell, B. P., J. V. J. Letter, et al. (1991). Report 11: Two-dimensional Modeling. Technical Report HL-82-15: The Atchafalaya River Delta. Vicksburg, Mississippi, Waterways Experiment Station, United States Army Corps of Engineers: 200.

DuMars, A. J. (2002). Distributary Mouth Bar Formation and Channel Bifurcation in the Wax Lake Delta, Atchafalaya Bay, Louisiana. Department of Geology and Geophysics. Baton Rouge, Louisiana, Louisiana State University.

Edmonds, D. A. and R. L. Slingerland (2007). "Mechanics of river mouth bar formation: Implications for the morphodynamics of delta distributary networks." J. Geophys. Res. 112(F2): F02034.

Edmonds, D. A. and R. L. Slingerland (2010). "Significant effect of sediment cohesion on delta morphology." Nature Geosci 3(2): 105-109.

Flynn, K. M., W. H. Kirby, et al. (2006). "User's manual for Program PeakFQ, annual flood-frequency analysis using Bulletin 17B guidelines." from http://purl.access.gpo.gov/GPO/LPS97012.

Galloway, W. E. (1975). Process framework for describing the morphologic and stratigraphic evolution of deltaic depositional systems. Deltas, Models for Exploration. M. L. Broussard, Houston Geological Society: 87-98.

Geleynse, N., J. E. A. Storms, et al. (2010). "Modeling of a mixed-load fluvio-deltaic system." Geophys. Res. Lett. 37(5): L05402.

Geleynse, N., J. E. A. Storms, et al. (2011). "Controls on river delta formation; insights from numerical modelling." Earth and Planetary Science Letters 302(1-2): 217-226.

Hillen, M. (2009). Wave reworking of a delta: Process-based modelling of sediment reworking under wave conditions in the deltaic environment. Faculty of Civil Engineering and Geosciences. Delft, the Netherlands, Delft University of Technology.

Kim, W., D. Mohrig, et al. (2008). Land Building in the Delta of the Mississippi River: Is it Feasible?, Chapter 10. Coastal Louisiana Ecosystem Assessment & Restoration (CLEAR) Program: A tool to support coastal restoration. Volume IV. Final Report to Department of Natural Resources, Coastal Restoration Division, Baton Rouge, LA. Contract No. 2512-06-02. R. R. Twilley.

Lesser, G. R., J. A. Roelvink, et al. (2004). "Development and validation of a three-dimensional morphological model." Coastal Engineering 51(8-9): 883-915.

Mashriqui, H. S. (2003). Hydrodynamic and Sediment Transport Modeling of Deltaic Sediment Transport Processes: A Dissertation. Department of Civil and Environmental Engineering. Baton Rouge, Louisiana, Louisiana State University.

Mossa, J. (1996). "Sediment dynamics in the lowermost Mississippi River." Engineering Geology 45(1-4): 457-479.

Nemec, W. (2009). Deltas — Remarks on Terminology and Classification. Coarse-Grained Deltas, Oxford: 3-12.

Nittrouer, J. A., M. A. Allison, et al. (2008). "Bedform transport rates for the lowermost Mississippi River." J. Geophys. Res. 113(F3): F03004.

Olariu, C. and J. P. Bhattacharya (2006). "Terminal Distributary Channels and Delta Front Architecture of River-Dominated Delta Systems." JOURNAL OF SEDIMENTARY RESEARCH 76(2): 212-233.

Orton, G. J. and H. G. Reading (1993). "Variability of deltaic processes in terms of sediment supply, with particular emphasis on grain size." Sedimentology 40(3): 475-512.

Parker, G. and O. Sequeiros (2006). Large Scale River Morphodynamics: Application to the Mississippi Delta. Proceedings, River Flow 2006 Conference, Lisbon, Portugal, Sept. 6-8, 2006.

Penland, S., R. Boyd, et al. (1988). "Transgressive Depositional Systems of the Mississippi Delta Plain: A Model for Barrier Shoreline and Shelf Sand Development." Journal of Sedimentary Petrology 58(6): 932-949.

Ranasinghe, R., C. Swinkels, et al. "Morphodynamic upscaling with the MORFAC approach: Dependencies and sensitivities." Coastal Engineering In Press, Corrected Proof.

Roberts, H. H. (1998). "Delta Switching: Early Responses to the Atchafalaya River Diversion." Journal of Coastal Research 14(3): 882-899.

Roberts, H. H., R. D. Adams, et al. (1980). "Evolution of sand-dominant subaerial phase, Atchafalaya Delta, Louisiana." AAPG Bulletin 64(2): 264-279.

Roberts, H. H., J. M. Coleman, et al. (2003). "An Embryonic Major Delta Lobe: A New Generation of Delta Studies in the Atchafalaya-Wax Lake Delta System." Gulf Coast Association of Geological Societies Transactions 53: 690-703.

Roberts, H. H., N. Walker, et al. (1997). "Evolution of Sedimentary Architecture and Surface Morphology: Atchafalaya and Wax Lake Deltas, Louisiana (1973-1994)." Gulf Coast Association of Geological Societies Transactions XLVII: 8.

Roberts, H. H., N. D. Walker, et al. (2005). Effects of Cold Fronts on Bayhead Delta Development: Atchafalaya Bay, Louisiana, USA. High Resolution Morphodynamics and Sedimentary Evolution of Estuaries. D. M. FitzGerald and J. Knight, Springer Netherlands. 8: 269-298.

Roelvink, J. A. (2006). "Coastal morphodynamic evolution techniques." Coastal Engineering 53(2-3): 277-287.

Snedden, G. A., J. E. Cable, et al. (2007). "Sediment discharge into a subsiding Louisiana deltaic estuary through a Mississippi River diversion." Estuarine, Coastal and Shelf Science 71(1-2): 181-193.

Storms, J. E. A., M. J. F. Stive, et al. (2007). Initial Morphologic and Stratigraphic Delta Evolution Related to Buoyant River Plumes. Proceedings of the Sixth International Symposium on Coastal Engineering and Science of Coastal Sediment Process, New Orleans, Louisiana, American Society of Civil Engineers.

Swarzenski, C. M., United States. Army. Corps of Engineers. New. Orleans District, et al. (2003). Surface-water hydrology of the Gulf Intracoastal Waterway in South-Central Louisiana, 1996-99. Reston, Va.; Denver, CO, U.S. Dept. of the Interior, U.S. Geological Survey ; U.S. Geological Survey, Branch of Information Services [distributor].

USACE. (2006). "Stage Data - Atchafalaya Bay Near Eugene Island (LA) " Retrieved February 10, 2011, from http://www.mvn.usace.army.mil/cgi-bin/watercontrol.pl?88550.

USACE (2009). LOUISIANA COASTAL PROTECTION AND RESTORATION (LACPR): FINAL TECHNICAL REPORT. New Orleans, Louisiana, U.S. Army Corps of Engineers.

USACE (2010). APPENDIX A-HYDRODYNAMIC ADH MODELING FOR THE 2010 ATCHAFALAYA BASIN FLOODWAY SYSTEM MR&T FLOW LINE. 2010 ATCHAFALAYA BASIN FLOODWAY SYSTEM MR&T FLOW LINE. New Orleans, LA, U.S. Army Corps of Engineers, New Orleans District, Hydraulics and Hydrologic Section: 82.

USACE (2010). APPENDIX D -HEC-6T SEDIMENT MODELING, ATCHAFALAYA BASIN, LOUISIANA, TECHNICAL APPENDIX, VOLUME 3. 2010 ATCHAFALAYA BASIN FLOODWAY SYSTEM MR&T FLOW LINE, U.S. Army Corps of Engineers: 188.

USGS (2005). Depicting Coastal Louisiana Land Loss, U.S. Department of the Interior, U.S. Geological Survey.

USGS. (2011). "National Water Information System data available on the World Wide Web (Water Data for the Nation)." Retrieved March 23, 2011, from http://waterdata.usgs.gov/nwis/dv?cb_00060=on&format=html&begin_date=1986-06-01&end_date=2011-03-22&site_no=07381590&referred_module=sw.

USGS. (2011). "National Water Information System data available on the World Wide Web (Water Quality Samples for the Nation)." Retrieved February 18, 2011, from http://nwis.waterdata.usgs.gov/nwis/qwdata/?site_no=07381590&agency_cd=USGS&inventory_output=0&rdb_inventory_output=file&TZoutput=0&pm_cd_compare=Greater%20than&radio_parm_cds=parm_cd_list&radio_multiple_parm_cds=30209%0A70331%0A80154%0A80155%0A%0A&format=html_table&qw_attributes=0&qw_sample_wide=wide&rdb_qw_attributes=0&date_format=YYYY-MM-DD&rdb_compression=file&submitted_form=brief_list.

van Heerden, I. L. and H. H. Roberts (1988). "Facies development of Atchafalaya Delta, Louisiana; a modern bayhead delta." AAPG Bulletin 72(4): 439-453.

van Rijn, L. C. (1984). "Sediment Transport, Part I: Bed Load Transport." Journal of Hydraulic Engineering 110(10): 1431-1456.

van Rijn, L. C. (1984). "Sediment Transport, Part II: Suspended Load Transport." Journal of Hydraulic Engineering 110(11): 1613-1641.

Wamsley, T. V., D. Vann Stutts, et al. (2008). Surge and Wave Modeling for the Louisiana Coastal Protection and Restoration Study. Coastal Engineering 2008: Proceedings of the 31st International Conference, Hamburg, Germany.

Wellner, R., R. Beaubouef, et al. (2005). "Jet-Plume Depositional Bodies—The Primary Building Blocks of Wax Lake Delta." Gulf Coast Association of Geological Societies Transactions 55: 867-909.

Winer, H. S. (2007). Re-engineering the Mississippi River as a Sediment Delivery System. Coastal Sediments 2007, New Orleans, Louisiana.

Wright, L. D. (1977). "Sediment transport and deposition at river mouths: A synthesis." Geological Society of America Bulletin 88(6): 857-868.

Wright, L. D. and J. M. Coleman (1973). "Variations in Morphology of Major River Deltas as Functions of Ocean Wave and River Discharge Regimes." AAPG Bulletin 57(2): 370-398.

Yuill, B., D. Lavoie, et al. (2009). "Understanding Subsidence Processes in Coastal Louisiana." Journal of Coastal Research: 23-36.

Appendix A – Hydrodynamic Calibration Results

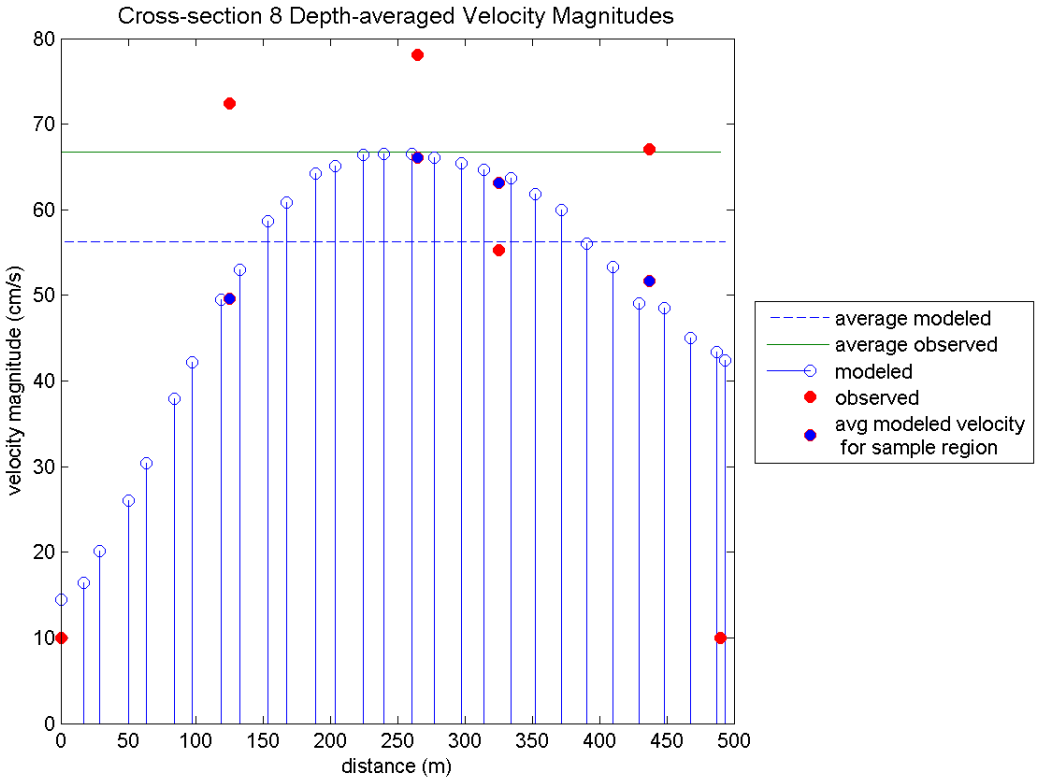

Figure A-1: Comparison of Modeled and Observed Depth-averaged Velocity Magnitudes at Cross-section 8

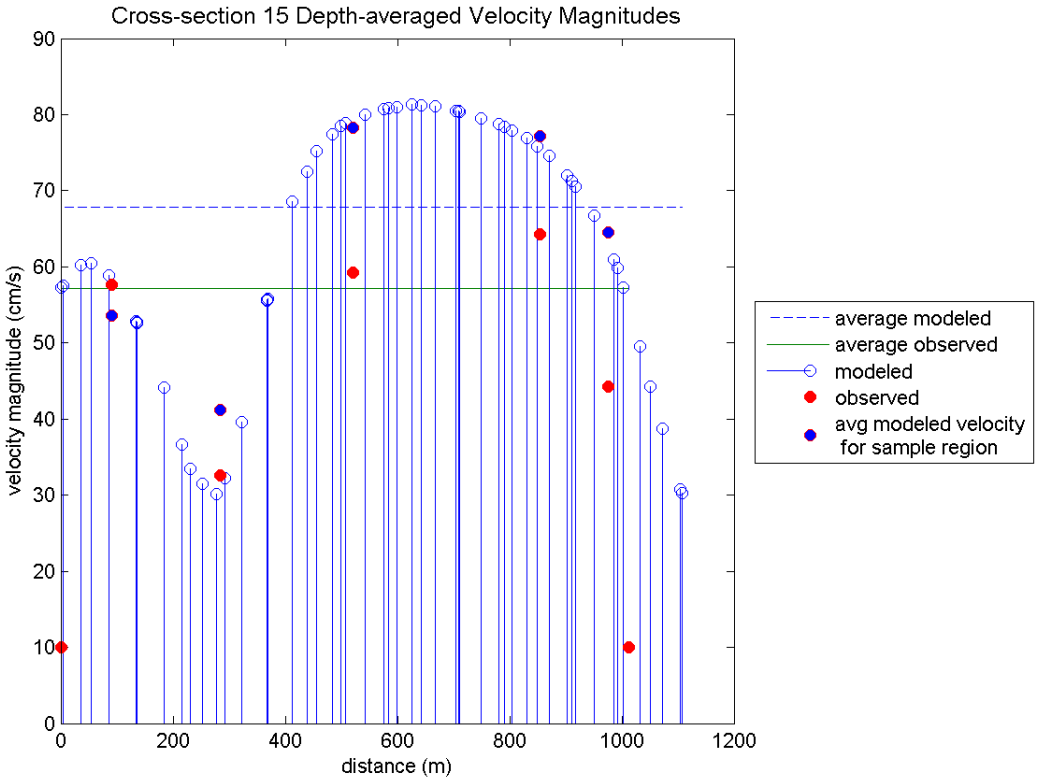

Figure A-2: Comparison of Modeled and Observed Depth-averaged Velocity Magnitudes at Cross-section 15

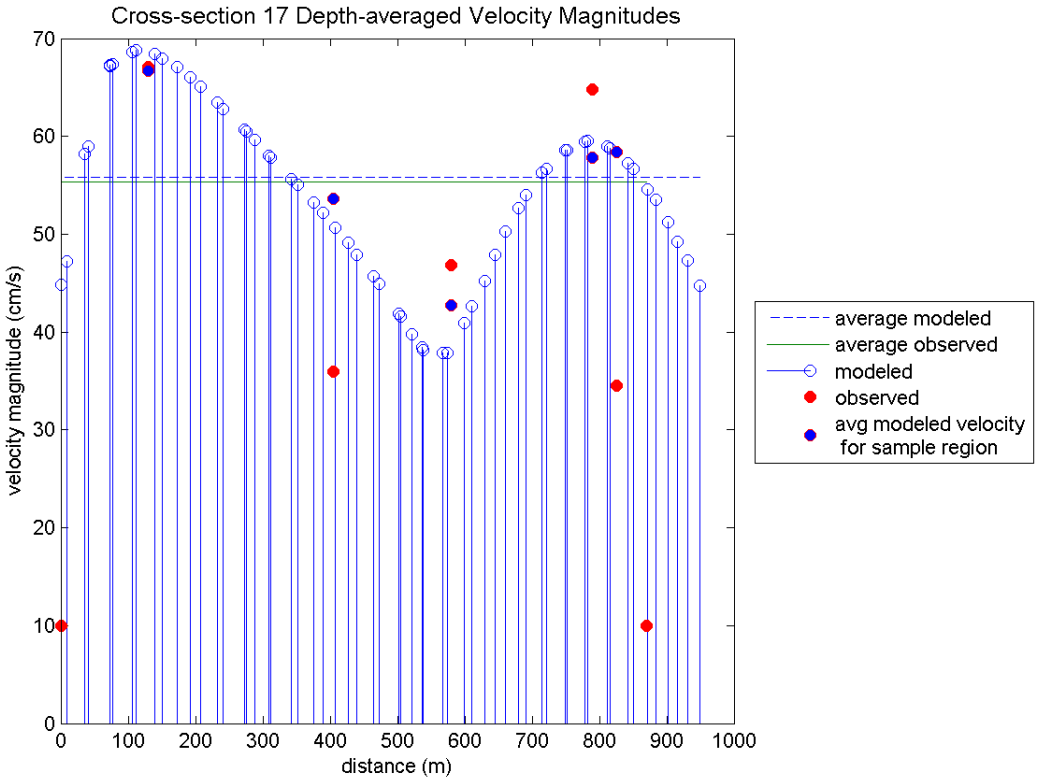

Figure A-3: Comparison of Modeled and Observed Depth-averaged Velocity Magnitudes at Cross-section 17

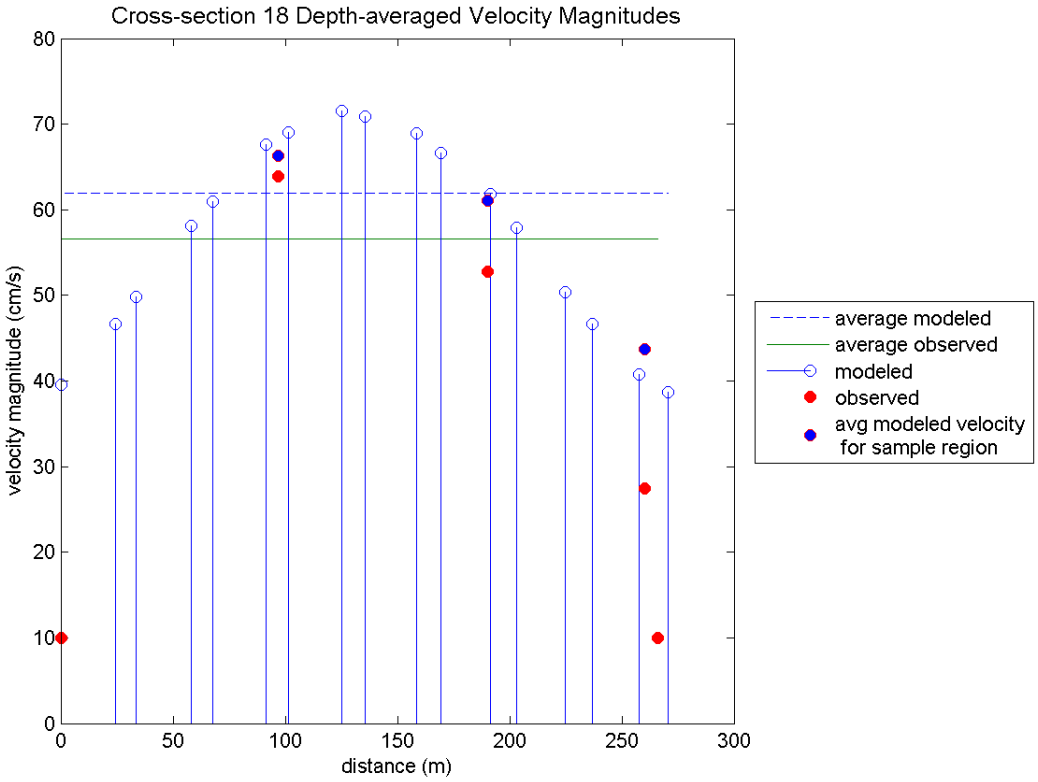

Figure A-4: Comparison of Modeled and Observed Depth-averaged Velocity Magnitudes at Cross-section 18

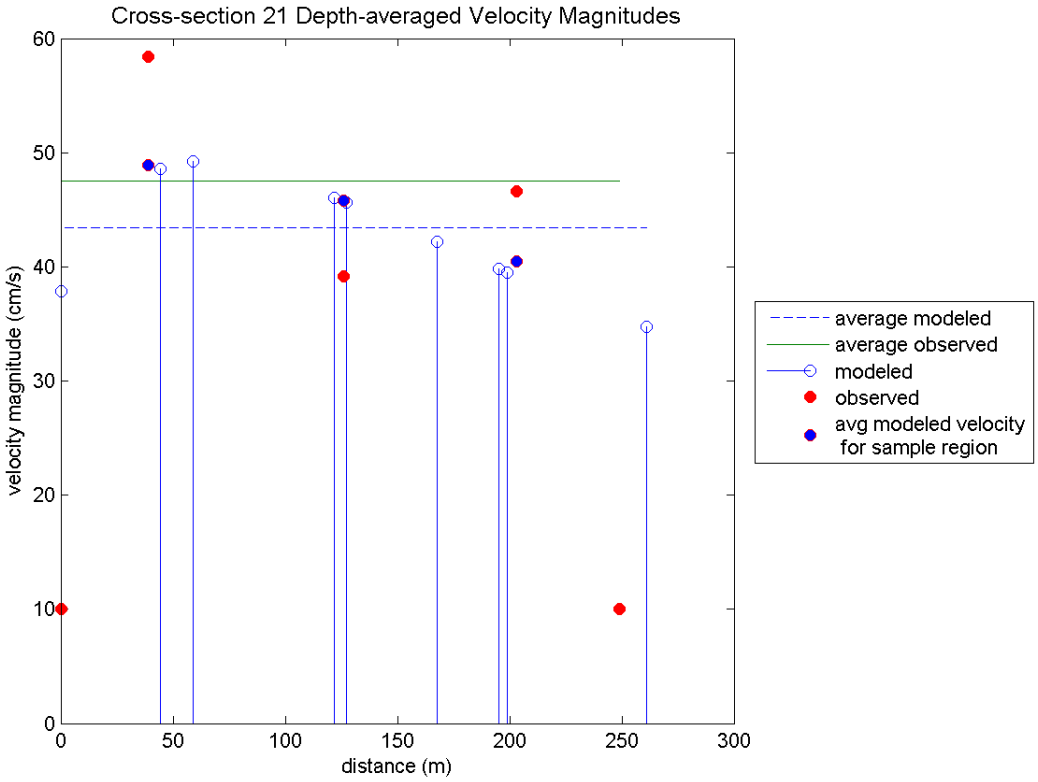

Figure A-5: Comparison of Modeled and Observed Depth-averaged Velocity Magnitudes at Cross-section 21

Appendix B – Transport Calibration Results

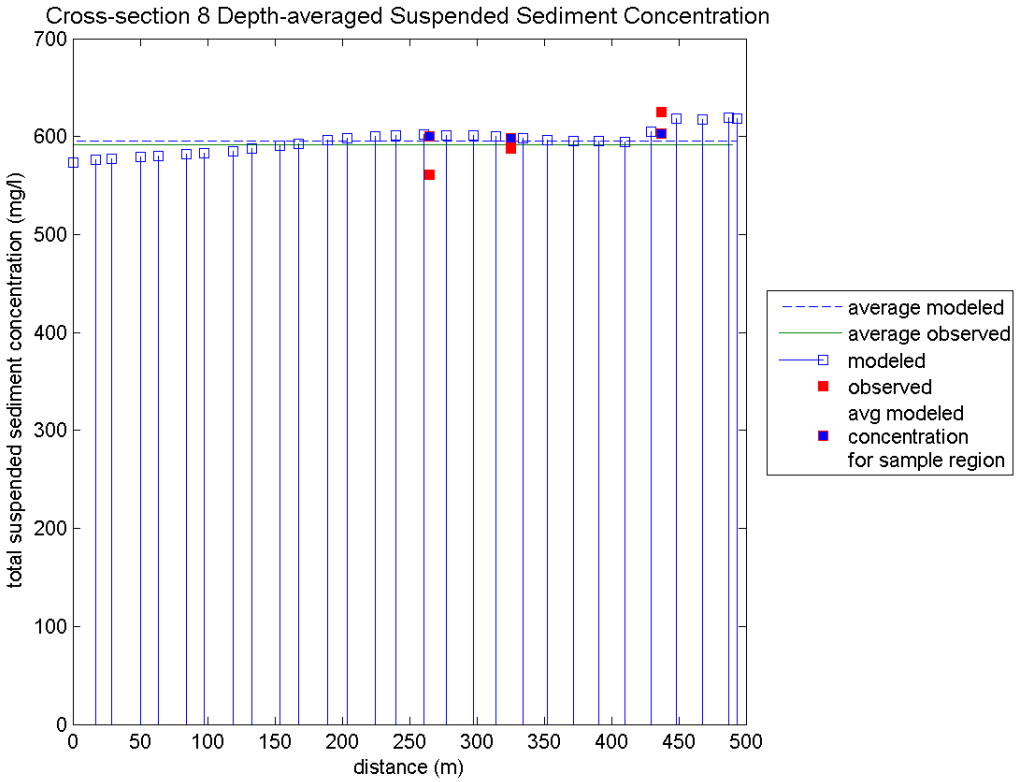

Figure B-1: Comparison of Modeled and Observed Suspended Sediment Concentrations at Cross-section 8

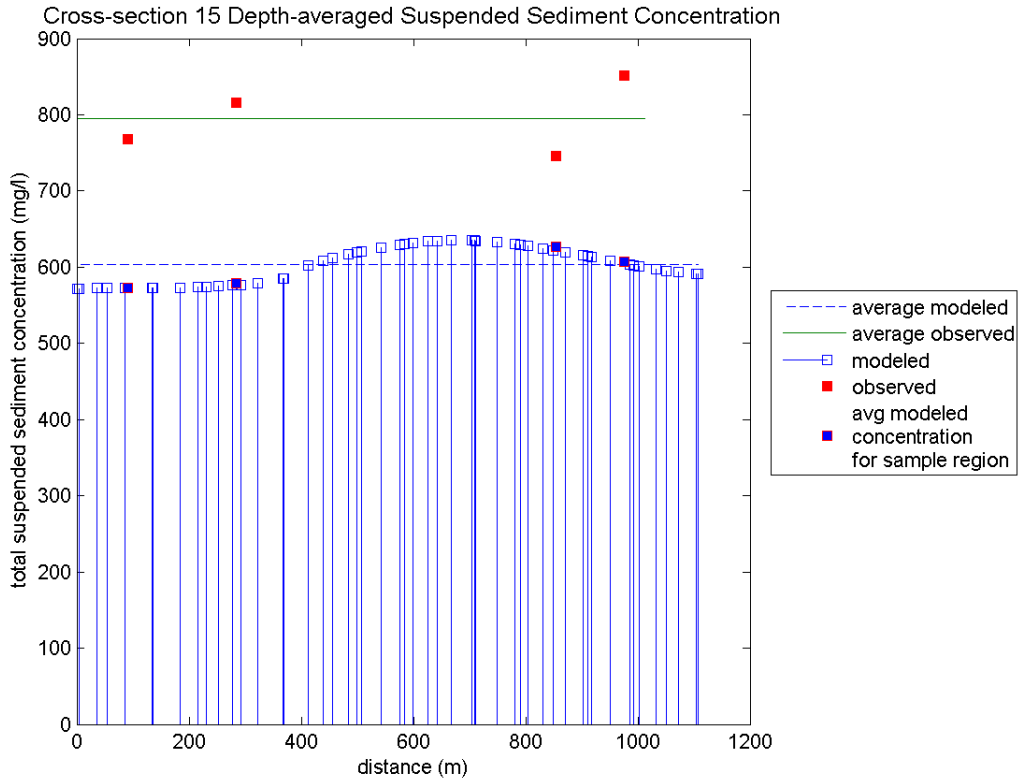

Figure B-2: Comparison of Modeled and Observed Suspended Sediment Concentrations at Cross-section 15

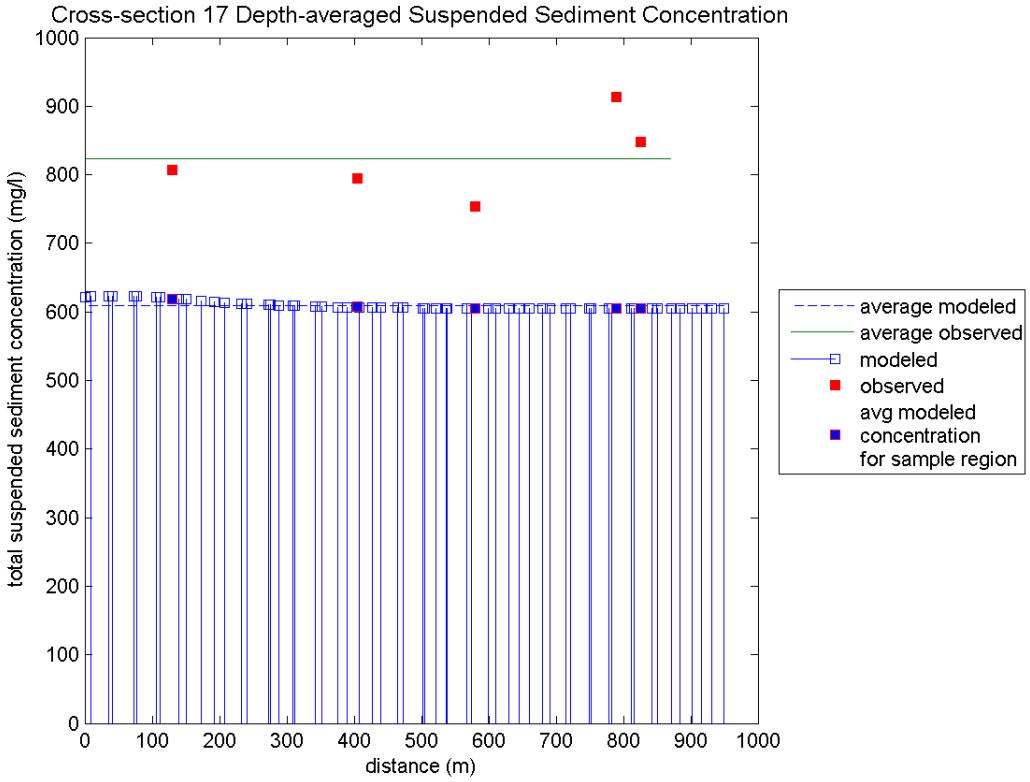

Figure B-3: Comparison of Modeled and Observed Suspended Sediment Concentrations at Cross-section 17

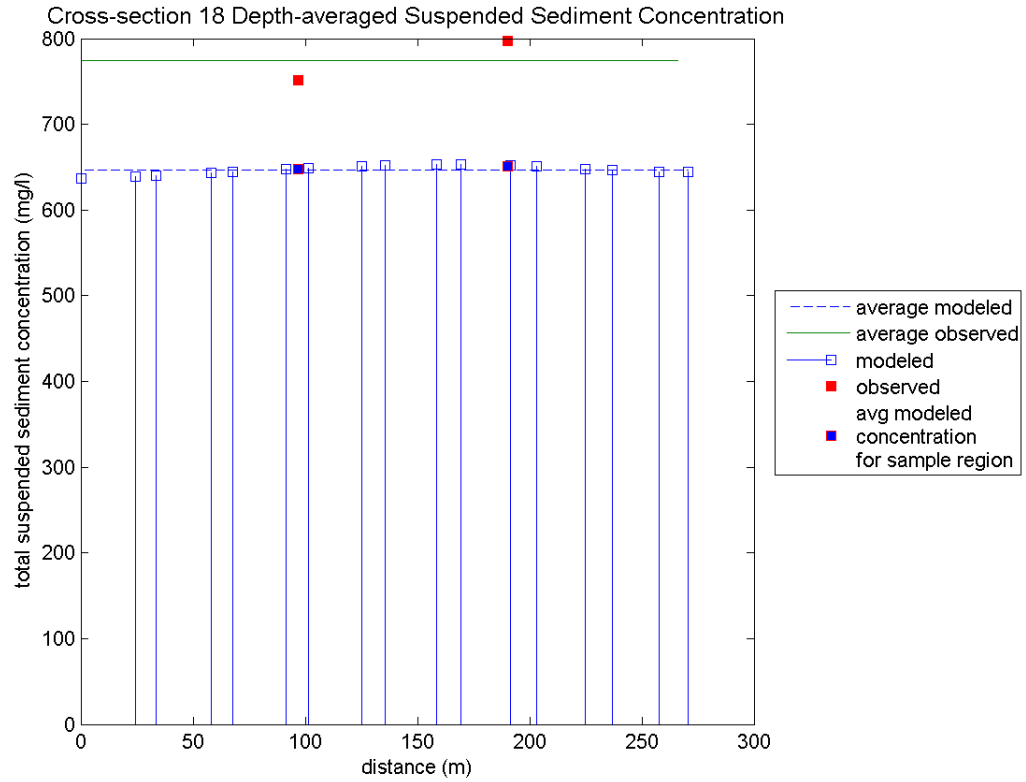

Figure B-4: Comparison of Modeled and Observed Suspended Sediment Concentrations at Cross-section 18

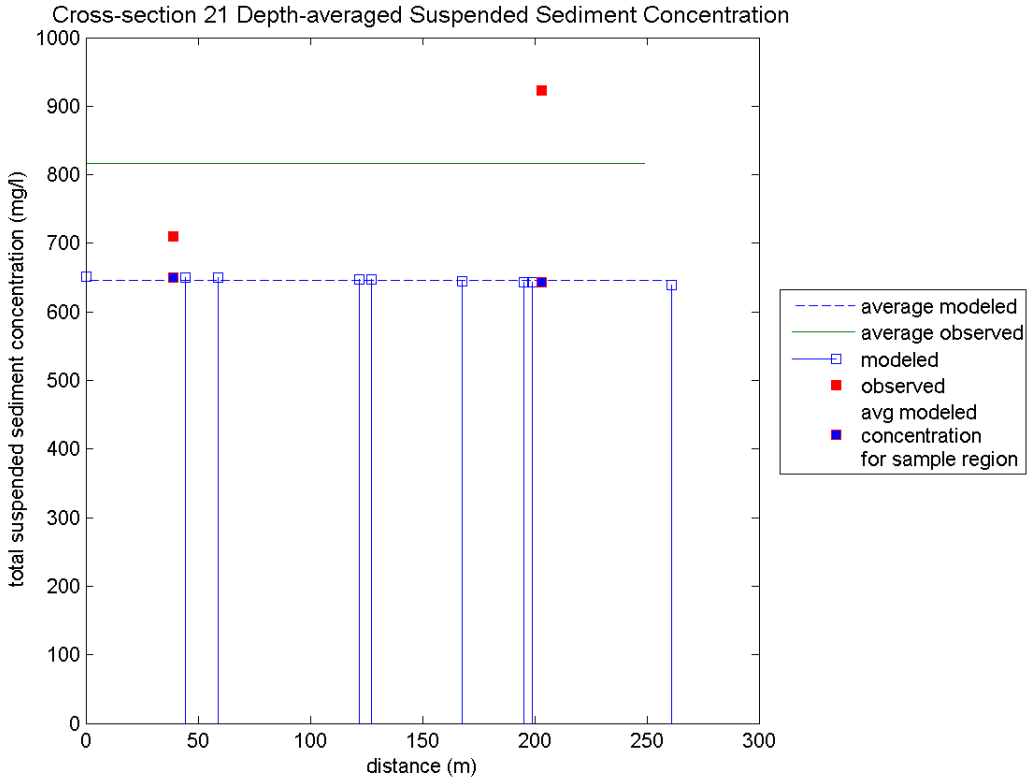

Figure B-5: Comparison of Modeled and Observed Suspended Sediment Concentrations at Cross-section 21

Appendix C – Model Sensitivity

Though some inaccuracies in the simulation of prototype morphological development can be explained by neglected processes and other consequences of modeling assumptions, the causes of the incessant channel narrowing and incision, unrealistic upstream accretion, and inadequate mouth bar development were not immediately clear from model results. In an attempt to gain more insight on causes for these misrepresentations, several more simulations were run with alterations in various parameters. This analysis differs from a traditional investigation of model sensitivity where parameters are systematically altered and the resulting variation in model results is examined; instead, only one alternative value for each parameter is investigated in an effort to efficiently improve simulation of prototype morphology. Table C-1 below gives an overview of the sensitivity runs and parameters that were altered for each simulation.

Table C-1: Overview of model sensitivity analysis

run	parameters	symbol	long term simulation value	sensitivity run value	units
base case	same settings as long term run, but with single discharge level and higher MorFac				
s001	offshore water level boundary		0.32	0	m
s002	depth location in computational grid		depth at grid cell centers	depth at grid cell corners	-
s003	horizontal eddy diffusitivity		10	1	m^2/s
s004	time step	Δt	1	0.5	min
s006	sand fraction grain size	d50	100	150	µm
s007	critical shear stress for cohesive sediment deposition	TcrDep	0.05	1000	N/m^2
s009	critical shear stress for erosion of cohesive sediments	TcrEro	0.5	1	N/m^2
s008	non-cohesive sediment transport calibration parameters	Sus	0.75	0.5	-
		Bed	1	0.5	-
s010	minimum water depth for sediment computations	SedThr	0.1	0.5	m
s013	Fall velocity	ws	0.00025	0	m/s
s014	sediment transport formulation		Van Rijn, 1993	Engelund-Hansen	-

In order to complete the necessary model sensitivity runs more efficiently, a change in the boundary condition discretization strategy was needed. In the long term morphological simulation, multiple discharge levels per morphologic year and the included spin-up intervals result in a model runtime of over six days. For the multiple sensitivity runs, model runtimes were reduced with the use of a single, representative channel-forming discharge that only occurs for a fraction of the year with the

assumption that all morphologic change occurs during the represented period. The fraction of the year that the discharge is applied (flood intermittency factor) is chosen such that the bedload transported by the applied discharge during the shortened period is equal to the mean annual bedload transport (Parker and Sequeiros 2006). The channel-forming discharge level and corresponding intermittency factor for the Wax Lake Outlet were previously found to be 4800 m^3/s and 0.35, respectively (Kim, Mohrig et al. 2008). Table C-2 below gives the hydrodynamic and morphologic periods simulated for the sensitivity runs that include the use of a higher MorFac for shorter simulation times. Sediment concentration boundary conditions were determined with the rating curves described in section 3.6.3, though inflow coarse sediment concentration was not prescribed in favor of an equilibrium condition similar to that used in the long-term simulation. Table C-3 gives the imposed sediment boundary conditions used for each run.

Table C-2: Channel-forming discharge level hydrodynamic and morphologic times of occurrence

Discharge (m^3/s)	Intermittency factor	Hydrodynamic Days (days)	MorFac	Morphologic days (days)	Morphologic Days with flood intermittency (days)
4800	.35	3.5	182.5	638.75	1825

Table C-3: Upstream boundary conditions – single channel-forming discharge level and corresponding mud suspended sediment concentration

Discharge (m^3/s)	Sediment Transport (tons/day)	Total suspended sediment concentration (mg/l)	Percent finer than .0625 mm (%)	Sand suspended sediment concentration (mg/l)	Mud suspended sediment concentration (mg/l)
4800	142680	312	81.8	equilibrium	255

Base Case

The first simulation uses the same parameter settings as the production run described in chapters 5 and 6 but with the constant imposed boundary conditions given in table C-3. Figure C-1 below gives the resulting delta morphology after the five year simulation for the base case; the following figure C-2 gives the difference between the final bed levels for the base case simulation and the production run. Results are qualitatively similar to the results of the production run simulation, reproducing channel narrowing and incision, upstream accretion of depositional lobes, excessive basinward mud deposition, and the development of incipient mouth bars. Slightly less excessive prodelta mud deposition is observed, though this is expected considering the lack of any periods of low flow in the base case simulation.

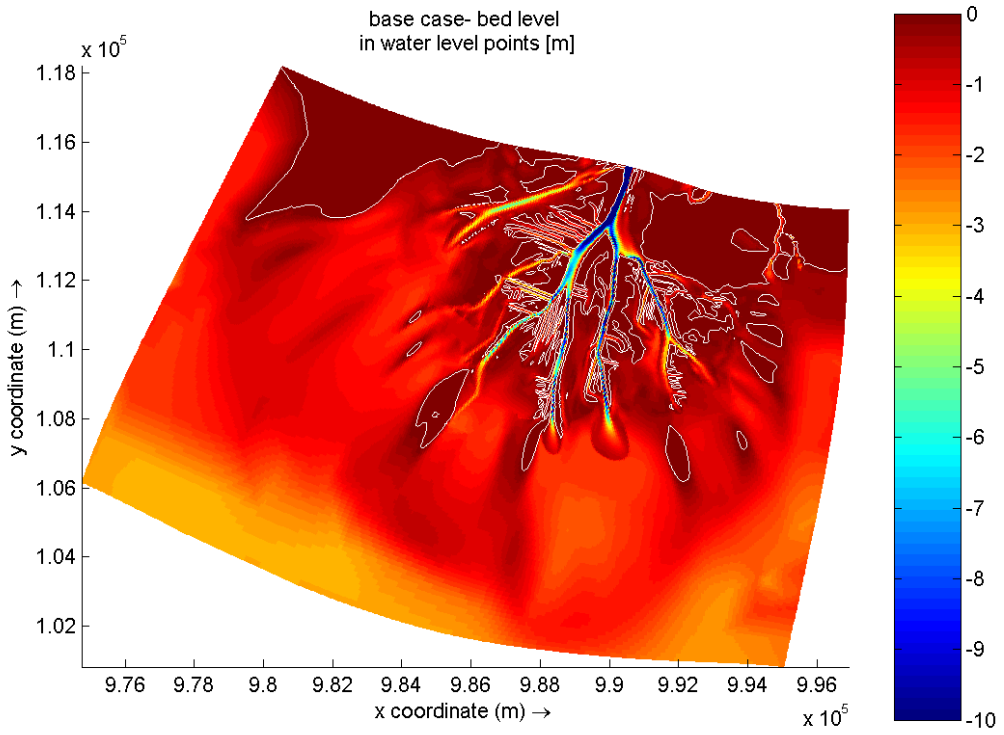

Figure C-1: Base case bathymetry of developing Wax Lake Delta and receiving basin after five years of morphologic simulation along with 0 m contour line. Upper and Lower color limits were defined so that elevations between limits could be viewed with more clarity.

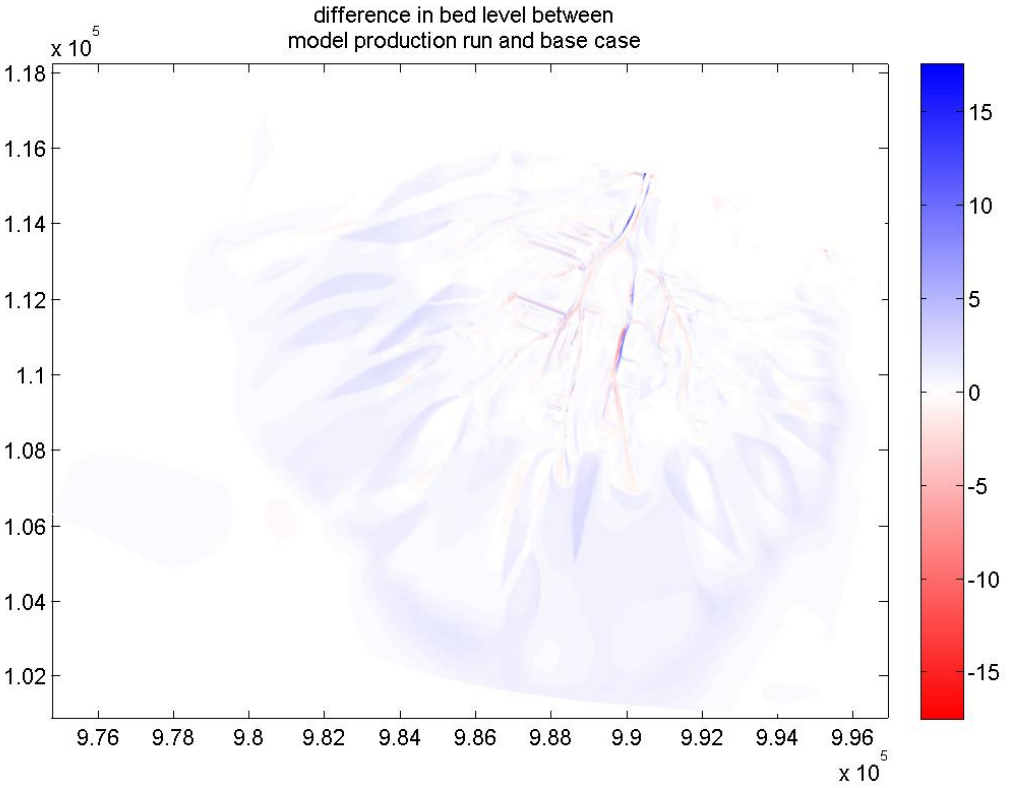

Figure C-2: Difference between final delta bed levels in model production run and base case. Positive values indicate higher bed levels in the production run, and negative values indicate lower bed levels in the production run.

The results of subsequent model sensitivity runs with altered parameters were then compared to the results from the base case. Though quantitative differences in resulting delta bed levels were present in all sensitivity runs, most parameter alterations did not result in significant improvements in prototype morphology simulation. Table C-4 below summarizes the findings of the sensitivity analysis with comments on any significant deviations from the results of the base case simulation.

Table C-4: Summary of sensitivity analysis findings

run	Altered parameters	Effect on resulting delta morphology
s001	offshore water level boundary	Slightly improved mouth bar development, increase in spurious grid-oriented channel incision
s002	depth location in computational grid	No significant difference from base case results
s003	horizontal eddy diffusitivity	Fully-formed mouth bar and channel bifurcation develops, excessive channel incision still present
s004	time step	No significant difference from base case results
s006	sand fraction grain size	No significant difference from base case results
s007	critical shear stress for cohesive sediment deposition	Mud deposition increases over most of the delta, results unrealistic
s009	critical shear stress for erosion of cohesive sediments	No significant difference from base case results
s008	non-cohesive sediment transport calibration parameters	No significant difference from base case results
s010	minimum water depth for sediment computations	No significant difference from base case results
s013	Fall velocity	No mud deposition, no significant effect on coarse depositional features
s014	sediment transport formulation	No channel incision and narrowing

Reduced Horizontal Eddy Diffusitivity

As noted in table C-4 above, the sensitivity run with a reduced horizontal eddy diffusitivity results in the development of a fully-formed mouth bar deposit at the mouth of Greg Pass that has aggraded sufficiently to induce flow bifurcation. Figure C-3 below gives the resulting delta morphology after the five year simulation for the s003 run described, and the following figure C-4 plots the difference between the final bed levels for the s003 run and the base case.

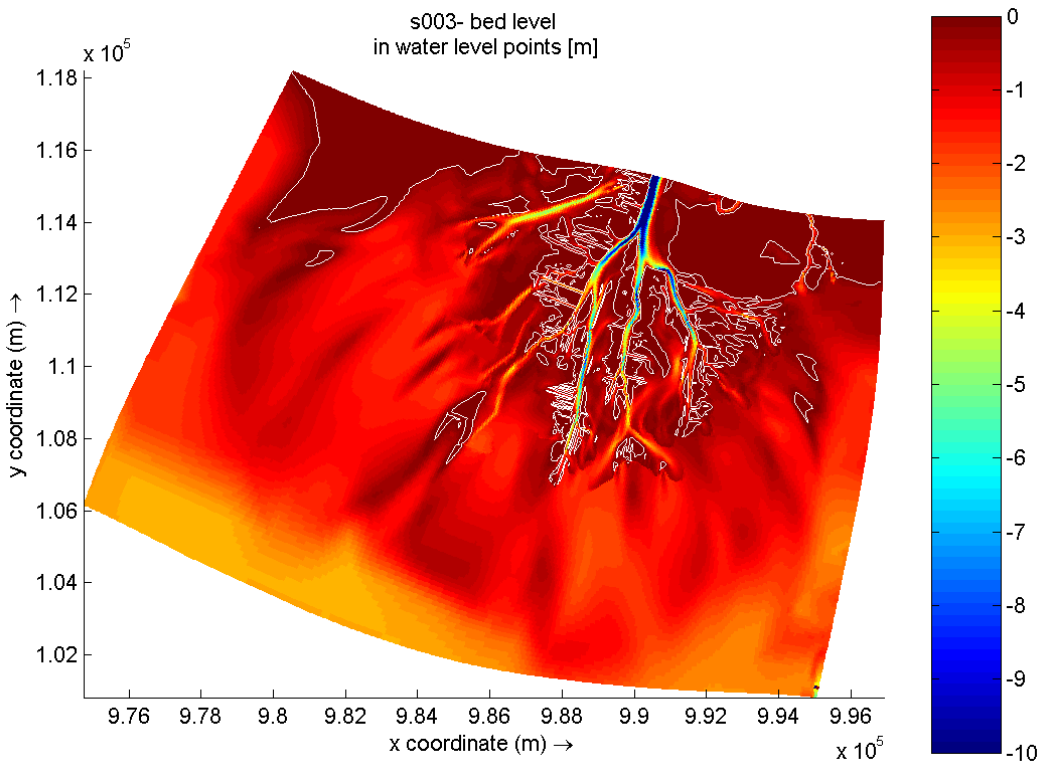

Figure C-3: s003 bathymetry of developing Wax Lake Delta and receiving basin after five years of morphologic simulation along with 0 m contour line. Upper and Lower color limits were defined so that elevations between limits could be viewed with more clarity.

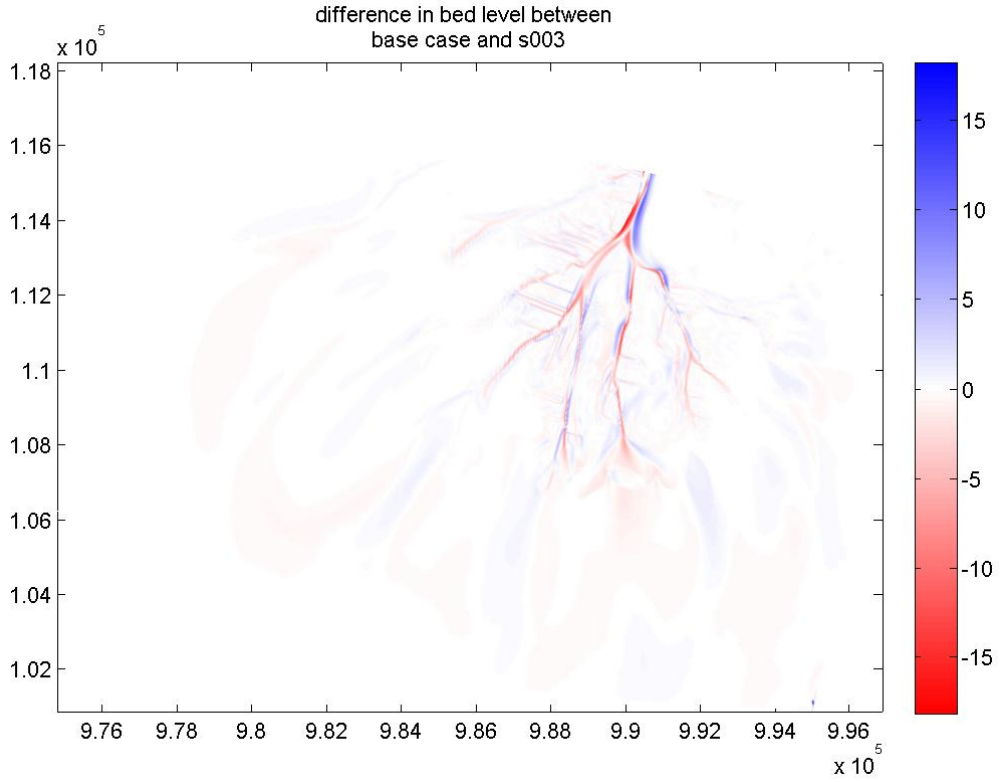

Figure C-4: Difference between final delta bed levels in base case and run s003. Positive values indicate higher bed levels in the base case, and negative values indicate lower bed levels in the base case.

Disabled Mud Deposition

The sensitivity run s013 prevented any mud deposition from occurring by setting the mud sediment fraction fall velocity equal to 0 m/s. This of course prevents the excessive prodelta deposition observed in the prototype run and base case; however, the possible effects of the reduced basinward deposition on developments within the delta could also be assessed. Figure C-5 below gives the resulting delta morphology after the five year simulation for the s013 run described, and the following figure C-6 plots the difference between the final bed levels for the s003 run and the base case. Examination of figure C-6 shows that while the prodelta mud deposition does not occur, there is no significant effect on delta depositional lobe and distributary channel development.

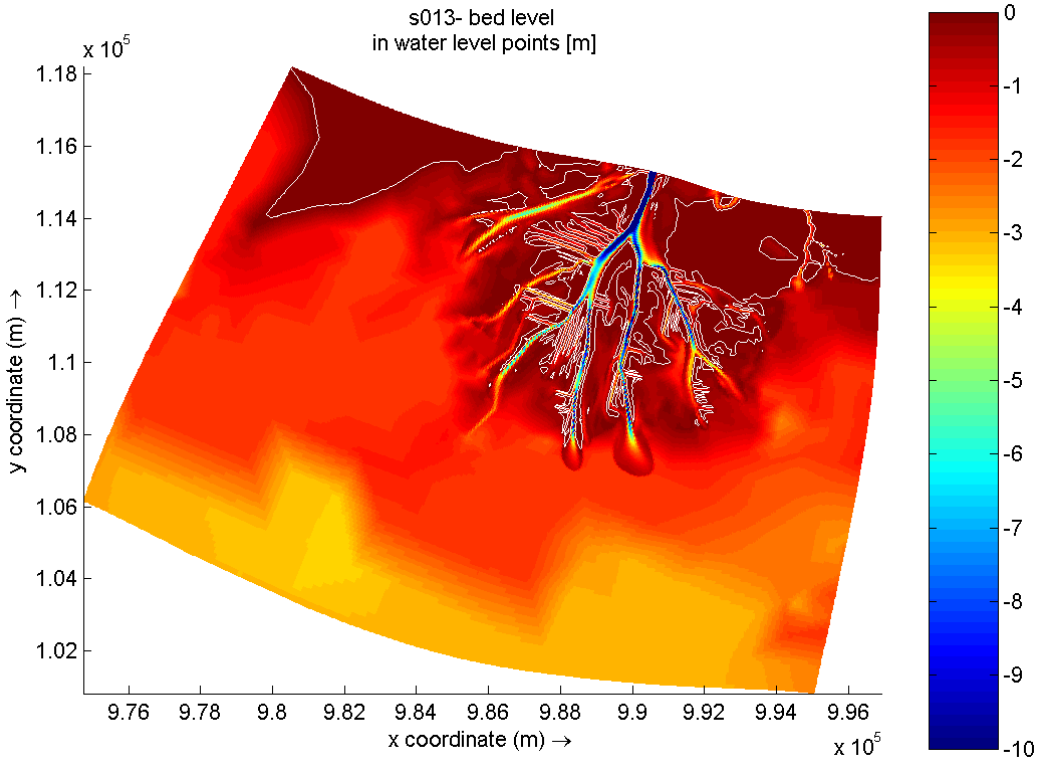

Figure C-5: s013 bathymetry of developing Wax Lake Delta and receiving basin after five years of morphologic simulation along with 0 m contour line. Upper and Lower color limits were defined so that elevations between limits could be viewed with more clarity.

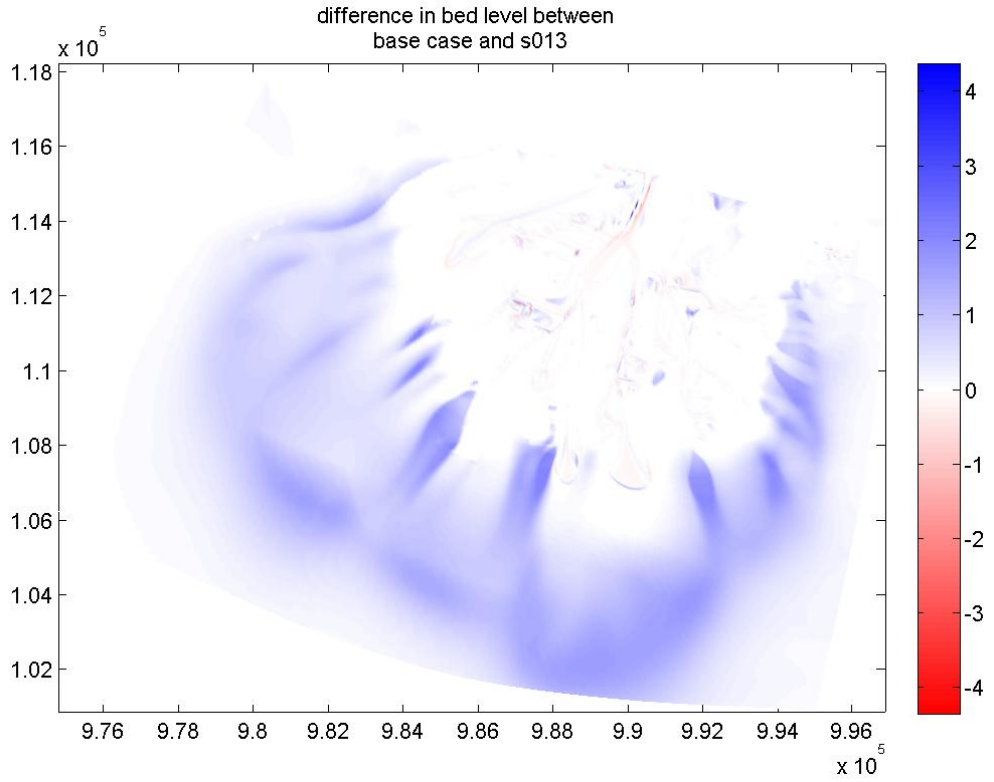

Figure C-6: Difference between final delta bed levels in base case and run s013. Positive values indicate higher bed levels in the base case, and negative values indicate lower bed levels in the base case.

Alternative Non-Cohesive Transport Formulation

The sensitivity run s014 implemented an alternative non-cohesive sediment transport formula, the Engelund-Hansen formulation instead of the Van Rijn, 1993 formula used in all other simulations. Though the model was unable to complete the full simulation run, examination of preliminary results indicates that the excessive channel incision and narrowing that characterize all other simulations do not occur while the prototype process of mouth bar formation continues with incipient jet deposit progradation. Figure C-6 below gives the resulting delta morphology after approximately 1 year of simulation in the s014 run described.

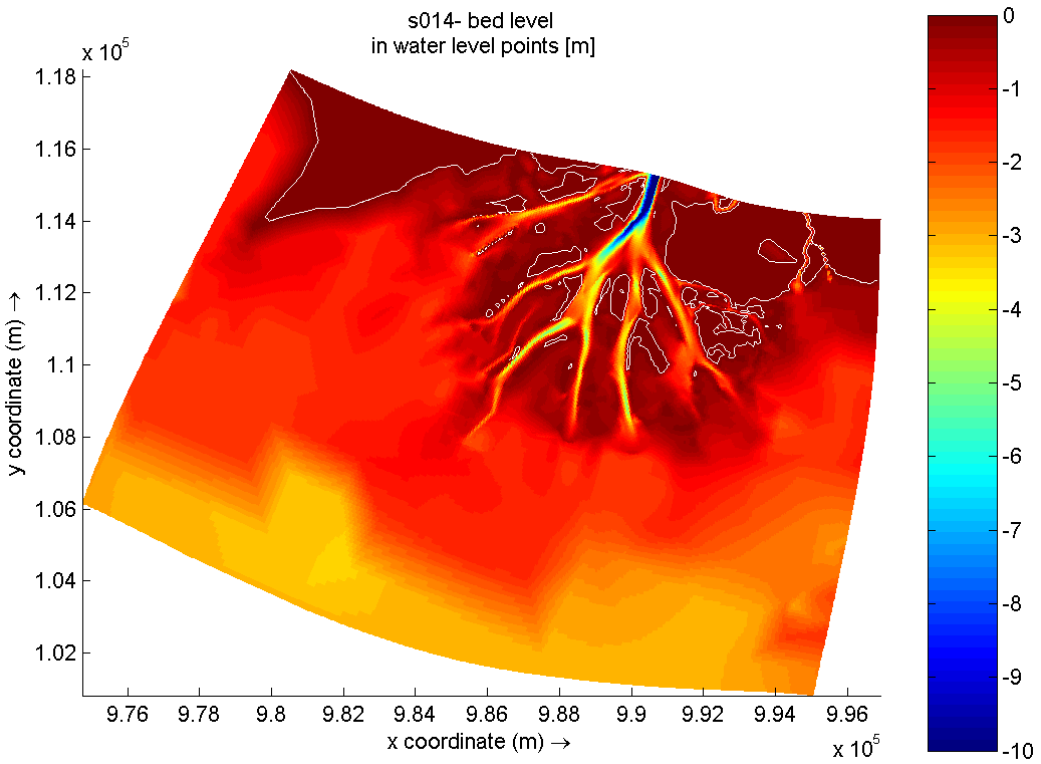

Figure C-7: s014 bathymetry of developing Wax Lake Delta and receiving basin after five years of morphologic simulation along with 0 m contour line. Upper and Lower color limits were defined so that elevations between limits could be viewed with more clarity.